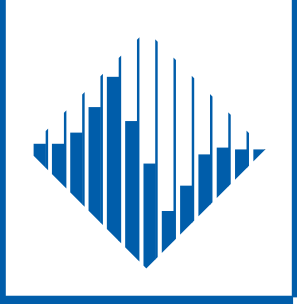

PACIFIC EARTHQUAKE ENGINEERING
RESEARCH CENTER

Evaluation of Ground Motion Selection and Modification Methods: Predicting Median Interstory Drift Response of Buildings

PEER Ground Motion Selection and Modification Working Group

Curt B. Haselton, Editor
California State University, Chico

PEER 2009/01
JUNE 2009

Evaluation of Ground Motion Selection and Modification Methods: Predicting Median Interstory Drift Response of Buildings

PEER Ground Motion Selection and Modification Working Group

Curt B. Haselton, Editor

Department of Civil Engineering
California State University, Chico

PEER Report 2009/01
Pacific Earthquake Engineering Research Center
College of Engineering
University of California, Berkeley

June 2009

CONTRIBUTING AUTHORS AND REVIEWERS

Jack W. Baker	Stanford University
Yousef Bozorgnia	Pacific Earthquake Engineering Research Center
Christine A. Goulet	URS Corporation
Curt B. Haselton	California State University, Chico
Erol Kalkan	United States Geological Survey
Nico Luco	United States Geological Survey
Tom Shantz	California Department of Transportation
Nilesh Shome	Applied Insurance Research (AIR) Worldwide
Jonathan P. Stewart	University of California, Los Angeles
Polsak Tothong	Applied Insurance Research (AIR) Worldwide
Jennie Watson-Lamprey	Watson-Lamprey Consulting
Farzin Zareian	University of California, Irvine

ABSTRACT

Nonlinear dynamic analysis of structures is becoming increasingly prevalent in code and regulatory documents prescribing design and analysis. A recurring challenge for both practicing engineers and developers of such documents is the selection and modification of ground motions for these nonlinear dynamic analyses. Nonlinear structural response is often highly sensitive to the selection and modification of input ground motions, and many ground motion selection and modification (GMSM) methods have been proposed. No systematic studies exist that provide impartial guidance to engineers regarding appropriate methods for use in a specific analysis application; thus engineers are left to make an important decision that is virtually uninformed.

The purpose of this report is to provide the engineering community with a foundation, backed by comprehensive research, for choosing appropriate ground motion selection and modification methods for predicting the median drift response of buildings. To this end, the approach taken in this report is (a) to select and scale ground motions using a wide variety of proposed methods, (b) to use these ground motions as inputs to nonlinear dynamic structural analyses, and then (c) to study differences in the resulting structural response predictions in order to identify what GMSM decisions are most crucial. By studying a large number of GMSM methods and analyzing a variety of structures, this report quantitatively compares many of the GMSM methods available to the engineering community.

This report presents the methodology developed by the GMSM Program and the results obtained using 14 ground motion selection and modification techniques (25 if variations of those 14 are considered separately) to analyze four reinforced concrete frame and wall buildings. The results show that for the classes of buildings considered here, one can improve the prediction of structural response by appropriately taking into account higher-mode and nonlinear properties (in addition to elastic first-mode properties) of the buildings when selecting and scaling ground motion records. This is often accomplished through selection based on appropriate spectral shape, or through use of inelastic methods. The specific results of this report are intended to provide practical guidance for those selecting and scaling ground motions for buildings, and the overall methodology provides a general framework for future evaluation of other ground motion selection and scaling techniques and other classes of engineered structures.

The PEER Ground Motion Selection and Modification Program plans to continue these types of evaluations in order to bring further quantitative rigor to the use of ground motions for

the analysis of buildings, and also to initiate such research for a wider range of engineering problems (e.g., bridges, nuclear structures, earthen dams, site response). This report should thus be considered as an initial building block toward future studies that will grow increasingly comprehensive.

ACKNOWLEDGMENTS

This study was sponsored by the Pacific Earthquake Engineering Research Center's (PEER's) Program of Applied Earthquake Engineering Research of Lifelines Systems supported by the California Department of Transportation and the Pacific Gas and Electric Company. Any opinions, findings, conclusions or recommendations expressed in this publication are those of the authors and do not necessarily reflect those of the funding agencies.

Funding was also provided to Christine Goulet from the National Sciences and Engineering Research Council of Canada. This funding is also greatly appreciated.

This project has been highly collaborative and has involved many members from the GMSM community. Some of these contributors spent many hours on this study, and the project team would like to thank the contributing researchers and practitioners for their time and efforts in providing ground motion record suites, and/or providing feedback and advice regarding the project scope and direction. Without their collaborations and efforts, this work could not have been achieved. These contributors are as follows:

Arzhang Alimoradi	John A. Martin & Associates
Paolo Bazzurro	Applied Insurance Research (AIR) Worldwide
Charles Kircher	Kircher and Associates
Albert Kottke	University of Texas, Austin
Coleen McQuoid	University of California, Berkeley
Praveen Malhotra	FM Global
Jack Moehle	University of California, Berkeley
Farzad Naeim	John A. Martin & Associates
Maury Power	AMEC Geomatrix Consultants
Ellen Rathje	University of Texas, Austin
Brian Skyers	Skyers and Associates
Jonathan Stewart	University of California, Los Angeles
Gang Wang	AMEC Geomatrix Consultants
Andrew Whittaker	State University of New York, Buffalo
Bob Youngs	AMEC Geomatrix Consultants

The authors would also like to thank the GMSM Program Management Committee for their efforts and guidance in this work: Norm Abrahamson, Yousef Bozorgnia, Nico Luco, and Tom Shantz.

CONTENTS

LIST OF FIGURES

LIST OF TABLES

1 Introduction and Objectives

Authors: J. W. Baker, C. B. Haselton, J. Watson-Lamprey

1.1 MOTIVATION AND BACKGROUND

Nonlinear dynamic analysis of structures is becoming increasingly prevalent in code and regulatory documents prescribing design and analysis. A recurring challenge for both practicing engineers and developers of these documents is the selection and modification of ground motions for these nonlinear dynamic analyses. Nonlinear structural response is often highly sensitive to the selection and modification of input ground motions. Many ground motion selection and modification methods have been proposed, but virtually no systematic studies exist that provide impartial guidance to engineers regarding appropriate methods for use in a specific analysis application. Thus, engineers are left to make an important decision that is virtually uninformed. This is problematic because, as will be seen in this report, predicted structural response can vary dramatically depending on the chosen ground motion selection and modification method. The engineer's choice of ground motion selection and modification method can lead to costly overdesign of structures, or worse, dangerous underdesign of structures.

1.2 OVERALL OBJECTIVES OF PEER GMSM PROGRAM, AND SPECIFIC OBJECTIVES OF THIS STUDY

To address this issue, the Pacific Earthquake Engineering Research (PEER) Center established the Ground Motion Selection and Modification (GMSM) Program, and this report is the first major product of this Program. The overall mission of the GMSM Program is to provide practical guidance and tools to the engineering community regarding ground motion selection and modification methods, while at the same time advancing the state of research in this area. In addition to the focus on technical advancements, the GMSM Program is also focused on creating

community consensus regarding appropriate GMSM methods. In the attempt to work toward this goal, this research project has directly involved many members of the ground motion community (listed in the acknowledgements section of this report), and the GMSM Program has coordinated two technical workshops (in fall 2006 and fall 2007).

The objective of this specific report is to provide the engineering community with a foundation, backed by comprehensive research, for choosing appropriate ground motion selection and modification methods for predicting the median drift response of buildings. To this end, the approach taken in this report is to (a) select and scale ground motions using a wide variety of proposed methods, (b) use these ground motions as inputs to nonlinear dynamic structural analyses, and then (c) study differences in the resulting structural response predictions in order to identify what GMSM decisions are most crucial. By studying a large number of GMSM methods, and analyzing a variety of structures, this report quantitatively compares many of the GMSM methods available to the engineering community.

The specific results of this report are intended to provide practical guidance for those selecting and scaling ground motions for buildings, and the overall methodology provides a general framework for future evaluation of other ground motion selection and scaling techniques and other classes of engineered structures. The PEER Ground Motion Selection and Modification Program plans to continue these types of evaluations, in order to bring further quantitative rigor to the use of ground motions as inputs for structural analysis. This report should thus be considered as an initial building block toward future studies that will grow increasingly comprehensive.

1.3 SCOPE OF STUDY

One challenge when evaluating GMSM techniques is to specify the purpose of the structural analysis for which the ground motions are to be used. A second challenge is that a wide variety of structural systems may be evaluated using nonlinear dynamic analyses, and the type of system being considered may impact the optimal method for selecting and modifying ground motions. The following subsections outline the assumed analysis goals considered in this study, and briefly introduce the structures that were used; more detail will be provided in the following chapters.

1.3.1 Assumed Goal of Dynamic Analysis

This report focuses on the use of dynamic analysis for predicting the response of a structure to a future ground motion with a known magnitude and distance (and also a known spectral acceleration value at the fundamental period of the structure, $Sa(T_1)$). This report looks specifically at predicting the maximum interstory drift ratio (MIDR) response (the maximum IDR over building height). The recommendations of this report are based on predicting MIDR, and the recommendations will likely differ for some other structural responses (e.g., peak floor accelerations or element force demands). The focus on MIDR was decided because it is a parameter of great interest for both code-based design checks as well as performance-based engineering assessments, and there is much research experience in predicting this response parameter. Future studies should consider a broader range of the response parameters.

One issue that immediately arises when examining data of this type is that the responses are necessarily probabilistic in nature due to variability among ground motions. Some of the GMSM methods included in this report will focus on predicting the complete probability distribution of MIDR response (i.e., the mean, or median, response as well as a standard deviation of responses). However, this report will focus on methods that have the goal of accurately predicting only the *median* MIDR structural response associated with ground motions having a given magnitude and distance (and also known $Sa(T_1)$). This focus on median responses is partly to limit the scope of the study and make the study tractable, and partly because median response (or the closely related mean or "average" response) is of primary interest in the nonlinear dynamic analysis requirements of current building codes (ICC 2006; ASCE 2005).

The focus on estimating response for a given magnitude and distance (and possibly $Sa(T_1)$) is because such estimates are believed to be valuable in a variety of analysis situations. For example, many performance-based or risk-based evaluations require that one (a) use probabilistic seismic hazard analysis to identify an $Sa(T_1)$ amplitude that is exceeded with a given probability, (b) use deaggregation to identify the most likely causal magnitudes and distances for that $Sa(T_1)$, and then (c) select and scale ground motions to match those identified parameters (e.g., Goulet et al. 2007). An alternative analysis situation might be one where an analyst specifies a "scenario" earthquake with a given magnitude and distance, and wants to obtain the resulting structural response. For evaluations incorporating multiple

magnitude/distance pairs or multiple $Sa(T_1)$ levels, the approaches studied here can be used to select and scale each of the multiple sets of ground motions needed for such an evaluation.

It should be clearly stated that this assumed analysis goal is somewhat different from the situation specified in current building codes (ICC 2006; ASCE 2005). These code requirements provide a fixed target spectrum, typically based on a uniform hazard spectrum, and then require the use of ground motions which *exceed* that spectrum over a *range of periods*. Because such an approach specifies spectral acceleration values over a range of periods, and the probability of simultaneously exceeding the multiple spectral values is not known, the resulting structural response results are of little use in performance-based assessments. Thus, while building-code-based ground motion selection methods will be considered here along with other methods (for comparative purposes), they are not the sole focus of this report.

1.3.2 Ground Motion Selection and Modification Methods Considered

To limit this current research effort to a manageable scope, the ground motion modification methods evaluated in this report are those that rely on selecting recorded ground motions and (possibly) scaling their amplitudes. Methods that use spectrum compatibilization (i.e., modification of the frequency content of a ground motion) and methods that simulate ground motions are not included here. Such methods are left for possible future extensions of this study. Even given this narrowing of the scope, a wide variety of methods have been proposed for selecting ground motions from a large library of recorded motions, and then scaling those motions. An overview of these methods is presented in Chapter 2. In total, 14 methods (25 in method variations are included) are evaluated in this report, with 22 researchers and practitioners participating in this study by submitting sets of ground motions.

One other decision that must be made is how many ground motions will be used for analysis. Because of record-to-record variability, two ground motions selected and scaled using an identical procedure will produce different structural responses. When comparing predictions from multiple GMSM methods, this variability can obscure differences in median (or average) response, and so using a larger number of records can enable more precise detection of differences between methods. On the other hand, analysts are often reluctant to use large numbers of ground motions for analysis, due to the extra effort required to obtain and interpret

the results. To balance between these two conflicting positions, the decision was to obtain four sets of seven ground motions for each GMSM method being considered. This was decided because seven ground motions are required by the building code in order to use the average structural response (ASCE 2005), and obtaining four sets selected using the same method allows us to measure the variability in the median prediction between the four sets. The 28 ground motions can also be examined as a single group, to more accurately estimate the median (and average) response prediction for each method. Although four sets of seven ground motions were requested from all participants in this project, for various reasons a few methods use differing numbers of ground motions.

1.3.3 Structures Considered

Table 1.1 briefly summarizes the structural models evaluated in this report, which are described in more detail in Chapter 3. These four reinforced concrete structural models were selected because the models are rigorous, and the structures are fairly realistic while being generic enough for the results to be as generalizable as possible, (since many structural systems behave like frames, walls, or some combination of the two). These specific four buildings were chosen to capture some variation in height (4–20 stories) and first-mode period (0.97–2.63 sec), and variation in the level of expected nonlinearity in response for the target ground motion (Building B is highly nonlinear, Building D is mildly nonlinear, and Buildings A and C are between these two extremes). Additionally, Buildings B and D were selected to identify any differences between a shear wall building and a moment-frame building having the same number of stories. Buildings A, B, and C are modeled in OpenSees (OpenSees 2006) and Building D is modeled in Drain-2DX (Prakash 1993). Note that the tallest building used in this study is 20 stories, so this report does not directly address the question of selecting motions for extremely tall structures.

Table 1.1 Four structural models used for comparison of GMSM methods.

Building	*Stories*	*Type*	*Code Compliance*	T_1 *(s)*
A	4	Modern special moment frame	2003 IBC	0.97
B	12	Modern special moment frame	2003 IBC, ASCE 7-02, ACI 318-02	2.01
C	20	Modern special moment frame	2003 IBC, ASCE 7-02, ACI 318-02	2.63
D	12	Modern (ductile) planar shear wall	ACI 319-02	1.20

Even though maximum interstory drift ratio (MIDR) is the focus on this current report, a wide variety of structural response parameters were recorded from each structural analysis (e.g., maximum interstory drifts of each story, maximum accelerations of each floor, and maximum plastic rotations of each element). These responses are fully documented in Appendix C.

1.4 SUMMARY

This report represents a study of a wide variety of ground motion selection and scaling techniques (14 methods, with 25 total variations), and draws conclusions based on structural response predictions for four buildings.

While any single report must necessarily limit its scope in terms of the types of structures and types of ground motion modification/simulation approaches considered, this study was carefully planned so that this document provides findings that are relevant to many of the types of ground motion selection and scaling techniques in common use today. In addition, the four structures were selected carefully (Section 1.3.3) so the findings are as generalizeable as possible. Because of this careful building selection, the intuition gained from studying these four buildings should be applicable over a somewhat broader range of cases than only buildings having these specific configurations.

Perhaps most importantly, this report provides the first objective third-party evaluation of the structural response results obtained from a wide variety of common GMSM techniques, most of which have never been systematically compared. The results should thus provide evidence for

the important discussions that often take place among analysts regarding "correct" techniques for selecting and scaling ground motions. In addition, the evaluation approach used in this study will be equally appropriate for future comparisons of other GMSM techniques (e.g., simulation and spectrum compatibilization) and other structures (e.g., geotechnical structures and bridges). Accordingly, the authors intend for this report to launch further studies examining the various GMSM techniques for a wider range of engineering problems (e.g., bridges, nuclear structures, earthen dams, site response, etc.).

1.5 OUTLINE OF REPORT

Chapter 2 of this report summarizes the GMSM methods considered in this study, including discussion of the objectives of each method, and the manner in which we group the methods into categories. Chapter 3 then provides more detail regarding the approach taken for comparing and evaluating the GMSM methods; this includes discussion of the buildings and the ground motion scenarios used in this study. Part of this evaluation process involves creating a prediction of the "true response" (to be used as a comparison point when evaluating the GMSM methods), and Chapters 4 and 5 discuss prediction of this "true" response. Chapters 6–10 present the detailed results for the five test-bed cases considered in this study. Chapter 11 then summarizes and interprets the results for each of the five cases, presents the final conclusions and recommendations of this study, and then discusses proposed future research.

2 Overview of GMSM Methods Investigated

Author: N. Luco

2.1 INTRODUCTION

As pointed out in the introduction of this report (Chapter 1), there are many methods of ground motion selection and modification (GMSM) available to use for nonlinear response history analysis of structures. Two of the first tasks of the PEER GMSM Program were (1) to compile a list of known GMSM methods and (2) to decide which of those methods would be investigated in this study. The results of those tasks are summarized in this chapter.

To date more than 40 different GMSM methods and method variants have been identified. We have reviewed these candidate methods, categorized them by their objective, and used this to select the subset of methods to be investigated in this report. We then grouped methods within this subset according to similarities in their procedures for selecting and modifying (i.e., scaling) ground motions. These groupings allow us to better generalize the method comparisons, as well as to more readily observe differences between methods that are nominally similar.

2.2 OBJECTIVES OF GMSM METHODS

Different GMSM methods may have different objectives. In order to determine which GMSM methods to investigate in this study, we looked at the possible objectives of GMSM methods. By the "objective" of a method we mean the ultimate intent of the nonlinear response history analyses conducted using the ground motions selected and modified by the GMSM method. For example, the Building Code Selection and Scaling methods 200–209 (listed later in Table 2.1)

aim to estimate an average building response parameter (or "engineering demand parameter" in the PEER equation) for a given 5%-damped spectral acceleration at the fundamental period of the building, $Sa(T_1)$, and an associated earthquake magnitude, M, and source-to-site distance, R. On the other hand, the "ATC-58 35% Draft" method 101 (also listed later in Table 2.1) aims to estimate the full probability distribution (e.g., average and standard deviation) of building response for a given $Sa(T_1)$, M, and R. We have identified four general objectives that encompass those of the known methods we compiled. These four objectives are explained below. As explained in Chapters 1 and 3 (Sections 1.3.1 and 3.4), the main objective focused on in this report is Objective 4.

2.2.1 Objective 1: Probability Distribution of Structural Response for a Given *M* and *R*

The first of the four candidate objectives we identified is to predict the probability distribution (e.g., average and dispersion) of structural response for an earthquake of a given M and R (and possibly, as in the case of this report, a style of faulting or source mechanism of the earthquake, F, and a 30-m shear wave velocity of the building site, $V_{s,30}$). An example of a GMSM method with Objective 1 is one that simply selects ground motions from earthquakes having close to the target M and R (and F and $V_{s,30}$, hereafter omitted for brevity). The nonlinear response history analysis results from this example method can be used to predict both the average and the dispersion of structural response for the given M and R, at least if a relatively large number of ground motions are selected. We know of several existing Objective 1 methods, including some that are expected to work even when relatively few ground motions are selected, but Objective 1 methods are not within the scope of this report.

2.2.2 Objective 2: Average Structural Response for a Given *M* and *R*

The second objective we identified is similar to the first except that instead of predicting the probability distribution of structural response, only the median (or, more generally, the average) structural response is predicted. Like Objective 1, Objective 2 is a prediction for a given M and R (and F, $V_{s,30}$) — in other words, a given earthquake scenario. An example of a GMSM method that aims at Objective 2 is one that selects earthquake ground motions that have close to the target M and R, similarly to an Objective 1 method, but then spectrum-matches or spectrum-

compatibilizes the motions to a median response spectrum for the given M and R obtained from a ground motion prediction equation (or attenuation relation). We know of several Objective 2 methods, some of which rely on spectrum matching and some that do not, but Objective 2 methods are not within the scope of this report.

Despite the fact that Objectives 1 and 2 both predict a median structural response, it is important to keep in mind that it is not necessarily fair to compare the results of these predictions, particularly if relatively few (e.g., seven) ground motions are selected by the methods. An Objective 1 method that also predicts the dispersion of structural response (or the probability distribution of response) is not designed to minimize the standard error of the predicted median, unlike a typical Objective 2 method. Therefore, one would expect the median predictions from Objective 2 methods to vary less between one set of selected ground motions and another.

2.2.3 Objective 3: Probability Distribution of Structural Response for a Given $Sa(T_1)$ and Associated M and R

The third objective we identified is, like Objective 2, similar to the first except that instead of predicting the probability distribution of structural response for an *earthquake* scenario of a given M and R, it predicts the distribution of response for a *ground motion* scenario defined by a given $Sa(T_1)$ and associated M and R (as well as F and $V_{s,30}$). Note that such a ground motion scenario requires a priori knowledge of the structure, namely its fundamental period T_1, whereas an earthquake scenario given in Objectives 1 and 2 does not; Objective 1 and 2 methods require only M and R. A few examples of GMSM methods that aim at Objective 3 are summarized briefly in Section 2.4.3, including the ATC-58 35% Draft method 101 mentioned above. A study focused on Objective 3 methods is a potential topic of future research within the PEER GMSM Program, but that is not the focus of this current study.

2.2.4 Objective 4: Average Structural Response for a Given $Sa(T_1)$ and Associated M and R

The fourth and last of the objectives we identified is to predict the median (or average) structural response (like Objective 2) for a given $Sa(T_1)$, M, and R (like Objective 3). As an example

alluded to above (in Section 2.2), we contend that the Building Code Selection and Scaling methods 200–209 (listed later in Table 2.1) aim at Objective 4. It is clear that the objective of the building code (e.g., ASCE/SEI 7-05) GMSM method is to predict the average (here median) structural response, for a given ground motion scenario (i.e., the maximum considered earthquake ground motion) that includes in its definition M, R, and source mechanism (see, e.g., Section 16.1.3.1 of ASCE/SEI 7-05). We interpret the ground motion portion of this scenario to be an MCE $Sa(T_1)$ value rather than an MCE response spectrum, because the annual probability of the former is readily available (e.g., from the U.S. Geological Survey). All of the selected GMSM methods that aim at Objective 4 are listed later in Table 2.1. As explained in Chapters 1 and 3 (Sections 1.3.1 and 3.4), Objective 4 is the primary focus of this report.

Similarly to it not necessarily being fair to compare the median structural response predictions from GMSM methods that aim at Objectives 1 and 2, for reasons explained above in Section 2.2.2, the same is true of Objectives 3 and 4. Even so, this report does include some Objective 3 methods with the Objective 4 methods focused upon in this report (as shown later in Table 2.1). However, care is taken when comparing the predictions from Objective 3 with Objective 4 methods, by often excluding the Objective 3 methods from the summary statistics presented in the later results chapters (Chapters 6–11). Particularly when comparing the precision (see Chapter 10) of the respective GMSM methods, though, it is important to keep in mind the difference between these objectives. Comparisons of methods that aim at Objective 3 or 4 (for a given *ground motion* scenario) with Objective 1 or 2 (for a given *earthquake* scenario) are more inappropriate, and hence are not included as part of this report.

2.3 LIST OF GMSM METHODS INVESTIGATED

To date more than 40 different GMSM methods and method variants have been identified. For reasons explained in the next section, 14 of the 40 methods are investigated in this report (17 methods if variants are included). A method number, descriptive name, and primary contributor for each of those 17 methods are listed in Table 2.1. Also indicated in the table are the objective (numbered 1–4) of the method, and the group number (I–V) that each method is assigned to. The objectives were described in Section 2.2, and the groups are described later in Section 2.4.

Table 2.1 GMSM methods investigated in this report.

method #	*method Name*	*Primary Contributor, Affiliation*	*Objective #*	*Group #*
100	$Sa(T_1)$ Scaling with Bin Selection	N. Shome, AIR Worldwide	3	I
101	ATC-58 35% Draft method	F. Zareian, UC Irvine	3	I
200–209	Building Code Selection & Scaling — methods A–J	Jack Baker, Stanford Univ.	4	II
300	Conditional Mean Spectrum Selection with Scaling	Jack Baker, Stanford Univ.	4	III
301	Genetic Algorithm Selection to match CMS	A. Alimoradi, Martin & Assocs.	4	III
302	Semi-Automated Selection & Scaling to match CMS	E. Rathje, Univ. of Texas	4	III
303	Design Ground Motion Library (DGML) — Objective 4	G. Wang, Geomatrix	4	III
304	Design Ground Motion Library (DGML) — Objective 3	G. Wang, Geomatrix	3	III
400	Target Spectrum Based on Epsilon Correlations	C. Goulet, URS Corporation	3	IV
401	ε Selection with Sde(T1) Scaling	P. Tothong, AIR Worldwide	3	IV
402	ATC-63 method Applied to MIDR — Far-Field Set	C. Haselton, CSU Chico	4	IV
403	ATC-63 method Applied to MIDR — Near-Field Set	C. Haselton, CSU Chico	4	IV
500	$S_{di}(T_1,d_y)$ Scaling	P. Tothong, AIR Worldwide	4	V
501	Vector of Record Properties Identified by Proxy	J. Watson-Lamprey, UC Berkeley	4	V
502a	Inelastic Response Surface Scaling — 1st Mode	T. Shantz, Caltrans	4	V
502b	Inelastic Response Surface Scaling — 1st-2nd Modes	T. Shantz, Caltrans	4	V
503	$IM_{1II\&2E}$ Scaling	N. Luco, USGS	4	V

In order to arrive at the GMSM methods listed in Table 2.1 above, we first selected from all known methods those that aim at Objective 4 (defined above in Section 2.2.4 and also discussed later in Section 3.4). We then added methods that aim at Objective 3 (defined in Section 2.2.3) except when such methods had an already-selected variant that aims at Objective 4. In one case, namely methods 303 (for Objective 4) and method 304 (for Objective 3), we selected both variants. The 17 selected GMSM methods (variants included) were then grouped according to similarities in their procedure for selecting and modifying ground motions. The five groups we identified, labeled Groups I–V in Table 2.1, are described below in Section 2.4.

The grouping of methods described in the preceding paragraph is important for two main reasons. The first is that it is most fair to compare methods that aim at the same objective. As mentioned above, we selected for comparison those methods that aim at Objective 4, and in some cases Objective 3, but not Objectives 1 and 2. The differences between these four objectives are explained in the next subsection. The second main reason is that grouping methods whose procedures for selecting and modifying ground motions are similar allows us to better generalize the comparison results, as well as to more readily observe differences between methods that are nominally similar. The ground motion selection and modification procedures for the five groups we identified are briefly summarized in the next section.

2.4 BRIEF SUMMARIES OF GMSM METHODS

In this section we provide brief summaries of the GMSM methods listed in Table 2.1, which, as mentioned in the preceding section, are grouped according to similarities in their procedure for selecting and modifying ground motions. Such grouping allows us to better generalize the method comparison results and more readily observe differences between methods that are nominally similar.

The brief summaries in this section are presented by GMSM Group (I–V), sometimes describing a particular method in the group but mostly referring to the method summaries provided in Appendix A for more details. In each summary (i.e., subsection) below we first describe how the methods within the group *select* ground motions, and then we describe how they *modify* (or *scale*) those ground motions. In some cases a large number of candidate ground motions are modified before selection of the final set, but we still summarize the selection before

the modification and simply note this reversal in the order of operations. In each summary we also note the specific objective(s) of the GMSM methods in the group.

2.4.1 Group I: Selection by *M* and *R* and Scaling to $Sa(T_1)$

The Group I, or "$Sa(T_1)$," methods select ground motions from earthquakes of magnitude (M) and distance (R) as close as possible to that of the scenario of interest. For example, for the M7 scenario that is used in this study (with M=7 and R=10 km, as defined in Section 3.3), method 101 selected ground motions with M=6.2–7.6 and R=1.0–17.5 km. In addition to M and R, the Group I methods may consider other earthquake, site, or ground motion parameters, such as the style of faulting or source mechanism of the scenario earthquake (e.g., strike-slip in the case of the PEER GMSM Program focus) and/or the type of soil at the site of interest (e.g., 400 m/s shear wave velocity for the top 30 m of the soil profile, Vs30). If all of these selection criteria result in more than the target number of ground motions, the Group I methods select from them randomly. For example, Group I method 101 randomly selects 11 ground motions from the 50 listed in Table 2.2. In contrast, if the selection criteria result in too few ground motions, the criteria are relaxed.

Table 2.2 Example of candidate ground motion from which Group I method 101 selects randomly.

Table B-3 Bin 1–Near-Fault Ground Motions

Designation	Event	Station	M [1]	r [1]
NF1, NF2	Kobe 1995	SAC 2/50 for Los Angeles	6.9	3.4
NF3, NF4	Loma Prieta 1989		7.0	3.5
NF5, NF6	Northridge 1994		6.7	7.5
NF7, NF8	Northridge 1994		6.7	6.4
NF9, NF10	Tabas 1974		7.4	1.2
NF11, NF12	Elysian Park 1 (simulated)		7.1	17.5
NF13, NF14	Elysian Park 2 (simulated)		7.1	10.7
NF15, NF16	Elysian Park 3 (simulated)		7.1	11.2
NF17, NF18	Palos Verdes 1 (simulated)		7.1	1.5
NF19, NF20	Palos Verdes 2 (simulated)		7.1	1.5
NF21, NF22	Cape Mendocino 04/25/92	89156 Petrolia	7.1	9.5
NF23, NF24	Chi-Chi 09/20/99	TCU053	7.6	6.7
NF25, NF26	Chi-Chi 09/20/99	TCU056	7.6	11.1
NF27, NF28	Chi-Chi 09/20/99	TCU068	7.6	1.1
NF29, NF30	Chi-Chi 09/20/99	TCU101	7.6	11.1
NF31, NF32	Chi-Chi 09/20/99	TCUWGK	7.6	11.1
NF33, NF34	Duzce 11/12/99	Duzce	7.1	8.2
NF35, NF36	Erzinkan 03/13/92 17:19	95 Erzinkan	6.9	2.0
NF37, NF38	Imperial Valley 10/15/79	5057 El Centro Array #3	6.5	9.3
NF39, NF40	Imperial Valley 10/15/79	952 El Centro Array #5	6.5	1
NF41, NF42	Imperial Valley 10/15/79	942 El Centro Array #6	6.5	1
NF43, NF44	Kobe 01/16/95 20:46	Takarazu	6.9	1.2
NF45, NF46	Morgan Hill 04/24/84 04:24	57191 Halls Valley	6.2	3.4
NF47, NF48	Northridge 1/17/94 12:31	24279 Newhall	6.7	7.1
NF49, NF50	Northridge 1/17/94 12:31	0637 Sepulveda VA	6.7	8.9

1. M = moment magnitude; r = closest site-to-fault-rupture distance

The ground motion modification applied by the Group I methods is relatively simple: each selected ground motion is scaled in amplitude (i.e., by multiplying the ground motion acceleration values by a scaling factor) such that its $Sa(T_1)$ value is equal to the scenario $Sa(T_1)$ value. The scaling factor applied is equal to the ratio of the scenario $Sa(T_1)$ value to the $Sa(T_1)$ value of each un-scaled ground motion. An example of the response spectra resulting from this type of scaling is provided in Figure 2.1.

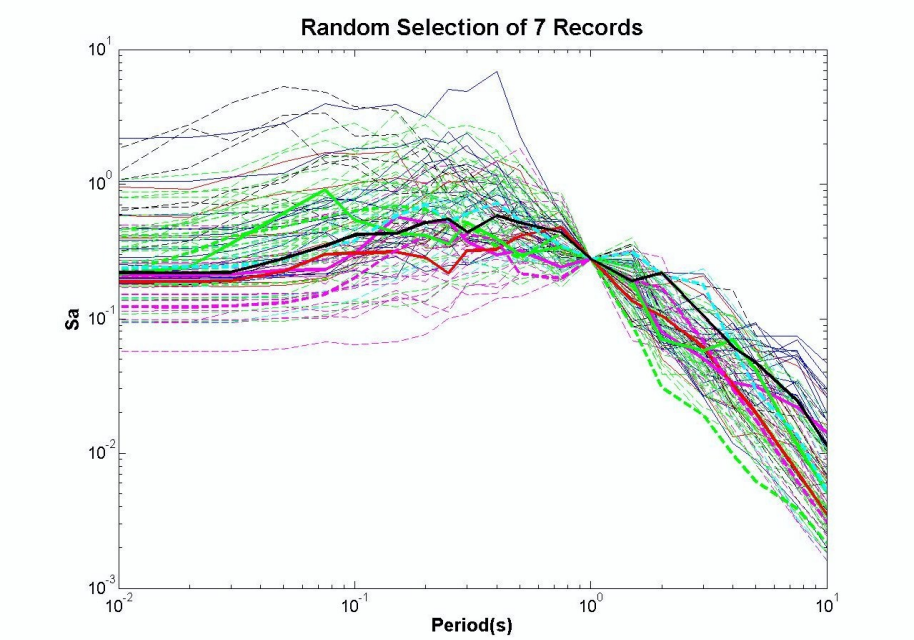

Fig. 2.1 Example of response spectra resulting from simple amplitude scaling of ground motions to scenario *Sa*(T_1). Seven thicker lines are response spectra for ground motions selected randomly from full set of records that match *M, R,* etc., selection criteria (thinner lines).

The objective targeted by the Group I methods is Objective 3, i.e., to predict the probability distribution of structural response for a ground motion scenario defined by a given $Sa(T_1)$ and associated M and R.

2.4.2 Group II: Selection and Scaling Using Uniform Hazard Spectrum (UHS)

The Group II, or "UHS," methods select ground motions whose response spectra, allowing for simple amplitude scaling of each ground motion (and thereby its response spectrum) are as close as possible to a target uniform hazard spectrum (UHS). In other words, these methods select ground motions whose "spectral shapes" are similar to the spectral shape of the target UHS. The target UHS is typically that from which the scenario $Sa(T_1)$ is taken. For this study, however, the scenario $Sa(T_1)$ was not read from a UHS, so the target UHS was taken to be a site-specific UHS in which all the spectral acceleration values, including $Sa(T_1)$, are one (for the M7.5 scenario defined in Chapter 3) or two (for the M7 scenario) standard deviations above the median

response spectrum for the earthquake scenario (i.e., an $\varepsilon = +1.0$ or $\varepsilon = +2.0$ response spectrum). In addition to spectral shape, the Group II methods may consider other earthquake, site, or ground motion parameters in selecting ground motions. For examples, please see the Appendix A summary for methods 200–209.

As mentioned in the preceding paragraph, the ground motion modification applied by the Group II methods is simple amplitude scaling. Unlike the Group I methods, however, the considered Group II methods do not scale the ground motions to the scenario $Sa(T_1)$. Instead, they scale each ground motion such that its response spectrum "closely matches" the UHS, and then scale upward slightly, if necessary, to ensure that the average response spectrum across the selected and scaled ground motions exceeds the UHS, consistent with procedures specified in SEI/ASCE 7-05 (ASCE 2005). For more information, please see the Appendix A summary for methods 200–209.

The objective targeted by the Group II methods is Objective 4, i.e., to predict the average (median) structural response for a ground motion scenario defined by a given $Sa(T_1)$ and associated M and R.

2.4.3 Group III: Selection and Scaling Using Conditional Mean Spectrum (CMS)

The Group III, or "CMS," methods are similar to the Group II (UHS) methods except that a conditional mean spectrum (CMS; Baker and Cornell 2006) is used as the target spectral shape for selecting ground motions instead of a UHS. The target CMS is calculated for the scenario $Sa(T_1)$, M, and R (and F, $V_{s,30}$, etc.) using the procedure described in the Appendix A summary for method 10. The CMS represents the *expected* response spectrum for the defined ground motion scenario, which is based on a target $Sa(T_1)$ value at a *single period*, as well as its associated M and R (and F, $V_{s,30}$, etc.). This is in contrast to the UHS, which represents equally rare $Sa(T)$ values at *many periods* (including T_1) simultaneously.

A comparison of the UHS and CMS used in this study is provided in Figure 2.2. In addition to spectral shape, the Group III methods 301 and 303–304 consider other earthquake, site, and ground motion parameters in selecting ground motions. For more information, see the Appendix A summaries for these methods.

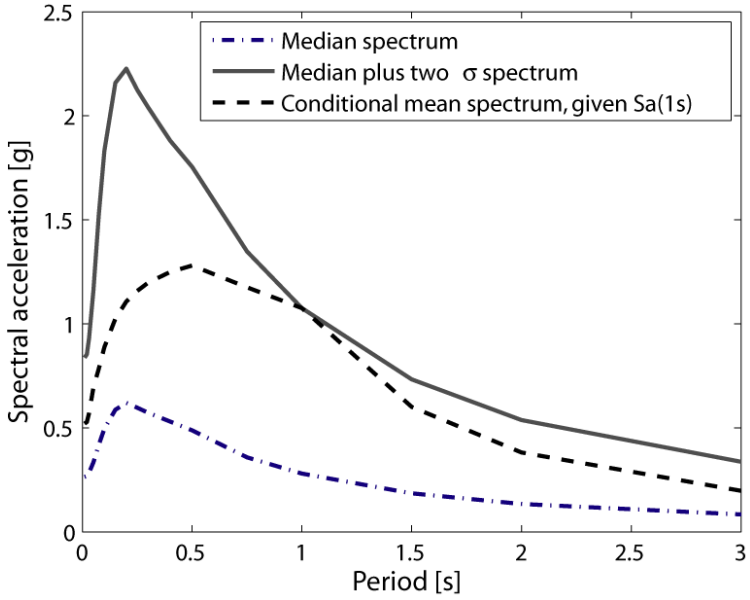

Fig. 2.2 Comparison of CMS and UHS (labeled "Median plus two σ spectrum") used in this study.

Similarly to the Group I and II methods, the ground motion modification applied by the Group III methods is simple amplitude scaling. Methods 300 and 303–304 scale the ground motions to the scenario $Sa(T_1)$, like the Group I methods, whereas methods 301 and 302 scale to closely match the target CMS, more like the Group II methods. The Appendix A summaries for methods 301 and 302 provide more information on how they "closely match" the target response spectrum.

All but one of the Group III methods target Objective 4. The exception is method 304, which targets Objective 3. It is important to note a difference in the selection and modification (i.e., scaling) between these methods for Objective 4 versus 3. Whereas the former (methods 300, 301, 302, and 303) typically select or scale ground motions such that the response spectrum for each closely matches the target CMS, the latter method (method 304) selects ground motions so as to reflect not only the conditional (given $Sa(T_1)$, M, and R) mean spectral acceleration at each period (i.e., the CMS) but also the conditional standard deviation of the spectral acceleration at each period. Methods 300 and 302 could be modified to reflect this standard deviation, and thereby to also target Objective 3.

2.4.4 Group IV: Selection and Scaling Using Proxy for CMS

The Group IV, or "ε," methods are similar to the Group III (CMS) methods except that they use ε as a proxy for the spectral shape of the CMS. That is, the Group IV methods (with the exception of methods 402–403, as explained below) select ground motions whose ε at the fundamental period of the building, denoted $\varepsilon(T_1)$, is as close as possible to the $\varepsilon(T_1)$ of the ground motion scenario (e.g., $\varepsilon(T_1)$=2 in the case of the M7 scenario defined in Chapter 3). The parameter $\varepsilon(T_1)$ is defined as the number of (logarithmic) standard deviations that $Sa(T_1)$ is above its median value for the scenario M and R. In addition to ε, the Group IV methods may consider other earthquake (e.g., M and R), site (e.g., Vs30), and ground motion parameters in selecting ground motions. In fact, these other parameters alone are used for selection in the Group IV methods 402–403 which, unlike the other Group IV methods, use $\varepsilon(T_1)$ *after* the nonlinear response history analyses under the selected and modified ground motions have been carried out; see the Appendix A method summaries for details.

Like the Group I–III methods, the ground motion modification applied by all but one of the Group IV methods is simple amplitude scaling to the scenario $Sa(T_1)$. No modification/scaling is applied in method 400.

Like the Group I methods, but unlike those in Groups II–III, the Group IV methods 400–401 target Objective 3. The Group IV methods 402–403, however, are designed to target Objective 4, although slight variants could allow them to instead target Objective 3.

2.4.5 Group V: Selection and Scaling Considering Inelastic Spectral Displacement

The Group V, or "inelastic," methods select, in the case of method 501 or 502a–b, ground motions whose properties related to inelastic spectral displacement (see method summaries in Appendix A for more information) are as close as possible to corresponding properties estimated for the ground motion scenario. These selections are made after the ground motion scaling described in the next paragraph. Method 502b also considers, in selecting ground motions, how well the scaled ground motion fits the CMS at the second-mode period of the particular building. In the case of method 500 or 503, the ground motions are selected randomly.

The ground motion modification applied by the Group V methods is in the case of method 501, simple amplitude scaling to the scenario $Sa(T_1)$. In the case of method 502a–b, each ground motion is iteratively scaled in amplitude to "fit" the target inelastic displacement surface (IDS) for the ground motion scenario. An example of a target IDS and the IDS for a candidate ground motion is shown in Figure 2.3; see the Appendix A summary of method 502a–b for more information. In the case of method 500 or 503, each ground motion is iteratively scaled in amplitude to match, respectively, the inelastic spectral displacement, $S_{di}(T_1,d_y)$, or the intensity measure $IM_{1I\&2E}$ (Luco and Cornell 2007) estimated for the scenario. The latter intensity measure reflects the spectral acceleration at the second-mode period of the particular building of interest.

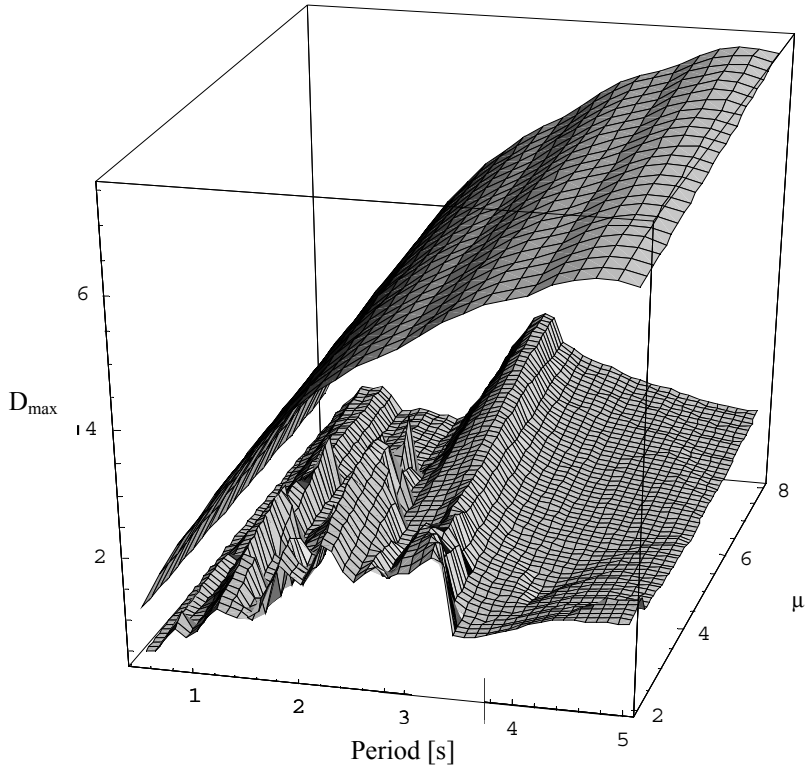

Fig. 2.3 Example of inelastic displacement surface (IDS) for candidate ground motion (lower surface) that is iteratively scaled in amplitude to fit target IDS (upper surface) in methods 502a–b.

The Group V methods target Objective 4 (median building response for a ground motion scenario), since like the Group II–III methods, they select and modify/scale ground motions to match anticipated properties other than those directly specified in the ground motion scenario (namely a UHS, CMS, or property related to inelastic spectral displacement).

2.5 SUMMARY

For investigation in this report, the PEER GMSM Program has compiled a list of 14 methods (17 after including variants) for selecting and modifying ground motion records for nonlinear response history analysis, developed by researchers and practitioners in the broader community. This list is a subset of known methods limited to methods consistent with the assumed goal of the nonlinear analysis that is within the scope established in Chapter 1; this goal is, namely, prediction of the average structural response (specifically maximum interstory drift ratio) for a ground motion scenario defined by a spectral acceleration at the fundamental period of the structure, $Sa(T_1)$, and an associated earthquake magnitude, M, and source-to-site distance, R. This objective (labeled Objective 4) is explained in more detail in Section 2.2.4 above, along with another closely related but different objective (Objective 3), and two others that are not investigated in this report (Objectives 1–2).

As indicated in the Table 2.1 list, the 17 methods investigated in this report are grouped, according to similarities in their procedures for selecting and modifying ground motions. The GMSM methods in each of the five groups identified are summarized briefly in Section 2.4. More detailed summaries of each individual method are provided in Appendix A.

3 Research Approach: Ground Motion Scenarios, Structures, Analysis Objectives, and Point of Comparison

Author: C. B. Haselton

3.1 OVERVIEW OF RESEARCH APPROACH

The purpose of this study is to provide the engineering community with a foundation, backed by comprehensive research, for choosing appropriate GMSM methods to predict median MIDR structural response. This requires an objective evaluation of a large number of the GMSM methods currently available in the literature.

To complete this evaluation, several test-bed cases were developed to be used in comparing the prediction capabilities of the various GMSM methods. These test-bed cases consist of four structures and two ground motion scenarios; these cases are discussed in detail in this chapter, and are summarized as follows:

- Case 1: Building A (4-story RC special moment frame), M7 ground motion scenario
- Case 2: Building B (12-story RC special moment frame), M7 ground motion scenario
- Case 3: Building C (20-story RC special moment frame), M7 ground motion scenario
- Case 4: Building D (12-story RC shear wall), M7 ground motion scenario
- Case 5: Building C (20-story RC special moment frame), M7.5 ground motion scenario

In order to provide a comprehensive evaluation of GMSM methods, it is not enough to simply compare the predictions from each method; we must have some estimate of the true response, to which the individual estimates can be compared. Due to our lack of complete data and knowledge, there is no way to know *exactly* what will happen in a future earthquake; even so, for comparative purposes, we create a "high-end prediction" (or "point of comparison"),

which we consider to be the *best* possible prediction of structural response. This prediction involves a great deal of effort (many ground motions, much statistical analysis, etc.), which is warranted for this research study, but would not be feasible for typical projects. In this project, we compare the simpler GMSM method predictions with this more comprehensive prediction, in order to show which simpler GMSM methods can be used in order to obtain the correct response prediction with a reasonable amount of effort (i.e., without completing a HEP).

Before starting to look at each GMSM method and make comparisons, the GMSM Working Group made an important decision. The group could have used the GMSM methods from various researchers, and selected motions "in-house" using those methods. Instead, the GMSM Working Group decided to request that the GMSM method *authors themselves* complete the selections and submit ground motion sets for each Case. This decision was made for two primary reasons: (1) this avoided misinterpretation of the GMSM methods, and more importantly (2) this created dialogue with the GMSM method authors and facilitated their direct input and review of this project. This was important, because the goal of this project is to not only provide guidance on appropriate GMSM methods, but also to begin creating *community consensus* regarding which methods should be used.

To involve as many GMSM method authors as possible, several public solicitations were announced, asking the ground motion community to submit sets of records; these solicitations are documented in Appendix C. The first solicitation was distributed in 2006 and asked for a single set of seven records for Case 1. Later solicitations expanded the requests to include Cases 1–4, and some researchers were asked to submit ground motions for Case 5 (for comparative purposes). In addition to the request for ground motion sets, the GMSM Working Group also invited these method authors to two PEER GMSM Workshops, where the preliminary results were presented for their review, and where the authors were asked to provide feedback and advice on the project direction and methods. A summary of this progression is as follows:

- Phase One Pilot Study (Case 1):
  - Fall 2006 — First public solicitation sent, for Case 1.
  - October 16, 2006 — Ground motion sets due for Case 1.
  - October 27, 2006 — PEER GMSM Workshop 1, to present preliminary results from Case 1 and to solicit feedback/advice from method authors and ground motion community members.

- November 17, 2006 — COSMOS Annual Meeting, were final Case 1 results were presented.

- Phase Two (Cases 2–5):
  - April 2007 — Second public solicitation sent, for Cases 2–5 (and also for Case 1, for those not involved in phase one).
  - June 4, 2007 — Ground motion sets due for Cases 2–5.
  - October 8, 2006 — PEER GMSM Workshop 2, to present preliminary results from Cases 2–4 and to solicit feedback/advice from method authors and ground motion community members.
  - November 9, 2006 — COSMOS Annual Meeting, were final Cases 2–4 results were presented.

The close collaboration with many members of the ground motion community (through the workshops, and more informally during the process of selecting records, completing the structural analyses, and distributing the results) was a critical part of this project.

3.2 STRUCTURAL DESIGNS AND STRUCTURAL MODELING

The structural designs and models used for this study were carefully selected to ensure that the results of this study are (a) based on realistic and reviewed structural designs that are representative of what would be designed in practice, (b) based on well-vetted analytical models that capture the important modes of structural response, and (c) applicable to a reasonably wide range of structural heights and systems.

3.2.1 Structural Designs

Four structural designs were selected for use in testing the GMSM methods considered in this study. These four designs are summarized in Table 3.1, and include three reinforced concrete (RC) special moment-frame structures (4, 12, and 20 stories), and one 12-story ductile RC wall structure. These four buildings were chosen because they are representative of modern design (for which most performance-based assessments are performed), capture variation in height (4-20 stories) and fundamental period (0.97–2.63 sec), and include two structural systems (RC

frames and walls). Note that frame buildings of any material (RC, steel, etc.) behave similarly, so the results of this study should be reasonably applicable to other types of frames as well.

Additionally, this study is purposefully avoiding direct prediction of structural collapse (the focus here is on pre-collapse interstory drift response; discussed later in Section 2.4). Due to this, these specific building designs were selected because they have a reasonably low rate of collapse for the ground motion scenarios used in this study (the scenarios are defined later in G66

Section 3.3). Under the ground motion scenarios used in this study, this set of buildings provides a range of levels of nonlinearity, with Building B being most nonlinear, Building D being least nonlinear, and Buildings A and C being between these two extremes.

Table 3.1 Four structural models used for comparison of GMSM methods.

Building	*Stories*	*Type*	*Code Compliance*	*$T_1 - T_3$ [s]*
A	4	Modern RC special moment frame	2003 IBC, ASCE 7-02, ACI 318-02	0.97, 0.35, 0.18
B	12	Modern RC special moment frame	2003 IBC, ASCE 7-02, ACI 318-02	2.01, 0.68, 0.39
C	20	Modern RC special moment frame	2003 IBC, ASCE 7-02, ACI 318-02	2.63, 0.85, 0.46
D	12	Modern (ductile) RC planar shear wall	None specifically, but consistent with modern planar wall design	1.20, 0.19, 0.07

Building A is a 4-story four-bay perimeter frame design, which comes from the recent "Benchmarking" study completed by the PEER Center (Goulet et al. 2007, Haselton et al. 2008), and has been studied in detail as part of that project.

Buildings B and C consist of three-bay frame that were designed as part of both the ATC-63 project (ATC 2008) and a recent doctoral dissertation by Haselton (2006). These designs were reviewed by a practicing engineer as part of the ATC-63 project.

Building D is a more generic structure wall that was designed for a recent doctoral dissertation by Zareian (2006).

3.2.2 Structural Modeling

The models for Buildings A, B, and C were developed by Haselton (Haselton 2006, ATC 2008) using the OpenSees platform (OpenSees 2007), and the model for Building D was developed by Zareian (2006) using the Drain-2DX platform (Prakash 1993). The frame and wall models both employ the element model recently developed by Ibarra, Medina, and Krawinkler (2005), which was implemented into Drain-2DX by the developers, and implemented into OpenSees by Altoontash (2004). Figure 3.1 shows the monotonic behavior and the cyclic behavior of the model. This model is capable of capturing the important behavior from yield up to collapse of the structure, specifically including both *in-cycle* strength degradation (which accounts for effects of rebar buckling and other modes of rapid strength loss, and is shown by the negative slope in Fig. 3.1a–b) and *between-cycle*, or "*cyclic*" deterioration (the strength loss shown between cycles in Fig. 3.1b). In this study, "collapse" is used to describe side-sway collapse, in which the building becomes dynamically unstable, and the displacements increase without bounds.

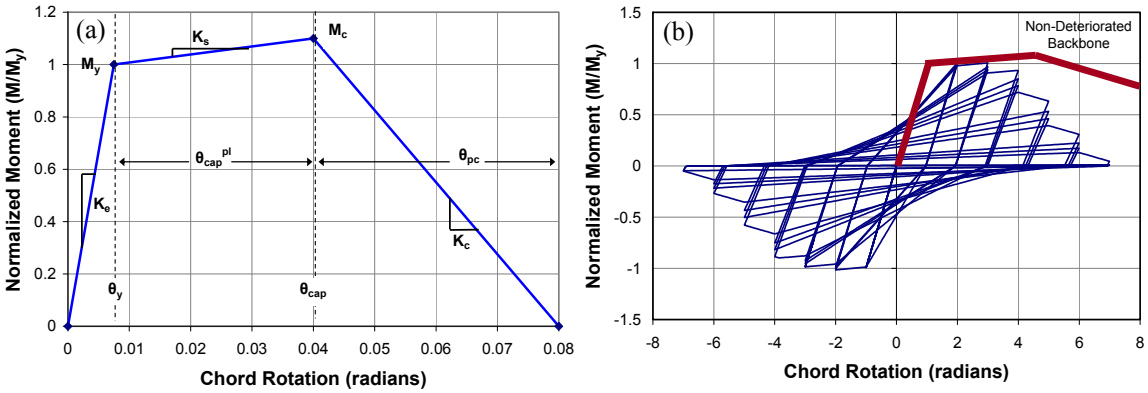

Fig. 3.1 Monotonic and cyclic behavior of component model used in this study. Element model and hysteretic rules were developed by Ibarra, Medina, and Krawinkler; figure after Haselton and Deierlein (2007, Chapter 4).

To create the models for the beams and columns of the RC frame structures, the above element model was carefully calibrated to results of over 250 experimental tests (Haselton and Liel et al. 2008). Figure 3.2 shows an example comparison between experimental and calibrated response (for one of the tests that shows a negative post-capping stiffness in the experimental response).

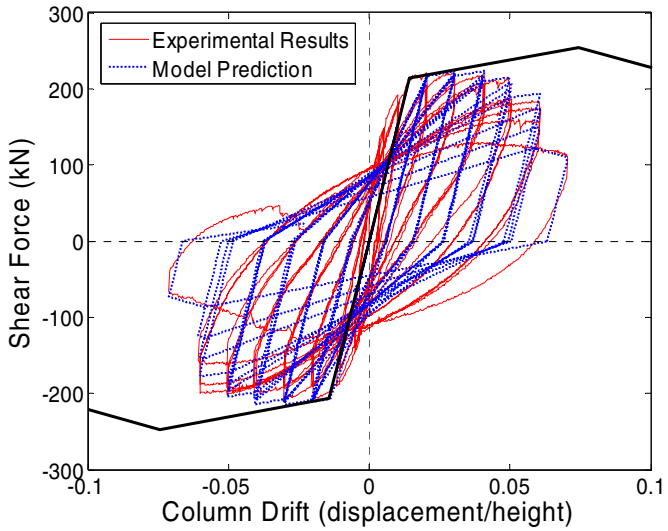

Fig. 3.2 Example calibration of monotonic and cyclic behavior of frame element model used in this study. Figure after Haselton and Liel et al. (2008).

Figure 3.3 presents the static pushover curves for Buildings A, B, C, and D. These pushover curves show base shear versus roof drift ratio, and are based on use of the lateral load distribution from the equivalent static procedure of ASCE7-02 (ASCE 2002). These pushover curves clearly show the capability of each model to "cap" and loose strength through a negative system-level stiffness. This structural modeling capability is necessary to accurately predict highly nonlinear response.

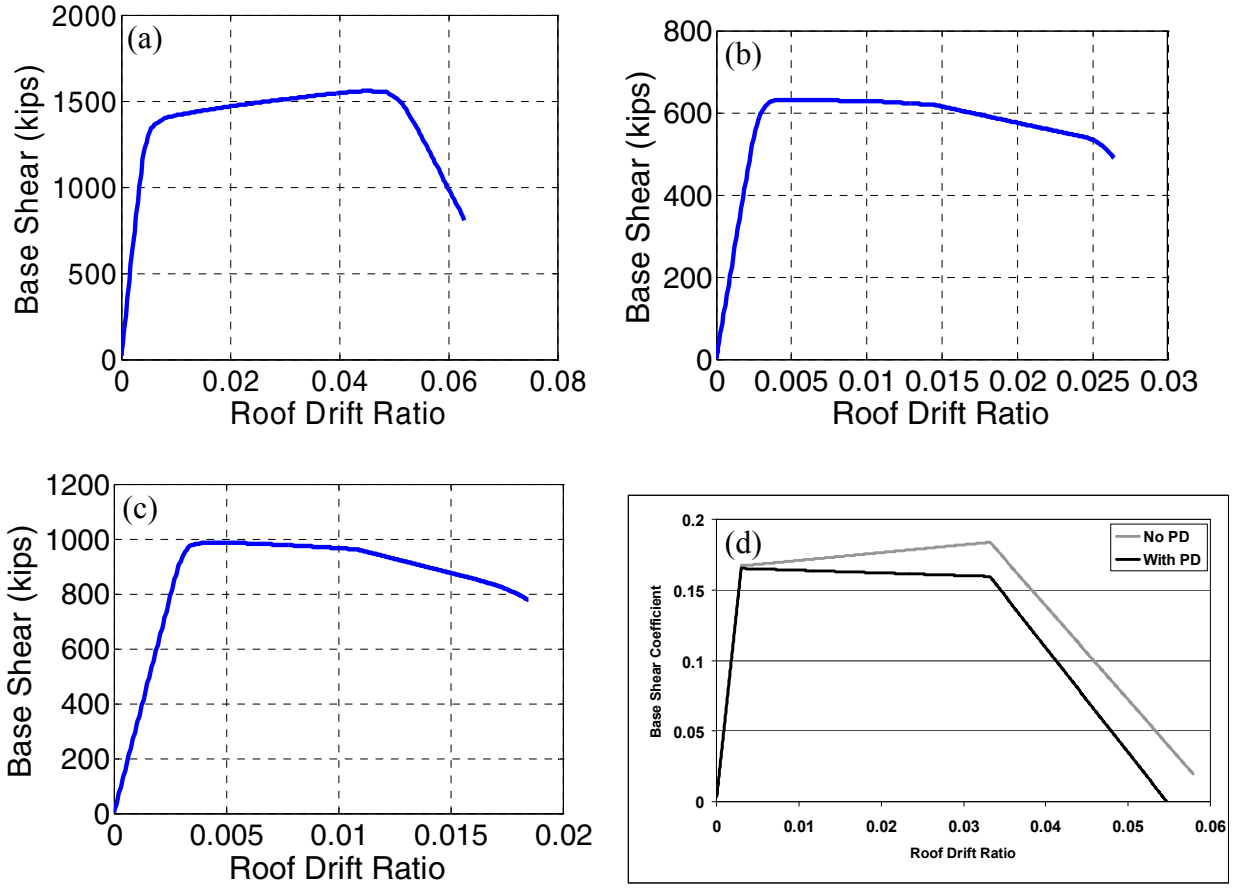

Fig. 3.3 Static pushover curves for Buildings A, B, C, and D, respectively, using lateral load distribution from ASCE7-05 (ASCE 2005). Relative to ASCE7-02 design levels (seismic design category D, S_1 = 0.6g, soil type D), static overstrength values of Buildings A–C are 2.3, 1.7, and 1.6, respectively.

Figure 3.4 shows the collapse modes for Building A (if the ground motion level is increased to be large enough to cause structural collapse, which is not the case for most of the analyses done as part of this study). This figure is shown to illustrate the capability of the structural model to directly simulate response up to collapse; all structural models used in this study have this capability. For this study, a building is said to have collapsed if dynamic instability occurs, causing the interstory drifts to increase without bounds; practically, collapse is said to have occurred if the interstory drift exceeds 15%.

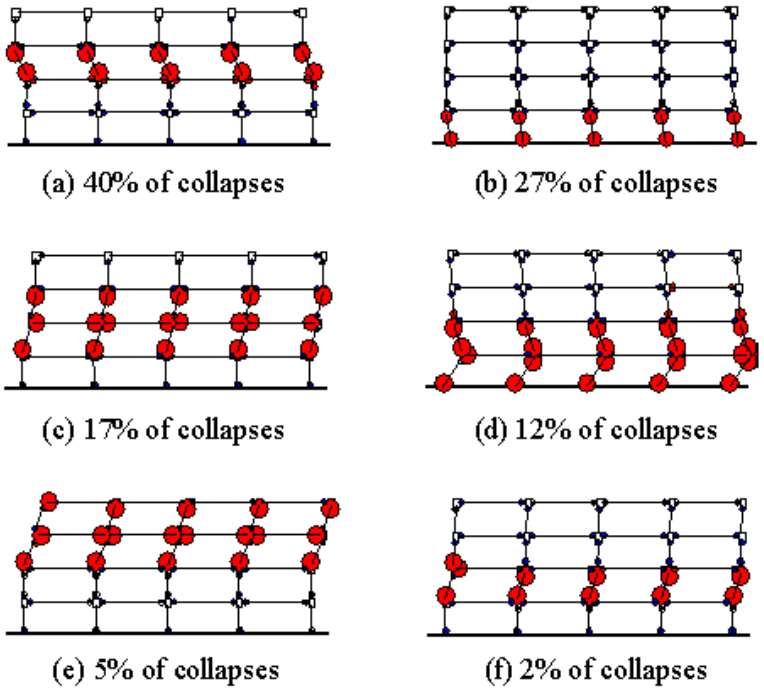

Fig. 3.4 Collapse modes of Building A, to illustrate behavior and capabilities of analytical model. After Goulet et al. (2007).

Further documentation of the structural modeling can be found in the dissertations, papers, and reports which discuss these models (Ibarra et al. 2005; Goulet et al. 2007; Haselton 2006; Haselton and Liel et al. 2008; and Zareian 2006).

3.3 GROUND MOTION SCENARIOS — M7 AND M7.5

For purposes of selecting sets of ground motions and comparing the structural response predictions, two target ground motion scenarios were developed, as follows:

- M7 scenario: A M7.0 earthquake occurring on a strike-slip fault, at a site that is 10 km from the fault rupture on soil with Vs,30 of 400 m/s (shear wave velocity for the top 30 m of the soil profile). The ground motion for this scenario is also constrained to have a spectral acceleration demand at the building's first-mode Sa(T1) that is two standard deviations above the median predicted value (using the Campbell and Bozorgnia 2008

attenuation model). This type of ground motion event is also often referred to as a "+2ε motion." This scenario is used for Buildings A, B, C, and D.

- M7.5 scenario: This is the same as the M7 scenario but is a M7.5 event, and the ground motion has an Sa(T1) value that is only one standard deviation above the median predicted value (i.e., a "+1ε motion"). This scenario is used only for Building C, for purposes of comparison to the results from the M7 scenario.

These two ground motion scenarios were selected carefully to be consistent with typical 2% in 50-year motions and maximum considered earthquake (MCE) ground motions used in current building code provisions (ASCE 2005) for high seismic sites in California. These "+ε motion" scenarios were selected because 2%-in-50-year and MCE ground motions have Sa values that are larger than the median Sa associated with the controlling scenario event (thus being "+ε motions"). Haselton (Haselton et al. 2008; ATC 2008) used the full set of United States Geological Survey (USGS) deaggregation data (Harmsen et al. 2001) and showed that the average ε value is 1.35 for a 2%-in 50-year motion at high seismic California sites, with some sites reaching up to ε = 2.0. Additionally, GMSM group member experience from site-specific hazard analyses have shown that these ε levels, or higher, are common for 2%-in-50-year or MCE motions in California. Additionally, in some regions the MCE level is governed by a deterministic cap of one standard deviation above the median spectral acceleration from a characteristic event, so in this case an ε = 1.0 motion is appropriate. The M7 and M7.5 scenarios were chosen to represent this range of ε values from 1.0 to 2.0.

Figure 3.5 shows the median spectra for the M7 and M7.5 scenarios, as well as the +ε demands for each building (at the fundamental period of the respective building). Figure 3.5a shows this for the M7 scenario, with the associated +2ε demands for all buildings, and Figure 3.1b shows this for the M7.5 scenario, with the associated +1ε demand for only Building C (because the M7.5 scenario is only used for Building C).

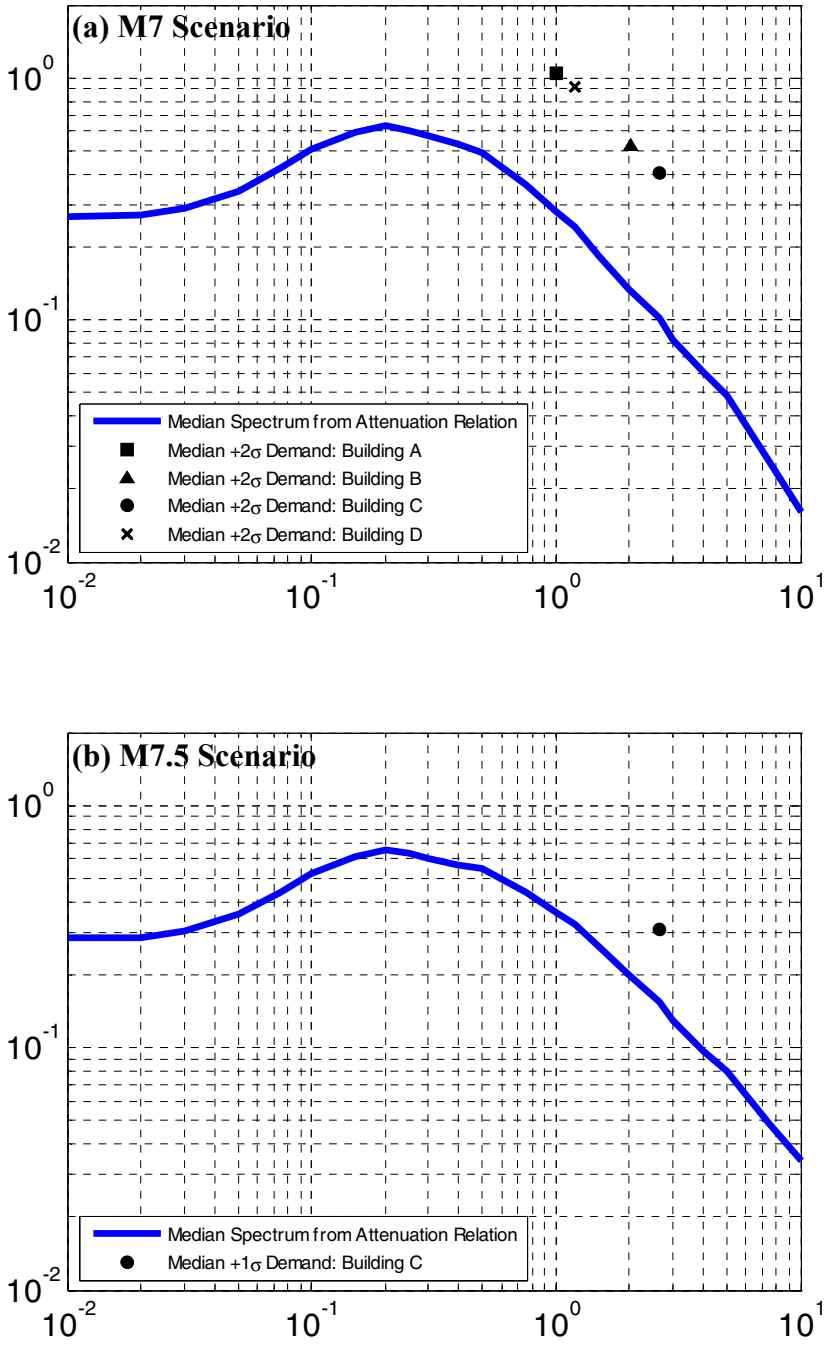

Fig. 3.5 Median expected acceleration spectra (from Campbell and Bozorgnia 2008 model) and median + 1-2σ demands consistent with ground motion scenarios, for (a) M7 scenario and (b) M7.5 scenario.

3.3.1 Application of Ground Motion Scenarios to Evaluate Inelastic-Based Methods

It should be noted that these ground motion scenarios are defined based on site and source parameters, as well as *elastic spectral acceleration* values. This presents a fundamental difficulty for inelastic GMSM methods because inelastic methods do not use elastic spectral values to quantify the ground motion intensity. This requires the inelastic-based methods to include some type of mapping that relates the defined elastic spectral values to the inelastic spectral values that are needed as input to the inelastic-based methods. The later chapters suggest that this step is problematic, and may have caused some of the resulting prediction inaccuracies of the inelastic-based methods.

3.4 OBJECTIVE OF NONLINEAR DYNAMIC ANALYSIS

Chapter 2 (Section 2.2) discusses some of the common objectives of nonlinear dynamic analysis. This report focuses on predicting the maximum interstory drift response (MIDR), which is the maximum interstory drift value for any story over the height of the building. Other structural responses were recorded and archived during the structural analyses, for use in later studies, but the expressed goal for this study is the prediction of MIDR response. Future studies may consider other response parameters.

We additionally narrowed the scope of this study to prediction of the *median* MIDR response, as opposed to the full distribution of response. Therefore, this report focuses on Objective 4, as discussed earlier in Section 2.2.4. This decision was made because results of the preliminary pilot studies (2006 COSMOS annual meeting) clearly showed that accurate prediction of even the median is difficult, so we decided to be sure that "we can walk before we try to run." Predicting the full distribution of response is a topic that we recommend for future study because it an important topic and is the natural next step beyond this current study.

The next question is related to the number of ground motions desired to achieve the prediction of the median MIDR. The decision was made to use sets of seven ground motions, because this is consistent with the current requirements of the ASCE 7-05 building code (ASCE 2005). For each GMSM method, we requested four independent sets of seven ground motions. This was done (a) to allow comparison between the median values of each set in order to

understand the consistency in the median prediction and (b) to allow use of a combined set of 28 records in order to compute a more stable estimate of the median response.

In summary, when comparing the GMSM methods considered in this study, the goal of the nonlinear dynamic analysis is to predict the *median MIDR* response using a set of *seven* ground motions. In this study, the various GMSM methods are judged based on their ability to predict this response consistently and accurately for the four structures and two ground motion scenarios that are used as test beds in this study.

3.5 COMPARISON TO POINT OF COMPARISON (ALSO TERMED HIGH-END PREDICTION)

The previous sections discussed the fact that we are comparing median structural response predictions (maximum interstory drift ratio) using five test-bed cases. However, if the goal is to determine which GMSM methods produce accurate and precise predictions of structural response, simple comparisons are not enough; we must have some estimate of the true response, which we can compare against.

Chapters 4 and 5 present the methodology to create the prediction of the true response. We do not claim that this is the absolute truth (since knowing the absolute truth would require that we have perfect knowledge of what will happen in future seismic events), but we rather claim that this is the best possible prediction given the ground motion data available and given the current level of knowledge in seismology and structural engineering. Accordingly, we do not call this the true response but rather term it the point-of-comparison (POC) or the high-end prediction (HEP). Creating the POC prediction of MIDR for a specific building involves:

(a) selecting a large ground motion bin for the ground motion scenario of interest (98 records for the M7 scenario and 192 for the M7.5 scenario),

(b) completing structural analyses using the ground motions scaled by factors of 1, 2, 4, and 8,

(c) carefully creating an empirical regression equation relating the structural response (MIDR) to important ground motion parameters (e.g., $Sa(T_1)$, $Sa(2T_1)$, etc.), and then

(d) integrating the MIDR regression equation over the proper distributions of the ground motion parameters (using dispersion estimates from PEER-NGA attenuation models) do obtain the median estimate of MIDR response (note that his also provides an estimate of

the variability of MIDR, but that is not utilized in this current study because this study is focused on the median response).

Chapters 4 and 5 present a detailed description of the methodology used to create the POC predictions. Chapter 4 first presents the basic POC methodology, and provides preliminary POC values. Chapter 5 builds upon Chapter 4 and looks more deeply at questions regarding how collapse cases should be treated, as well as questions regarding the function form and appropriate parameters for use in the regression models. For later studies that employ this POC methodology, the modifications suggested in Chapter 5 should be included with the methodology of Chapter 4.

For purposes of this study, the results of Chapter 4 are the values used in the later comparisons of GMSM methods contained in Chapters 6–11. The updated POC results of Chapter 5 were not used in the later chapters because a *blind POC prediction was desired*, and the Chapter 5 work was completed *after* the structural analysis results were compiled for Chapters 6–11. Even so, the preferred POC values from Chapter 5 do not vary widely from those of Chapter 4, so this decision would not affect the conclusions of this report.

3.6 SUMMARY

The goal of this study is to complete an objective evaluation of many of the GMSM methods available in the literature, and use this to provide guidance regarding which methods can be used to obtain accurate and precise predictions of structural response. This study focuses on predicting the median value of the maximum interstory drift ratio (MIDR) using a set of seven ground motions. To compare GMSM methods, test-bed cases are utilized; these include four structures (ranging from 4-20 stories, and including RC frames and a shear wall) along with two ground motion scenarios (M7 with $\varepsilon = 2.0$, and M7.5 with $\varepsilon = 1.0$). To determine which predictions are most accurate, the point-of-comparison (or high-end prediction) value is developed (which involves a great deal of effort), and used as a yardstick to judge the predictions from the various methods. The methods that consistently provide predictions close to the POC (or HEP) are then recommended for use so that highly accurate predictions can be obtained with a reasonable amount of effort (i.e., without needing to develop a POC, which is very time consuming).

4 Point of Comparison

Author: J. Watson-Lamprey

4.1 INTRODUCTION

In order to evaluate the prediction accuracy of various GMSM methods, we must establish an estimate of the true response. To highlight the fact that our data and knowledge of ground motion behavior is limited and that we will never know the true response, this prediction is termed the point-of-comparison (POC) or, alternatively, the high-end prediction. This current report focuses solely on the prediction of *median* structural response, but the goal of the POC prediction is to predict both median and variability, since future studies may investigate prediction of the full distribution of response. Consistent with the scope of this report, this chapter focuses on predicting the median value of the interstory drift ratio for the most damaged story (median MIDR), though this POC method is generally applicable to any structural response parameter.

This chapter presents the methodology used for this POC prediction, and Chapter 5 includes evaluation and additional complexity applied to the methodology described in this chapter. For example, this chapter does not explicitly include consideration of structural collapse for all cases; this is addressed in Chapter 5. For the specific modern structures used in this report, collapse cases have virtually no effect on the POC prediction.

In order to estimate the true response (termed the POC prediction), the first, simplest method would be to compile a large number of unscaled ground motion records that are consistent with the magnitude, distance, soil conditions, and spectral acceleration of interest, use these records for structural analyses, and then compute the median interstory drift response of the structure. Unfortunately, this method is not an option because there are no records that match the

magnitude, distance, and the desired ground motion for the ground motion scenarios utilized in this study. Therefore, we must consider other options for obtaining an approximate prediction of the POC. There are a number of other possible approaches to this.

The second option would be to calculate the POC using the results from a bin of records with *similar* magnitudes, distances, and spectral acceleration (ε) values. This option is appealing because it is conceptually clear and is similar to the simple solution outlined above. However, this is not possible because obtaining enough records would require that the ranges of the ground motion bin be very large. This would result in an inaccurate response prediction, so this option was rejected.

A third option would be to calculate the POC value using the bin of records from option two, but correct (scale) the records to produce the proper variability at a single spectral value. This approach does not address the variability at other spectral values, which are also significant.

A fourth option is to expand the range of the ground motion bin, in order to utilize a large number of records in the structural analyses. Then, to develop an empirical regression model that predicts the structural response parameter (in this case, median MIDR) conditioned on the ground motion parameters. This regression model can then be used, integrated together with pre-existing models for the ground motion intensity measures, to calculate the distribution of the structural response parameter (in this case, median MIDR). This option does not suffer from the same drawbacks as the previous approaches, and this is the method utilized in this chapter.

In summary, the approach to obtaining the POC prediction consists of the following steps. This approach provides a useful comparison by which to evaluate the other GMSM method considered in this study, since it is considered to provide a precise estimate of the distribution of MIDR under the ground motion scenarios of interest in this study.

1. Perform structural analysis using a large number of representative ground motions both scaled and unscaled, and record the response parameter of interest (e.g., maximum interstory drift ratio, or *MIDR*) from each analysis, along with all relevant properties of each input ground motion (e.g., spectral acceleration values at periods of interest).
2. Use regression analysis to create a predictive equation that relates the ground motion properties to the observed structural responses.

3. Use ground motion prediction equations (along with correlation models) to predict the distribution of ground motion properties that will occur during the scenario earthquake of interest.
4. Evaluate the regression equation over the predicted distribution of ground motion properties, to compute the distribution of structural response.

4.2 EQUATIONS FOR CALCULATING DISTRIBUTION OF AN EDP

The probability of a structural response parameter, also termed an engineering demand parameter (*EDP*), exceeding some value *edp* given the earthquake scenario can be written as follows, where *Eqk* represents the given magnitude, distance, soil type, and style-of-faulting.

$$P(EDP > edp \mid Eqk) \tag{4.1}$$

All that is necessary to complete the evaluation is an estimate of the distribution of *EDP* given *Eqk*. Such estimates can be obtained for ground motion intensity measures using ground motion prediction equations, but there are no such estimates available for most structures. Ground motion prediction equations employ seismological principles to guide selection of a functional form and to extrapolate to large magnitudes and close distances where there are few records and the results are of engineering significance. No equivalent set of principles exist for structures, thus for the rare ground motions that are of the greatest engineering significance the uncertainties in such an equation would be large.

Instead, we rely on the more stable relationship between *EDP*s and ground motion intensity measures to obtain the distribution of response. If we use one ground motion intensity measure (*IM*) to model the *EDP,* we can evaluate the probability of *EDP* exceeding some value *edp* through the following equation.

$$P\left(EDP > edp \mid Eqk\right) = \int_0^\infty f_X\left(x \mid Eqk\right) P\left(EDP > edp \mid x\right) dx \tag{4.2}$$

where x is an *IM*, and f is the probability density function of *x* given *Eqk*. More commonly, the EDP is a function of multiple ground motion intensity measures. For the case of two intensity measures, X and Y, the equation becomes the following.

$$P\left(EDP > edp \mid Eqk\right) = \int_0^\infty \int_0^\infty f_{X,Y}\left(x, y \mid Eqk\right) P\left(EDP > edp \mid x, y\right) dxdy \tag{4.3}$$

Using conditional probabilities, the following is true.

$$f_{X,Y}(x,y \mid Eqk) = f_X(x \mid Eqk) f_{Y|X}(y \mid Eqk, x) \tag{4.4}$$

Combining the above equations, the final equation is as follows.

$$P(EDP > edp \mid Eqk) = \int_0^\infty \int_0^\infty f_X(x \mid Eqk) f_{Y|X}(y \mid Eqk, x) P(EDP > edp \mid x, y) dxdy \tag{4.5}$$

Extrapolating further for the case of three intensity measures, the following equation can be used.

$$P(EDP > edp \mid Eqk) = \int_0^\infty \int_0^\infty \int_0^\infty f_{X,Y,Z}(x,y,z \mid Eqk) P(EDP > edp \mid x,y,z) dxdydz \tag{4.6}$$

Again, using conditional probabilities, the following is true.

$$f_{X,Y,Z}(x,y,z \mid Eqk) = f_{X,Y}(x,y \mid Eqk) f_{Z|X,Y}(z \mid Eqk, x, y) \tag{4.7}$$

Combining the above equations, the final equation is shown as follows.

$$P(EDP > edp \mid Eqk) = \int_0^\infty \int_0^\infty \int_0^\infty f_X(x \mid Eqk) f_{Y|X}(y \mid Eqk, x) f_{Z|X,Y}(z \mid Eqk, x, y) P(EDP > edp \mid x,y,z) dxdydz \tag{4.8}$$

The *IM*s are commonly log-normally distributed, therefore, it is more convenient to evaluate this integral using the standard normal distribution instead of the log-normal distribution. Making this modification, we normalize the ground motion intensity measure distributions and the equation for calculating the probability of an EDP exceeding some value *edp*, as follows.

$$P(EDP > edp \mid Eqk) = \int_{-\infty}^\infty \int_{-\infty}^\infty \int_{-\infty}^\infty f_{\varepsilon_x}(e_x) f_{\varepsilon_{y|x}}(e_{y|x}) f_{\varepsilon_{z|x,y}}(e_{z|x,y}) P(EDP > edp \mid x,y,z) de_x de_{y|x} de_{z|x,y} \tag{4.9}$$

where f is the standard normal probability distribution. The ground motion parameters are defined through equations of the following form.

$$\ln x = \overline{\ln x \mid Eqk} + \varepsilon_x \sigma_x \tag{4.10}$$

where $\overline{\ln x \mid Eqk}$ is the mean ln*x* given *Eqk*, and σ_x is the standard deviation of ln*x* from a ground motion prediction equation.

$$\ln y \mid x = \overline{\ln y \mid Eqk, x} + \varepsilon_{y|x} \sigma_{y|x} \tag{4.11}$$

$$\overline{\ln y \mid Eqk, x} = \overline{\ln y \mid Eqk} + \rho_{x,y} \varepsilon_x \sigma_y \tag{4.12}$$

$$\sigma_{y|x} = \sqrt{1-\rho_{x,y}^2}\,\sigma_y \tag{4.13}$$

$$\rho_{x,y}^2 = \frac{\left(\sum \ln x \ln y - n\overline{\ln x}\,\overline{\ln y}\right)^2}{\left(\ln x^2 - n\overline{\ln x}^2\right)\left(\ln y^2 - n\overline{\ln y}^2\right)} \tag{4.14}$$

$$\ln z \mid x, y = \overline{\ln z \mid Eqk, x, y} + \varepsilon_{z|x,y}\sigma_{z|x,y} \tag{4.15}$$

$$\overline{\ln z \mid Eqk, x, y} = \overline{\ln z \mid Eqk} + \rho_{x,z}\varepsilon_x\sigma_z + \rho_{y|x,z}\varepsilon_{y|x}\sigma_z \tag{4.16}$$

$$\sigma_{z|x,y} = \sqrt{1-\rho_{x,z}^2}\sqrt{1-\rho_{y|x,z}^2}\,\sigma_z \tag{4.17}$$

$$\rho_{y|x,z}^2 = \frac{\left(\sum \ln y \mid x \ln z - n\overline{\ln y \mid x}\,\overline{\ln z}\right)^2}{\left(\ln y \mid x^2 - n\overline{\ln y \mid x}^2\right)\left(\ln z^2 - n\overline{\ln z}^2\right)} \tag{4.18}$$

where the ε and σ are total ε and total σ. The total σ is calculated from the intra-event σ and interevent σ using the following equation.

$$\sigma_{x,T}^2 = \sigma_x^2 + \tau_x^2 \tag{4.19}$$

where σ is the intra-event standard deviation, and τ is the interevent standard deviation.

The total correlation coefficient should not be calculated from the total residuals. The total residuals are not normally distributed and this procedure will provide incorrect results. To calculate the total correlation coefficient we use the following equation.

$$\rho_{\varepsilon_{x,T},\varepsilon_{y,T}}^2\sigma_{x,T}\sigma_{y,T} = \rho_{\varepsilon_x,\varepsilon_y}^2\sigma_x\sigma_y + \rho_{\eta_x,\eta_y}^2\tau_x\tau_y \tag{4.20}$$

where ε is the intra-event normalized residual and η is the interevent normalized residual.

To evaluate the integral it is more convenient to discretize the ε values as follows.

$$P\left(EDP > edp \mid Eqk\right) = \sum_{\varepsilon_{x,i}=-\infty}^{\infty}\sum_{\varepsilon_{y|x,j}=-\infty}^{\infty}\sum_{\varepsilon_{z|x,y,k}=-\infty}^{\infty} p_{\varepsilon_x}\left(e_{x,i}\right)p_{\varepsilon_{y|x}}\left(e_{y|x,j}\right)p_{\varepsilon_{z|x,y}}\left(e_{z|x,y,k}\right)P\left(EDP > edp \mid x_i, y_j, z_k\right) \tag{4.21}$$

where

$$p_\varepsilon\left(e_l\right) = P\left(\frac{e_l + e_{l-1}}{2} < e < \frac{e_{l+1} + e_l}{2}\right) \tag{4.22}$$

We recall that ε has the standard normal distribution so we can evaluate this using the following equation.

$$p_{\varepsilon}(e_l) = \Phi\left(\frac{e_l + e_{l-1}}{2}\right) - \Phi\left(\frac{e_{l+1} + e_l}{2}\right) \tag{4.23}$$

All that remains is to evaluate the probability of *EDP* greater than some value *edp*.

The probability density function of the response is bi-modal, with one part containing the probability of collapse, and the second a log-normal distribution of *EDP* values. The probability of an *EDP* being greater than some value *edp* is then the probability that the structure has collapsed, and the probability of *EDP* greater than *edp* given that the structure has not collapsed. We write this as follows.

$$\begin{aligned} &P(EDP > edp \mid x,y,z) = \\ &\quad P(collapse \mid x,y,z) + P(EDP > edp \mid x,y,z,no\,collapse)P(no\,collapse \mid x,y,z) \end{aligned} \tag{4.24}$$

The probability of the collapse and non-collapse states is one. We can re-write the equation

$$\begin{aligned} &P(EDP > edp \mid x,y,z) = \\ &\quad P(collapse \mid x,y,z) + P(EDP > edp \mid x,y,z,no\,collapse)(1 - P(collapse \mid x,y,z)) \end{aligned} \tag{4.25}$$

We estimate the probability of collapse by performing a maximum-likelihood regression using the results of the nonlinear structural model.

We can evaluate the probability of *EDP* being greater than *edp* given no collapse by noting that ln*EDP* is normally distributed.

$$P(EDP > edp \mid x,y,z,no\ collapse) = 1 - \Phi\left(\frac{\overline{\ln EDP \mid x,y,z,no\ collapse} - \ln edp}{\sigma_{\ln EDP \mid x,y,z,no\ collapse}}\right) \tag{4.26}$$

To evaluate the previous equation, the estimates are needed for the mean of ln*EDP* and the standard deviation of ln*EDP* given *x*, *y, z*. These estimates are obtained by performing nonlinear dynamic structural analyses using the large bin of ground motions and then performing a regression on the *EDP* values for all of the non-collapse cases.

This procedure results in a distribution of *EDP* for an earthquake of a given magnitude, distance, etc., but we are also interested in defining the distribution of an *EDP* given a defined ground motion intensity measure. To reflect this conditioning on a given value of a ground motion intensity measure, the following equation is used, which is similar to Equation (4.21) but where the summation over the ground motion intensity measure is removed.

$$P\left(EDP > edp \mid Eqk, x\right) = \sum_{\varepsilon_{y|x,j}=-\infty}^{\infty} \sum_{\varepsilon_{z|x,y,k}=-\infty}^{\infty} p_{\varepsilon_{y|x}}\left(e_{y|x,j}\right) p_{\varepsilon_{z|x,y}}\left(e_{z|x,y,k}\right) P\left(EDP > edp \mid x_i, y_j, z_k\right) \quad (4.27)$$

The above equation is evaluated in the same way as Equation (4.21). The final POC value is the median *edp* from the distribution calculated using Equation (4.28).

4.3 STRUCTURAL ANALYSIS

For the M7 scenario, we are interested in the nonlinear response of the structure for a M7.0 strike-slip earthquake that occurs 10 km from our site, and where the ground motion has $\varepsilon(T_1) = +2.0$. To accurately estimate the mean and variability of ln*EDP* for this scenario, we must select records that span the range of significant ground motion intensity measures. The task is complicated by the fact that the most significant ground motion intensity measures are unknown before performing the structural analyses and interpreting the structural response predictions. We know from prior studies that spectral acceleration values at the modal periods of the structure will be important for predicting the interstory drift response. We also know that magnitude and distance may have some effect on response because they have an effect on many ground motion intensity measures. We thus select a suite of records with 6.75 < magnitude < 7.25 and distance < 20 km (98 time series in all) from which to begin our analyses. The ground motion records selected can be found in Appendix D. We additionally scale these records by factors of 1, 2, 4, and 8 to ensure that large spectral acceleration values are captured. Much previous research has shown that such large upward scaling can lead to biased structural response predictions, but this is accounted for in the later regression analyses that are preformed on the resulting structural response data. We will specifically examine the validity of this upward scaling in a later section.

The scaled ground motions are then used to perform nonlinear dynamic structural analyses, and the desired engineering demand parameter are recorded for each ground motion. These results are then used, along with the ground motion intensity measures, to develop a regression model of the *EDP* as a function of the *IM*s. Appendix D includes the MIDR responses utilized to create the POC predictions, and Appendix C provides full documentation of a larger number of EDPs (including MIDR, but also many other EDPs) for each of the four buildings used in this study (Section C.7 and the electronic appendix files).

An additional analysis was performed for Building C using an expanded set of ground motions to develop a point-of-comparison prediction for the M7.5 scenario. Documentation of the expanded ground motion set (192 motions) can be found in Appendix D along with the MIDR values for the four buildings used in this study. Similarly to the M7 scenario, Appendix C includes documentation of a larger number of EDPs (Section C.8 and the electronic appendix files).

4.4 DEVELOPMENT OF FUNCTIONAL FORM FOR REGRESSION EQUATIONS THAT PREDICT EDP BASED ON GROUND MOTION INTENSITY MEASURES

A model of the *EDP* as a function of ground motion intensity is desired to capture the significant relationships between *EDP* and *IM*. The goal is to develop a model that is robust with regard to magnitude, distance, and scale factor. Prior research was used to guide selection of potentially significant *IM*s. This section provides an example of model development for Building A, which is a modern 4-story reinforced concrete frame structure (with a fundamental period of 1.0 sec).

We begin with a simple model of *EDP* as a function of spectral acceleration at the fundamental period of the structure. This relationship is demonstrated in Figure 4.1.

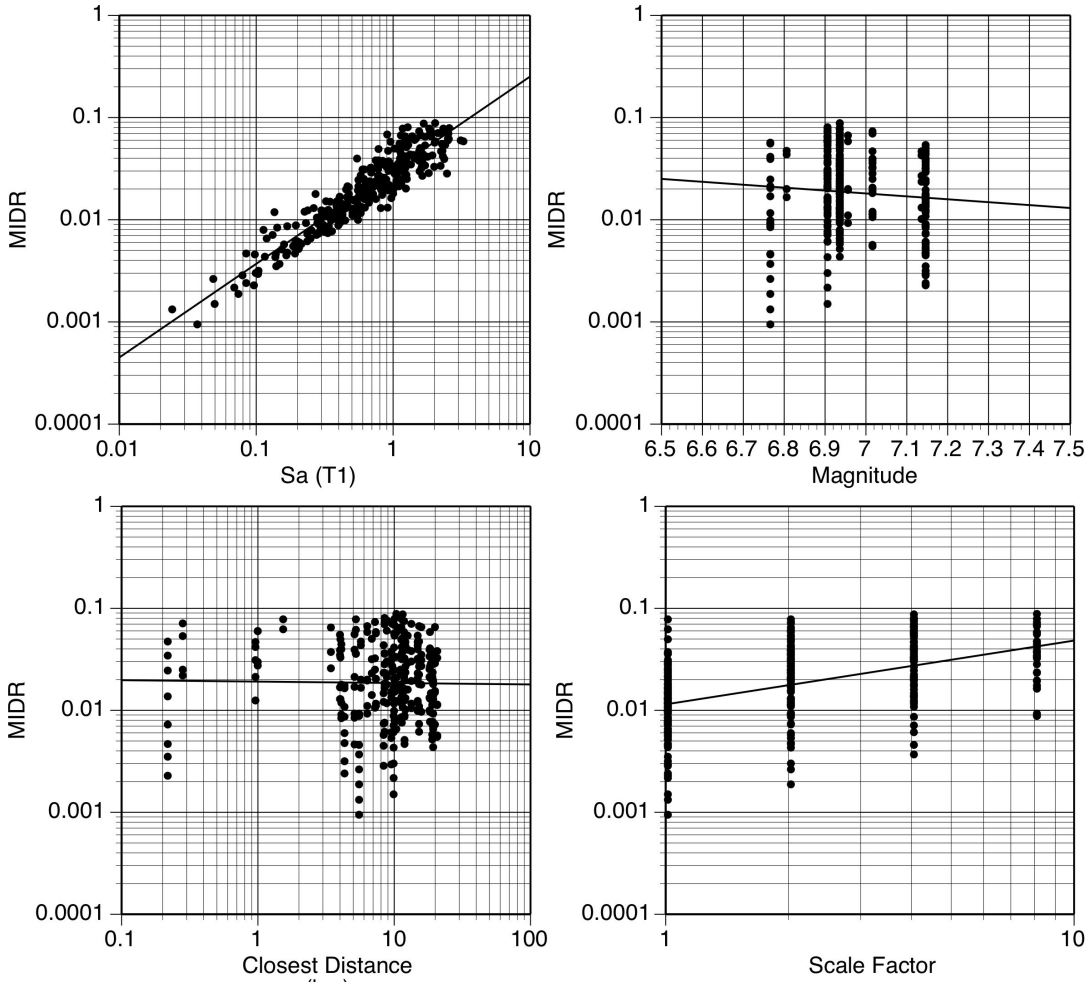

Fig. 4.1 Maximum interstory drift ratio as a function of spectral acceleration at fundamental period of structure. R^2 = 0.87.

We can see from Figure 4.1 that spectral acceleration at the fundamental period of the structure is indeed a strong predictor of our selected engineering demand parameter, with an R^2 value of 0.87. We fit a simple model to this relationship and use the residuals from the model to examine the predictive ability of spectral acceleration at two times the fundamental period of the structure. This relationship is demonstrated in Figure 4.2.

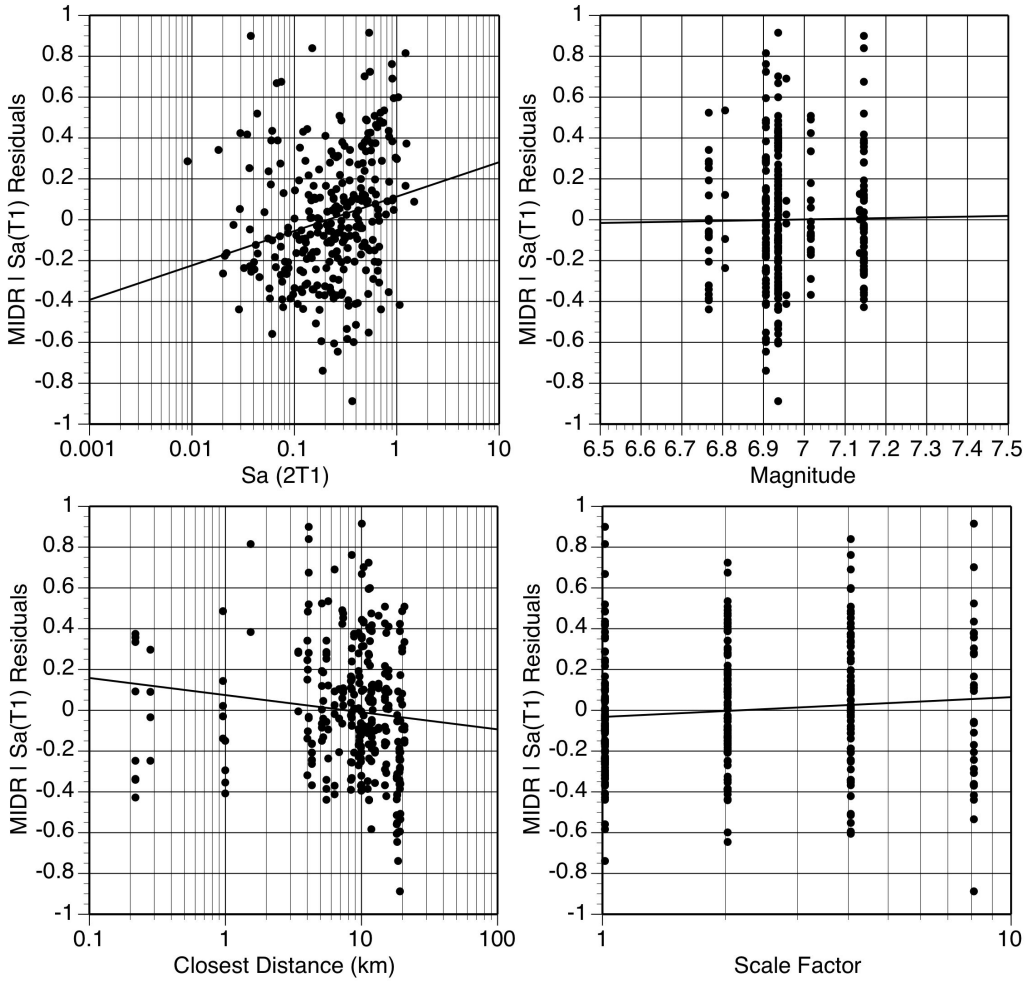

Fig. 4.2 Residuals of maximum interstory drift ratio as a function of spectral acceleration at fundamental period vs. spectral acceleration at two times fundamental period of structure. $R^2 = 0.048$.

We see that even given knowledge of spectral acceleration at the fundamental period, there is still a trend in the residuals with the spectral acceleration at twice the fundamental period. To account for this trend, we now fit a simple model of MIDR as a function of these two spectral accelerations, and examine the residuals to look for a possible dependence on spectral acceleration at the second1-mode period, as shown in Figure 4.3.

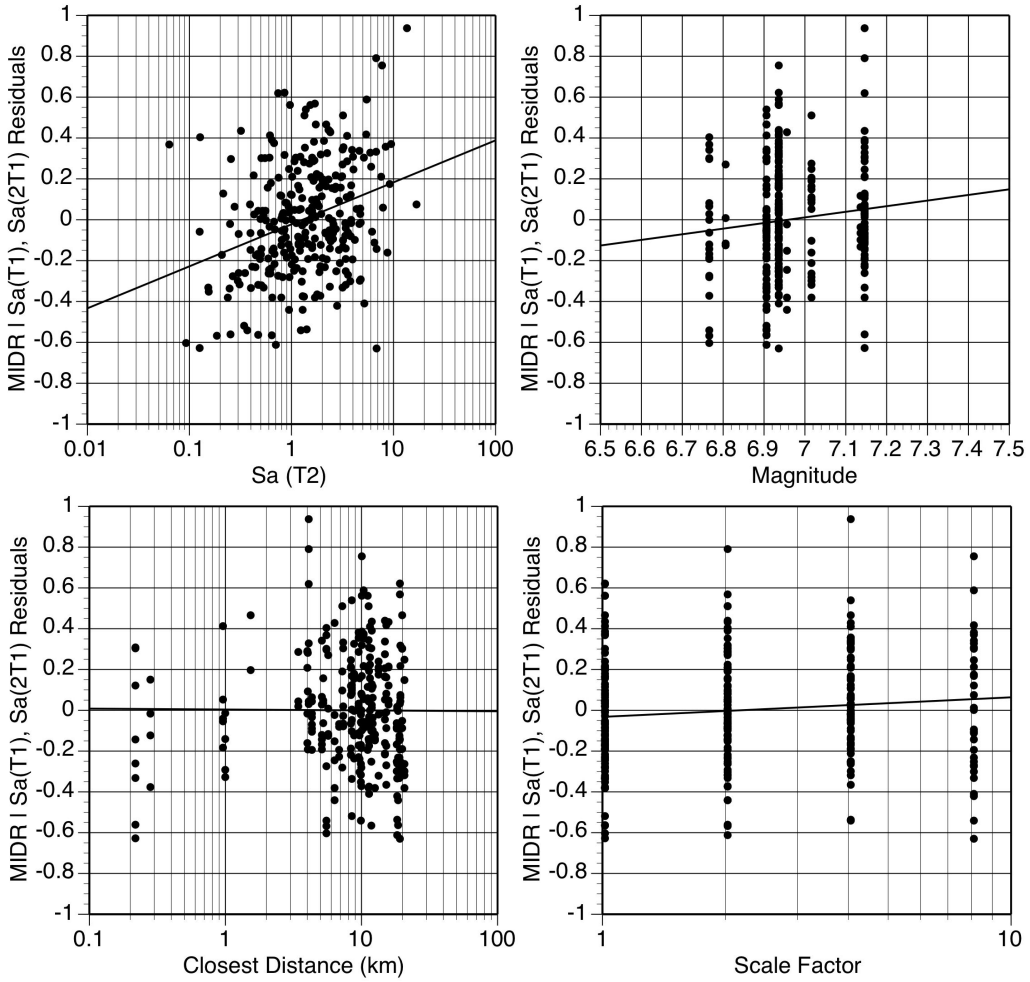

Fig. 4.3 Residuals of maximum interstory drift ratio as a function of spectral acceleration at fundamental period and two times fundamental period vs. spectral acceleration at second-mode period of structure. $R^2 = 0.090$.

A trend is apparent in the spectral acceleration values at the second-mode period, so accounting for the spectral acceleration at the second-mode period will improve the prediction of MIDR. We expand the simple regression model to include the second-mode period and look at the dependence of the residuals on spectral acceleration at the third-mode period and peak ground velocity in Figures 4.4 and 4.5. Additionally, Figure 4.6 checks trends between the residuals and magnitude, distance, and scale factor.

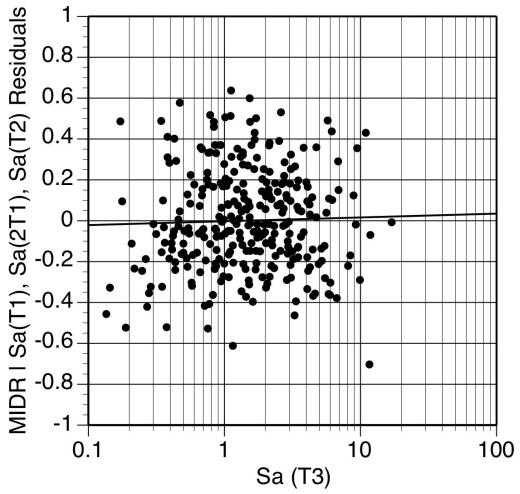

Fig. 4.4 Residuals of maximum interstory drift ratio as a function of spectral acceleration at fundamental period, two times fundamental period, and second-mode period vs. spectral acceleration at third-mode period of structure. R^2 = 0.00088.

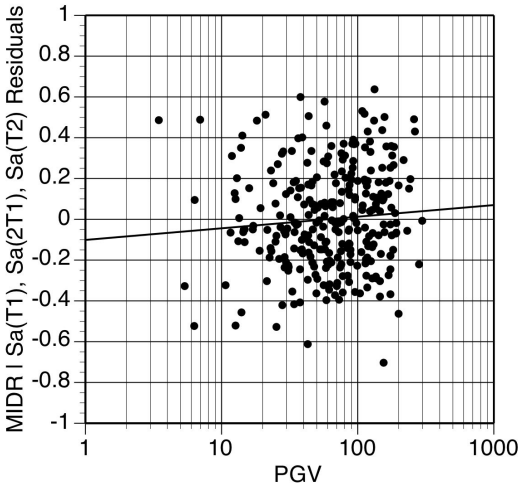

Fig. 4.5 Residuals of maximum interstory drift ratio as a function of spectral acceleration at fundamental period, two times fundamental period, and second-mode period vs. peak ground velocity. R^2 = 0.0065.

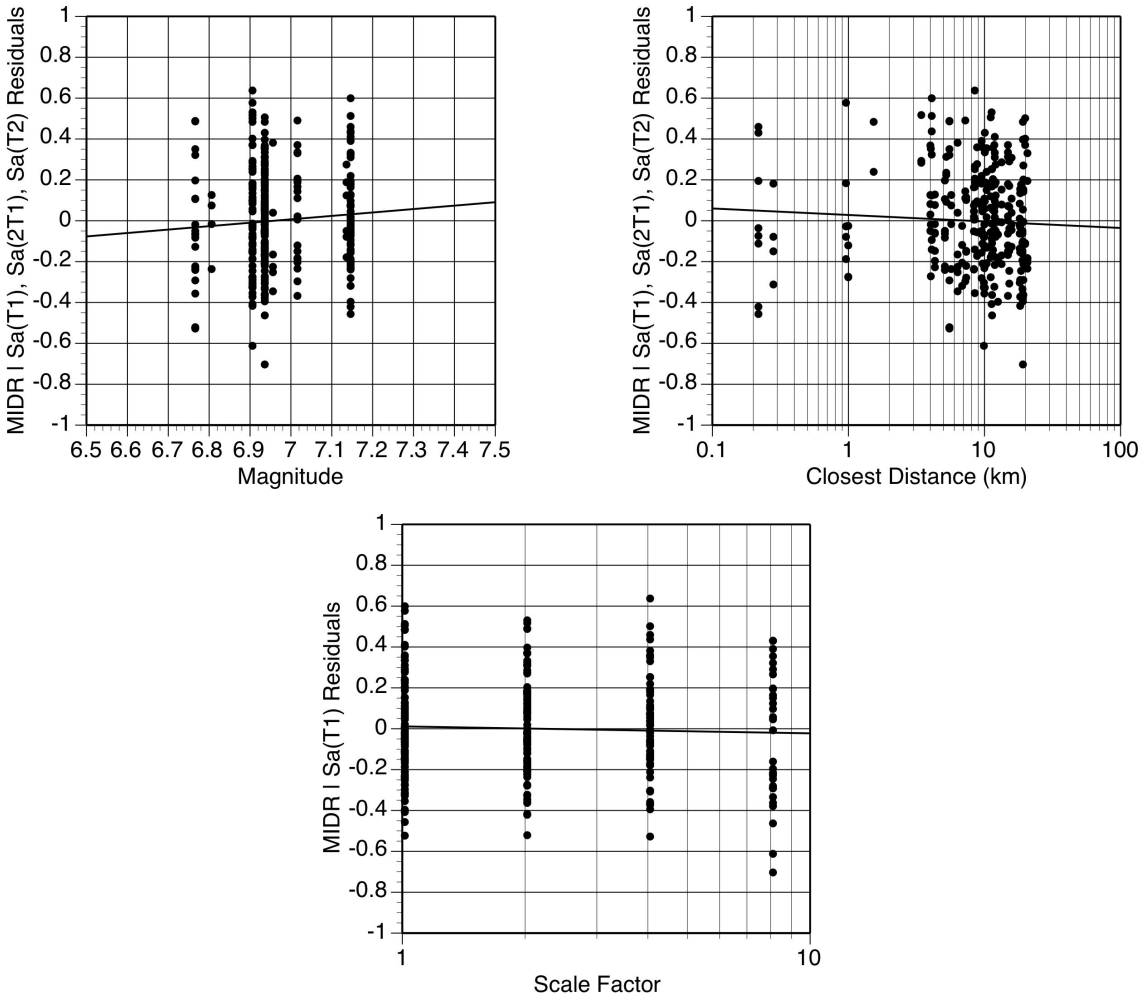

Fig. 4.6 Residuals of maximum interstory drift ratio as a function of spectral acceleration at fundamental period, two times fundamental period, and second-mode period vs. magnitude, distance, and scale factor.

Figures 4.4 and 4.5 show that there is a minor trend between the residuals and the Sa(T3) and the peak ground velocity. Both possible linear models have R^2 values of less than 0.01. Neither of these terms were included in the regression model because their effect was judged to be insignificant. Figure 4.6 similarly shows that the regression model is robust with respect to magnitude, distance, and scale factor.

4.5 SELECTED FUNCTIONAL FORM AND MODEL FITTING

Based on the results of the sensitivity analysis in the previous section, the following functional form was selected to model the *EDP*.

$$\ln EDP = b_1 + b_2 \ln Sa_{T1} + b_3 \ln Sa_{T1}^{\ 2} + b_4 \ln Sa_{2T1} + b_5 \ln Sa_{2T1}^{\ 2} + b_6 \ln Sa_{T2} + b_7 \ln Sa_{T2}^{\ 2} \qquad (4.28)$$

For the sake of expediency, this functional form was used for each of the four structures and the probability of collapse was assumed to be zero for all cases. Chapter 5 evaluates these simplifying assumptions by also looking at other possible parameters, functional forms, and collapse evaluations.

The regression models were fit using the standard least-squares approach. The spectral periods used for each of the four buildings are given in Table 4.1, and the resulting regression coefficients are given in Table 4.2.

Table 4.1 MIDR regression model spectral periods for Buildings A–C.

Period (sec)	A	B	C	D
T1	1.0	2.0	2.6	1.2
2T1	2.0	4.0	5.2	2.4
T2	0.4	0.7	0.85	0.2

Table 4.2 MIDR regression model coefficients for Buildings A–C.

Coefficient	A	B	C	D
$\mathbf{b_1}$	-2.93	-2.15	-2.00	-3.961
$\mathbf{b_2}$	0.304	0.277	0.236	0.376
$\mathbf{b_3}$	-0.111	-0.0470	-0.0353	-0.0846
$\mathbf{b_4}$	0.856	1.02	1.06	0.577
$\mathbf{b_5}$	0.158	0.131	0.128	0.0943
$\mathbf{b_6}$	0.224	0.363	0.387	0.134
$\mathbf{b_7}$	-0.0156	-0.00487	-0.0391	0.0259

An additional model was developed for Building C using an expanded set of ground motions to create a point of comparison for the M7.5 scenario. The resulting coefficients are presented in Table 4.3.

Table 4.3 Magnitude 7.5 MIDR regression model coefficients for Building C.

Coefficient	C
b_1	-1.63
b_2	0.162
b_3	-0.0692
b_4	1.39
b_5	0.185
b_6	0.338
b_7	-0.0394

The resulting regression model for Building A is shown in Figure 4.7, for a range of pseudo-spectral acceleration values.

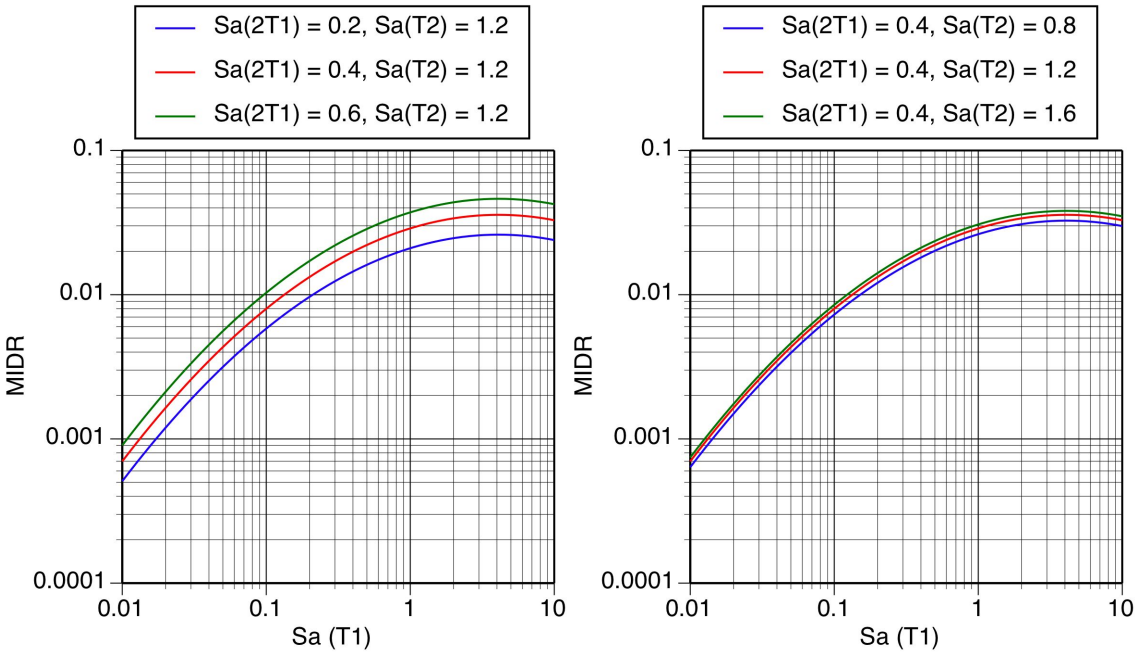

Fig. 4.7 Regression model to predict MIDR for Building A, under varying levels of spectral demand.

The regression models developed in this section are integrated with ground motion prediction equations, according to Section 4.2, in order to compute the final POC for the ground motion scenario of interest. This is discussed in the following section.

4.6 POINT OF COMPARISON (POC)

The point of comparison (POC) desired for use in this report is the median EDP given the occurrence of the M7 scenario or the M7.5 scenario (as defined in Section 3.3). This is computed by using Equation (4.28), and then computing the median of the resulting distribution. In order to evaluate Equation (4.28), the distribution EDP responses given ground motion parameters is required (i.e., the predictive equation from Section 4.5, along with the associated standard deviation of the residuals), as well as the distribution of those ground motion parameters. The specific ground motion parameters required are listed as follows.

$$\overline{\ln Sa(T_1)} \mid Eqk, \quad \overline{\ln Sa(2T_1)} \mid Eqk, \quad \overline{\ln Sa(T_2)} \mid Eqk$$

$$\sigma_{\ln Sa(T_1),T}, \quad \sigma_{\ln Sa(2T_1),T}, \quad \sigma_{\ln Sa(T_2),T}$$

$$\rho_{\varepsilon_{\ln Sa(T1),T},\ln Sa(2T1),T}, \quad \rho_{\varepsilon_{\ln Sa(T1),T},\ln Sa(T2),T}, \quad \rho_{\varepsilon_{\ln Sa(T2),T},\ln Sa(2T1)|\ln Sa(T1),T}$$

The median spectral values and total standard deviations are calculated using Campbell and Bozorgnia[1] (2006). These values can be found in Table 4.4.

Table 4.4 Spectral values and total standard deviation from Campbell and Bozorgnia (2006) NGA model for M7 strike-slip earthquake 10 km from a site with a 30-m shear wave velocity of 400 m/s.

Building	A		B		C		D	
Period	PSA (g)	σ_T	PSA (g)	σ_T	PSA (g)	σ_T	PSA (g)	σ_T
T1	0.530	0.623	0.134	0.682	0.102	0.686	0.242	0.631
2T1	0.134	0.693	0.0610	0.691	0.0490	0.747	0.112	0.685
T2	0.280	0.673	0.387	0.644	0.322	0.655	0.631	0.618

The correlation coefficients are calculated using the intra-event and interevent normalized residuals from Campbell and Bozorgnia (2008). For the sake of expediency the third correlation coefficient is neglected. These correlation coefficients can be found in Table 4.5.

Table 4.5 Correlation coefficients from Campbell and Bozorgnia (2008) NGA model for total normalized residuals.

Correlation Coefficient	A	B	C	D
$\rho_{\varepsilon_{\ln Sa(T1),T},\ln Sa(2T1),T}$	0.78	0.75	0.77	0.73
$\rho_{\varepsilon_{\ln Sa(T1),T},\ln Sa(T2),T}$	0.62	0.62	0.60	0.39

Using these values, Equation (4.28) can be evaluated for each of the structures. The resulting cumulative distribution function is shown in Figure 4.8, for the example case of Building A. The point of comparison is the median structural response value given the M7 scenario; this is shown to be 2.7% interstory drift in Figure 4.8. For comparison, Figure 4.8 also shows the distribution of MIDR response conditioned on a M7.0 event at a distance of 10 km, but without the conditioning on the motion being an ε = +2.0 motion (as described for the M7 scenario in Section 3.3).

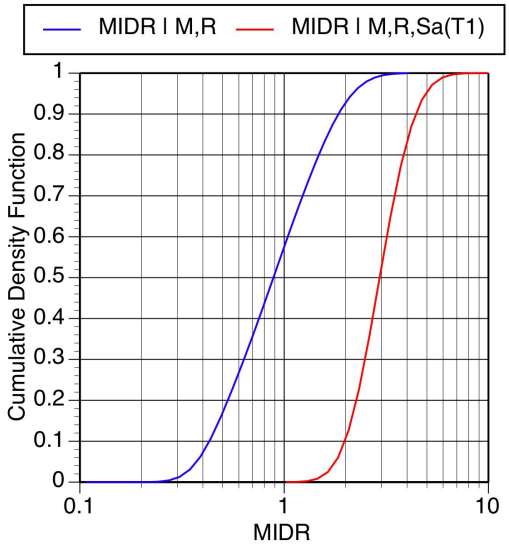

Fig. 4.8 Cumulative distribution function of MIDR | M, R, and MIDR | M, R, Sa(T_1).

[1] The following values were used as representative for the Campbell and Bozorgnia model: Z_{TOR} = 0, Z_{Vs30} = 2 km, and δ = 90 degrees.

The final point-of-comparison values for each of the four buildings are listed in Table 4.6.

Table 4.6 Points of comparison.

Building	Magnitude 7 | Sa_{T1} (2ε)	Magnitude 7.5 | Sa_{T1} (1ε)
A	0.027	--
B	0.022	--
C	0.019	0.016
D	0.0108	--

4.7 SUMMARY

This chapter summarized the approach to predict the true response of the structure. Recognizing that we do not have complete knowledge of future seismic ground motions, this is termed the point of comparison (POC). This chapter presented the POC prediction methodology, as well as the POC predictions of the median MIDR for Buildings A, B, C, and D for the M7 scenario, as well as Building C for the M7.5 scenario.

The POC results from Table 4.6 of this chapter are the values used in the later comparisons of GMSM methods contained in Chapters 6-11.

Chapter 5 builds upon the results of this chapter, and looks more deeply at questions regarding how collapse cases should be treated, as well as questions regarding the function form and appropriate parameters for use in the regression models.

5 Evaluation of Point-of-Comparison Methodology

Primary Author: J. W. Baker

Associate Author: N. Shome

5.1 INTRODUCTION

The point-of-comparison (POC) methodology proposed in Chapter 4 provides a potentially highly accurate approach for determining the distribution of structural response to be expected from a specified scenario earthquake and ground motion intensity. The general approach of this methodology consists of the following steps:

1. Perform structural analysis using a large number of representative ground motions, and record the response parameter of interest (e.g., maximum interstory drift ratio, or *MIDR*) from each analysis, along with all relevant properties of each input ground motion (e.g., spectral acceleration values at periods of interest).
2. Use regression analysis on these data to define a predictive equation that relates the ground motion properties to the observed structural response levels.
3. Use ground motion prediction equations (along with correlation models) to predict the distribution of ground motion properties that will occur during the scenario earthquake of interest.
4. Evaluate the regression equation over the predicted distribution of ground motion properties, to get the distribution of structural response.

This approach requires too much analysis effort to be feasible in practical design situations, but it is potentially very useful for the studies in the following five chapters of this

report, as it may provide a precise estimate of the distribution of *MIDR* under the scenario earthquakes of interest here.

While the POC methodology is intended to provide robust and reliable predictions, it was determined that an independent evaluation of the procedure was desirable due to the relative lack of experience with this procedure and the importance of the POC predictions in the following report chapters. This chapter presents a limited independent effort to develop regression equations for the POC, using standard model building tools from the field of regression analysis. The ground motion and structural response data in this chapter are identical to the data used in Chapter 4. The stages of model development will be described and justified in detail for an example building to illustrate the chosen approach, and summary results will be presented for all buildings and scenarios used in this report. The results will serve several purposes. First, they will provide a verification that the predictions obtained in Chapter 4 are correct in the sense of being consistent with the structural response results obtained from many hundreds of dynamic structural analyses. Second, these results will help to quantify how sensitive the final *MIDR* prediction is to minor changes in the predictive model. Finally, the results will help to highlight remaining uncertainties with this methodology to be addressed by future research. Thus, while the effort expended to develop these models was much less than the effort expended to develop the original models of Chapter 4, the results are believed to provide a useful evaluation of the methodology.

5.2 ANALYSIS APPROACH

The approach taken here is to use classical regression analysis model building approaches to quickly construct and evaluate a variety of predictive models that specify the distribution of *MIDR* for a given set of ground motion properties. The final result of these analyses is a predictive model of the form

$$MIDR = g(\mathbf{X}) + \upsilon \tag{5.1}$$

where $\mathbf{X}$ is a vector of ground motion properties (such as spectral accelerations at various periods), $g(\mathbf{X})$ is a function that predicts the mean value of *MIDR*, and υ is a zero-mean random variable representing the remaining observed variability in *MIDR* that is not explained by $g(\mathbf{X})$. Because υ is often observed to be lognormally distributed (as opposed to being normally

distributed, which is useful for several reasons regression analysis), Equation 5.1 is often formulated slightly differently, as a prediction of ln*MIDR*

$$\ln MIDR = g'(\mathbf{X}) + \upsilon' \tag{5.2}$$

where $g'(\mathbf{X})$ represents the prediction of ln*MIDR*, and υ' represents the zero-mean (and now normally distributed) prediction error. Note that this assumption of normally distributed prediction errors is not completely correct when the structure sometimes collapses. A generalization of the model to account for that case is discussed below.

The predictive function $g'(\mathbf{X})$ will be calibrated empirically using regression analysis on the ground motions and response data discussed previously. The results below will focus on what form that predictive function should take, and what predictor variables should be included in the vector **X**. Once the $g'(\mathbf{X})$ predictive model is calibrated, it can be used to predict the probability that a ground motion with properties **X**=**x** causes an *MIDR* greater than *y* (throughout this chapter, capital letters will denote random variables, and lower case letters will denote numerical values that those random variables may take).

$$\begin{aligned} P(\ln MIDR > \ln y \mid \mathbf{X} = \mathbf{x}) &= P(g'(\mathbf{x}) + \upsilon' > \ln y) \\ &= P(\upsilon' > \ln y - g'(\mathbf{X})) \\ &= P\left(\frac{\upsilon'}{\sigma_{\upsilon'}} > \frac{\ln y - g'(\mathbf{x})}{\sigma_{\upsilon'}}\right) \\ &= 1 - \Phi\left(\frac{\ln y - g'(\mathbf{x})}{\sigma_{\upsilon'}}\right) \end{aligned} \tag{5.3}$$

where the notation "|**X**=**x**" is used to denote that the probability prediction is made conditional on a given set of ground motion parameter values **x**, $g'(\mathbf{x})$ is the predictor function evaluated at **x**, $\sigma_{\upsilon'}$ is the standard deviation of υ' (a value that is easily obtained during the regression analysis), and $\Phi(\ )$ is the cumulative distribution function for a standard normal random variable (Benjamin and Cornell 1970). In the final line of Equation 5.3, we have taken advantage of the fact that $\upsilon'/\sigma_{\upsilon'}$ has a standard normal distribution (i.e., a normal distribution with zero mean and unit standard deviation), so that $P(\upsilon'/\sigma_{\upsilon'} \le z) = \Phi(z)$.

Once the predictive model $g'(\mathbf{X})$ has been built, Equation 5.3 can be used to predict the distribution of *MIDR*, given occurrence of the earthquake scenario of interest. Recall that in this report, the earthquake scenarios of interest consist of a given earthquake magnitude and distance,

as well as spectral acceleration value at the structure's first-mode period ($Sa(T_1)$). This prediction is made by using Equation 5.3 to predict the probability that a ground motion with parameters **x** causes a given *MIDR* value to be exceeded, and then combining that information with the probabilities that various values of **x** will be observed during the earthquake scenario using the total probability theorem (Benjamin and Cornell 1970). If we define the earthquake scenario by $M = m$, $R = r$, $Sa(T_1) = sa$, then we can write

$$P(\ln MIDR > \ln y \mid M = m, R = r, Sa(T_1) = sa) = \iiint_{M,R,Sa(T_1)} P(\ln MIDR > \ln y \mid \mathbf{X} = \mathbf{x}) f_{\mathbf{X}|M,R,Sa(T_1)}(\mathbf{x} \mid m, r, sa)\, dm\, dr\, dsa \quad (5.4)$$

where $f_{\mathbf{X}|M,R,Sa(T_1)}(\mathbf{x} \mid m, r, sa)$ denotes the conditional probability density function of **X**, given *M*, *R* and $Sa(T_1)$ (loosely speaking, this is proportional to the probability that **X**=**x**, given the earthquake scenario). Since *M*, *R* and $Sa(T_1)$ are specified by this conditioning, if those terms are included in the vector **X** they are known with certainty. Fortunately, because logarithmic spectral acceleration values at multiple periods within a given ground motion are known to have a joint normal distribution with previously computed correlation coefficients (Baker and Jayaram 2008; Jayaram and Baker 2008), if the vector **X** is composed of logarithmic spectral acceleration values, then $f_{\mathbf{X}|M,R,Sa(T_1)}(\mathbf{x} \mid m, r, sa)$ is very easy to compute. In fact, the distribution of X is exactly specified by the conditional mean spectrum in this case (Baker and Cornell 2006). In part because the distribution of **X** is so easy to compute in this case, the predictions below are functions of logarithmic spectral acceleration values. (Additional reasons for this choice include the fact that spectral acceleration values are good predictors of response, as well as the fact that ln*Sa* and ln*MIDR* values often have approximately linear relationships.) Once Equation 5.4 has been computed, it can be used to determine the median *MIDR* for the scenario (i.e., the *y* value for which Equation 5.4 is equal to 0.5).

One significant limitation of the model building in this chapter is that only spectral acceleration values at a few periods were considered as predictors. This in part because only those predictors were considered in Chapter 4, and in part due to schedule constraints during this project.

Given the details of this approach described above, it may be useful to anticipate the effectiveness of various ground motion selection approaches in reproducing the structural response results from Equation 5.4. Ground motions selected to match the conditional mean

spectrum are internally consistent with the calculations of Equation 5.4, so they are expected to produce comparable response estimates. On the other hand, ground motions selected to match a uniform hazard spectrum will differ in their estimated response because a uniform hazard spectrum is not a true representation of the ground motion parameter **X** associated with occurrence of M, R and $Sa(T_1)$. And ground motions selected to match an inelastic response spectrum will produce comparable structural response results only if the inelastic spectral targets are consistent with the M, R, and (elastic) $Sa(T_1)$ value specified by the earthquake scenario; we will see later that the inelastic targets used by some methods may in fact not be consistent, leading to unintended variations in structural response results.

5.3 REGRESSION ANALYSIS: NON-COLLAPSE RESPONSES FOR BUILDING B

To demonstrate the analysis procedure used in this chapter, the ground motion and structural response data for the M7 scenario and Building B is used here. The approach and results will be presented in parallel. For reference, the Chapter 4 point-of-comparison value for this building was 0.022.

In this section, only the ground motions that do not cause collapse are used, and it is temporarily assumed that the probability of collapse is zero for the purpose of computing a median MIDR. This assumption will be relaxed below, once a prediction of the probability of collapse is obtained.

5.3.1 Model 1: Predictive Equation from Chapter 4

The first regression model attempted here was the exact functional form used in Chapter 4:

$$E[\ln MIDR] = b_0 + b_1 \ln Sa(T_1) + b_2 \ln Sa(T_1)^2 + b_3 \ln Sa(2T_1) + b_4 \ln Sa(2T_1)^2 + b_5 \ln Sa(T_2) + b_6 \ln Sa(T_2)^2 \quad (5.5)$$

where the notion $E[\ ]$ is used to denote an expected (or mean) value, and T_i denotes the period of the ith-mode of vibration of the structure of interest. The b_j coefficients were then determined using least-squares regression (i.e., by selecting the coefficients that minimize the sum of the squared errors between the observed and predicted ln*MIDR* values from the calibration data set). The coefficients obtained from this procedure are shown in Table 5.1. The "Estimate" column of

this table provides the estimated coefficients. The "s.e." column provides the standard errors for these estimates (because the estimates are uncertain due to the finite sample of data used for calibration). These estimates and standard errors can then be used to compute the p-values shown in the third column of the table. Note that the data in this table are part of the standard output from most popular regression and numerical analysis software packages such as R, S-Plus and Matlab (Fox 2002; Matlab Inc. 2005). A p-value states the probability that a coefficient value at least as large as the computed value would be observed if in fact there was no real relationship between the predictor variable and ln*MIDR*. Put another way, we would get non-zero coefficients for even nonsensical predictor variables, although those coefficients would have large standard errors relative to the estimated coefficients. The p-value test thus identifies estimates with a high probability of being observed if in fact the associated variable has no predictive ability. By convention, predictors with p-values of less than 0.05 are removed from the regression model. Further information on regression analysis and p-value tests are available from the many textbooks describing regression analysis (e.g., Kutner et al. 2004; Weisberg 1985). Note also that in general, there are many other tools available for statistical model building, but only p-values were used here because of the very limited time available to perform this evaluation.

Table 5.1 Regression coefficient summary for model of Equation 5.5.

	Estimate	s.e.	p-value
b_0	-2.12	0.13	0.00
b_1	0.29	0.07	0.00
b_2	-0.05	0.02	0.02
b_3	1.05	0.10	0.00
b_4	0.14	0.02	0.00
b_5	0.36	0.03	0.00
b_6	-0.01	0.02	0.71

In Table 5.1, all parameters appear to be statistically significant, except for the $\ln Sa(T_2)^2$ term associated with b_6. Using this model to evaluate Equation 5.4, we find that the POC is equal to 0.0224, which is essentially identical to the result in Chapter 4.

5.3.2 Model 2: Linear Terms Only

The second model considered uses the same predictor variables as Model 1 but excludes the quadratic *Sa* terms. This revision is made because one of the quadratic terms in Model 1 was not statistically significant and because polynomial functional fits can sometimes produce unreasonable predictions when extrapolated. Model 2 takes the following form.

$$E[\ln MIDR] = b_0 + b_1 \ln Sa(T_1) + b_2 \ln Sa(2T_1) + b_3 \ln Sa(T_2) \tag{5.6}$$

The estimated coefficients for this model are shown in Table 5.2. All coefficients for this model are statistically significant. This functional form is also computationally convenient because it is a linear function of all predictor parameters. The linear form means that the mean value of ln*MIDR* associated with the earthquake scenario can be computed by simply evaluating the function using the mean values of all predictor variables (Benjamin and Cornell 1970), and the exponential of the mean ln*MIDR* is the median *MIDR* of interest (this mean/median relationship holds because *MIDR* is lognormally distributed). Evaluating this function at the mean $Sa(T_i)$ values associated with the M7 scenario earthquake yields a POC value of 0.0215, which is comparable to the results from Chapter 4 and Model 1 above. Model 2 is thus deemed slightly preferable to Model 1, as it is simpler than Model 1, provides a comparable POC estimate, and facilitates a straightforward computation of the POC due to its linear functional form (although an argument could certainly also be made that the statistically significant quadratic parameters should be retained in the model).

Table 5.2 Regression coefficient summary for the model of Equation 5.6.

	Estimate	s.e.	p-value
b_0	-2.97	0.06	0.00
b_1	0.44	0.04	0.00
b_2	0.30	0.03	0.00
b_3	0.35	0.03	0.00

5.3.3 Model 3: Linear Terms Only and $Sa(T_3)$

Because of questions as to whether $Sa(T_3)$ is also an important predictor for some buildings, Model 2 was expanded to include $Sa(T_3)$ as a predictor:

$$E[\ln MIDR] = b_0 + b_1 \ln Sa(T_1) + b_2 \ln Sa(2T_1) + b_3 \ln Sa(T_2) + b_4 \ln Sa(T_3) \quad (5.7)$$

The estimated coefficients for this model are shown in Table 5.3. All previous predictor variables remain statistically significant in this model, and the additional $\ln Sa(T_3)$ predictor is also statistically significant. Thus, it appears that $Sa(T_3)$ should have been included in the model of Chapter 4. Using this model for the point of comparison yields a POC of 0.0211, which is comparable to (but slightly less than) the models above.

Table 5.3 Regression coefficient summary for model of Equation 5.7.

	Estimate	s.e.	p-value
b_0	-3.01	0.07	0.00
b_1	0.46	0.04	0.00
b_2	0.29	0.03	0.00
b_3	0.28	0.04	0.00
b_4	0.08	0.03	0.01

5.3.4 Model 4: Linear Terms and Scale Factor

To test for scale factor bias, Model 3 was expanded to include the scale factor as a regression term.

$$E[\ln MIDR] = b_0 + b_1 \ln Sa(T_1) + b_2 \ln Sa(2T_1) + b_3 \ln Sa(T_2) + b_4 \ln Sa(T_3) + b_5 SF \quad (5.8)$$

where *SF* is the scale factor of the ground motion. The estimated coefficients for this model are shown in Table 5.4. The scale factor is not statistically significant, and its estimated coefficient is also nearly equal to zero, indicating that ground motions with large scale factors behave exactly the same as unscaled ground motions in terms of their relationship between *Sa* values and *MIDR*. Model 3 is thus preferable to Model 4, due to its simplicity. Incidentally, if Model 4 were to be used (by evaluating the equation with a target scale factor of 1.0, assuming we are interested in the response from unscaled ground motions), it would result in a POC of 0.0206, which differs from the Model 3 result only by a small amount, as expected.

Table 5.4 Regression coefficient summary for model of Equation 5.8.

	Estimate	s.e.	p-value
b_0	-3.06	0.08	0.00
b_1	0.46	0.04	0.00
b_2	0.27	0.03	0.00
b_3	0.29	0.04	0.00
b_4	0.07	0.03	0.04
b_5	0.01	0.01	0.20

5.3.5 Results from Different Models

Recall that we have considered so far only a very limited number of potential predictor variables. In order to review the robustness of the selection of the predictor variables in Model 3, we further consider all possible combinations of spectral accelerations at up to three different periods between 0.25s and 8.0s as predictor variables in addition to spectral acceleration at the first-mode period (T_1). The regression results for all the cases (around 60 million) show that predictions using Sa at periods of 2.01s, 0.65s, 2.44s, and 3.83s have a standard deviation of regression error (υ') of 0.24, versus 0.25 for Model 3. The variation of regression error only for a subset of all the cases ($\sigma_{\upsilon'} < 0.30$) is shown in Figure 5.1. The figure shows that the optimized model has a slightly better ability to predict MIDR than Model 3 above. Model 3, on the other hand, is appealing in that the predictor variables are known to be related to the dynamic response characteristics of structures. We have plotted in Figure 5.2 the expected MIDR of Building B for the mean spectrum *Sa* conditioned on $Sa(T_1)$. The conditional mean spectrum is estimated at different percentiles of $Sa(T_1)|M,R$. This figure also demonstrates that the difference in the results between Model 3 and the optimized model (*Optm. Model*) is not significant.

Additionally we have considered an alternative model (*Alt. Model*) which has a similar functional form to Model 3, but the independent variables except $Sa(T_1)$ are formulated as a ratio of logarithm of spectral accelerations, (i.e., $\ln(Sa(T_i))/\ln(Sa(T_1))$. This model has the advantage of reducing the potential collinearity compared to Model 3 where the predictor variables have significant correlation (Shome and Cornell 1999). The regression error of this model is, however, 0.32. Hence the predictive ability of the alternative model is significantly lower than Model 3, and also the fitted model as shown in Figure 5.2 has somewhat questionable shape at high $Sa(T_1)$.

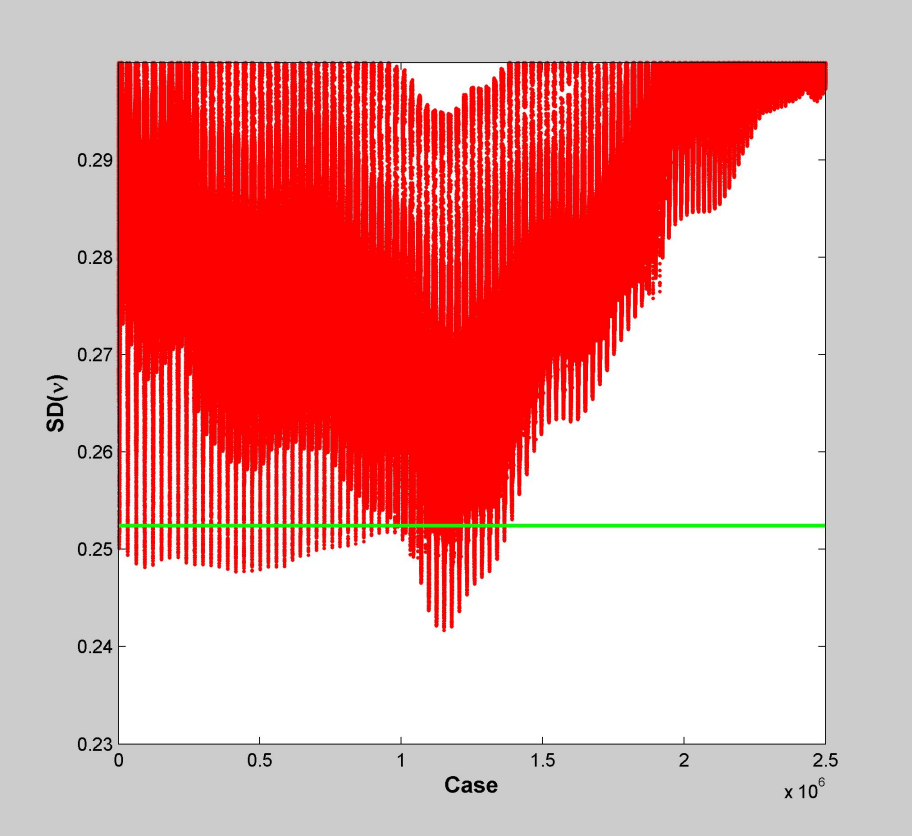

Fig. 5.1 Variation of standard deviation of regression error for regression model that has functional relationship similar to Model 3 but has different independent variables. Independent variables for each case are combinations of Sa at three different periods and Sa(T_1). Green line shows regression error for Model C.

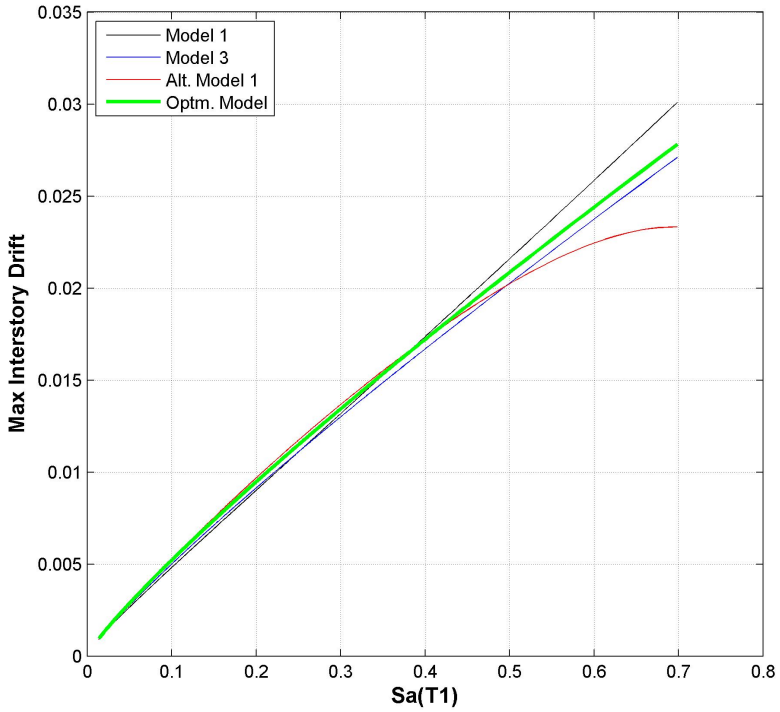

Fig. 5.2 Variation of maximum interstory drift ratio (MIDR) for conditional mean spectrum Sa at a given Sa(T_1). Conditional mean spectrum is estimated at different percentiles of Sa(T1)|M,R.

5.3.6 Final Model Results

In conclusion, this brief model building effort resulted in the selection of Model 3 (Eq. 5.7) for prediction of non-collapse *MIDR*. In general, Model 3 has excellent predictive ability as indicated by its R^2 value of 0.93, which indicates that the predictive equation explains 93% of the variance in ln(*MIDR)* observed in the raw data. Finally, in order to evaluate Equation 5.3, we note that $\sigma_{v'} = 0.251$ for this model.

5.4 PROBABILITY OF COLLAPSE MODELING: BUILDING B

The previous results in this chapter were all obtained using only the ground motions that did not cause the building to collapse. Some of the ground motions did cause collapse, however, and those must also be accounted for when predicting a true median *MIDR*. The approach taken to

incorporate collapse follows the approach of Shome and Cornell (2000), but uses a logistic regression equation to determine the probability of collapse. First, the distribution of *MIDR* from non-collapse ground motions is accounted for by using the model of the previous section. Second, all ground motions are classified as causing collapse or not causing collapse, and the probability that a given ground motion will cause collapse is then predicted using logistic regression (e.g., Agresti 2002). Logistic regression is perhaps the most widely used statistical technique for modeling categorical data (such as collapse/non-collapse). The complete set of assumptions underlying this approach are given by Agresti (2002), and the function used to make this prediction is of the form

$$P(Collapse \mid \mathbf{X} = \mathbf{x}) = \frac{1}{1 + e^{-(b_0 + b_1 x_1 + b_2 x_2 + \ldots)}} \tag{5.9}$$

where again $\mathbf{X}$ is a vector of ground motion properties, and $\mathbf{x} = [x_1, x_2, \ldots, x_n]$ are the numerical values that $\mathbf{X}$ takes. An example plot of this functional form, as a function of a single x parameter, is shown in Figure 5.3.

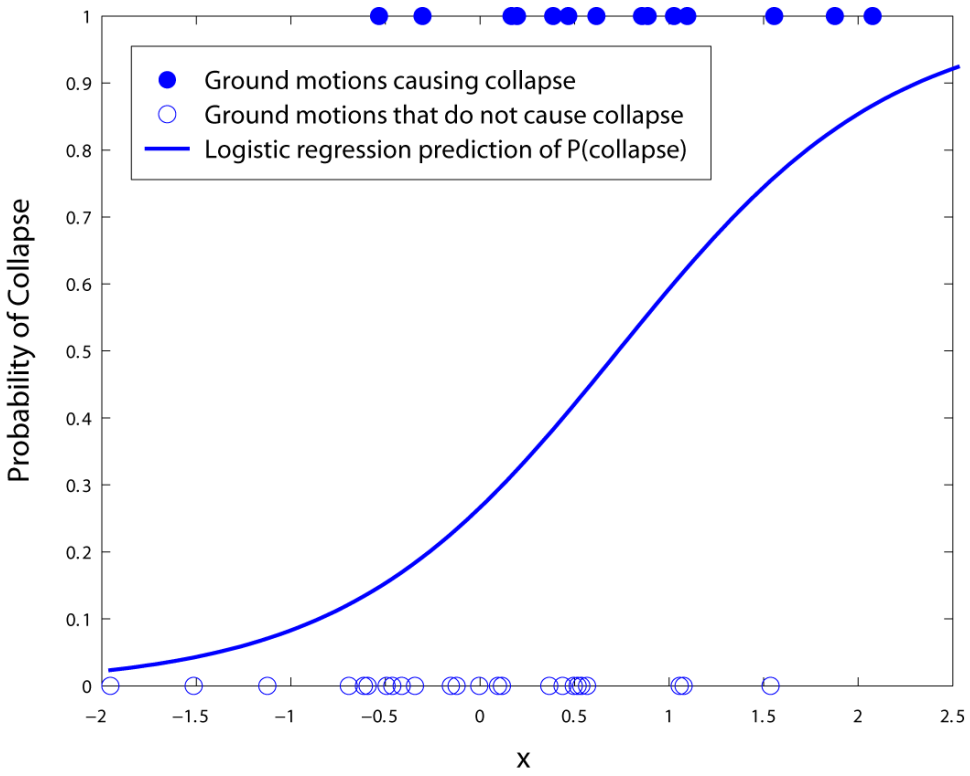

Fig. 5.3 Schematic illustration of predicting P (collapse) as a function of generic ground motion property, *x*, using logistic regression applied to collapse/non-collapse results.

Third, the collapse and non-collapse predictions are recombined using the total probability theorem (Shome and Cornell 2000). The probability of exceeding a given *MIDR* level is equal to the probability of collapse and the probability of exceeding the *MIDR* level given that the building did not collapse. Mathematically, this can be written,

$$\begin{aligned} P(\ln MIDR > \ln y \mid \mathbf{X} = \mathbf{x}) \quad &= P(Collapse \mid \mathbf{X} = \mathbf{x}) \\ &+ \left(1 - P(Collapse \mid \mathbf{X} = \mathbf{x})\right) \\ &\cdot \left(P(\ln MIDR > \ln y \mid \mathbf{X} = \mathbf{x},\ no\ collapse)\right) \end{aligned} \tag{5.10}$$

where $P(\ln MIDR > \ln y \mid \mathbf{X} = \mathbf{x},\ no\ collapse)$ is the non-collapse prediction of Equation 5.3 evaluated using the regression model of Section 5.3 (and where "no collapse" has been added to the notation to emphasize that this prediction is only for the non-collapse data). Once the inputs to this equation have been obtained, it will be possible to compute a median *MIDR*, accounting

explicitly for the probability of collapse. All that remains to complete this computation is to choose a suitable model for predicting $P(Collapse \mid \mathbf{X} = \mathbf{x})$. The following subsections explore potential predictive models. To distinguish from the non-collapse models, the following models are denoted with letters rather than numbers (i.e., "Model A," Model B," etc.).

5.4.1 Model A: Only $Sa(T_1)$ and $Sa(2T_1)$ as Predictors

The first model considered uses only $Sa(T_1)$ and $Sa(2T_1)$ as predictors. This was done to follow the preliminary model considered in Chapter 4, which was developed under the plausible assumption that higher-mode responses (and thus $Sa(T_2)$, $Sa(T_3)$, etc.) may not be important predictors of collapse occurrence. The initial predictive function is thus

$$P(Collapse) = \frac{1}{1 + e^{-(b_0 + b_1 \ln Sa(T_1) + b_2 \ln Sa(2T_1))}} \tag{5.11}$$

and the estimated regression coefficients are shown in Table 5.5. As with linear regression, the standard errors and p-values for each regression coefficient are easily obtained from most statistical software packages. We see from the table that both predictor variables are statistically significant.

Table 5.5 Regression coefficient summary for model of Equation 5.11.

	Estimate	s.e.	p-value
b_0	6.25	1.00	0.00
b_1	2.05	0.48	0.00
b_2	3.59	0.65	0.00

We are interested in the probability of collapse predicted by this model under the M7 earthquake scenario (which is described in Section 3.3). The calculation is completed by using Equation 5.11 and the associated coefficients summarized in Table 5.5, substituting the value of $Sa(T_1 = 2.01s) = 0.524g$ that is consistent with the M7 scenario, and then integrating over the conditional distribution of $Sa(2T_1 = 4.02s)$ which is conditioned on the above value of $Sa(T_1)$; this conditional distribution is defined in Baker and Cornell (2006). Using this calculation, the estimated $P(Collapse)$ for this model is 0.25.

5.4.2 Model B: $Sa(T_1)$, $Sa(2T_1)$, $Sa(T_2)$ and $Sa(T_3)$ as Potential Predictors

As a revision to Model A, we now consider $Sa(T_2)$ and $Sa(T_3)$ as additional potential predictors, for consistency with the non-collapse prediction models developed previously. The predictive equation for Model B is

$$P(Collapse) = \frac{1}{1+e^{-(b_0+b_1 \ln Sa(T_1)+b_2 \ln Sa(2T_1)+b_3 \ln Sa(T_2)+b_4 \ln Sa(T_3))}} \tag{5.12}$$

and the estimated regression coefficients are shown in Table 5.6. The estimated $P(Collapse)$ from this model is 0.09, which is considerably smaller than the estimate of Model A. The new predictor variable $Sa(T_3)$ is statistically significant, so it will be retained in the final model. The $Sa(T_2)$ predictor is not statistically significant (which is somewhat surprising given that $Sa(T_3)$ was significant). $Sa(T_2)$ was, however, found to be significant for the comparable analyses of Building C.

Table 5.6 Regression coefficient summary for model of Equation 5.12.

	Estimate	s.e.	p-value
b_0	4.87	1.10	0.00
b_1	1.56	0.58	0.01
b_2	3.98	0.74	0.00
b_3	0.54	0.57	0.34
b_4	1.16	0.50	0.02

Given the results from the previous paragraph, the Model B prediction was revised slightly to remove $Sa(T_2)$ a predictor. The following revised model was then used

$$P(Collapse) = \frac{1}{1+e^{-(b_0+b_1 \ln Sa(T_1)+b_2 \ln Sa(2T_1)+b_3 \ln Sa(T_3))}} \tag{5.13}$$

resulting in the following coefficient estimates.

Table 5.7 Regression coefficient summary for model of Equation 5.13.

	Estimate	s.e.	p-value
b_0	4.99	1.09	0.00
b_1	1.77	0.53	0.00
b_2	3.94	0.73	0.00
b_3	1.48	0.38	0.00

As expected, all remaining predictors are significant. The estimated $P(Collapse)$ from this model is also 0.09, indicating that the inclusion or omission of $Sa(T_2)$ as a predictor does not practically impact the $P(Collapse)$ estimate in this case.

For brevity, in the summary results presented below for the other buildings, Model B refers to a model in which all statistically significant $Sa(T_i)$ variables are included as predictors. For this building, Model B is therefore represented by Equation 5.13, but for some other buildings $Sa(T_2)$ is also included in Model B.

5.4.3 Model C: Model B Predictors and Scale Factor

As a final model variation, we consider scale factor as a predictor to check for remaining scaling bias. Adding this predictor to Equation 5.13 gives

$$P(Collapse) = \frac{1}{1+e^{-(b_0+b_1 \ln Sa(T_1)+b_2 \ln Sa(2T_1)+b_3 \ln Sa(T_3)+b_4 SF)}} \tag{5.14}$$

The resulting coefficients are summarized in Table 5.8.

Table 5.8 Regression coefficient summary for model of Equation 5.14.

	Estimate	s.e.	p-value
b_0	4.03	1.15	0.00
b_1	2.05	0.55	0.00
b_2	3.95	0.78	0.00
b_3	0.97	0.44	0.03
b_4	0.35	0.12	0.00

The scale factor is statistically significant in this case, indicating that there is some scaling bias (i.e., the b_4 coefficient is positive, indicating that a ground motion scaled up to a given set of *Sa* values is more likely to cause collapse than an unscaled ground motion having the same *Sa* values). To adjust for this scale factor effect in the point-of-comparison calculation, we evaluate Equation 5.14 using $SF = 1.0$. This model produces an estimated $P(Collapse)$ of 0.05. This model also includes all statistically significant predictors (from among the limited set of predictors variables considered in this study), so it is the proposed model for predicting collapse of Building B.

5.4.4 Binary Regression Results from Different Models

Recall again that we have considered so far only a very limited number of potential predictor variables to estimate the collapse probability. It is interesting to note here that, unlike the non-collapse predictive models, changes to the predictive model for collapse resulted in dramatic changes to the estimated $P(Collapse)$, with predictions ranging from 0.05 to 0.22. This suggests that much care is needed when identifying an appropriate predictive model for collapse when using the point-of-comparison methodology. Hence, following the approach in Section 5.3.5, we have considered a large number of spectral accelerations at two different periods and the ground-motion scale factor in addition to $Sa(T_1)$ as the predictor variables. The regression results for all the cases (around 300,000) show that a prediction using Sa at periods of 2.01s, 4.88s and 0.76s has the deviance of the fit, $D(P_C, \theta)$, (which is defined as the -2 times the log-likelihood of the model at the solution vector) equal to 96 (versus 103 for Model C). Analogous to the residual sum of squares in linear regression, the goodness-of-fit of a generalized linear model can be measured by the deviance. It is a very useful for comparing two models and the difference of the deviance between two models follows approximately chi-squared (χ^2) distribution with degrees of freedom equal to the difference between the numbers of parameters in the two models (see McCullagh and Nelder (1989) for details on deviance and generalized linear model, GLM). The variation of $D(P_C, \theta)$ for all the cases is shown in Figure 5.4. The deviance for Model C is shown in the figure by the green line. We have also plotted in Figure 5.5 the expected P_C for the mean spectrum *Sa* conditioned on $Sa(T_1)$ in line with what we have done in Section 5.3.5 (Fig. 5.2),

which demonstrated that the difference in the results between Model C and the optimized model is not significant.

Additionally we have considered two alternative models to determine the sensitivity of P_C to different functional forms for the regression model. The first model is a logistic regression model, which has the same functional form as Model C, but the independent variables except $Sa(T_1)$ are the ratio of logarithm of spectral accelerations at a period and the logarithm of $Sa(T_1)$. The basis of the selection of this model is explained in Section 5.3.5. The second model also has the similar functional relationship as Model C, but we have used *probit* regression instead of logistic regression used in Model C (details of the probit regression can be found in Agresti (2002). Regression analysis shows that the deviance of the fit is 139.9 for the first model and 103.5 for the second model (versus 102.6 from Model C). So the predictive ability of the probit model is not better than Model 3 and also the expected P_C from the fitted model as shown in Figure 5.5 is also not significantly different from that of Model C. Also, based on the results of deviance (higher compared to Model C) and the plot in Figure 5.5. (higher probability of collapse compared to other models), we can state that the alternative model for the ratio of spectral accelerations is even worse than Model C. Note that when we use $Sa(T_2)$ instead of $Sa(T_3)$ as the predictor variable in Model C (referred to as Model D), we also get results very similar to Model C for Building B (see Fig. 5.5). So we find that Model C works very well for Building B even though other models would have worked equally well. We have chosen here Model C, since the model works well also for all the other buildings.

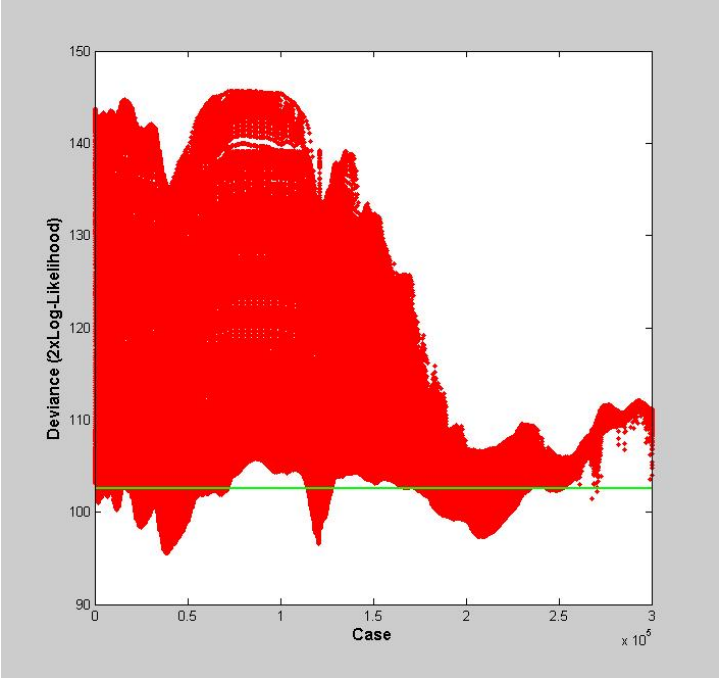

Fig. 5.4 Variation of deviance of fit for logistic regression model similar to Model C. Independent variables for each case are combinations of *Sa* at two different periods, $Sa(T_1)$ and ground-motion scaling factor. Green line shows deviance of Model C fit.

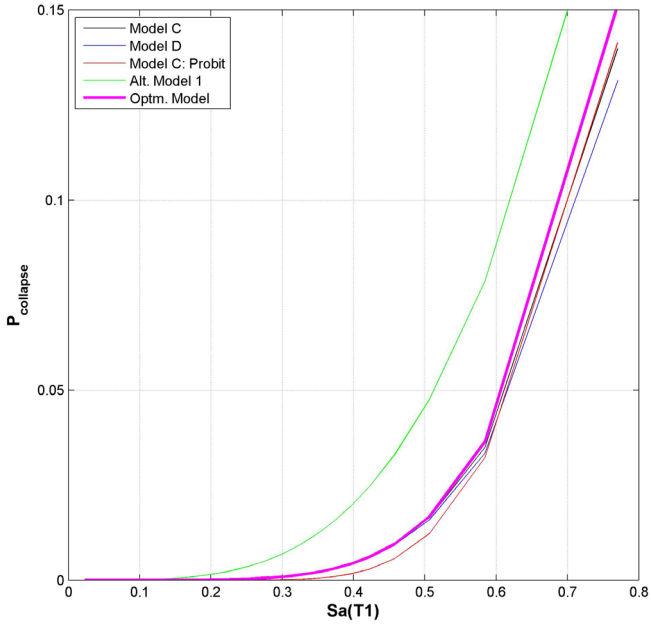

Fig. 5.5 Variation of probability of collapse (PC) from different regression models for conditional mean spectrum *Sa* at a given $Sa(T_1)$. Conditional mean spectrum is estimated at different percentiles of $Sa(T_1)|M,R$.

5.4.5 Final Model Results

The proposed $P(Collapse)$, P_C, for Building B under the M7 scenario is 0.05. Other analysis results are also available to help judge whether these $P(Collapse)$ estimates are reasonable. Based on extensive previous analysis of this structure as part of the ATC-63 project (Applied Technology Council 2008; Haselton and Deierlein 2008), an estimated $P(Collapse)$ of 0.01 was obtained independently of this effort (Curt Haselton, personal communication, 2008). Further, as will be seen in Chapter 7 to follow, the ground motion selection methods found to work well produce an approximate $P(Collapse)$ estimate that is very near to zero. These additional estimates suggest that the true $P(Collapse)$ is likely near to zero, lending further support to the selection of Model C above, given that it produced the smallest estimated $P(Collapse)$. These additional estimates also suggest that perhaps the Model C estimate is still too high as well, and that further important predictor variables exist that would bring the POC estimate down further. That question is left for future more general investigation into the point-of-comparison methodology, and Model C is proposed for use here.

5.5 FINAL POC ESTIMATE FOR BUILDING B

Combining the non-collapse distribution of *MIDR* from Section 5.3 (which produced a median *MIDR* of 0.021) with the $P(Collapse)$ prediction from Section 5.4 (which produced a P(Collapse) estimate of 0.05), using Equation 5.10, we obtain a final median *MIDR* estimate of 0.0220. This estimate is identical to the comparable POC estimate obtained in Chapter 4 using different predictor variables and functional forms for the needed predictive equations. Discussion of this comparison will be deferred until after comparable results are presented for the other buildings.

5.6 SUMMARY OF RESULTS FOR ALL BUILDINGS SUBJECTED TO M7 SCENARIO

The above procedure was repeated for all buildings considered in this report. For brevity, the POC results are summarized in Table 5.9, and intermediate results such as individual regression coefficients are omitted. In Table 5.9, the model names (Model 1, Model 2, etc.), refer to the models having the same functional forms used in the sections above (but with new coefficients

estimated using response data for each individual building). The POC values from the preferred models are shaded in the table. A few brief comments about differences between models are also included in the following paragraphs.

For Building A (the building discussed in the most detail in Chapter 4), the POC identified here was larger than the Chapter 4 POC, but by less than 10%. The preferred regression model for this building was Model 2, as some quadratic terms were not statistically significant, and $Sa(T_2)$, $Sa(T_3)$, and the scale factor were not statistically significant predictors. It is not surprising that *Sa* values at higher-mode periods were not useful predictors, as this is a low-rise building whose interstory drifts are dominated by first-mode response. Collapse was a non-factor for this building, with the probability of collapse essentially equaling zero in all cases. The final POC estimate of 0.029 differs by about 10% from the value of 0.027 reported in Chapter 4.

For Building C, all spectral acceleration predictors (i.e., $Sa(T_1)$, $Sa(2T_1)$, $Sa(T_2)$ and $Sa(T_3)$) were found to be significant predictors of non-collapse response, and the scale factor was also significant. Probability of collapse was also found to depend upon all *Sa* values and the scale factor. The final POC estimate of 0.0188 is essentially identical to the value of 0.019 reported in Chapter 4. Note in Table 5.9 that, as with Building B, the $P(Collapse)$ estimates varied dramatically as the predictive equation was modified. If a larger $P(Collapse)$ estimate had been obtained (e.g., if Model A had be chosen to estimate $P(Collapse)$), then the final POC reported here would have been significantly larger, and would have differed from the result in Chapter 4.

For Building D, $Sa(T_1)$, $Sa(2T_1)$, and $Sa(T_3)$ were found to be significant predictors of non-collapse response. $Sa(T_2)$ and the scale factor were not significant for this building. Collapse was not an issue for this building, with none of the models predicting non-zero collapse probabilities. The final POC estimate of 0.0167 differs from the Chapter 4 estimate of 0.019 by approximately 10%.

Table 5.9 Summary of POC results for all buildings.

		Building			
	Analysis Case	**A**	**B**	**C**	**D**
	Report Chapter	6	7	8	9
Reference POC	Chapter 4 POC	0.0270	0.0220	0.0190	0.0110
POC estimated from non-collapse responses only	Model 1	0.0290	0.0224	0.0200	0.0108
	Model 2	0.0291	0.0215	0.0188	0.0110
	Model 3	0.0292	0.0210	0.0180	0.0107
	Model 4	0.0297	0.0206	0.0167	0.0108
Estimated P(Collapse)	Model A	0.01	0.22	0.22	0.00
	Model B	0.01	0.09	0.02	0.00
	Model C	0.00	0.05	0.01	0.00
Final POC estimate	Final POC, accounting for collapse	**0.0291**	**0.0220**	**0.0167**	**0.0107**
		Preferred Models			

5.7 BUILDING C SUBJECTED TO M7.5 SCENARIO

The final case to be considered is Building C, but subjected to the M7.5 scenario rather than the M7 scenario. There are two options for evaluating the POC in this case. The first option is to use the regression model developed using the previous set of ground motions (i.e., the regression equation used to produce the results in Table 5.9) but evaluate the model at the *Sa* values associated with the M7.5 scenario rather than the M7 scenario. The second option is to use a new set of ground motions (with magnitudes of approximately 7.5, rather than the M7 ground motions used above) to develop new predictive equations, and evaluate the new predictive equations at the *Sa* values associated with the M7.5 scenario. Both options are considered here. Both the M7 and M7.5 ground motion sets are documented in Appendix B.

There are two simplifications that ease this comparison. First, with both options the probability of collapse is negligible, so we can focus on the non-collapse model only. Second, the same predictor variables are statistically significant in both cases, so in both cases the preferred predictive equation is of the form:

$$E[\ln MIDR] = b_0 + b_1 \ln Sa(T_1) + b_2 \ln Sa(2T_1) + b_3 \ln Sa(T_2) + b_4 \ln Sa(T_3) \qquad (5.15)$$

If using the first option described above, then the estimated coefficients are obtained from regression on the ground motions with magnitudes of approximately 7. The resulting coefficients

are reported in Table 5.10, and all coefficients are seen to be statistically significant. *The estimated POC obtained using option one is 0.0148.*

Table 5.10 Regression coefficient summary for model of Equation 5.15, obtained using ground motions with magnitudes of approximately 7.0.

	Estimate	s.e.	p-value
b_0	-2.96	0.08	0.00
b_1	0.42	0.04	0.00
b_2	0.28	0.03	0.00
b_3	0.29	0.04	0.00
b_4	0.12	0.03	0.00

If using the second method, then the same procedure is performed using regression on the ground motions with magnitudes of approximately 7.5. The resulting coefficients are reported in Table 5.11, and all coefficients are again seen to be statistically significant. *The estimated POC obtained using option two is 0.0172. The POC of 0.016 reported in Chapter 4 falls in between these two estimates.* The Chapter 4 estimate was obtained using all ground motions (i.e., both those with magnitudes of approximately 7, and those with magnitudes of approximately 7.5), but when that approach was tried here, it resulted in an estimate of approximately 0.017; differences between the two chapters may be due to differences in the functional forms of the predictive equations, and in the predictor variables used.

Table 5.11 Regression coefficient summary for model of Equation 5.15, obtained using ground motions with magnitudes of approximately 7.5.

	Estimate	s.e.	p-value
b_0	-2.40	0.05	0.00
b_1	0.53	0.04	0.00
b_2	0.45	0.03	0.00
b_3	0.12	0.05	0.01
b_4	0.15	0.04	0.00

The difference of greater than 15% between these two estimates is somewhat troubling. While on one hand we might expect some difference in results when using input ground motions

having differing magnitudes, on the other hand this difference is surprisingly large for a relatively small change in earthquake magnitude, especially when the predictive equation has already accounted for any differences in spectral acceleration values at four periods that are expected to be good proxies for the effect of magnitude on spectral shape. Further, if we compare the coefficient estimates in Table 5.10 to those in Table 5.11, we see that some coefficients increase and some decrease, suggesting no systematic effect of magnitude on these coefficients.

While the predictive equation is a complex 5-dimensional relationship between the spectral values and *MIDR*, we can get some idea of how the relationship differs between the two ground motion sets using the plots of variable pairs shown in Figures 5.6–5.9. Note that these plots are presented in log scale, since logarithms of the variables are used in the predictive equation. While there appear to be some differences between the two ground motion sets, the variation is not easily explained using common engineering and seismology intuition. Note that the figures show the MIDR results for both the M7 and M7.5 sets of ground motions for ground motion scale factors of 1.0, 2.0, 4.0, and 8.0; additionally, records that cause collapse are excluded from the figures.

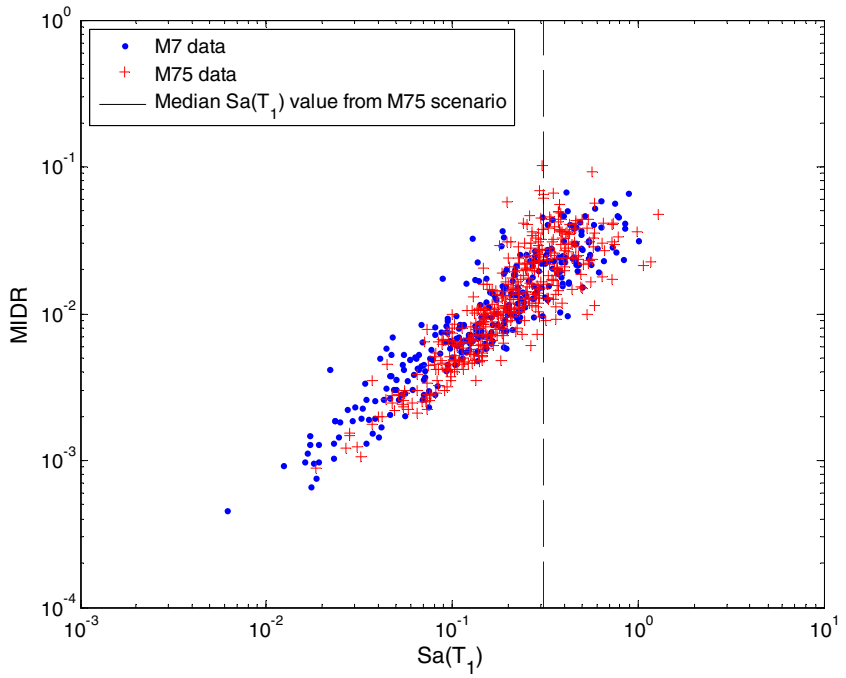

Fig. 5.6 *Sa*(T_1) versus MIDR, from two sets of ground motion data of interest.

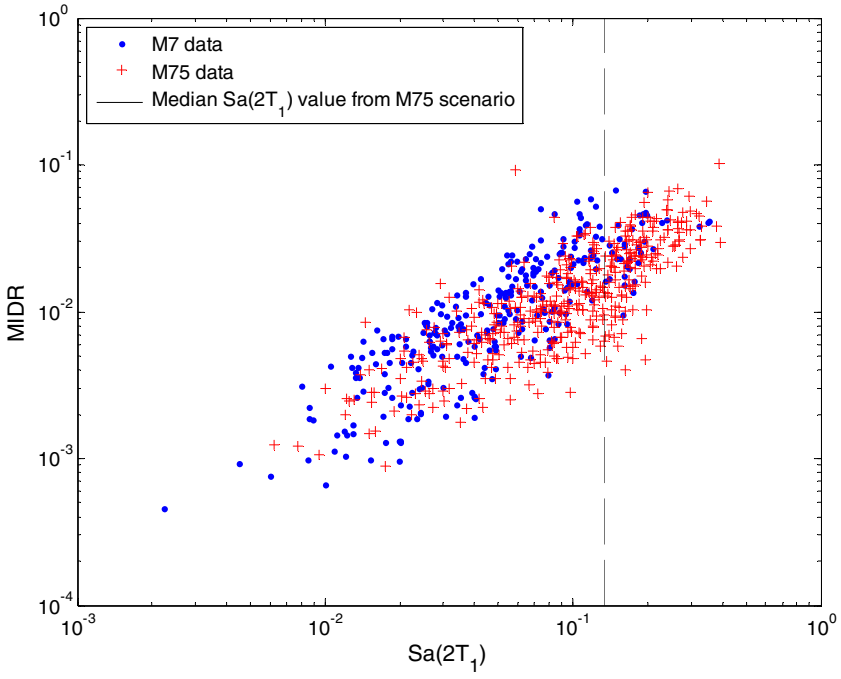

Fig. 5.7 *Sa*($2T_1$) versus MIDR, from two sets of ground motion data of interest.

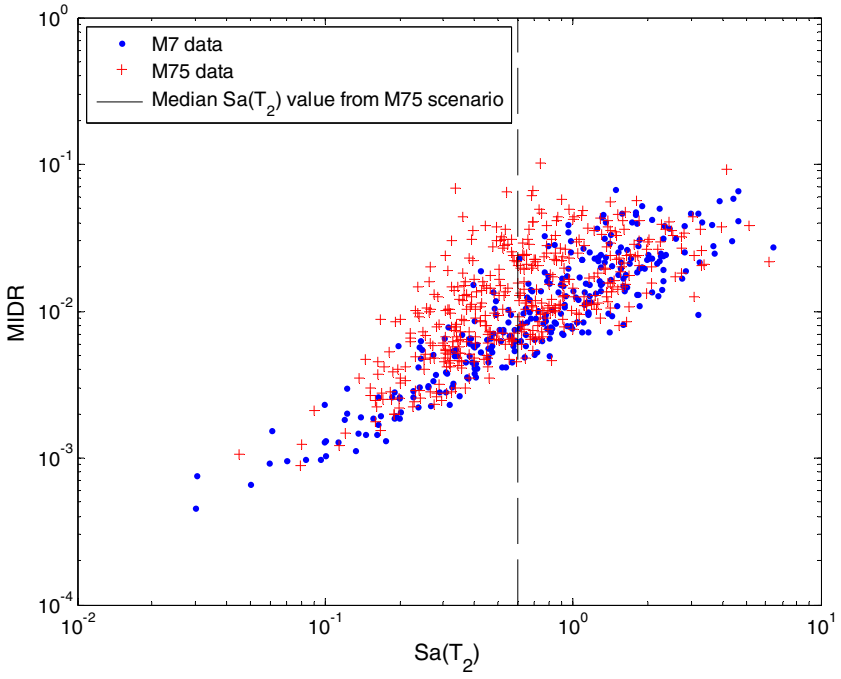

Fig. 5.8 *Sa*(T2) versus MIDR, from two sets of ground motion data of interest.

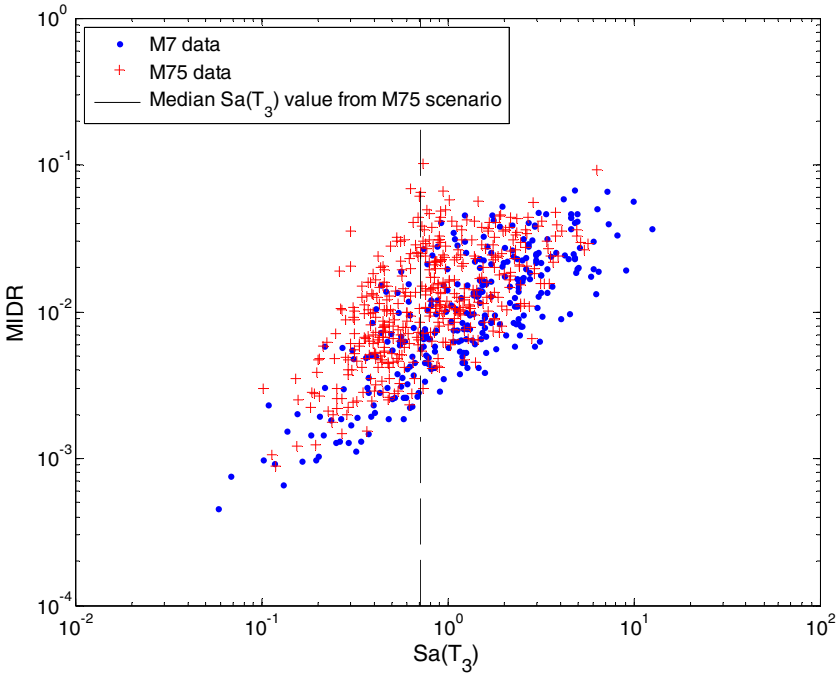

Fig. 5.9 *Sa*(T_3) versus MIDR, from two sets of ground motion data of interest.

One plausible resolution to this problem might be to simply propose using the POC of 0.0172 as it was obtained using the ground motions that most closely resemble the scenario earthquake of interest. But, as will be seen later in Chapter 10, the POC of 0.0148 much more closely matches the estimated *MIDR* values obtained from the most effective ground motion selection methods (where the effective methods are identified by their consistent match with the predicted POC in the four other building analysis cases). Because it is apparently unclear what the correct POC is in this case, the Chapter 10 analysis of this case will present results using both the 0.016 POC value from Chapter 4, and the 0.0148 value obtained here. A final resolution as to why the methodology produces unstable results in this case will be reserved for future more general research into the point-of-comparison methodology.

5.8 SUMMARY AND DISCUSSION

The point-of-comparison (POC) predictions of *MIDR* that were presented in Chapter 4 are an important foundational element of this report, as all other structural response predictions are reported relative to these estimates. One important stage in the point-of-comparison

methodology, as described in the introduction to this chapter, is development of the predictive equation using regression analysis. The purpose of this chapter was to derive predictive equations independently of the effort presented in Chapter 4, and to evaluate the extent to which differences in the identified predictive equation will result in changes to the estimated POC value. The results were presented for all four buildings considered in this report, and for both the M7 and M7.5 earthquake scenarios which are described in Chapter 3.

Predictions of the distribution of non-collapse *MIDR* for the four buildings under the M7 scenario were found to be in reasonable agreement with the comparable predictions from Chapter 4. While the functional forms and predictor variables selected here differ from those in Chapter 4, the final median *MIDR* predictions generally differed from the Chapter 4 predictions by less than 10%.

The probability-of-collapse predictions, on the other hand, differed significantly depending upon the variables chosen for use in the predictive equation. Building C, for example, resulted in probability of collapse predictions ranging from 1% to 22% depending upon the predictive model chosen. While the final predictive models selected here seem to agree with independent estimates of *P*(*Collapse*), the variation suggests that a poorly chosen predictive model could result in an grossly incorrect *P*(*Collapse*) prediction.

Building C was also studied under the M7.5 scenario, and the predicted median *MIDR* was found to be very sensitive to the set of ground motions used for calibration of the regression equation. More detailed analysis of the potential predictive equations found that the regression coefficients varied in a seemingly random manner with the ground motion set was varied. The correct median *MIDR* estimate was thus not obvious. Further work is needed to identify why this variation occurred.

In summary, with the exceptions noted in the two previous paragraphs, it appears that reasonable variations in the predictive model for *MIDR* generally result in changes to the final POC prediction of less than 10%. *This suggests that the POC numbers from Chapter 4, for the M7 event, can be interpreted as the true median MIDR* (*at least to within* +/- 10%) *for the purposes of evaluating ground motion selection methods in the following chapters.*

Finally, the variation in *MIDR* predictions caused by changes in the predictive model highlights the need to identify an accurate predictive model when using this approach. In order to obtain accurate and reproducible predictive models, the authors strongly advocate that analysts

make use of standard model selection tools such as the p-values used above for hypothesis testing. Many other model building tools, such as adjusted R^2 values, Akaike's information criterion, and stepwise regression are also very useful if the analyst has the time to use them (Burnham and Anderson 2002). These model building tools facilitate transparency in the regression model development, and make it more likely that a proposed prediction will be reproduced by another analyst repeating the methodology using the same data.

The effort expended to produce this chapter was necessarily much less than the effort expended to develop the original models of Chapter 4, but the results are nonetheless believed to provide useful qualitative information as to the stability of *MIDR* estimates obtained using the point-of-comparison methodology.

6 Findings for Modern 4-Story Reinforced Concrete Moment-Resisting Frame (Building A), Subjected to M 7.0 Scenario

Primary Author: C. A. Goulet

Associate Authors: F. Zareian, C. B. Haselton

6.1 INTRODUCTION AND OVERVIEW

This chapter is the first of five to provide structure-specific results and discussions. The results presented in this chapter are for the nonlinear dynamic response history analysis simulations of the 4-story structure labeled "Building A." An overview of the earthquake scenario and structural model is presented here for convenience, but more detailed information on these topics is available in Chapter 3. The purpose of the analyses discussed here is to evaluate how different ground motion selection and modification (GMSM) methods perform in predicting the median of maximum interstory drift ratio (MIDR) for different structures. The performance and accuracy of the results is based on the comparison of predictions relative to the point of comparison (POC) described in Chapter 4, using the ratio of predictions for a given method to the POC prediction. In each structure-specific chapter, the results are presented following the GMSM groups introduced in Chapter 2. The average of ratios for a given group of GMSM methods provides the basis for evaluating that group of GMSM.

6.1.1 Summary of Modern 4-Story Reinforced Concrete Frame (Building A)

Building A is a modern 4-story moment-resisting frame structural system with periods in the first through third modes of T = 0.97, 0.35, and 0.18 sec. The building was designed according to

2003 IBC, with a base shear coefficient V = 0.09W where W is the weight of the building. This design corresponds to an overstrength factor Ω = 2.3. The moment-resisting frame is modeled with nonlinear beam–column elements for which nonlinearity is concentrated at element end-points (e.g., lumped plasticity). The building is modeled and analyzed using OpenSEES (OpenSEES 2006). The information about component behavior properties, such as plastic hinge rotation capacity, are evaluated based on member sizes. Further information about the model can be found in Section 3.2 and in Haselton and Deierlein (2007).

6.1.2 Comparison to Other Chapters (Ground Motion Scenario and Building)

The current chapter presents the results of simulations for a 4-story building (Building A) for the M7 Scenario (M_w = 7.0, R = 10 km, ε = 2.0). This same ground motion scenario is considered in Chapters 7, 8, and 9, while Chapter 10 considers an additional M7.5 Scenario.

Building A is a ductile special moment-resisting frame structural system designed according to a current design code (2003 IBC) and it was selected to represent low-rise structural systems, which comprise a large portion of the building stock in California. Details about the design characteristics of this structure can be found in Section 3.2 and in Haselton and Deierlein (2006). For Building A and the M7 scenario, the point-of-comparison MIDR is 2.7% (Section 4.6).

6.1.3 Ground Motion Sets

Ground motion sets were selected according to the approach described in Section 3.4, which is the same method utilized for each building and ground motion scenario (Chapters 6–10).

Appendix C provides detailed documentation of each ground motion set, and the structural response predictions resulting from the set. This electronic Appendix includes Excel spreadsheet files with the ground motion filenames (from the PEER-NGA database; PEER 2006), the scale factors, and the resulting structural responses (including MIDR, individual drifts, floor accelerations, and many others). Also included are figure files showing the scaled acceleration spectra for each ground motion set.

6.2 METHOD GROUPS

The following sections present the structural response results by method groups. The grouping criteria are described in Chapter 2 but a summary is presented here for convenience. Please refer to Chapter 2 for a detailed description of each group.

- Group I: Sa(T_1) scaling (with magnitude and distance bin selection)
- Group II: building code methods (matching the uniform hazard spectrum over a given period range)
- Group III: conditional mean spectrum (CMS) matching
- Group IV: methods using a proxy for the CMS (e.g., selection based on ε)
- Group V: methods based on inelastic-response

6.3 RESPONSE RESULTS FOR GROUP I METHODS [SA(T_1) SCALING]

The Group I methods involve selecting records from a ground motion bin (magnitude and distance), and then scaling the set of records to a target Sa(T_1) level. Table 6.1 and Figure 6.1 present the MIDR response predictions for the two Group I methods. Method 100 corresponds to a generic GMSM method that uses Sa(T_1) as a basis for scaling ground motion records with a proper bin selection. Method 101 is the GMSM method recommended in the ATC-58 35% draft document in which the selection is limited to a group of 50 pre-selected records. Compared to the POC, the Sa(T_1) class of GMSM methods overestimate the median of MIDR by 48%. Method 101 provides four sets of 11 records with a median overprediction of 63%; an average of two records per set lead to structural collapse (collapse is discussed in Section 3.2.2).

Table 6.1 Median MIDR responses for sets of seven ground motions selected and scaled using Sa(T_1) methods.

					Individual Sets		All Subsets Combined	
Method Number	Method Tag	Method Name	Set Index	Num. of Rec.	Median MIDR	Ratio to POC	Median MIDR	Ratio to POC
100	4	Sa(T_1) Scaling with Bin Selection	1	7	0.0332	1.23	0.0340	1.26
100	4	Sa(T_1) Scaling with Bin Selection	2	7	0.0324	1.20		
100	4	Sa(T_1) Scaling with Bin Selection	3	7	0.0381	1.41		
100	4	Sa(T_1) Scaling with Bin Selection	4	7	0.0349	1.29		
101	67	ATC-58 35% Draft Method	1	11	0.0518	1.92	0.0439	1.63
101	67	ATC-58 35% Draft Method	2	11	0.0420	1.56		
101	67	ATC-58 35% Draft Method	3	11	0.0443	1.64		
101	67	ATC-58 35% Draft Method	4	11	0.0435	1.61		
				Median:	0.0401	**1.48**	--	--
				Average:	0.0400	1.48	--	--
				C.O.V.:	--	0.17	--	--
				Minimum:	0.0324	1.20	--	--
				Maximum:	0.0518	1.92	--	--

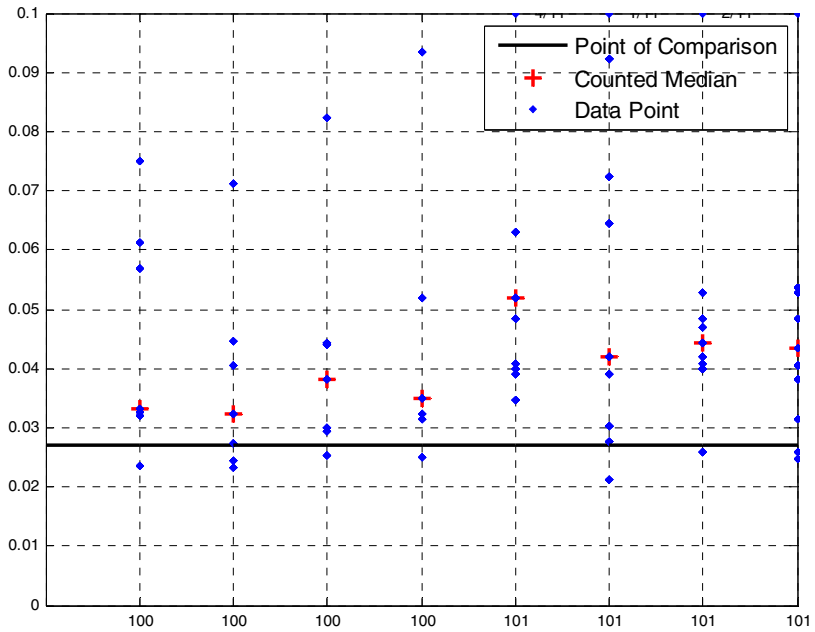

Fig. 6.1 Maximum interstory drift ratio responses for sets of seven ground motions scaled using Sa(T_1) methods.

Figure 6.2 shows the scaled acceleration spectra for methods 100 and 101. The solid black line shows the ground motion prediction equation (GMPE) prediction for the M7 scenario, and the blue dashed line shows the conditional mean spectrum (CMS, see Section 2.4.3) constrained at T_1=0.97 sec for the M7, ε=2 scenario. The red lines in Figure 6.2 represent the individual spectra from the four sets of records scaled to the target Sa(T_1) = 1.05g, and the dotted black line shows the median spectrum of the individual records. This figure shows that compared to the CMS, the median spectrum for both methods has larger spectral acceleration values for periods larger than T_1. As a result, it is expected that as Building A develops nonlinear behavior and an effective first-mode period elongation, larger estimates of MIDR would be observed from these Group I methods. Also note that the median spectra of the sets are higher than the CMS for periods shorter than T_1, suggesting that higher modes might also contribute to the response overestimation (this is especially true for method 100). As shown in Table 6.1, methods 100 and 101 overestimate the median of MIDR by an average of 26% and 69%, respectively. This overestimation of MIDR appears to be due to the incompatibility of the spectral shape of the scaled ground motion records in this class with the CMS for Building A and the M7 scenario.

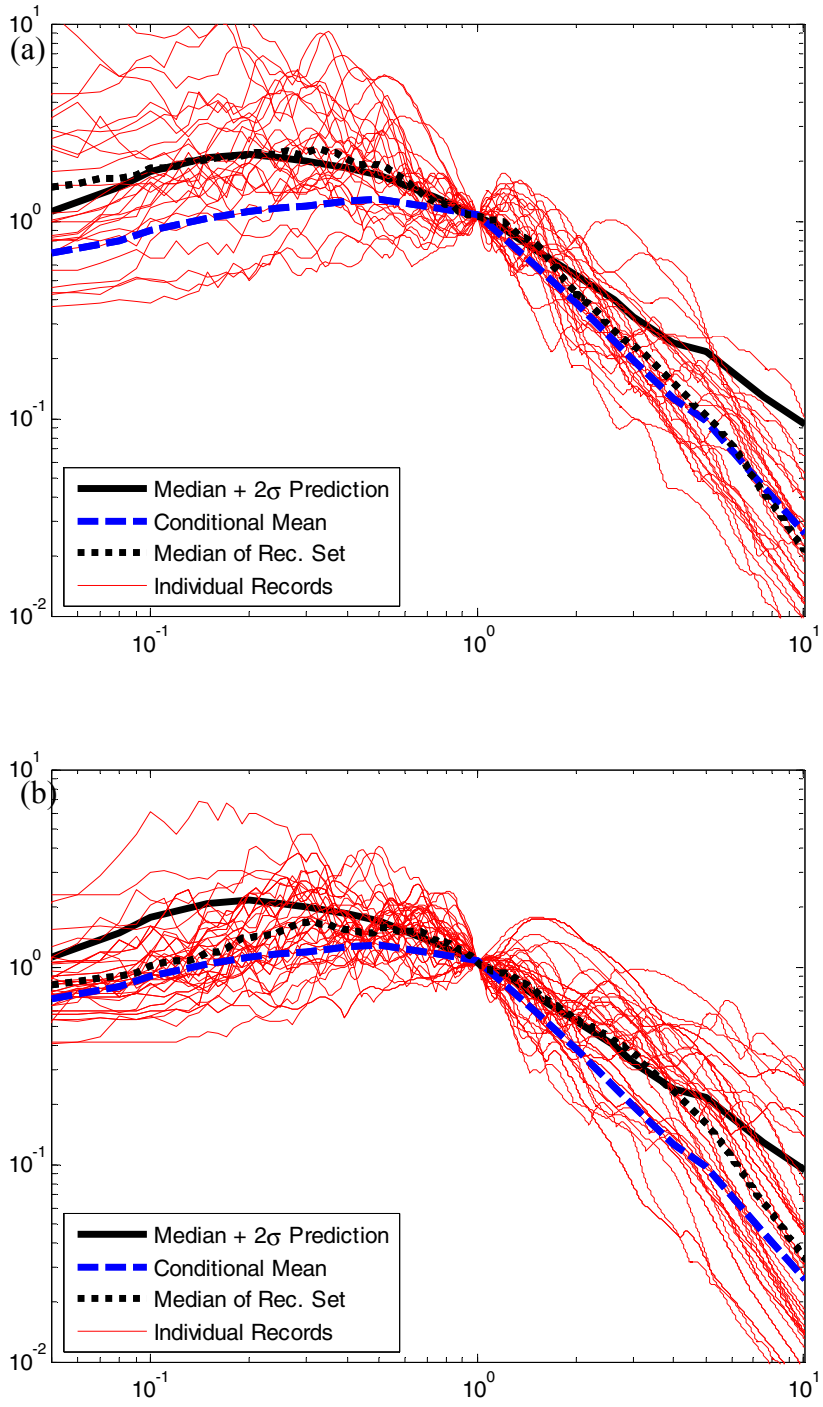

Fig. 6.2 Scaled acceleration spectra for 28 records (4 sets of 7 records each) selected with Sa(T1) scaling methods: (a) method 100 and (b) method 101.

6.4 RESPONSE RESULTS FOR GROUP II METHODS (BUILDING CODE–BASED METHODS THAT MATCH UNIFORM HAZARD SPECTRUM)

The Group II method presented in this section is based on the Uniform Building Code (UBC 1997). Table 6.2 and Figure 6.3 present the MIDR predictions for the single GMSM method (method 200) from Group II. A larger number of building code methods are presented for some of the other structures (specifically Chapters 7–8), but this chapter included only one of these methods. Compared to the POC, this method results in a median 40% overestimation of MIDR. Figure 6.4 shows the spectra for the four sets of seven records selected and scaled using method 200. The median spectrum for the selected and scaled records falls above the CMS for the first three modal periods of Building A. The scatter in estimation of the median of MIDR using method 200 is due to the large scatter in spectral values at periods larger than $T_1 = 0.97$ sec (see Fig. 6.4).

Table 6.2 Median MIDR responses for sets of seven ground motions selected and scaled using Group II methods (matching uniform hazard spectrum).

					Individual Sets		All Subsets Combined	
Method Number	Method Tag	Method Name	Set Index	Num. of Rec.	Median MIDR	Ratio to POC	Median MIDR	Ratio to POC
200	9980/39	Building Code Selection and Scaling - Method A	1	7	0.0373	1.38	0.0379	1.40
200	9980/39	Building Code Selection and Scaling - Method A	2	7	0.0413	1.53		
200	9980/39	Building Code Selection and Scaling - Method A	3	7	0.0380	1.41		
200	9980/39	Building Code Selection and Scaling - Method A	4	7	0.0377	1.40		
				Median:	0.0379	**1.40**	--	--
				Average:	0.0386	1.43	--	--
				C.O.V.:	--	0.05	--	--
				Minimum:	0.0373	1.38	--	--
				Maximum:	0.0413	1.53	--	--

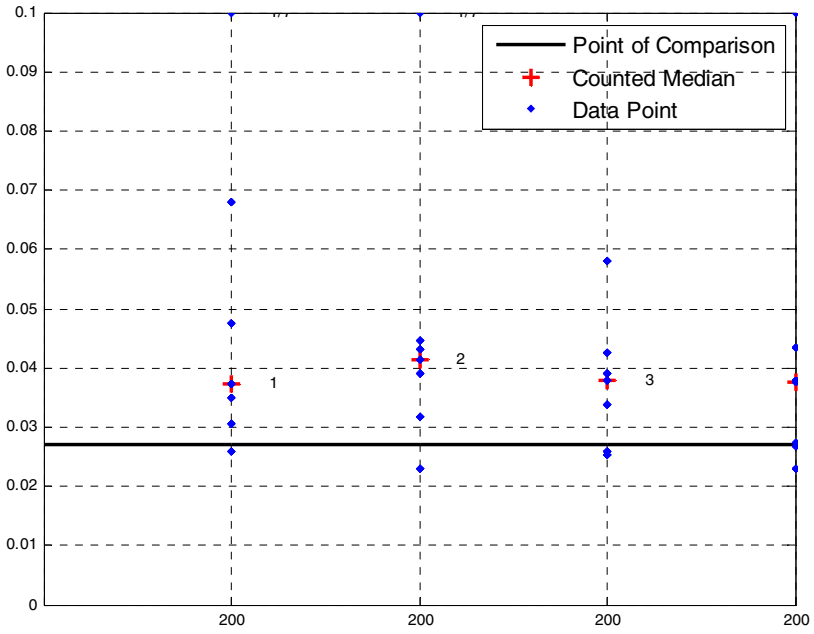

Fig. 6.3 Maximum interstory drift ratio responses for sets of seven ground motions selected and scaled using a Group II method (matching uniform hazard spectrum).

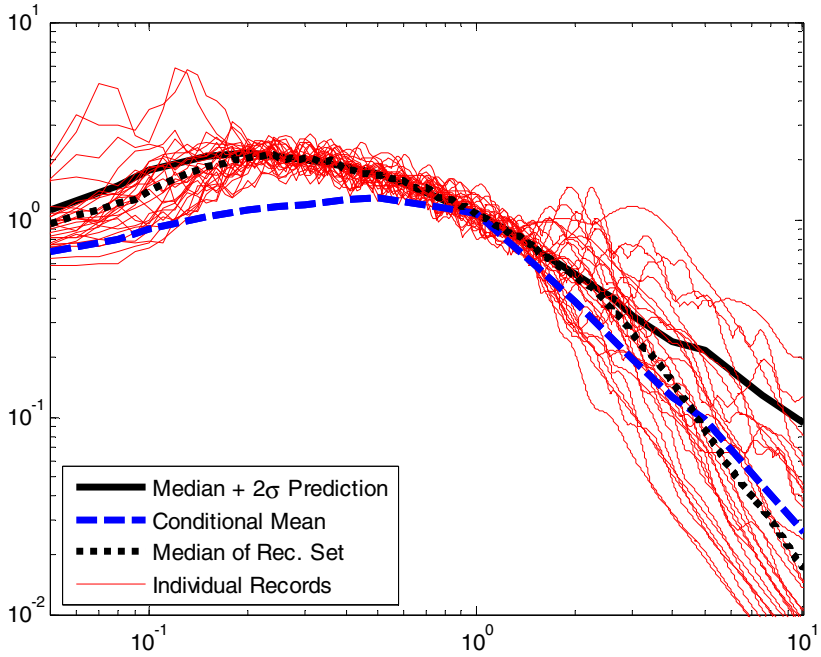

Fig. 6.4 Scaled acceleration spectra for 28 records (4 sets of 7 records each) selected with building code scaling method 200.

6.5 RESPONSE RESULTS FOR GROUP III METHODS [METHODS THAT MATCH CONDITIONAL MEAN SPECTRUM (CMS)]

For this building and scenario, the best estimates of median MIDR are provided by the methods that try to match the CMS. Recall that for the CMS, the spectral acceleration at T_1 is defined and the rest of the spectrum is obtained by correlations of expected values at other periods. The CMS, due to the way it is constructed, has the ability to represent the *correct* general spectral shape of a single earthquake scenario, while the UHS, by definition, comprises contributions from multiple earthquake scenarios.

Table 6.3 and Figure 6.5 present the median of MIDR predictions using the three individual Group III methods. These methods lead to a median overestimation of MIDR by +4% compared to the POC. Figure 6.6 shows the methods 300 and 304 scaled spectra, it is expected that the scatter in estimation of median MIDR will be larger for method 304, since method 304 is aimed to predict both the median and dispersion of response (Objectives 3 and 4) rather than just the median response (Objective 4). Table 6.3 shows the results of this additional scatter in the

predictions; the method 304 estimates of the median of MIDR vary from 3% underestimation to 53% overestimation of the POC, while the method 300 estimates vary only from +1% to +9% above the POC.

Table 6.3 Median MIDR responses for sets of seven ground motions selected and scaled using Group III methods.

					Individual Sets		All Subsets Combined	
Method Number	Method Tag	Method Name	GM Set Index	Number of Records	Median MIDR	Ratio to POC	Median MIDR	Ratio to POC
300	10	Conditional Mean Spectrum Selection with Scaling	1	7	0.0275	1.02	0.0274	1.01
300	10	Conditional Mean Spectrum Selection with Scaling	2	7	0.0294	1.09		
300	10	Conditional Mean Spectrum Selection with Scaling	3	7	0.0273	1.01		
300	10	Conditional Mean Spectrum Selection with Scaling	4	7	0.0274	1.02		
301	15	Genetic Algorithm Selection (to match CMS)	1	7	0.0451	1.67	0.0451	1.67
302	24	Semi-Automated Selection & Scaling (to match CMS)	1	7	0.0287	1.06	0.0287	1.06
304	45	Design Ground Motion Library (DGML) (Objective 3-4)	1	7	0.0370	1.37	0.0367	1.36
304	45	Design Ground Motion Library (DGML) (Objective 3-4)	2	7	0.0294	1.09		
304	45	Design Ground Motion Library (DGML) (Objective 3-4)	3	7	0.0261	0.97		
304	45	Design Ground Motion Library (DGML) (Objective 3-4)	4	7	0.0412	1.53		
				Median:	0.0281	**1.04**	--	--
				Average:	0.0309	1.14	--	--
				C.O.V.:	--	0.23	--	--
				Minimum:	0.0273	1.01	--	--
				Maximum:	0.0451	1.67	--	--

*For consistency of comparisons, Objective 3 method is not included in the summary statistics.

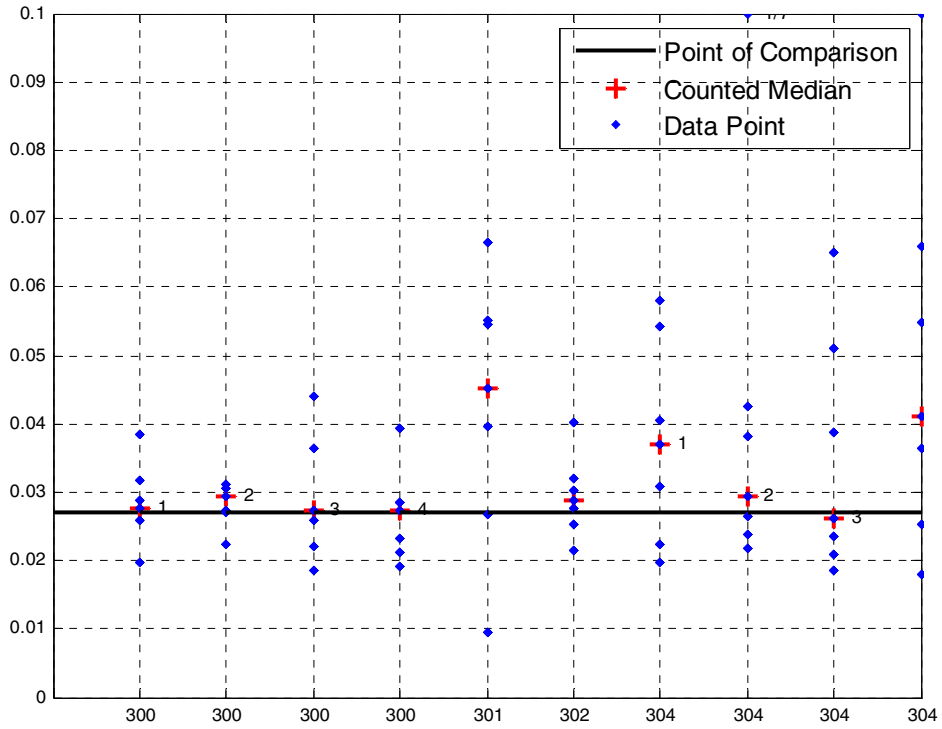

Fig. 6.5 Maximum interstory drift ratio responses for sets of seven ground motions selected and scaled using Group III methods.

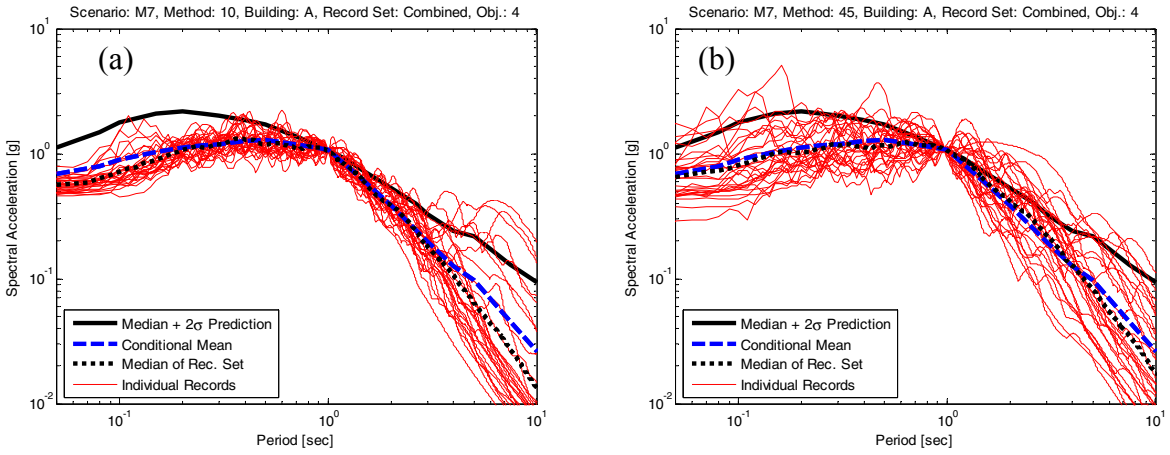

Fig. 6.6 Scaled acceleration spectra for two Group III methods: (a) method 300 and (b) method 304.

6.6 RESPONSE RESULTS FOR GROUP IV METHODS (METHODS THAT USE EPSILON PROXY FOR CMS)

The Group IV methods use an *indicator* of the spectral shape (or a *proxy* for the spectral shape), rather than directly matching the shape of the CMS. This indicator is (or at least involves) the parameter epsilon (ε), which is defined as the number of standard deviations between the natural logarithm of an observed Sa(T) value and the natural logarithm of the median Sa(T) value predicted by a GMPE. In this section, methods that use epsilon (ε) as a proxy for spectral shape in the selection and scaling process are evaluated. Because these methods indirectly consider the CMS spectral shape, we expect that the median of MIDR can be estimated with a similar accuracy to that of Group III methods.

Table 6.4 and Figure 6.7 present results for two methods that use ε as a proxy for the CMS. Overall, the median overestimation of MIDR is 5% when these methods are used. method 400 underestimates the median compared to the POC by an average of 8%, whereas method 401 overestimates the median by 13%. This inconsistency between the results of two methods can be explained by studying the spectra of records used in each method. Figure 6.8 shows the spectra for the combined set of 28 records for methods 400 and 401. Comparison between the spectra of two sets of records shows that using ε as a proxy for CMS leads to records that tend to match the CMS well. However, Figure 6.8b shows that the median of the records obtained using method 401 is slightly above the CMS for periods larger than T_1. This results in an overestimation of the median of MIDR compared to POC with a relatively large scatter. Figure 6.8a shows results for method 400. This method was originally developed to scale pairs of records according to the geometric mean of their two horizontal components. For these simulations, the method was not modified and the scaling was applied to the geometric mean of the records, resulting in spectra that envelope the CMS with a fairly large variability (the spectra are not pinned at T_1). The median spectrum is slightly higher than the CMS at shorter periods (exciting higher modes) and slightly lower than the CMS at periods larger than T_1, creating a somewhat compensating effect with a net underprediction of the median MIDR. Further studies using records scaled relative to the individual components are required to validate the efficiency of this method.

Table 6.4 Median MIDR responses for sets of seven ground motions selected and scaled based on proxy for spectral shape.

					Individual Sets		All Subsets Combined	
Method Number	Method Tag	Method Name	Set Index	Num. of Rec.	Median MIDR	Ratio to POC	Median MIDR	Ratio to POC
400	20	Target Spectrum Based on Epsilon Correlations	1	7	0.0270	1.00	0.0248	0.92
400	20	Target Spectrum Based on Epsilon Correlations	2	7	0.0305	1.13		
400	20	Target Spectrum Based on Epsilon Correlations	3	7	0.0206	0.76		
400	20	Target Spectrum Based on Epsilon Correlations	4	7	0.0227	0.84		
401	31	ε Selection with $S_{de}(T_1)$ Scaling	1	7	0.0442	1.64	0.0305	1.13
401	31	ε Selection with $S_{de}(T_1)$ Scaling	2	7	0.0320	1.18		
401	31	ε Selection with $S_{de}(T_1)$ Scaling	3	7	0.0279	1.03		
401	31	ε Selection with $S_{de}(T_1)$ Scaling	4	7	0.0290	1.07		
				Median:	0.0285	**1.05**	--	--
				Average:	0.0292	1.08	--	--
				C.O.V.:	--	0.24	--	--
				Minimum:	0.0206	0.76	--	--
				Maximum:	0.0442	1.64	--	--

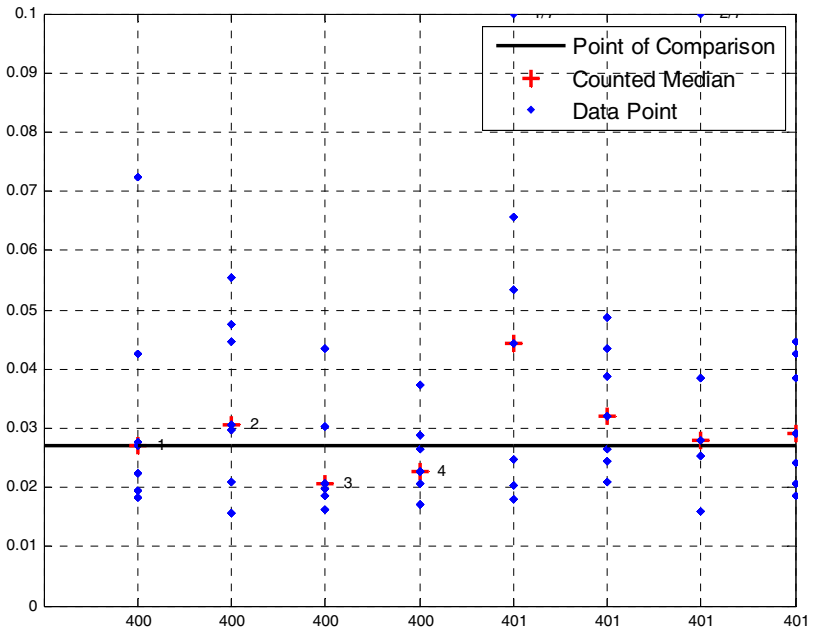

Fig. 6.7 Maximum interstory drift ratio responses for sets of seven ground motions selected and scaled using Group IV methods.

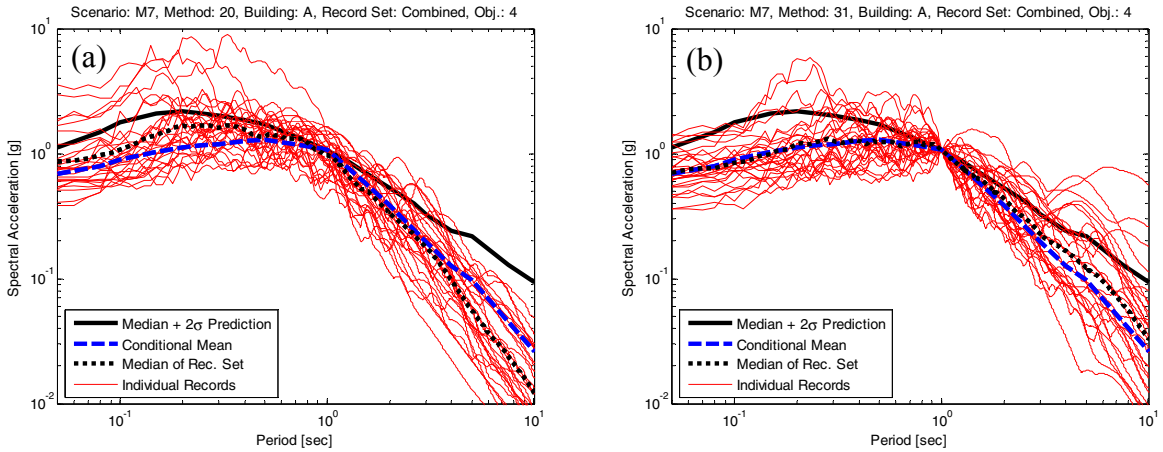

Fig. 6.8 Scaled acceleration spectra for combined set of 28 records selected using methods that use ε proxy for GMSM: (a) method 400, (b) method 401.

6.7 RESPONSE RESULTS FOR GROUP V METHODS (INELASTIC-BASED METHODS)

The Group V methods utilize some type of inelastic parameter (e.g., inelastic spectral displacement) and/or results of inelastic structural analysis (e.g., nonlinear static pushover) for the record selection and scaling.

Table 6.5 and Figure 6.9 present the MIDR predictions for four Group V methods. These methods result in a median overprediction of MIDR response by 28%. Table 6.5 shows that method 501 performs better and underpredicts the MIDR median by only 4%. Methods 500 and 503 overestimate the median MIDR by 40% and 39%, respectively. These methods were expected to work well because they consider nonlinear response. However, a problem arises when the target is defined based on elastic spectral ordinates (as is the case for the scenarios used in this study) and when the POC prediction is also based on elastic spectral values, because there is a mismatch between the elastic and inelastic metrics that requires a mapping between the two. This issue needs to be investigated further, and is discussed in Sections 3.3.1 and 5.2, respectively.

Figure 6.10 shows the individual spectra for each of the inelastic methods. Method 501 (Fig. 6.10b) is the one that provided the best prediction relative to the POC. Nonetheless, the spectra do not follow the CMS closely, but present the same compensation effects as for method 400 (see discussion above). The net result in this case is a slight overprediction of the median

MIDR (by 4%). For methods 500 and 503 (Figs. 6.10a and d), the median spectra closely follows the CMS for periods up to T_1, but lie above for larger periods. This seems to explain the larger overprediction in MIDR. Finally, method 502b (Fig. 6.10c) presents the opposite trend: the median spectrum is larger than the CMS for periods shorter that T_1, but agrees well with the CMS at larger periods. This leads to an overprediction due to a larger excitation of the higher-mode periods. This overprediction is much smaller than the one seen for methods 500 and 503 (17% compared to 39% or 40%) because the participation factors for higher modes is smaller than for the first mode.

Table 6.5 Median MIDR responses for sets of seven ground motions selected and scaled using Group V methods.

					Individual Sets		All Subsets Combined	
Method Number	**Method Tag**	**Method Name**	**Set Index**	**Num. of Rec.**	**Median MIDR**	**Ratio to POC**	**Median MIDR**	**Ratio to POC**
500	27	$S_{di}(T_1, dy)$ Scaling	1	7	0.0345	1.28	0.0378	1.40
500	27	$S_{di}(T_1, dy)$ Scaling	2	7	0.0391	1.45		
500	27	$S_{di}(T_1, dy)$ Scaling	3	7	0.0491	1.82		
500	27	$S_{di}(T_1, dy)$ Scaling	4	7	0.0364	1.35		
501	6	Vector of Record Properties Identified by Proxy	1	7	0.0285	1.06	0.0281	1.04
501	6	Vector of Record Properties Identified by Proxy	2	7	0.0276	1.02		
501	6	Vector of Record Properties Identified by Proxy	3	7	0.0232	0.86		
501	6	Vector of Record Properties Identified by Proxy	4	7	0.0310	1.15		
502a	11	Inelastic Response Surface Scaling (1st mode)	1	7	0.0317	1.17	0.0317	1.17
503	35	IM1I&2E Selection/Scaling	1	7	0.0314	1.16	0.0375	1.39
503	35	IM1I&2E Selection/Scaling	2	7	0.0388	1.44		
503	35	IM1I&2E Selection/Scaling	3	7	0.0461	1.71		
503	35	IM1I&2E Selection/Scaling	4	7	0.0362	1.34		
			Median:		0.0345	**1.28**	--	--
			Average:		0.0349	1.29	--	--
			C.O.V.:		--	0.21	--	--
			Minimum:		0.0232	0.86	--	--
			Maximum:		0.0491	1.82	--	--

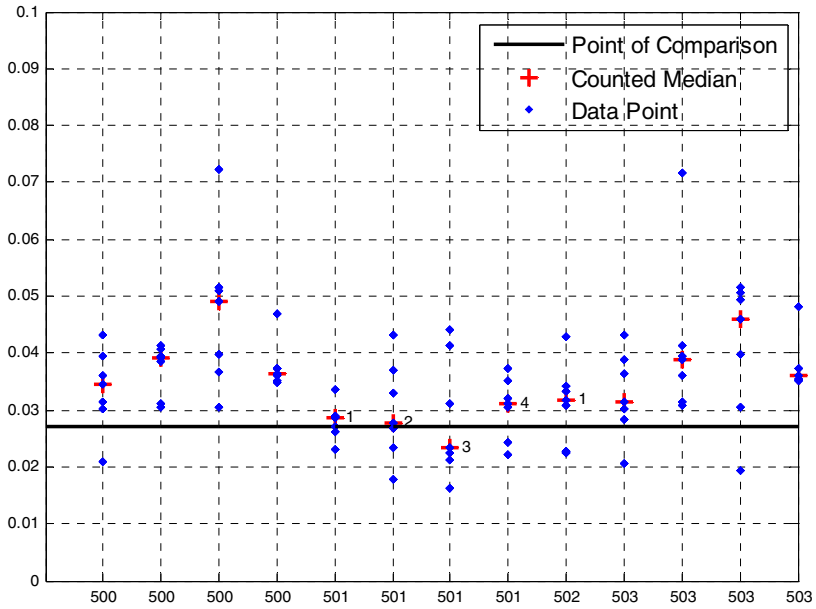

Fig. 6.9 Maximum interstory drift ratio responses for sets of seven ground motions selected and scaled using Group V methods.

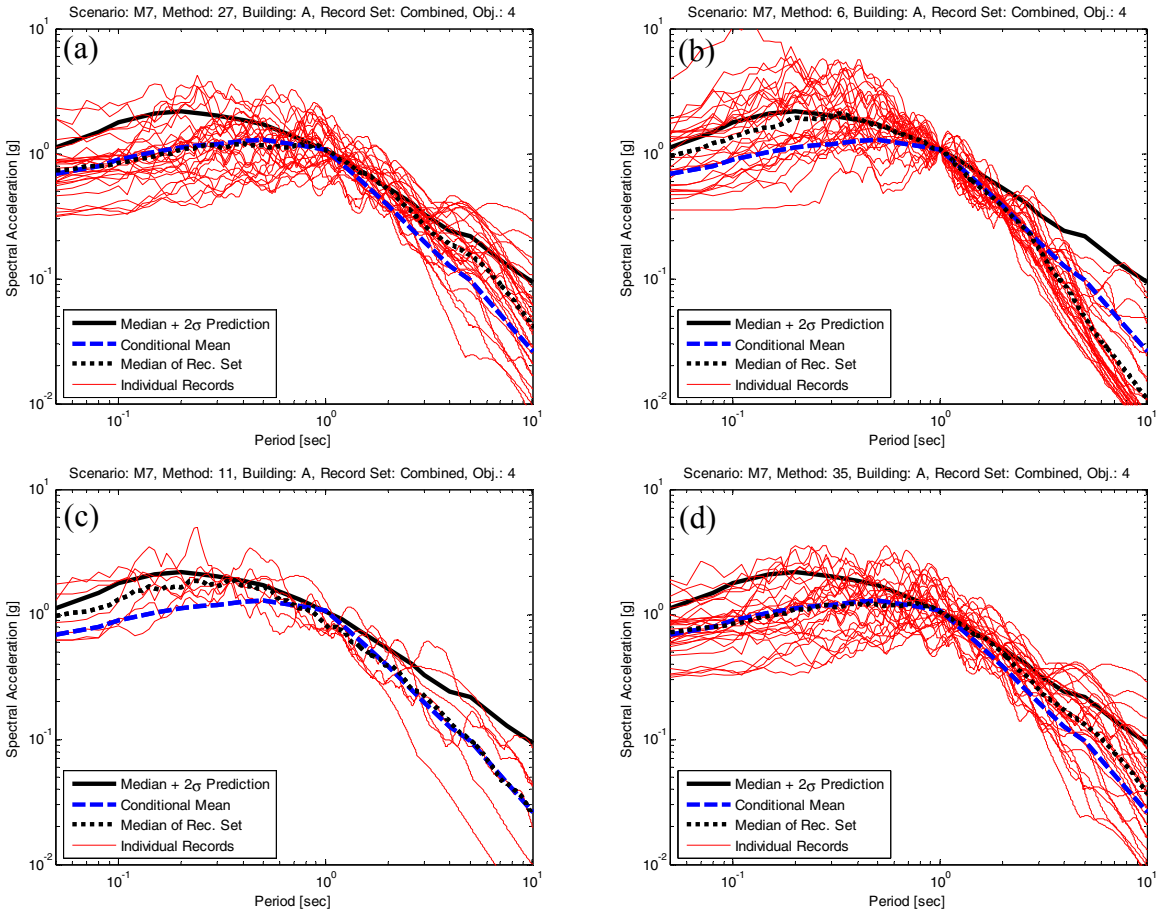

Fig. 6.10 Scaled acceleration spectra for records selected using inelastic methods for GMSM: (a) method 500, (b) method 501, (c) method 502b, (d) method 503.

6.8 SUMMARY AND CONCLUSIONS

6.8.1 Summary of Results by Method Group

Table 6.6 summarizes the prediction accuracies by method groups for this 4-story modern RC frame building. This table shows summary statistics for the estimation bias factor computed as the ratio of the median MIDR response to the point-of-comparison (POC) prediction. Note that the groups are not equally populated; for example, Group II consists of only a single method. The results show that Groups III (CMS matching) and IV (proxy for the CMS) methods result in a prediction that is fairly accurate (with a median overprediction of only 4% and 5% respectively), with coefficients of variation (c.o.v.) of 0.22–0.24. In contrast, methods that do not consider the spectral shape in any way (i.e., Groups I and II methods) lead to an overestimation

of the MIDR median of 40% and 48%. This shows the significance of considering spectral shape in the selection and scaling ground motions, at least for structures exhibiting a strong first-mode response such as this one. For this round of simulations, the Group V methods lead to an average overprediction of MIDR of 28% relative to the POC. A mismatch between the specified scenario (the *elastic* spectral acceleration of the building was provided as the target along with the scenario) and the method (based on *inelastic* response) mostly controls this discrepancy. Although inelastic methods were expected to perform well, this exercise simulation highlighted the implementation challenges these methods face in the correct state of engineering practice.

Based on the results of this chapter, the average prediction capability of the method groups can be ordered as follows. Note that these results are generalized for method groups only and that some methods might lead to a better prediction within a group.

- Group III [CMS matching]
- Group IV [proxy methods (e.g., ε)]
- Group V [inelastic-based methods]
- Group II [building code methods]
- Group I [$Sa(T_1)$ methods]

Note that these results are only applicable to this specific building (design and computer model) and scenario. The results for three different buildings are presented in Chapters 7-9 for this same M7 scenario.

Table 6.6 Summary of median of MIDR estimation bias factor by method group.

MIDR/POC	I: $Sa(T_1)$	II: UHS	III: CMS	IV: Proxy (i.e. ε)	V: Inelastic
Median:	1.48	1.40	1.04	1.05	1.28
Average:	1.48	1.43	1.14	1.08	1.29
C.O.V.:	0.17	0.05	0.22	0.24	0.21
Minimum:	1.20	1.38	1.01	0.76	0.86
Maximum:	1.92	1.53	1.67	1.64	1.82

6.8.2 Closing Comments

The discussions provided in this chapter include evaluation of a total of 12 GMSM methods in 5 classes, and highlights the importance of considering the spectral shape in selection and scaling of ground motion records for proper estimation of the median MIDR. This is true for the current structure and scenario combination. It was concluded that more accurate and precise estimation of the MIDR median can be provided by GMSM methods that utilize the CMS. The methods that use ε as a proxy for the spectral shape show fairly good MIDR predictions as well but exhibit a larger scatter.

The prediction capabilities of these methods will now be evaluated for three additional buildings for this same M7 scenario, and the results are presented in Chapters 7, 8, and 9. Chapter 10 then will present the results of Building C subjected to an M7.5 ground motion scenario, and then general conclusions based on all the structural simulations will be presented in Chapter 11.

7 Findings for Modern 12-Story Reinforced Concrete Moment-Frame Building (Building B) Subjected to M 7.0 Scenario

Primary Author: J. W. Baker

Associate Author: C. B. Haselton

7.1 INTRODUCTION AND OVERVIEW

In this chapter, we use 15 ground motion selection and modification (GMSM) methods (23 methods if variations are included) to predict the maximum interstory drift ratio (MIDR) response of a modern (ductile) 12-story reinforced concrete (RC) frame building (termed Building B). This building was investigated because it is a relatively mid-rise building somewhat sensitive to second-mode response, although less sensitive than the frame building studied in the following chapter (thus allowing for a study of the impact of varying contributions to second-mode response). Additionally, it was designed using current building codes and could thus represent a new building designed using performance-based design approaches (for which GMSM is important).

Following the pattern of Chapter 5, this chapter presents structural response results by the GMSM method group. For each group, the MIDR predictions are presented for the individual methods in that group, and the predictions are compared to the point of comparison (POC). For this building and scenario, the POC (i.e., the expected MIDR response) is 2.2% interstory drift (according to Section 4.6). Comparing the predicted responses to the POC serves as the basis for evaluating the prediction capability of the group of methods. When appropriate, the results of individual methods are also highlighted when their predictions differ substantially from other methods in their group.

This chapter concludes the observation that for this study, consideration of spectral shape appears to be critical. The most effective way to do this is by matching directly to the conditional mean spectrum. Unlike other chapters in this report, it is seen that for this building, some other advanced methods that rely on spectral shape proxies or inelastic predictors produce significant overestimations of response. Some basic explanations for this finding are presented below. The primary explanation for this discrepancy is that the results from inelastic-based methods (later referred to as numbers 500, 502, and 503) are not comparable with the POC, because the earthquake records are scaled to an Sdi target and not the Sa target. Thus, the results are not incorrect, but rather attempting to answer a different question. Future work will reconcile these results and compare them more generally.

7.1.1 Summary of Modern 12-Story Reinforced Concrete Building (Building B)

The structural model utilized in this chapter is a 12-story RC perimeter frame building designed according to the ASCE 7-02 (ASCE 2002) and ACI 318-02 (ACI 2002) design requirements, and modeled utilizing the OpenSEES open source software package (OpenSEES 2006). Section 3.2, describes the design and model in more detail. This model was created as part of the Applied Technology Council Project ATC-63 (FEMA 2009) and doctoral research by Haselton (Haselton and Deierlein 2007). In the course of those projects, the structural design was reviewed in detail by practicing structural engineers. The building fundamental period is 2.01 sec.

One unique property of this structure relative to the other buildings considered is that it collapses more often at the design ground motion level. In this study, "collapse" is used to describe side-sway collapse, in which the building becomes dynamically unstable, and the displacements increase without bounds. In some cases, four or more ground motions from a set of seven will cause collapse, and so for those cases a median response cannot be reported. In all cases, however, the median of the larger set of ground motions from a method (typically 28 ground motions) can be computed, so summary statistics can still be reported as usual.

7.1.2 Comparison to Other Chapters (Ground Motion Scenario, and Building)

The current chapter presents the results of simulations for a 12-story building (Building B) for the M7 scenario (M_w = 7.0, R = 10 km, ε = 2.0). This same ground motion scenario is considered in Chapters 6, 8, and 9, while Chapter 10 considers an additional M7.5 scenario.

Building B is a ductile special moment-resisting frame structural system designed according to a current design code (2003 IBC) and it was selected to represent mid-rise structural systems. Details about the design characteristics of this structure can be found in Section 3.2 and in Haselton and Deierlein (2007). For Building B and the M7 scenario, the point-of-comparison MIDR is 2.2% (Section 4.6).

7.1.3 Ground Motion Sets

Ground motion sets were selected according to the approach described in Section 3.4, which is the same method utilized for each building and ground motion scenario (Chapters 6–10).

Appendix C provides detailed documentation of each ground motion set, and the structural response predictions resulting from the set. This electronic Appendix includes Excel spreadsheet files with the ground motion filenames (from the PEER-NGA database; PEER 2006), the scale factors, and the resulting structural responses (including MIDR, individual drifts, floor accelerations, and many others). Also included are figure files showing the scaled acceleration spectra for each ground motion set.

7.2 METHOD GROUPS

The following sections present the structural response results by method groups. The results are presented following the groups established in Section 2.4. Chapter 2 explains the basis of each of these method groups

- Group I: Sa(T_1) scaling (with bin selection)
- Group II: building code methods (matching to the uniform hazard spectrum)
- Group III: conditional mean spectrum (CMS) matching
- Group IV: methods using a proxy for the CMS (e.g., selection based on ε)
- Group V: inelastic-based methods

7.3 RESPONSE RESULTS FOR GROUP I METHODS [SA(T_1) SCALING METHODS]

The Group I methods involve selecting records from a ground motion bin and then scaling the set of records to a target Sa(T_1) level. This is described in detail in Section 2.4.1.

Table 7.1 and Figure 7.1 present the maximum interstory drift ratio response predictions for the two Sa(T_1) methods. As compared to the POC, these methods have a median response overprediction of 55%. Note that at the top of Figure 7.1, points are shown at an MIDR of 0.08 if the given ground motion caused a collapse. Text labels by those points indicate what fraction of ground motions from the set caused collapse. The collapsed cases are considered when computing the counted median MIDR response, so if four or more out of a set of seven ground motions caused collapse, then no median value is reported in Table 7.1. Because counted medians are used to summarize these results, we avoid problems that would arise when considering a mean value of MIDR in the presence of collapses.

Table 7.1 Median MIDR responses for sets of seven ground motions scaled using Group I methods.

					Individual Sets		All Subsets Combined	
Method Number	Method Tag	Method Name	GM Set Index	Number of Records	Median MIDR	Ratio to POC	Median MIDR	Ratio to POC
100	4	Sa(T_1) Scaling with Bin Selection	1	7	0.0261	1.19	0.0366	1.66
100	4	Sa(T_1) Scaling with Bin Selection	2	7	0.0579	2.63		
100	4	Sa(T_1) Scaling with Bin Selection	3	7	*collapse*	*collapse*		
100	4	Sa(T_1) Scaling with Bin Selection	4	7	0.0264	1.20		
101	67	ATC-58 35% Draft Method	1	11	0.0276	1.25	0.0367	1.67
101	67	ATC-58 35% Draft Method	2	11	*collapse*	*collapse*		
101	67	ATC-58 35% Draft Method	3	11	0.0303	1.38		
101	67	ATC-58 35% Draft Method	4	11	0.0379	1.72		
				Median:	0.034	**1.55**	--	--
				Average:	--	--	--	--
				C.O.V.:	--	--	--	--
				Minimum:	0.026	1.19	--	--
				Maximum:	*collapse*	*collapse*	--	--

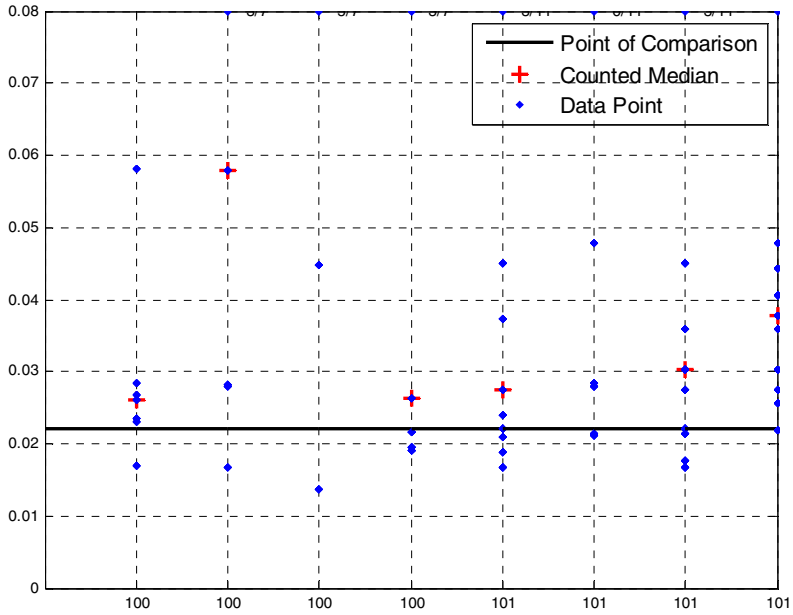

Fig. 7.1 Maximum interstory drift ratio responses for sets of seven ground motions scaled using Group I methods.

Table 7.1 shows that this overestimation is very consistent between the two methods. That is not universally the case, however, based on the corresponding results for other buildings. The two methods seem to produce comparable results overall, but the median response result for a given ground motion set varies based on the specific properties of those records. What is seen consistently, however, is that both of these methods consistently overpredict response relative to the POC or the more advanced methods considered below.

For further information, the response spectra of these two record sets are shown in Figure 7.2. If one takes the conditional mean spectrum as a target spectrum, we see that both of the methods in this section have spectra that typically exceed this target at short periods (and instead closely match the UHS), although they provide a reasonable match with the conditional mean spectrum at longer periods. The higher observed spectral values at short periods are likely the reason for the large response results observed from both of these methods; for this building, the second- and third-mode periods are 0.68 and 0.39 sec.

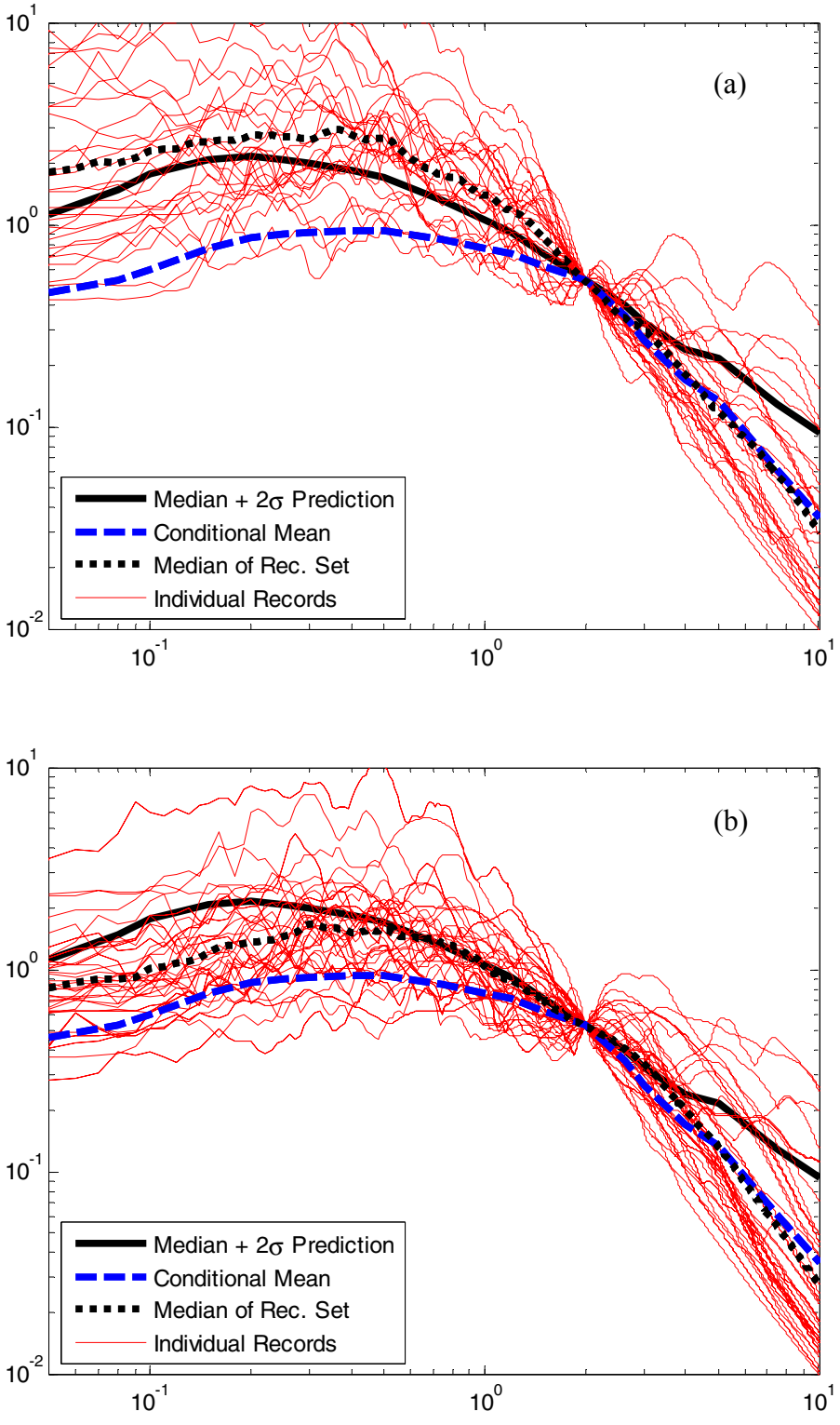

Fig. 7.2 Scaled acceleration spectra for 28 records (4 sets of 7 records each for Group I methods (a) 100 and (b) 101.

7.4 RESPONSE RESULTS FOR GROUP II METHODS (BUILDING CODE–BASED METHODS THAT MATCH UNIFORM HAZARD SPECTRUM)

The building code-based methods presented in this section include various interpretations of the requirements of the Uniform Building Code (UBC 1997) and the ASCE 7-05 (ASCE 2005). For brevity, the detailed differences between these sets are not presented here, but left to a forthcoming publication on this topic. Even so, the exhaustive results are presented below, to illustrate the variability in prediction that can result from the differences in various building code requirements, as well as differences in interpretation of these requirements.

Figure 7.3 illustrates a set of seven records selected using building code methods (method 206, set one). This illustrates that the median spectrum exceeds the uniform hazard spectrum (UHS) at all periods from $0.2T_1$ to $1.5T_1$, as required by the building code provisions. Note that for the M7 scenario used in this study, there is a single event with $M_w = 7.0$ and R = 10 km that defines the hazard; therefore, the UHS and the median + 2σ spectrum are identical.

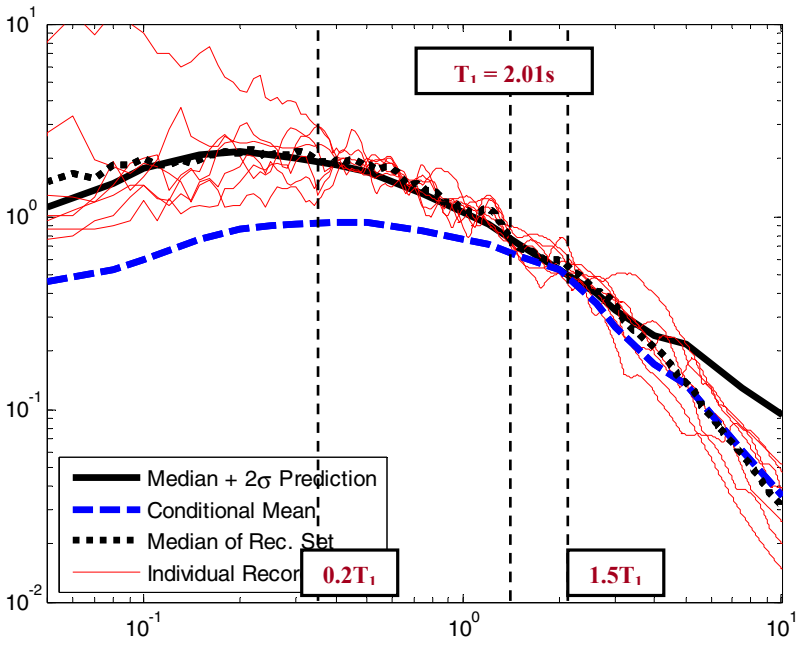

Fig. 7.3 Scaled acceleration spectra for one set of seven records selected using building code methods that match or exceed uniform hazard spectrum (method 206).

Table 7.2 and Figure 7.4 present the maximum interstory drift ratio response predictions for all variants of the building code-based methods. As compared to the POC, these methods have a median MIDR response overprediction of 39%. In addition, the scatter leads to a wide range of predictions from the various methods, from 20% to 87% above the POC. Some individual sets of seven records produce median predictions that are more than double the POC.

Table 7.2 Median MIDR responses for sets of seven ground motions selected and scaled using Group II methods.

					Individual Sets		All Subsets Combined	
Method Number	Method Tag	Method Name	GM Set Index	Number of Records	Median MIDR	Ratio to POC	Median MIDR	Ratio to POC
200	9980	Building Code Selection and Scaling - Method A	1	7	0.0266	1.21	0.0265	1.20
200	9980	Building Code Selection and Scaling - Method A	2	7	0.0211	0.96		
200	9980	Building Code Selection and Scaling - Method A	3	7	0.0320	1.45		
200	9980	Building Code Selection and Scaling - Method A	4	7	0.0165	0.75		
201	9981	Building Code Selection and Scaling - Method B	1	7	0.0266	1.21	0.0277	1.26
201	9981	Building Code Selection and Scaling - Method B	2	7	0.0465	2.11		
201	9981	Building Code Selection and Scaling - Method B	3	7	0.0320	1.45		
201	9981	Building Code Selection and Scaling - Method B	4	7	0.0200	0.91		
202	9982	Building Code Selection and Scaling - Method C	1	7	0.0487	2.21	0.0412	1.87
202	9982	Building Code Selection and Scaling - Method C	2	7	*collapse*	*collapse*		
202	9982	Building Code Selection and Scaling - Method C	3	7	0.0299	1.36		
202	9982	Building Code Selection and Scaling - Method C	4	7	0.0338	1.54		
203	9983	Building Code Selection and Scaling - Method D	1	7	0.0268	1.22	0.0272	1.24
203	9983	Building Code Selection and Scaling - Method D	2	7	*collapse*	*collapse*		
203	9983	Building Code Selection and Scaling - Method D	3	7	0.0204	0.93		
203	9983	Building Code Selection and Scaling - Method D	4	7	0.0287	1.30		
204	9984	Building Code Selection and Scaling - Method E	1	7	0.0286	1.30	0.0340	1.55
204	9984	Building Code Selection and Scaling - Method E	2	7	0.0299	1.36		
204	9984	Building Code Selection and Scaling - Method E	3	7	*collapse*	*collapse*		
204	9984	Building Code Selection and Scaling - Method E	4	7	*collapse*	*collapse*		
205	9985	Building Code Selection and Scaling - Method F	1	7	0.0328	1.49	0.0320	1.45
205	9985	Building Code Selection and Scaling - Method F	2	7	0.0412	1.87		
205	9985	Building Code Selection and Scaling - Method F	3	7	0.0312	1.42		
205	9985	Building Code Selection and Scaling - Method F	4	7	0.0271	1.23		
206	9986	Building Code Selection and Scaling - Method G	1	7	0.0361	1.64	0.0355	1.61
206	9986	Building Code Selection and Scaling - Method G	2	7	0.0489	2.22		
206	9986	Building Code Selection and Scaling - Method G	3	7	0.0350	1.59		
206	9986	Building Code Selection and Scaling - Method G	4	7	0.0279	1.27		
209	9989	Building Code Selection and Scaling - Method J	1	7	0.0268	1.22	0.0268	1.22
209	9989	Building Code Selection and Scaling - Method J	2	9	0.0268	1.22		
				Median:	0.031	**1.39**	--	--
				Average:	--	--	--	--
				C.O.V.:	--	--	--	--
				Minimum:	0.017	0.75	--	--
				Maximum:	*collapse*	*collapse*	--	--

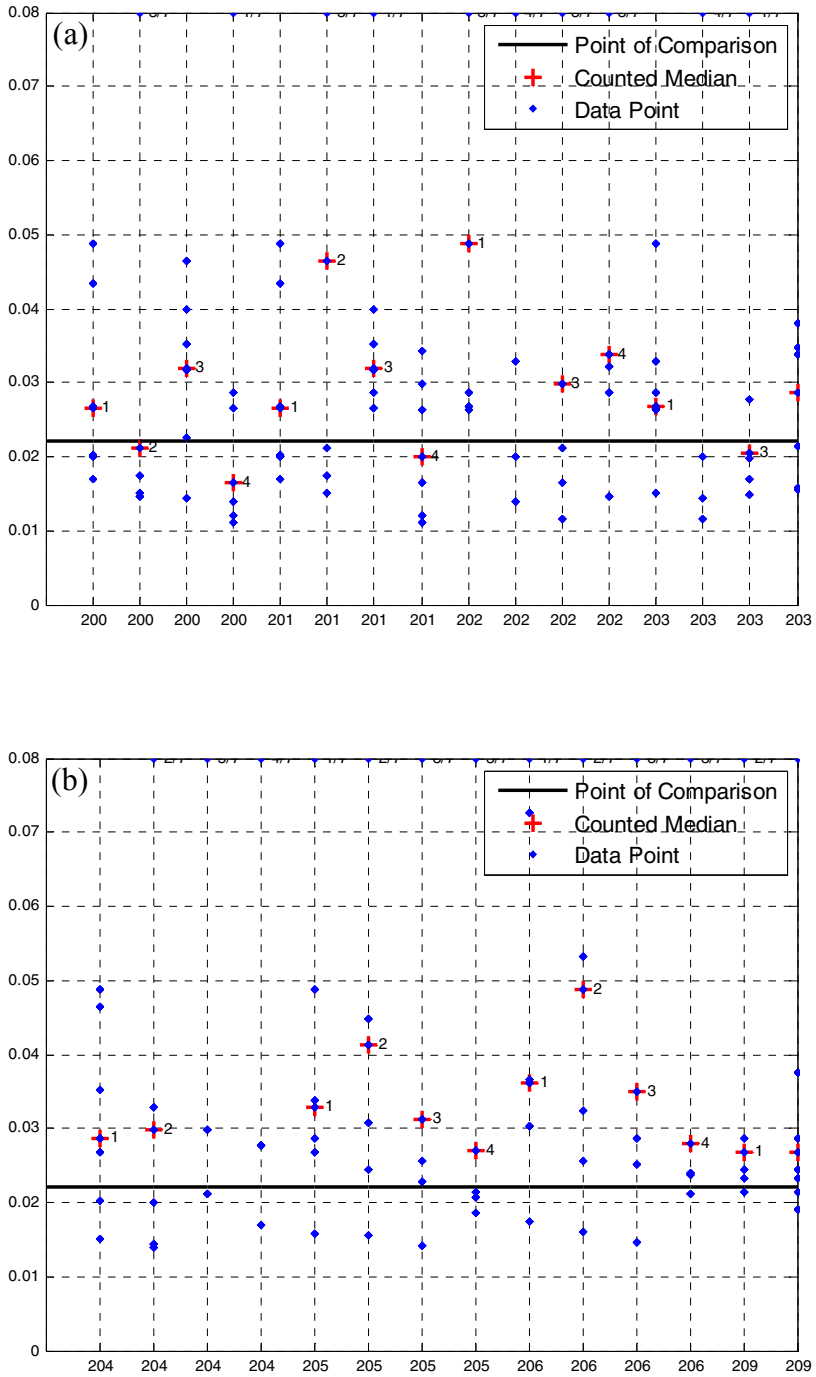

Fig. 7.4 Maximum interstory drift ratio responses for sets of seven ground motions selected and scaled using Group II methods.

7.5 RESPONSE RESULTS FOR GROUP III METHODS [METHODS THAT MATCH CONDITIONAL MEAN SPECTRUM (CMS)]

The methods discussed in this section match the conditional mean spectrum (CMS) using some type of numerical algorithm. The CMS, and the rationale for utilizing it for GMSM, is discussed in Section 2.4.3. Figure 7.5 shows the scaled acceleration spectra for a set of seven ground motions selected to match the CMS; this example is for method 300.

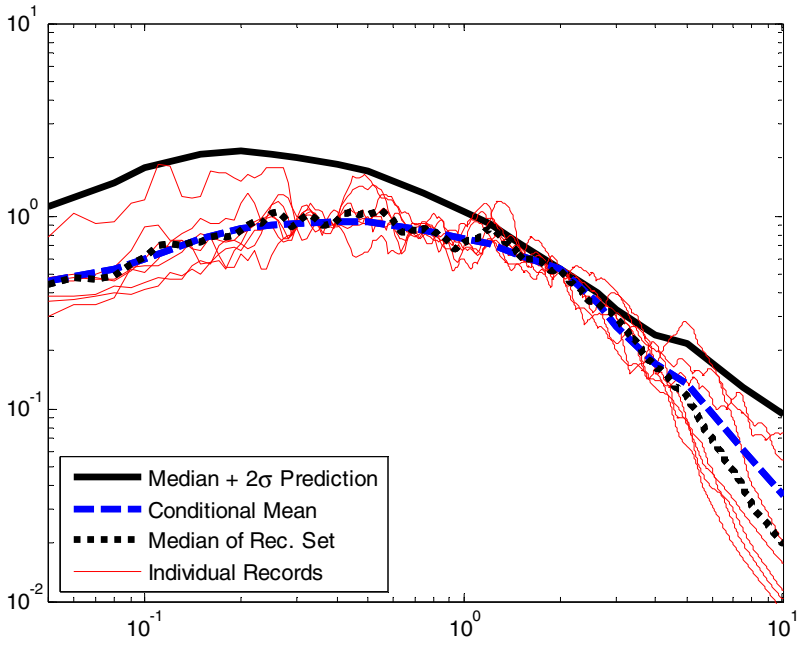

Fig. 7.5 Scaled acceleration spectra for one set of seven records selected to match conditional mean spectrum (method 300).

Table 7.3 and Figure 7.6 present the maximum interstory drift ratio response predictions from the five methods that match the CMS over a period range deemed important to structural response by the method author (e.g., method 300 matches between $0.2T_1$ and $2.0T_1$). The median prediction from these methods is only 1% larger than the POC, and the individual methods produce median predictions that are within 10% of the POC in almost all cases. This is the most accurate performance from among all the method sets considered in this chapter, and this observation is also consistent with observations from other chapters.

The exception to these accurate estimates is method 301, which produces a median prediction that is only 50% of the POC prediction. The response spectra of records selected using

that method are shown in Figure 7.7; looking at this figure, there are no obvious gross errors in the match the target spectrum. Looking at Figure 7.6, we see that method 301 produced three large responses and four very small responses. So the median was very sensitive to whether there were four large responses or four small responses from the set of seven. This points out a subtle difference between the objectives of method 301, and the objective being used in this report. This report focuses on the precise prediction of median interstory drift response, while method 301 is focused on creating a set of ground motions that fulfills building code requirements (which requires the *average* spectrum of the ground motion set to be above a specified target) with minimal scaling. Therefore, looking at median structural response is slightly outside of the intended purpose for which method 301 was created, and this should be considered when interpreting the results presented in Table 7.3.

Enforcing that the *average* spectrum meets the target, rather than matching the record spectra *individually* to the target spectra, may be the cause of the unusually large and small responses observed here for method 301.

Table 7.3 Median MIDR responses for sets of seven ground motions selected and scaled using Group III methods.

					Individual Sets		All Subsets Combined	
Method Number	Method Tag	Method Name	GM Set Index	Number of Records	Median MIDR	Ratio to POC	Median MIDR	Ratio to POC
300	10	Conditional Mean Spectrum Selection with Scaling	1	7	0.0229	1.04	0.0202	0.92
300	10	Conditional Mean Spectrum Selection with Scaling	2	7	0.0184	0.84		
300	10	Conditional Mean Spectrum Selection with Scaling	3	7	0.0164	0.75		
300	10	Conditional Mean Spectrum Selection with Scaling	4	7	0.0223	1.01		
301	15	Genetic Algorithm Selection (to match CMS)	1	7	0.0112	0.51	0.0112	0.51
302	24	Semi-Automated Selection & Scaling (to match CMS)	1	7	0.0185	0.84	0.0223	1.01
302	24	Semi-Automated Selection & Scaling (to match CMS)	2	7	0.0261	1.19		
303	78	Design Ground Motion Library (DGML) (Objective 4)	1	7	0.0270	1.23	0.0232	1.05
303	78	Design Ground Motion Library (DGML) (Objective 4)	2	7	0.0231	1.05		
303	78	Design Ground Motion Library (DGML) (Objective 4)	3	7	0.0185	0.84		
303	78	Design Ground Motion Library (DGML) (Objective 4)	4	7	0.0240	1.09		
304	45	Design Ground Motion Library (DGML) (Objective 3-4)	1	7	0.0223	1.01	0.0243	1.10
304	45	Design Ground Motion Library (DGML) (Objective 3-4)	2	7	0.0206	0.94		
304	45	Design Ground Motion Library (DGML) (Objective 3-4)	3	7	0.0468	2.13		
304	45	Design Ground Motion Library (DGML) (Objective 3-4)	4	7	0.0525	2.39		
				Median:	0.022	**1.01**	--	--
				Average:	0.021	0.94	--	--
				C.O.V.:	--	0.22	--	--
				Minimum:	0.011	0.51	--	--
				Maximum:	0.027	1.23	--	--

*For consistency of comparisons, Objective 3 method is not included in the summary statistics.

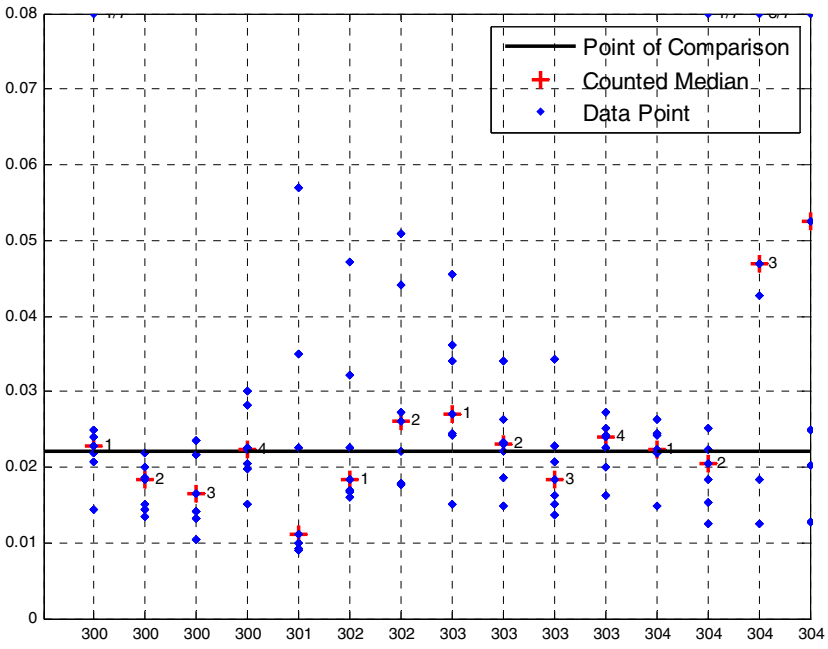

Fig. 7.6 Maximum interstory drift ratio responses for sets of seven ground motions selected and scaled using Group III methods.

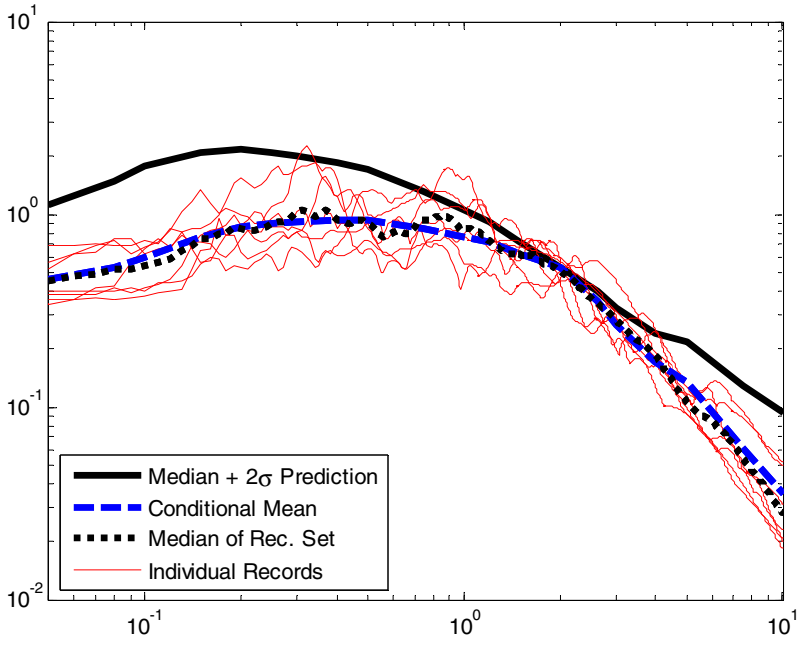

Fig. 7.7 Scaled acceleration spectra seven records selected to match conditional mean spectrum using a genetic algorithm (method 301).

7.6 RESPONSE RESULTS FOR GROUP IV METHODS (METHODS THAT USE EPSILON PROXY FOR CMS)

The Group IV methods use an *indicator* of the spectral shape (or a *proxy* for the spectral shape), rather than directly matching the shape of the CMS. This indicator is (or at least involves) the parameter epsilon (ε), which is defined as the number of standard deviations between the natural logarithm of an observed Sa(T) value and the natural logarithm of the median Sa(T) value predicted using an attenuation function.

Table 7.4 and Figure 7.8 present the results for the three Group IV methods. These methods result in a median 12% overprediction in response. While methods 400 and 401 produce overpredictions of response, method 403 appears to produce unbiased predictions. This is consistent with the results from other chapters.

Table 7.4 Median MIDR responses for sets of seven ground motions selected and scaled using Group IV methods.

					Individual Sets		All Subsets Combined	
Method Number	Method Tag	Method Name	GM Set Index	Number of Records	Median MIDR	Ratio to POC	Median MIDR	Ratio to POC
400	20	Target Spectrum Based on Epsilon Correlations	1	7	0.0260	1.18	0.0265	1.20
400	20	Target Spectrum Based on Epsilon Correlations	2	7	0.0171	0.78		
400	20	Target Spectrum Based on Epsilon Correlations	3	7	0.0281	1.28		
400	20	Target Spectrum Based on Epsilon Correlations	4	7	0.0234	1.06		
401	31	ε Selection with $S_{de}(T_1)$ Scaling	1	7	0.0162	0.74	0.0291	1.32
401	31	ε Selection with $S_{de}(T_1)$ Scaling	2	7	0.0346	1.57		
401	31	ε Selection with $S_{de}(T_1)$ Scaling	3	7	0.0404	1.84		
401	31	ε Selection with $S_{de}(T_1)$ Scaling	4	7	0.0293	1.33		
402	43	ATC-63 Method Applied to MIDR - Far-Field Set	1	44	0.0203	0.92	0.0203	0.92
403	48	ATC-63 Method Applied to MIDR - Near-Field Set	1	56	0.0230	1.05	0.0230	1.05
				Median:	0.025	**1.12**	--	--
				Average:	0.026	1.17	--	--
				C.O.V.:	--	0.29	--	--
				Minimum:	0.016	0.74	--	--
				Maximum:	0.040	1.84	--	--

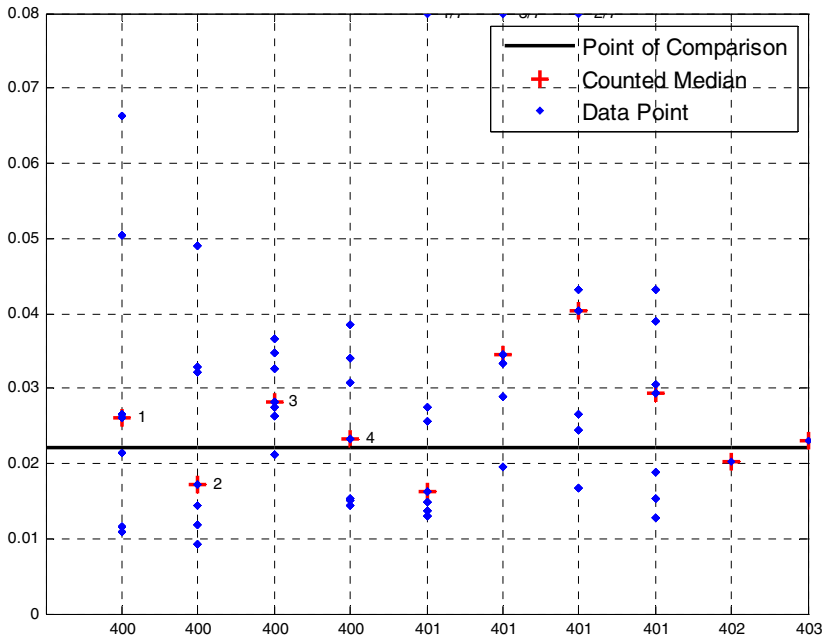

Fig. 7.8 Maximum interstory drift ratio responses for sets of seven ground motions selected and scaled using Group IV methods.

To better investigate method 401, Figure 7.9 shows the combined set of 28 records for this method; this shows that ε selection leads to records that match the CMS well, *on average*. Figure 7.10 shows the spectra for the individual sets of seven records, and these spectra explain the observed MIDR responses for each ground motion set (as shown in Table 7.4). Ground motion sets 1–2 (Fig. 7.10a–b) have spectral values much higher than the CMS for $T > T_1$ (T_1 = 2.63 sec.), and sets 3–4 (Fig. 7.10c–d) have spectral values lower than the CMS at the same periods; this observation correlates exactly with the observation that sets 1–2 greatly overpredict MIDR response and sets 3–4 underpredict response. Even though the average spectral shape tends to match the CMS (Fig. 7.9), the average results still have +33% bias because the ground motions with Sa values above the CMS at $T > T_1$ tend to produce larger predictions of response, as compared to the underestimation of response by using records with Sa values below the CMS at $T > T_1$ (i.e., unsymmetrical behavior).

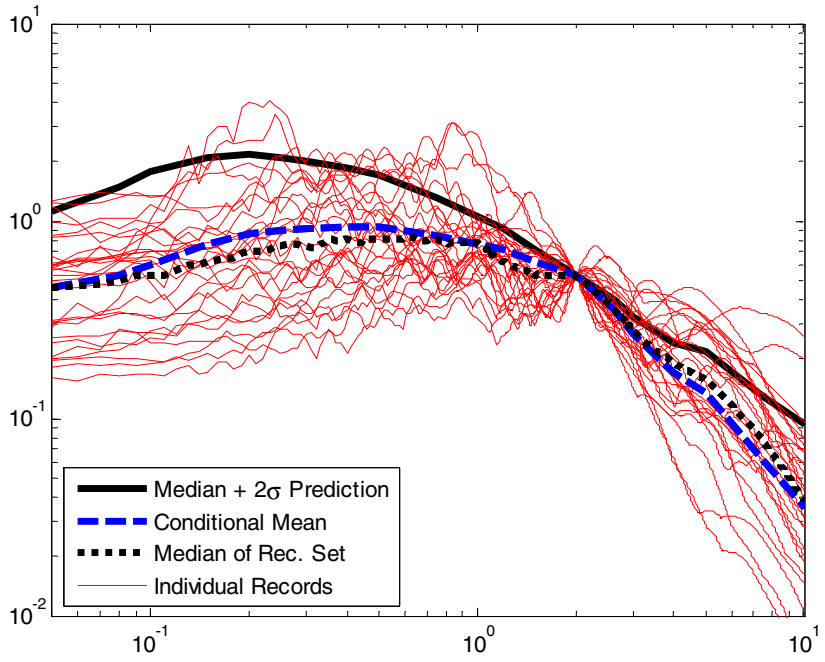

Fig. 7.9 Scaled acceleration spectra for combined set of 28 records selected based on ε (method 401).

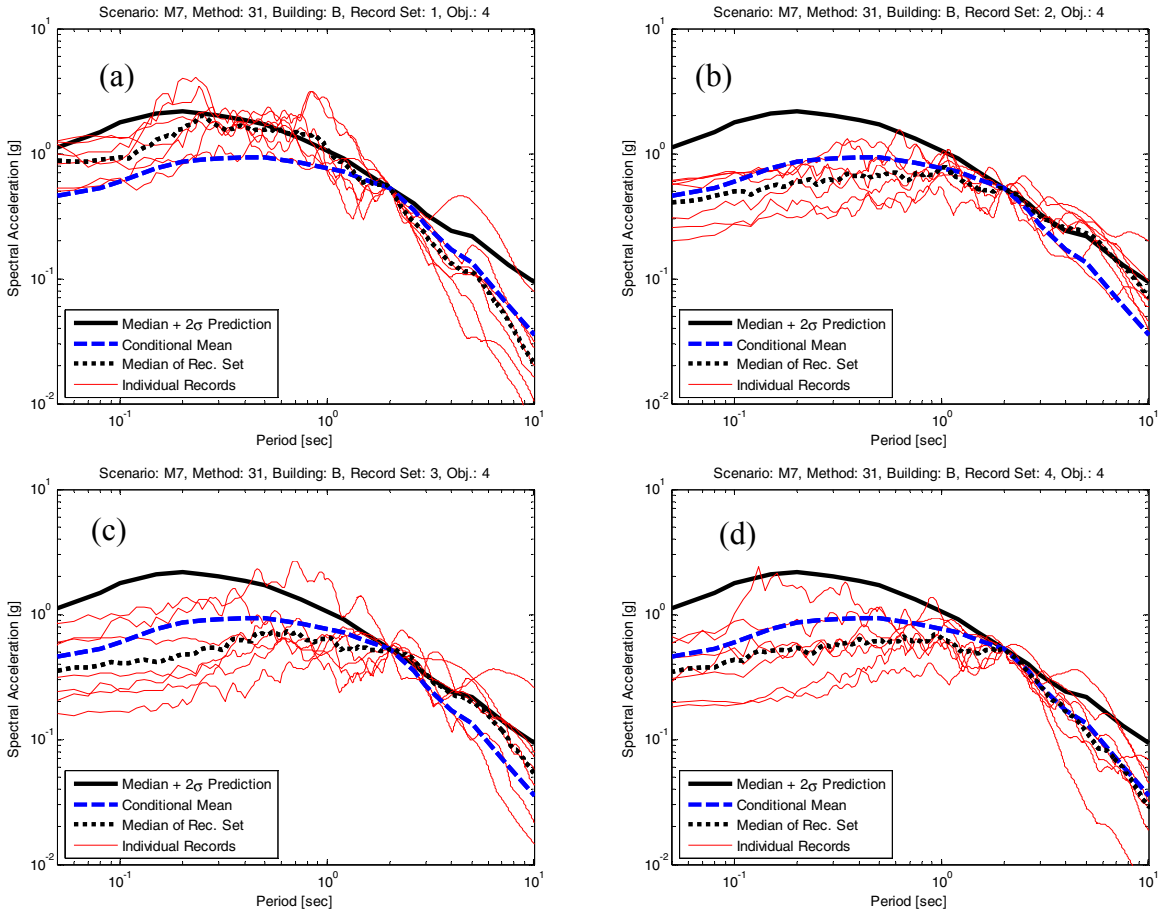

Fig. 7.10 Scaled acceleration spectra for each individual set of seven records selected based on ε (method 401).

The spectra from method 400 are also shown below in Figures 7.11 and 7.12. In this case, on average the records tend to be larger than the CMS at periods shorter than T_1. This may explain some of the overestimation of response relative to the POC. But interestingly, the response results from these records are on average smaller than the response results from the method 401 records, even though the method 401 records had smaller Sa values at short periods. This may be caused by the fact that the method 400 spectra fall off at longer periods more quickly that the method 401 spectra. Another possible explanation may be the variability in the response spectra. The spectra from method 400 generally have lower variability than the spectra from method 401 (near the fundamental period of the building), and according to the argument of the previous paragraph, this should result in the lower median responses that were observed. This

link between response spectra variability and median response requires further study to further justify the premise.

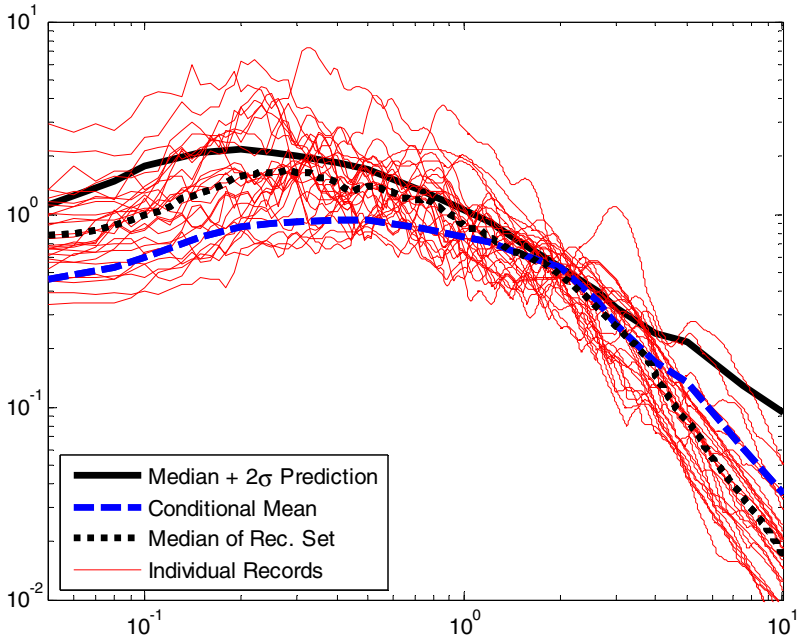

Fig. 7.11 Scaled acceleration spectra for combined set of 28 records selected using method 400.

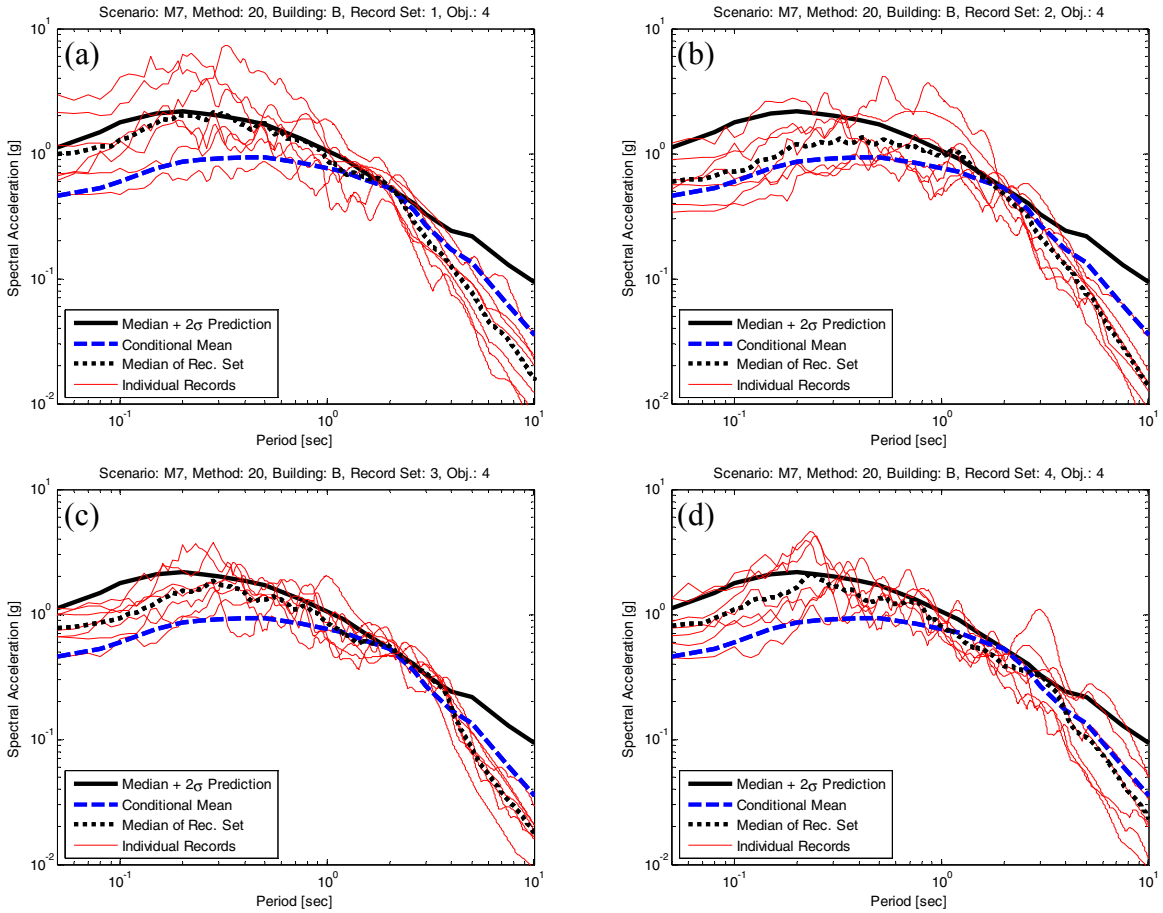

Fig. 7.12 Scaled acceleration spectra for each individual set of seven records selected using method 400.

7.7 RESPONSE RESULTS FOR GROUP V METHODS (INELASTIC-BASED METHODS)

The methods presented in this section utilize some type of inelastic parameter (e.g., inelastic spectral displacement) and/or results of inelastic structural analysis (e.g., nonlinear static pushover) to inform the record selection and scaling. Before discussing these results, let us note that an important caveat is that the records from methods 500 and 503 are scaled to the Sdi and IM1I&2E targets, respectively, rather than the Sa target. Consequently, the results may not necessarily be directly comparable with the ground motion scenarios (Section 3.3.1) and the creation of the POC (Section 5.2), since both of these are based on elastic spectral values. This discrepancy in targets may explain the discrepancy in response predictions observed below.

Figure 7.13 and Table 7.5 present the results for the four inelastic-based methods. These methods lead to a median 39% overestimation in response. This is an unusually high estimation given the expected effectiveness of these methods, and given their relatively better performance for predictions related to the other buildings considered. Given these unexpected results, these methods are considered individually in this section.

Table 7.5 Median MIDR responses for sets of seven ground motions selected and scaled using Group V methods.

					Individual Sets		All Subsets Combined	
Method Number	**Method Tag**	**Method Name**	**GM Set Index**	**Number of Records**	**Median MIDR**	**Ratio to POC**	**Median MIDR**	**Ratio to POC**
500	27	$S_{di}(T_1, dy)$ Scaling	1	7	0.0372	1.69	0.0330	1.50
500	27	$S_{di}(T_1, dy)$ Scaling	2	7	0.0432	1.96		
500	27	$S_{di}(T_1, dy)$ Scaling	3	7	0.0249	1.13		
500	27	$S_{di}(T_1, dy)$ Scaling	4	7	0.0301	1.37		
501	6	Vector of Record Properties Identified by Proxy	1	7	0.0183	0.83	0.0176	0.80
501	6	Vector of Record Properties Identified by Proxy	2	7	0.0161	0.73		
501	6	Vector of Record Properties Identified by Proxy	3	7	0.0203	0.92		
501	6	Vector of Record Properties Identified by Proxy	4	7	0.0162	0.74		
502a	11	Inelastic Response Surface Scaling (1st mode)	1	7	0.0464	2.11	0.0373	1.70
502a	11	Inelastic Response Surface Scaling (1st mode)	2	7	0.0327	1.49		
502b	11	Inelastic Response Surface Scaling (1st-2nd modes)	3	7	0.0312	1.42		
502b	11	Inelastic Response Surface Scaling (1st-2nd modes)	4	7	0.0402	1.83		
503	35	IM1I&2E Selection/Scaling	1	7	0.0287	1.30	0.0303	1.38
503	35	IM1I&2E Selection/Scaling	2	7	0.0378	1.72		
503	35	IM1I&2E Selection/Scaling	3	7	0.0250	1.14		
503	35	IM1I&2E Selection/Scaling	4	7	0.0325	1.48		
				Median:	0.031	**1.39**	--	--
				Average:	0.030	1.37	--	--
				C.O.V.:	--	0.31	--	--
				Minimum:	0.016	0.73	--	--
				Maximum:	0.046	2.11	--	--

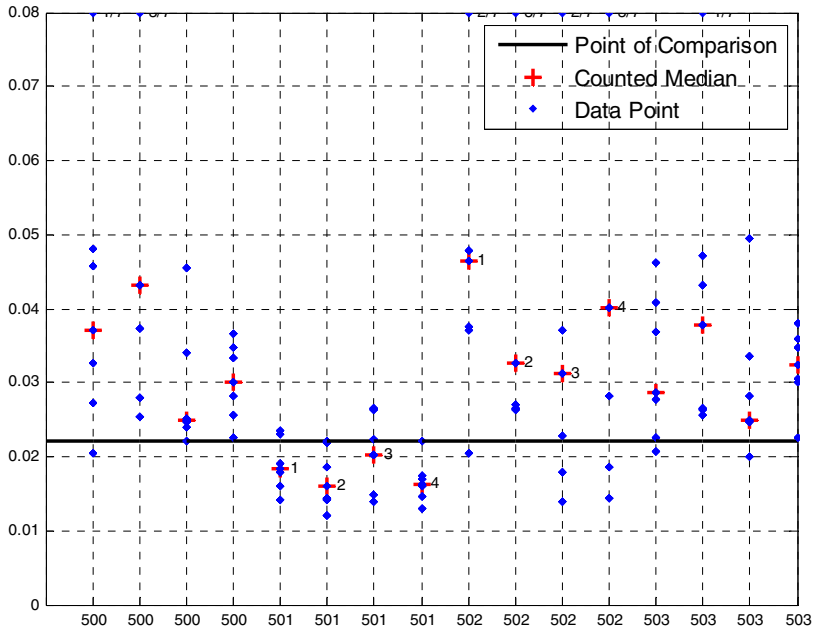

Fig. 7.13 Maximum interstory drift ratio responses for sets of seven ground motions selected and scaled using Group V methods.

The Sdi scaling method (method 500) selects records randomly and then scales records to match an inelastic spectral displacement value (at the first-mode building period) associated with the target Sdi scenario. The Sdi target is, for example, the +2ε Sdi rather than the +2ε Sa used to define the scenario. Figure 7.14 shows the response spectra from the four sets of records selected using this method.

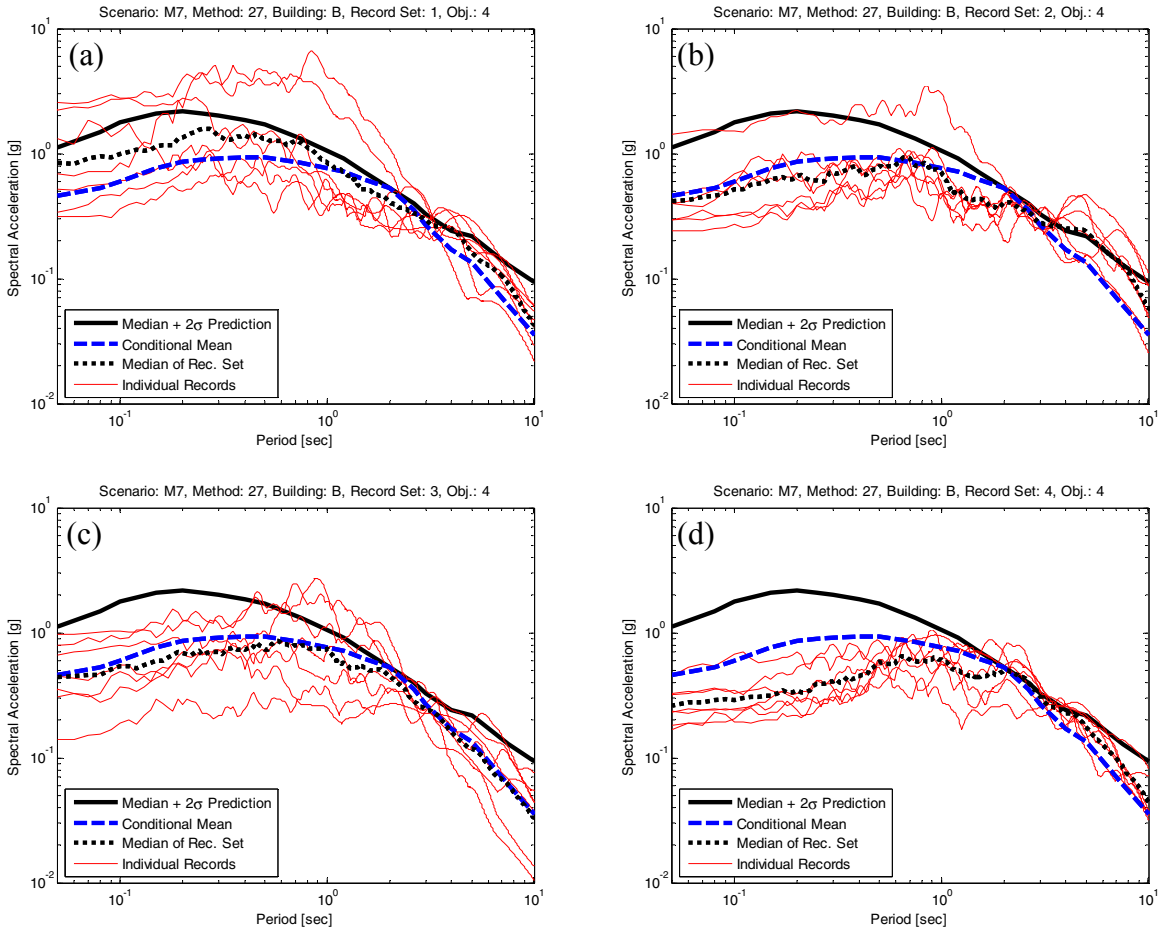

Fig. 7.14 Scaled acceleration spectra for two sets of seven records selected using method 500.

The vector of record properties identified by proxy method (method 501) is the only method in this group that shows an underprediction of response. Figure 7.15 shows that the spectra of records selected using this method. They closely match the CMS for the period range of interest here, which makes it somewhat surprising that only 4 out of the 28 selected records produce a response prediction larger than the POC (as seen in Fig. 7.13). The records are relatively weak in long-period energy, which may partly explain the low responses obtained.

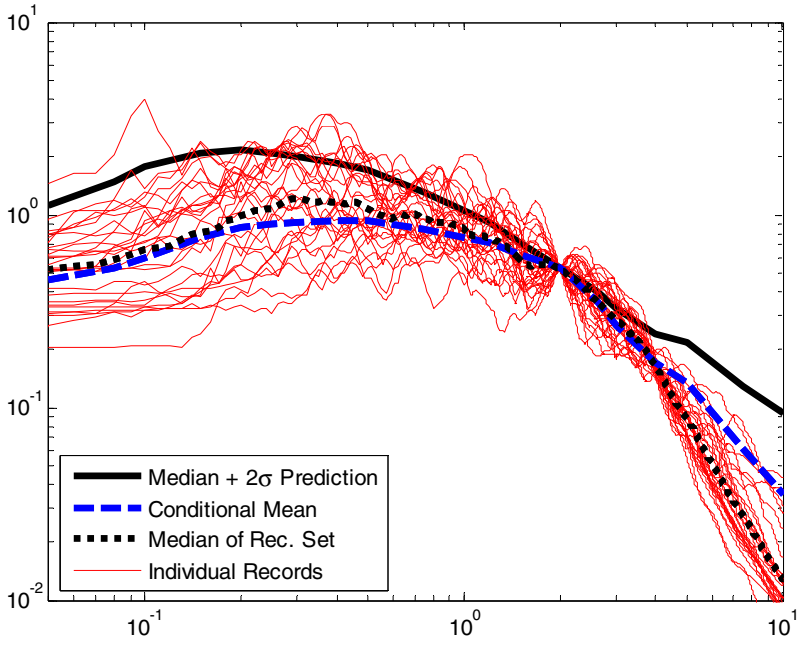

Fig. 7.15 Scaled acceleration spectra for combined set of 28 records selected based on vector of record properties identified by proxy (method 501).

The inelastic response surface scaling method (method 502) has two variants. Ground motion sets 1–2 were selected without considering a second-mode term, and sets 3–4 were selected including this term. To illustrate this difference, Figure 7.16 shows the scaled response spectra for all four ground motion sets. Unlike results obtained using this method for some other buildings in this report, all four ground motion sets overestimated the median MIDR.

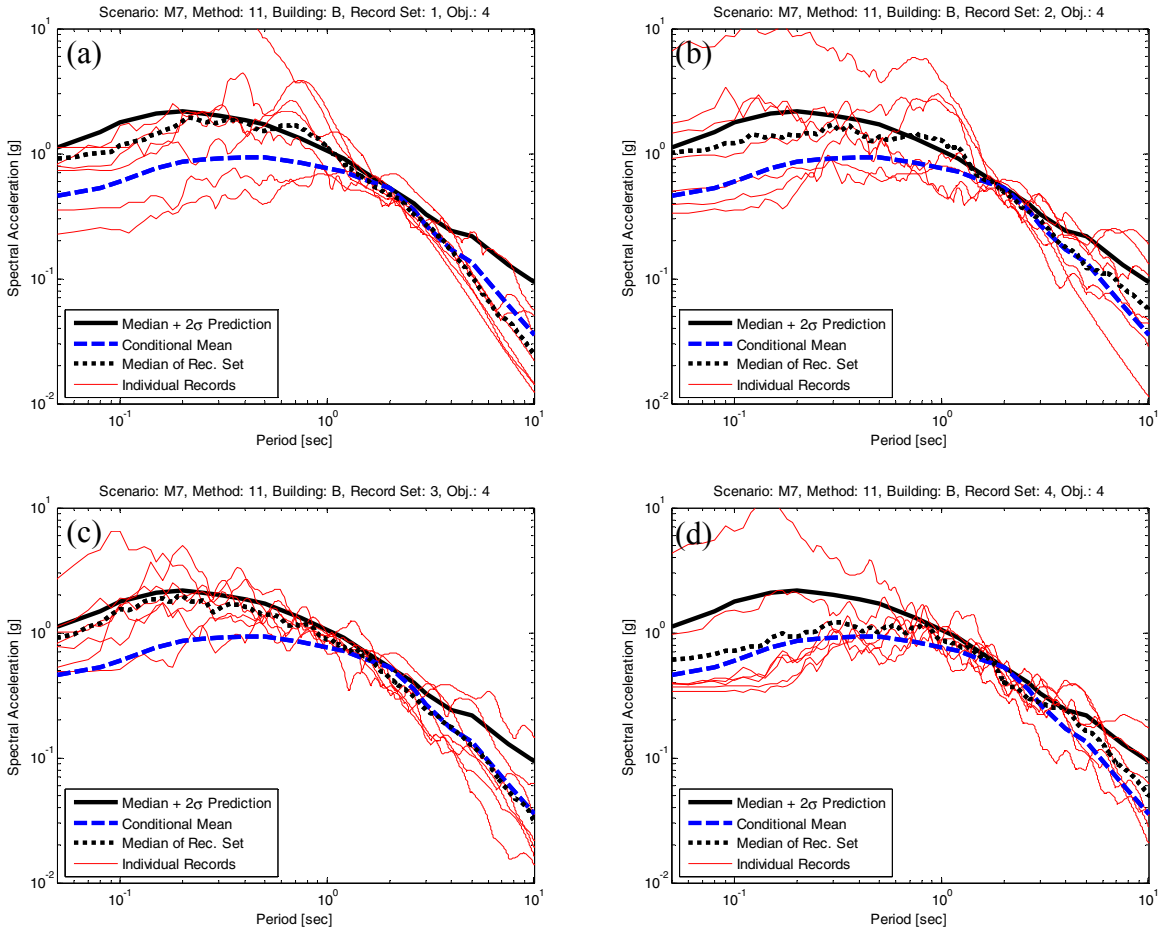

Fig. 7.16 Scaled acceleration spectra for two sets of seven records selected using two variants of inelastic response surface method (method 502): (a) and (b) selected without consideration of second mode, and (c) and (d) selected to account for second mode.

Method 503 is the final method in this category. It can be thought of as an extension of method 500, with a modification to account for the expected elastic spectral acceleration at the building's second-mode period. While for some other buildings this method has produced results in good agreement with the POC, here it overestimates the POC by 38%, which is not a significant improvement relative to method 500. Plots of the elastic response spectra are shown in Figure 7.17.

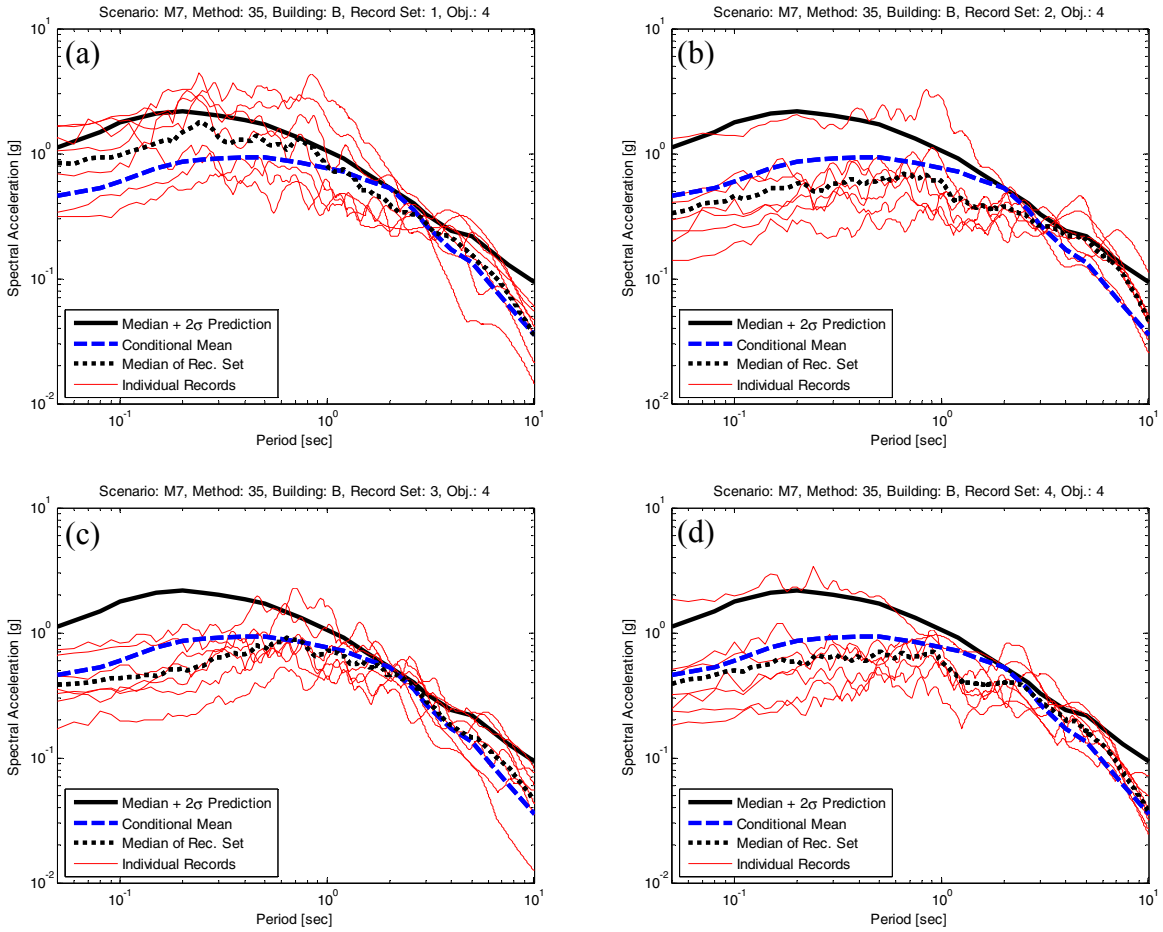

Fig. 7.17 Scaled acceleration spectra for two sets of seven records selected using two variants of inelastic response surface method (method 503): (a) and (b) selected without consideration of second mode, and (c) and (d) selected to account for second mode.

In general, the elastic response spectra are not particularly informative for identifying why the response results did not agree with the POC in this case. The results are also somewhat perplexing because these methods generally performed well for predicting the response of the other buildings. The fact that three of these methods did not use the basic Sa target may explain this variation; it does not mean that the methods are bad, but rather that they are designed for answering a different question than was posed here. Future efforts will be dedicated to resolving this observed discrepancy more completely.

7.8 SUMMARY AND CONCLUSIONS

7.8.1 Summary of Results by Method Group

Table 7.6 summarizes the prediction accuracies by method group for this building. This table shows summary statistics for the estimation bias factor computed as the ratio of median maximum interstory drift ratio (MIDR) response to the point-of-comparison (POC) prediction. This shows that the conditional mean spectrum (CMS) matching methods result in a prediction that is both highly accurate (with a median error of only 1%) and precise (with a coefficient of variation of only 0.22). In contrast, the methods that do not consider the CMS shape in any way (i.e., the UHS and Sa(T1) methods) lead to consistent overpredictions of response from 39–55%. (c.o.v.'s were not reported for these methods because they produced too many collapses to have median results for every set of seven ground motions.) This shows that for predicting structural response under an extreme ground motion scenario, consideration of spectral shape is important.

The inelastic methods generally produced overestimates of response (except for method 501, which underestimated the median response by 20%). These overestimates may be caused by differences in the target spectra from these methods relative to the target spectra for other methods (and for the POC). The consistent overestimations by the inelastic methods may come from the use of an inelastic target (e.g., S_{di}) that is too high the M7 scenario; if this is the case, further study may be able to remedy this bias problem. The results for methods scaling to the Sdi target are relatively consistent among each other. Future work should more completely resolve this issue.

The proxy methods, which indirectly incorporate CMS-like information, produced a slight overestimation (i.e., a median overestimation of 12%). This is smaller than any method class except the CMS methods. Both method Groups IV and V produced comparable c.o.v.'s of median responses, of approximately 0.3. This is slightly higher than the c.o.v. from the CMS methods.

Table 7.6 Summary of response estimation bias factor by method group.

MIDR/POC	I: Sa(T_1)	II: UHS	III: CMS	IV: Proxy (i.e. ε)	V: Inelastic
Median:	1.55	1.39	**1.01**	1.12	1.39
Average:	--	--	**0.94**	1.17	1.37
C.O.V.:	--	--	0.22	0.29	0.31
Minimum:	1.19	0.75	0.51	0.74	0.73
Maximum:	collapse	collapse	1.23	1.84	2.11

7.8.2 Closing Comments

This chapter presents many attempts to accurately predict the median MIDR response of a 12-story RC frame building (Building B), when subjected to a M_w = 7.0, R = 10 km, and ε = 2.0 ground motion scenario (the M7 scenario). These comparisons include 15 ground motion selection and modification (GMSM) methods (23 methods if variations are included), which come from five different method groups.

This chapter concludes that for Building B subjected to the M7 scenario, consideration of proper elastic spectral shape is critical when predicting MIDR under such an extreme ground motion. To obtain accurate and precise MIDR predictions, matching to the conditional mean spectrum (CMS) is the most effective to consider this proper spectral shape (for the Sa target).

8 Findings for Modern 20-Story Reinforced Concrete Moment-Frame Building (Building C), Subjected to Magnitude 7.0 Scenario

Primary Author: C. B. Haselton

Associate Author: J. W. Baker

8.1 INTRODUCTION AND OVERVIEW

In this chapter, we use 14 ground motion selection and modification (GMSM) methods (26 methods if variations are included) to predict the maximum interstory drift ratio (MIDR) response of a modern (ductile) 20-story reinforced concrete (RC) frame building (termed Building C). These results are used as a building block of the overall study, in order to determine which methods lead to unbiased and consistent predictions of the maximum interstory drift ratio response. This 20-story modern RC frame building model is specifically investigated because (a) it is a modern building for which nonlinear dynamic analysis may be employed as part of a performance-based design, or for performance assessment completed as part of the building code design procedures (ICC 2005, ASCE 2005), and (b) it is a relatively tall (mid-rise) building that is sensitive to the second mode, (c) this model was also used as part of the ATC-63 project, and the design and model have both already been scrutinized as part of that effort.

Following the pattern of Chapters 6-7, this chapter presents results by method groupings. For each group, the MIDR predictions are presented for the individual methods in that group, and the predictions are compared to the point of comparison (POC). For this building and scenario, the POC (i.e., the expected MIDR response) is 1.9% interstory drift (according to Section 4.6). Comparing the predicted responses to the POC serves as the basis for evaluating the

prediction capability of the group of methods. When appropriate, the results of individual methods are also highlighted when their predictions differ substantially from other methods in their group.

This chapter concludes with the observation that, for this study, consideration of spectral shape appears critical. The most effective way to do this is by matching directly to the conditional mean spectrum. Alternatively, this chapter finds that some of the inelastic-based and ε-based (proxy) methods also lead to predictions that are acceptably accurate and precise.

8.1.1 Summary of Modern 20-Story Reinforced Concrete Building (Building C)

The structural model utilized in this chapter is a 20-story RC perimeter frame building designed according to the ASCE 7-02 (ASCE 2002) and ACI 318-02 (ACI 2002) design requirements, and modeled utilizing the OpenSEES open source software package (OpenSEES 2006). Section 3.2, described the design and model in more detail, so please refer to that section if detailed information is desired. This model was created as part of the Applied Technology Council Project ATC-63 (FEMA 2009) and doctoral research by Haselton (Haselton and Deierlein 2007). In the course of those projects, the structural design was reviewed in detail by practicing structural engineers. The building fundamental period is 2.63 sec, and the second- and third-mode periods are 0.85 and 0.46 sec.

8.1.2 Comparison to Other Chapters (Ground Motion Scenario, and Building)

The current chapter presents the results of simulations for a 20-story building (Building C) for the M7 scenario (M_w = 7.0, R = 10 km, ε = 2.0). This same ground motion scenario is considered in Chapters 6, 7, and 9, while Chapter 10 considers an additional M7.5 scenario.

Building C is a ductile special moment-resisting frame structural system designed according to a current design code (2003 IBC) and it was selected to represent high-rise frame systems. A taller RC frame building is not considered in this study because most taller buildings consist of a dual structural system (frames and walls), and such designs and models were not readily available for use in this project. Details about the design characteristics of this structure can be found in Section 3.2 and in Haselton and Deierlein (2007). For Building C and the M7 scenario, the point-of-comparison MIDR is 1.9% (Section 4.6).

8.1.3 Ground Motion Sets

Ground motion sets were selected according to the approach described in Section 3.4, which is the same method utilized for each building and ground motion scenario (Chapters 6–10).

Appendix C provides detailed documentation of each ground motion set, and the structural response predictions resulting from the set. This electronic Appendix includes Excel spreadsheet files with the ground motion filenames (from the PEER-NGA database; PEER 2006), the scale factors, and the resulting structural responses (including MIDR, individual drifts, floor accelerations, and many others). Also included are figure files showing the scaled acceleration spectra for each ground motion set.

8.2 METHOD GROUPS

The following sections present the structural response results by method groups. The results are presented following the groups established in Section 2.4. Chapter 2 explains the basis of each of these method groups:

- Group I: Sa(T_1) scaling (with bin selection)
- Group II: building code methods (matching to the uniform hazard spectrum)
- Group III: conditional mean spectrum (CMS) matching
- Group IV: methods using a proxy for the CMS (e.g., selection based on ε)
- Group V: inelastic-based methods

8.3 RESPONSE RESULTS FOR GROUP I METHODS [SA(T_1) SCALING METHODS]

The Group I methods involve selecting records from a ground motion bin, and then scaling the set of records to a target Sa(T_1) level. This is described in detail in Section 2.4.1.

Table 8.1 and Figure 8.1 present the maximum interstory drift ratio response predictions for the two Group I methods. As compared to the POC, these methods have a median response overprediction of 36%. Figure 8.1 also shows that for selection and scaling using this group of methods, there is an average of 1.0 building collapse for each set of seven records.

Table 8.1 Median MIDR responses for sets of seven ground motions scaled using Sa(T_1) methods.

Method Number	Method Tag	Method Name	Set Index	Num. of Rec.	Individual Sets: Median MIDR	Individual Sets: Ratio to POC	All Subsets Combined: Median MIDR	All Subsets Combined: Ratio to POC
100	4	Sa(T_1) Scaling with Bin Selection	1	7	0.0289	1.52	0.0319	1.68
100	4	Sa(T_1) Scaling with Bin Selection	2	7	0.0521	2.74		
100	4	Sa(T_1) Scaling with Bin Selection	3	7	0.0381	2.01		
100	4	Sa(T_1) Scaling with Bin Selection	4	7	0.0281	1.48		
101	67	ATC-58 35% Draft Method	1	11	0.0204	1.07	0.0224	1.18
101	67	ATC-58 35% Draft Method	2	11	0.0228	1.20		
101	67	ATC-58 35% Draft Method	3	11	0.0223	1.17		
101	67	ATC-58 35% Draft Method	4	11	0.0235	1.24		
				Median:	0.026	**1.36**	--	--
				Average:	0.030	1.55	--	--
				C.O.V.:	--	0.36	--	--
				Minimum:	0.020	1.07	--	--
				Maximum:	0.052	2.74	--	--

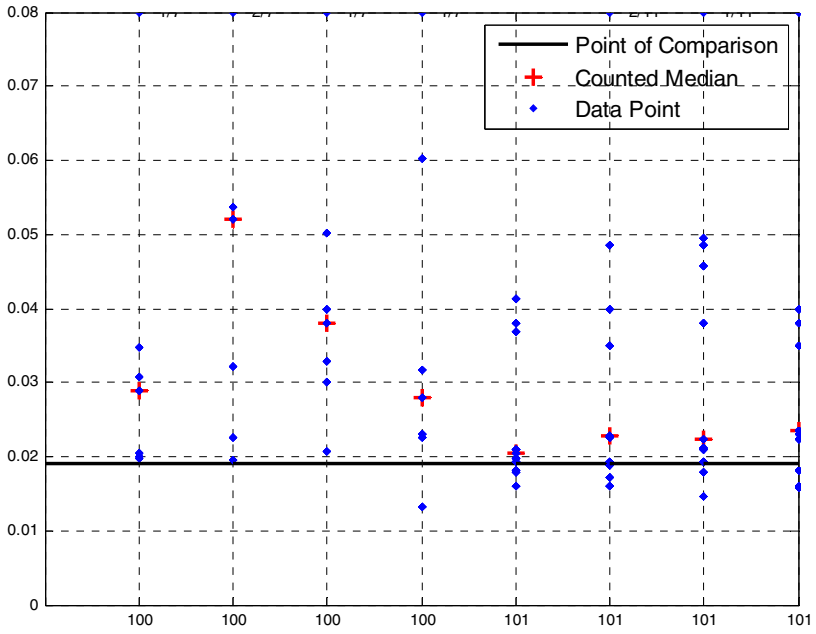

Fig. 8.1 Maximum interstory drift ratio responses for sets of seven ground motions scaled using Sa(T_1) methods.

Table 8.1 shows that this 36% overestimation is not consistent between the two methods. Method 100 leads to a median overestimation of 68% (with a large range of 48%–174% over the

POC prediction) and method 101 leads to only an 18% overprediction (with a range of only 7%–24% overprediction).

To identify possible reasons for the large difference between methods 100 and 101, the scaled acceleration spectra for the two methods are plotted in Figure 8.2; each figure shows all 28 spectra included in the four sets of seven records. This figure shows that the average spectral shape differs between the two sets. Compared to method 100, method 101 has an average spectrum that is lower for $T < T_1$ (T_1 = 2.63 sec.) and slightly lower for $T > T_1$. This causes both a reduction in higher-mode response, as well as a reduction in first-mode response (due to the reduction in spectral demands at $T > T_1$, where the building will be responding once it is damaged), and explains why the method 101 MIDR prediction is lower than that of the method 100 prediction.

These spectral shape differences result from fundamentally different ground motion bins being used for selection. Method 100 is based on selection from a M_w = 7.0 and R = 10 km bin, while the method 101 selection is based on a near-field bin containing many pulse-type motions.

Notice that method 101 results in a spectrum that is close to the CMS for T > T1 (T_1 = 2.63 sec.), leading to a response prediction that is closer to the POC as compared to other Group I methods (overprediction of 18%). This occurs only because the method 101 near-field ground motion set tends to have a spectral shape similar to the CMS when scaled to $Sa(T_1)$ in the period range of 2.5–3.0 sec. Once the fundamental period of the building is away from this period range, the difference between the CMS and the method 101 spectrum is larger. For this reason, using the method 101 for GMSM leads to larger overpredictions of response, in the order of 20%–70%, for the other three buildings used in this study (see Chapters 6, 7, and 9).

We emphasize that the ATC-58 method (method 101) utilized in this research was extracted from the ATC-58 35% draft document, and was still subject to change at the time of publication of this report. The ATC-58 project team has already indicated that spectral shape will be considered in future versions of the ATC-58 GMSM methodology, which can address the issue shown in these findings.

In summary, Group I methods generally lead to large overprediction of the MIDR response. In addition, the prediction is highly sensitive to both the ground motion bin used for selection (i.e., the typical spectral shapes of the motions in the bin) and the period, T1, used for ground motion scaling.

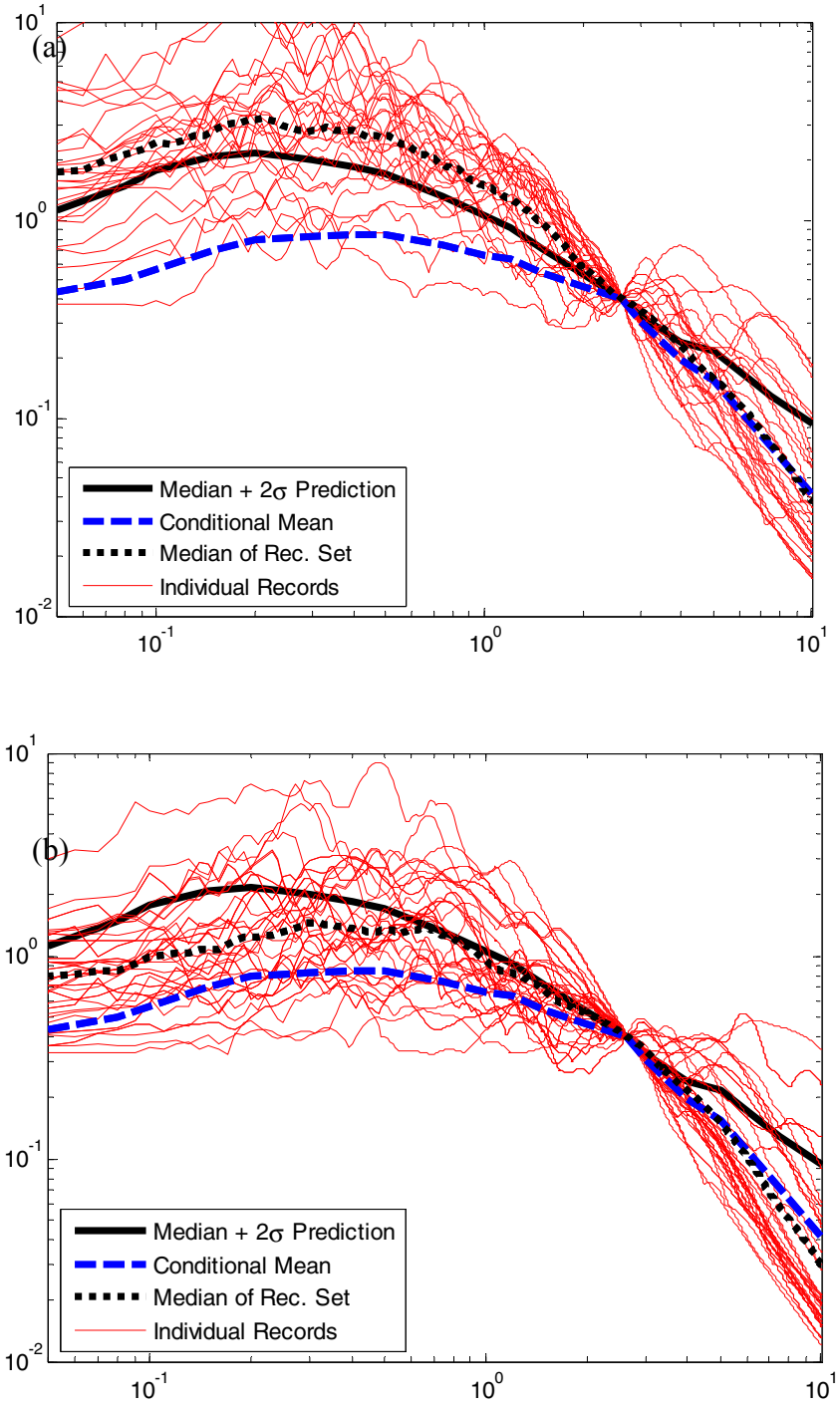

Fig. 8.2 Scaled acceleration spectra for 28 records (4 sets of 7 records each for Sa(T_1) scaling methods (a) 100 (top) and (b) 101 (bottom).

8.4 RESPONSE RESULTS FOR GROUP II METHODS (BUILDING CODE–BASED METHODS THAT MATCH UNIFORM HAZARD SPECTRUM)

The Group II methods presented in this section include various interpretations of the requirements of the Uniform Building Code (UBC 1997) and the ASCE 7-05 (ASCE 2005); these methods are discussed in Section 2.4.2. For brevity, the detailed differences between these sets are not presented here, but left to a forthcoming publication on this topic. Even so, the exhaustive results are presented below to illustrate the variability in prediction that can result from the differences in various building code requirements, as well as differences in interpretation of these requirements.

Figure 8.3 illustrates a set of seven records selected using Group II methods (method 206, set two). This illustrates that the median spectrum exceeds the uniform hazard spectrum (UHS) at all periods from $0.2T_1$ to $1.5T_1$, as required by the building code provisions. Note that for the M7 scenario used in this study, there is a single event with $M_w = 7.0$ and R = 10 km that defines the hazard; therefore, the UHS and the median + 2σ spectrum are identical.

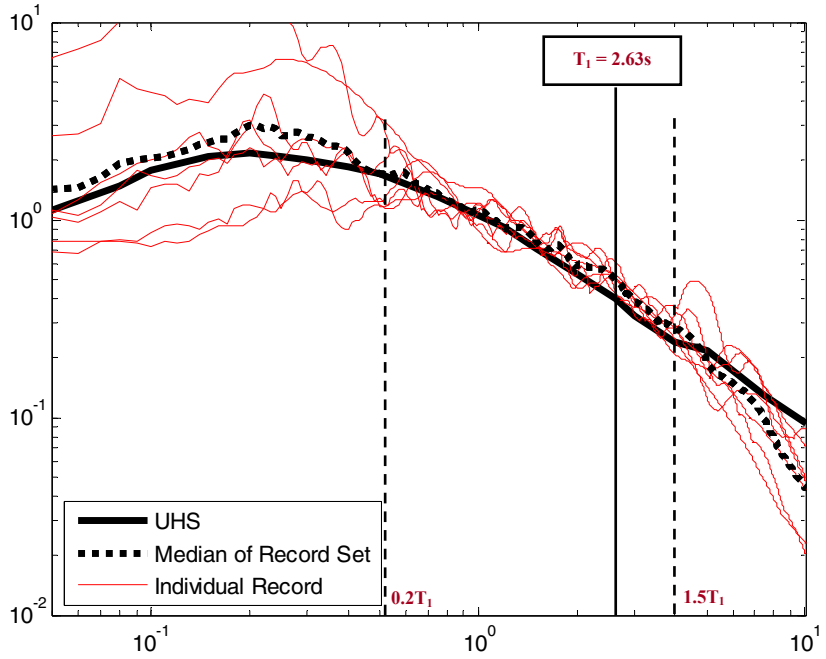

Fig. 8.3 Scaled acceleration spectra for one set of seven records selected using building code methods that match or exceed uniform hazard spectrum (method 206).

Table 8.2 and Figure 8.4 present the maximum interstory drift ratio response predictions for all variants of the Group II methods. As compared to the POC, these methods have a median MIDR response overprediction of 26%. In addition, the scatter leads to a wide range of individual predictions (for each set of seven records), from 10% below the POC to 110% above the POC. Figure 8.4 also shows that for selection and scaling using this group of methods, there is an average of 0.9 building collapses for each set of seven records.

Table 8.2 Median MIDR responses for sets of seven ground motions selected and scaled using Group II methods (matching uniform hazard spectrum).

					Individual Sets		All Subsets Combined	
Method Number	Method Tag	Method Name	Set Index	Num. of Rec.	Median MIDR	Ratio to POC	Median MIDR	Ratio to POC
200	9980	Building Code Selection and Scaling - Method A	1	7	0.0200	1.05	0.0227	1.19
200	9980	Building Code Selection and Scaling - Method A	2	7	0.0224	1.18		
200	9980	Building Code Selection and Scaling - Method A	3	7	0.0379	1.99		
200	9980	Building Code Selection and Scaling - Method A	4	7	0.0281	1.48		
201	9981	Building Code Selection and Scaling - Method B	1	7	0.0224	1.18	0.0254	1.34
201	9981	Building Code Selection and Scaling - Method B	2	7	0.0379	1.99		
201	9981	Building Code Selection and Scaling - Method B	3	7	0.0394	2.07		
201	9981	Building Code Selection and Scaling - Method B	4	7	0.0239	1.26		
202	9982	Building Code Selection and Scaling - Method C	1	7	0.0234	1.23	0.0234	1.23
202	9982	Building Code Selection and Scaling - Method C	2	7	0.0238	1.25		
202	9982	Building Code Selection and Scaling - Method C	3	7	0.0277	1.46		
202	9982	Building Code Selection and Scaling - Method C	4	7	0.0173	0.91		
203	9983	Building Code Selection and Scaling - Method D	1	7	0.0206	1.08	0.0221	1.16
203	9983	Building Code Selection and Scaling - Method D	2	7	0.0241	1.27		
203	9983	Building Code Selection and Scaling - Method D	3	7	0.0223	1.17		
203	9983	Building Code Selection and Scaling - Method D	4	7	0.0215	1.13		
204	9984	Building Code Selection and Scaling - Method E	1	7	0.0220	1.16	0.0227	1.19
204	9984	Building Code Selection and Scaling - Method E	2	7	0.0239	1.26		
204	9984	Building Code Selection and Scaling - Method E	3	7	0.0198	1.04		
204	9984	Building Code Selection and Scaling - Method E	4	7	0.0279	1.47		
205	9985	Building Code Selection and Scaling - Method F	1	7	0.0220	1.16	0.0265	1.39
205	9985	Building Code Selection and Scaling - Method F	2	7	0.0315	1.66		
205	9985	Building Code Selection and Scaling - Method F	3	7	0.0282	1.48		
205	9985	Building Code Selection and Scaling - Method F	4	7	0.0228	1.20		
206	9986	Building Code Selection and Scaling - Method G	1	7	0.0246	1.29	0.0307	1.62
206	9986	Building Code Selection and Scaling - Method G	2	7	0.0341	1.79		
206	9986	Building Code Selection and Scaling - Method G	3	7	0.0356	1.87		
206	9986	Building Code Selection and Scaling - Method G	4	7	0.0262	1.38		
207	9975	Building Code Selection and Scaling - Method H	1	7	0.0206	1.08	0.0260	1.37
207	9975	Building Code Selection and Scaling - Method H	2	7	0.0299	1.57		
207	9975	Building Code Selection and Scaling - Method H	3	7	0.0291	1.53		
207	9975	Building Code Selection and Scaling - Method H	4	7	0.0229	1.21		
208	9976	Building Code Selection and Scaling - Method I	1	7	0.0284	1.49	0.0240	1.26
208	9976	Building Code Selection and Scaling - Method I	2	7	0.0196	1.03		
208	9976	Building Code Selection and Scaling - Method I	3	7	0.0375	1.97		
208	9976	Building Code Selection and Scaling - Method I	4	7	0.0175	0.92		
209	9989	Building Code Selection and Scaling - Method J	1	7	0.0220	1.16	0.0226	1.19
209	9989	Building Code Selection and Scaling - Method J	2	9	0.0233	1.23		
				Median:	0.024	**1.26**	--	--
				Average:	0.026	1.36	--	--
				C.O.V.:	--	0.23	--	--
				Minimum:	0.017	0.91	--	--
				Maximum:	0.039	2.07	--	--

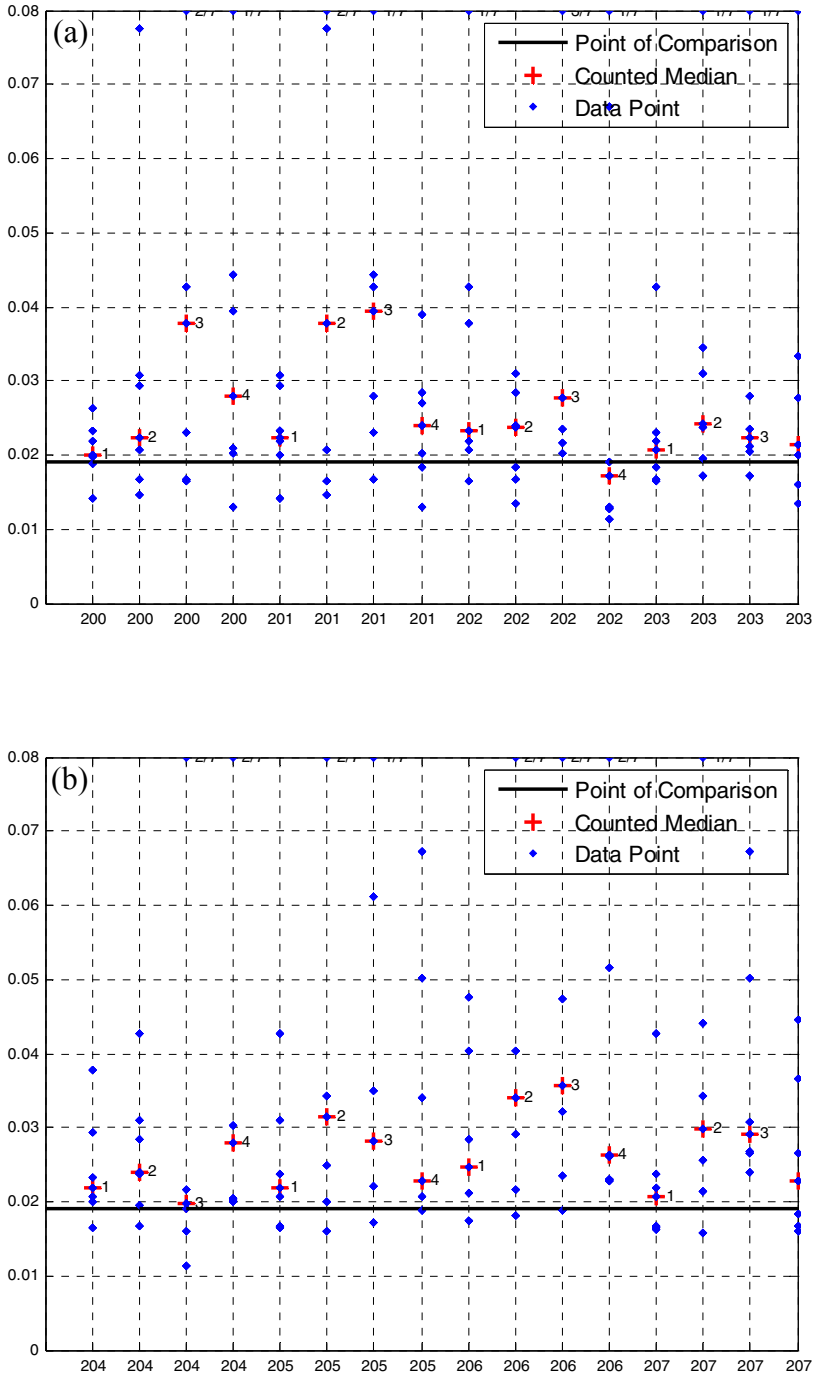

Fig. 8.4 Maximum interstory drift ratio responses for sets of seven ground motions selected and scaled using Group II methods (matching uniform hazard spectrum).

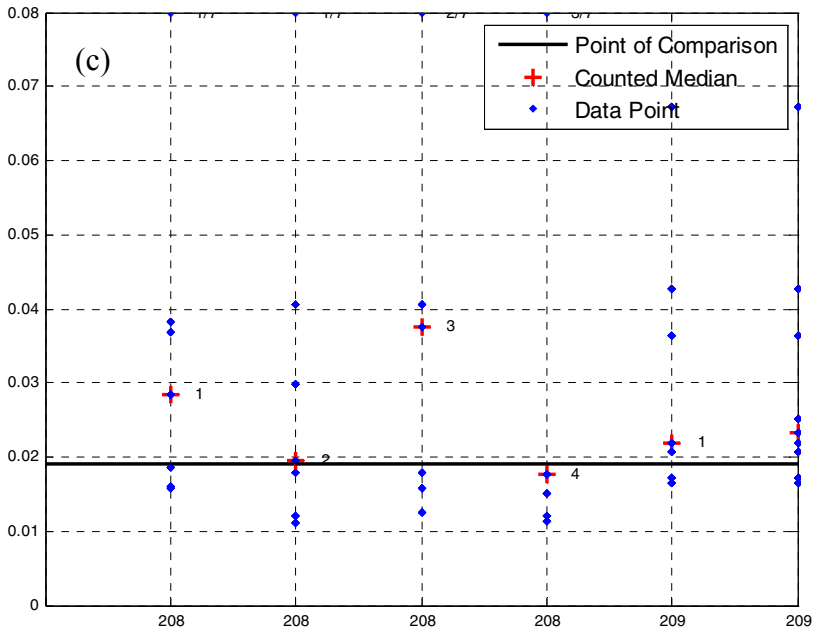

Fig. 8.4—*Continued*

8.5 RESPONSE RESULTS FOR GROUP III METHODS [METHODS THAT MATCH CONDITIONAL MEAN SPECTRUM (CMS)]

The Group III methods discussed in this section match the conditional mean spectrum (CMS) using some type of numerical algorithm. The CMS, and the rationale for utilizing it for GMSM, is discussed in Section 2.4.3. Figure 8.5 shows the scaled acceleration spectra for a set of seven ground motions selected to match the CMS; this example is for method 300.

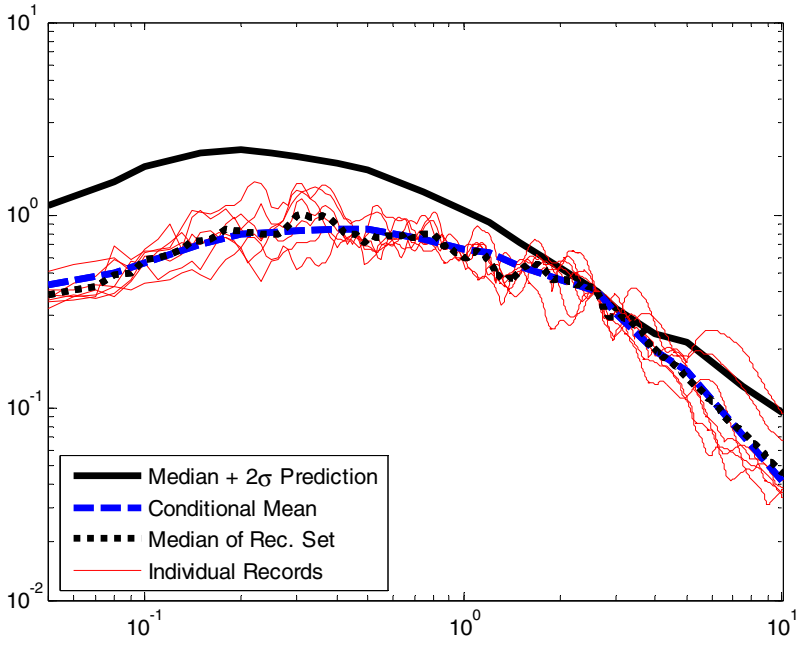

Fig. 8.5 Scaled acceleration spectra for one set of seven records selected to match conditional mean spectrum (method 300).

Table 8.3 and Figure 8.6 present the maximum interstory drift ratio response predictions from the five different methods that match the CMS over a period range deemed important to structural response by the method author (e.g., method 300 matches between $0.2T_1$–$2.0T_1$). The Group III methods lead to a typical MIDR response prediction being only 1% above the POC, with the median predictions from each set of seven records ranging within 15% of the POC (with method 304 being an exception, which is discussed below). Figure 8.6 also shows that for selection and scaling using this group of methods, there are no building collapses in any of the records sets.

Of the methods that have results for multiple ground motion sets, methods 300 and 303 provide the most accurate and consistent predictions.

Method 304 shows a biased and highly variable prediction, simply because it attempts to predict the full distribution of response (Objective 3), while the other methods aim to predict only median response (Objective 4). For comparison, method 303 shows that the DGML method provides a very accurate prediction when aiming to predict only median response (Objective 4).

For consistency in the comparisons of this chapter, the Objective 3 method (method 304) is excluded from the calculation of the summary statistics in Table 8.3.

Table 8.3 Median MIDR responses for sets of seven ground motions selected and scaled using Group III methods.

					Individual Sets		All Subsets Combined	
Method Number	Method Tag	Method Name	Set Index	Num. of Rec.	Median MIDR	Ratio to POC	Median MIDR	Ratio to POC
300	10	Conditional Mean Spectrum Selection with Scaling	1	7	0.0174	0.92	0.0186	0.98
300	10	Conditional Mean Spectrum Selection with Scaling	2	7	0.0198	1.04		
300	10	Conditional Mean Spectrum Selection with Scaling	3	7	0.0189	0.99		
300	10	Conditional Mean Spectrum Selection with Scaling	4	7	0.0195	1.03		
301	15	Genetic Algorithm Selection (to match CMS)	1	7	0.0192	1.01	0.0192	1.01
302	24	Semi-Automated Selection & Scaling (to match CMS)	1	7	0.0172	0.91	0.0203	1.07
302	24	Semi-Automated Selection & Scaling (to match CMS)	2	7	0.0222	1.17		
303	78	Design Ground Motion Library (DGML) (Objective 4)	1	7	0.0180	0.95	0.0190	1.00
303	78	Design Ground Motion Library (DGML) (Objective 4)	2	7	0.0218	1.15		
303	78	Design Ground Motion Library (DGML) (Objective 4)	3	7	0.0203	1.07		
303	78	Design Ground Motion Library (DGML) (Objective 4)	4	7	0.0188	0.99		
304	45	Design Ground Motion Library (DGML) (Objective 3-4)	1	7	0.0144	0.76	0.0158	0.83
304	45	Design Ground Motion Library (DGML) (Objective 3-4)	2	7	0.0287	1.51		
304	45	Design Ground Motion Library (DGML) (Objective 3-4)	3	7	0.0210	1.11		
304	45	Design Ground Motion Library (DGML) (Objective 3-4)	4	7	0.0154	0.81		
			***Median*:**		0.019	**1.01**	--	--
			***Average*:**		0.019	1.02	--	--
			***C.O.V.*:**		--	0.08	--	--
			***Minimum*:**		0.017	0.91	--	--
			***Maximum*:**		0.022	1.17	--	--

*For consistency of comparisons, Objective 3 method is not included in the summary statistics.

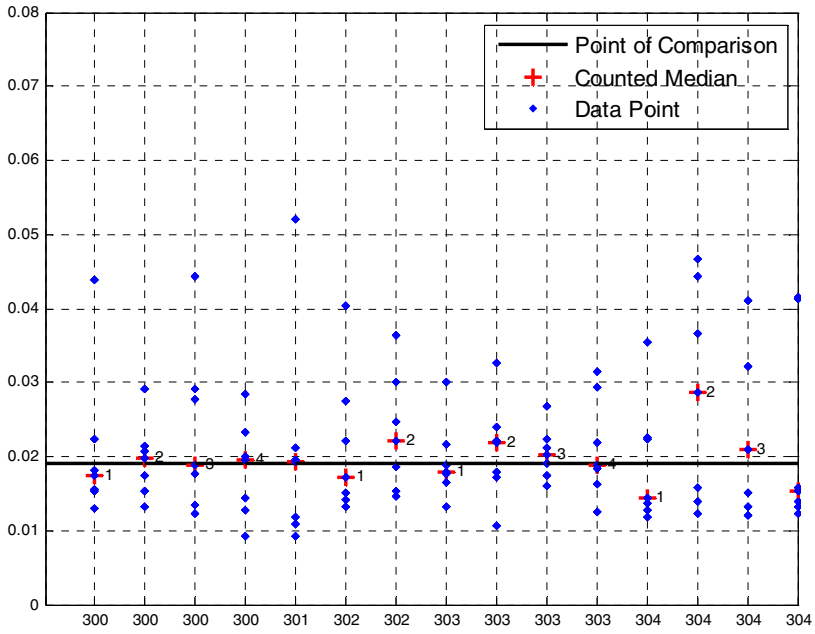

Fig. 8.6 Maximum interstory drift ratio responses for sets of seven ground motions selected and scaled using Group III methods.

8.6 RESPONSE RESULTS FOR GROUP IV METHODS (METHODS THAT USE EPSILON PROXY FOR CMS)

The Group IV methods use an *indicator* of the spectral shape (or a *proxy* for the spectral shape) rather than directly matching the shape of the CMS; these are discussed in Section 2.4.4. This indicator is (or at least involves) the parameter epsilon (ε), which is defined as the number of standard deviations between the natural logarithm of an observed Sa(T) value and the natural logarithm of the median Sa(T) value predicted using an attenuation function.

Table 8.4 and Figure 8.7 present the results for the four Group IV methods. These methods result in a median overprediction of 6%, and a scatter in the predictions that is larger as compared with the methods that directly match the CMS. This large scatter causes the median predictions (from each set of seven records) to typically range within +/-20% of the POC. The one exception is method 401, which is discussed further in this section. Figure 8.7 also shows that for selection and scaling using this group of methods, there is an average of 0.9 building collapses for each set of seven records.

Table 8.4 Median MIDR responses for sets of seven ground motions selected and scaled based on proxy for spectral shape.

					Individual Sets		All Subsets Combined	
Method Number	Method Tag	Method Name	Set Index	Num. of Rec.	Median MIDR	Ratio to POC	Median MIDR	Ratio to POC
400	20	Target Spectrum Based on Epsilon Correlations	1	7	0.0230	1.21	0.0215	1.13
400	20	Target Spectrum Based on Epsilon Correlations	2	7	0.0223	1.17		
400	20	Target Spectrum Based on Epsilon Correlations	3	7	0.0219	1.15		
400	20	Target Spectrum Based on Epsilon Correlations	4	7	0.0164	0.86		
401	31	ε Selection with $S_{de}(T_1)$ Scaling	1	7	0.0357	1.88	0.0218	1.15
401	31	ε Selection with $S_{de}(T_1)$ Scaling	2	7	0.0322	1.69		
401	31	ε Selection with $S_{de}(T_1)$ Scaling	3	7	0.0151	0.79		
401	31	ε Selection with $S_{de}(T_1)$ Scaling	4	7	0.0178	0.94		
402	43	ATC-63 Method Applied to MIDR - Far-Field Set	1	44	0.0153	0.81	0.0153	0.81
403	48	ATC-63 Method Applied to MIDR - Near-Field Set	1	56	0.0182	0.96	0.0182	0.96
				Median:	0.020	**1.06**	--	--
				Average:	0.022	1.15	--	--
				C.O.V.:	--	0.32	--	--
				Minimum:	0.015	0.79	--	--
				Maximum:	0.036	1.88	--	--

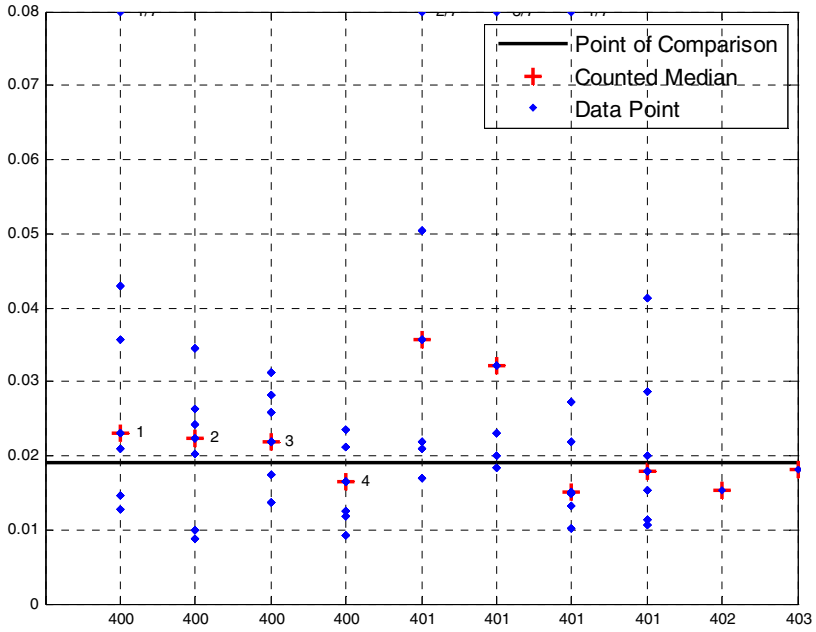

Fig. 8.7 Maximum interstory drift ratio responses for sets of seven ground motions selected and scaled using Group IV methods.

To better investigate method 401, Figure 8.8 shows the combined set of 28 records for this method; this shows that method 401 leads to records that match the CMS well, *on average*, though the variation of spectral content is significant between the individual sets of seven records. To illustrate this, Figure 8.9 shows the spectra for the individual sets of seven records, and these spectra explain the observed MIDR responses for each ground motion set (as shown in Table 8.4). Ground motion sets 1–2 (Fig. 8.9a–b) have spectral values much higher than the CMS for $T > T_1$ (T_1 = 2.63 sec.), and sets 3–4 (Fig. 8.9c–d) have spectral values lower than the CMS at the same periods; this observation correlates exactly with the observation that sets 1–2 greatly overpredict MIDR response and sets 3–4 underpredict response. Even though the average spectral shape tends to match the CMS (Fig. 8.8), the average results still have a slight +15% bias, possibly because the ground motions with Sa values above the CMS at $T > T_1$ tend to produce larger predictions of response, as compared to the underestimation of response by using records with Sa values below the CMS at $T > T_1$ (i.e., unsymmetrical behavior).

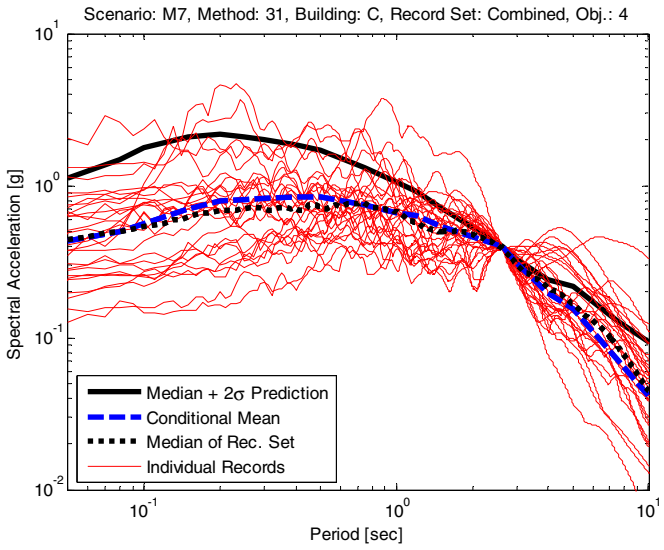

Fig. 8.8 Scaled acceleration spectra for combined set of 28 records selected based on ε (method 401).

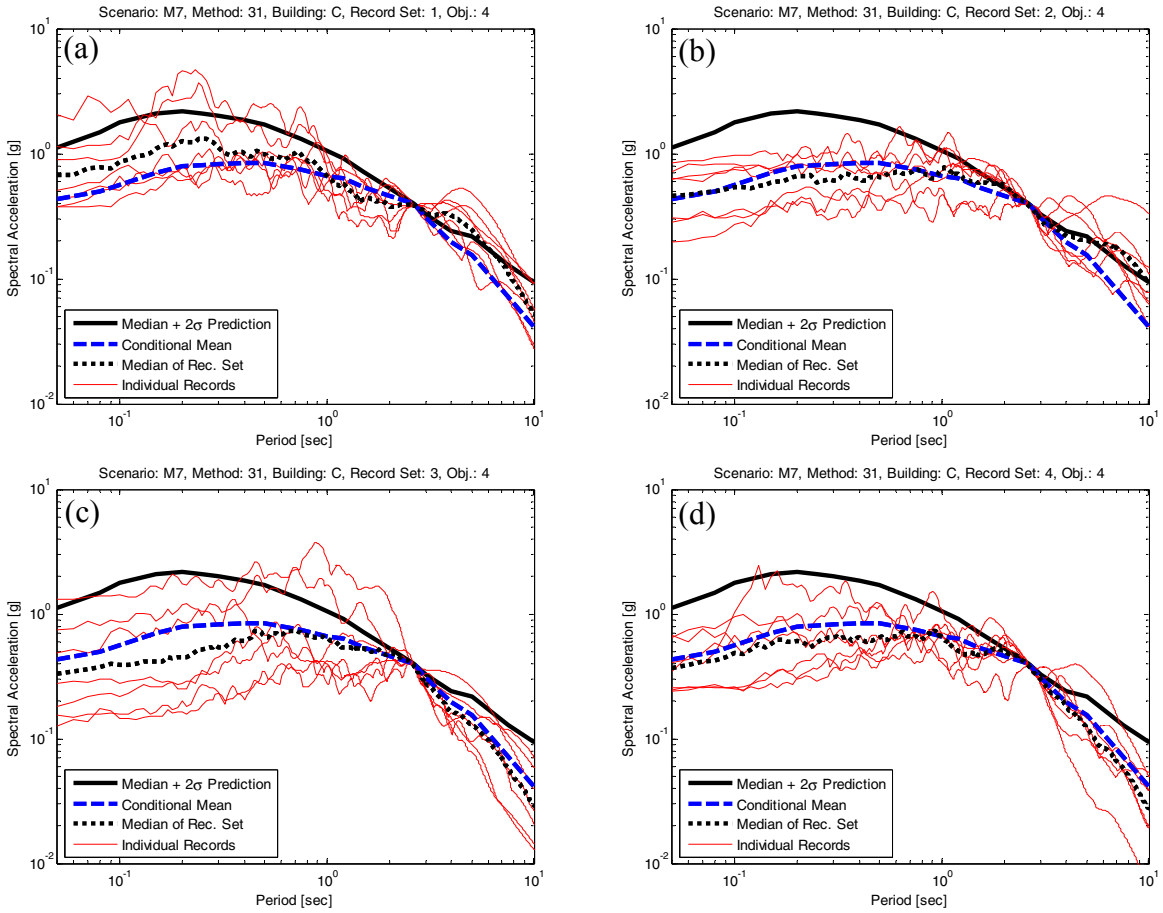

Fig. 8.9 Scaled acceleration spectra for each individual set of seven records selected based on ε (method 401).

To interpret the result of the method 400, Figure 8.10 shows the combined set of 28 records for this method. This shows an average spectrum that is fundamentally different from the CMS; the median spectrum decreases more rapidly that the CMS for $T > T_1$ and nearly matches the UHS for $T < T_1$. Figure 8.11 shows that the median spectra consistently have this shape for each of the individual sets of seven records. Even though this method has a spectral shape different from the CMS, it led to an overprediction of only 13%. Note that this method predicts higher second-mode response and lower first-mode response, as compared to the POC and CMS methods, but the *aggregate* response prediction is similar.

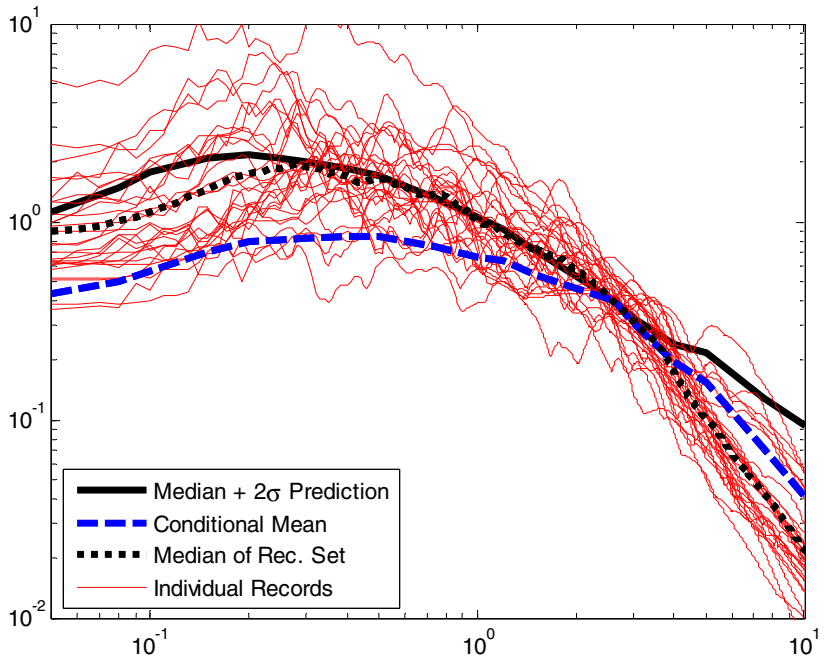

Fig. 8.10 Scaled acceleration spectra for combined set of 28 records selected using method 400.

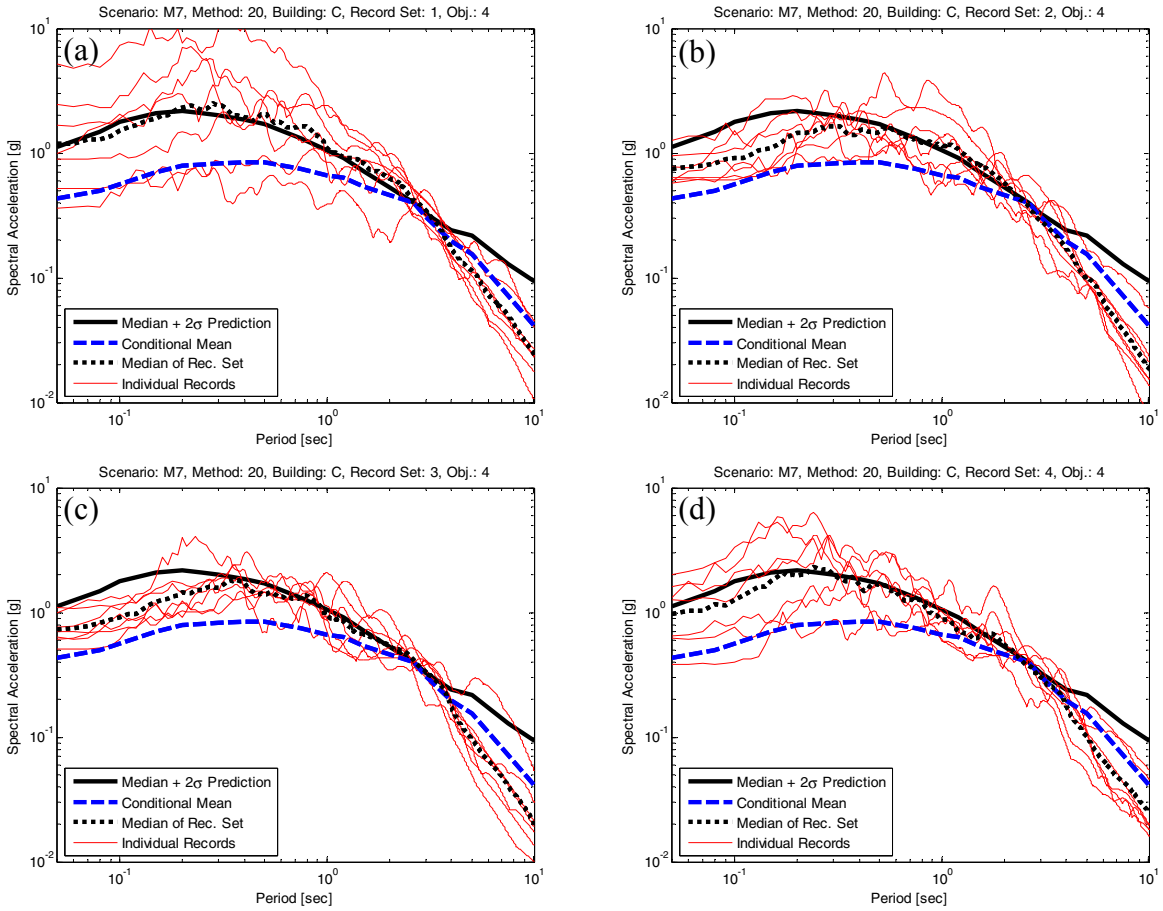

Fig. 8.11 Scaled acceleration spectra for each individual set of seven records selected using method 400.

The spectra for methods 402 and 403 are not shown because the ATC-63 method takes a slightly different approach to record selection and scaling. Due to the objectives of the ATC-63 project (where the method needed to be applicable to any building at any site, with the desire to use the same ground motion sets for all cases), the ATC-63 methods use the same far-field or near-field records set independent of the expected ε value for the ground motion scenario, and then uses results of a linear regression analysis to correct for the expected ε value for the specific scenario being considered. For Building C and the M7 scenario, this method led to 4% underprediction of MIDR response when using the near-field ground motion set and 19% underprediction using the far-field set. This result is similar for the other buildings used in this study, with the near-field set leading to a consistently accurate prediction and the far-field set underpredicting response by an average of about 20%.

8.7 RESPONSE RESULTS FOR GROUP V METHODS (INELASTIC-BASED METHODS)

The Group V methods utilize some type of inelastic parameter (e.g., inelastic spectral displacement) and/or results of inelastic structural analysis (e.g., nonlinear static pushover) to inform the record selection and scaling; these are discussed in Section 2.4.5.

Figure 8.12 and Table 8.5 present the results for the Group V methods. These methods lead to a median MIDR overprediction of 19%. This overprediction is somewhat higher than the Group IV methods, but the scatter in the inelastic-based predictions in substantially smaller. Even though the average overestimation is 19%, there are two methods (one of which is a submethod) in this group which produce a MIDR prediction that is very close to the POC. These methods are discussed individually in this section. Figure 8.12 also shows that for selection and scaling using this group of methods, there is an average of 0.4 building collapses for each set of seven records.

Sections 3.3.1 and 5.2 of this report discuss possible reasons why these inelastic methods result in biased response predictions. This comes from the fact that the M7 scenario and the POC methodology are both based on *elastic* spectral values, and this may be causing an inconsistency with the observed predictions from *inelastic* methods.

Table 8.5 Median MIDR responses for sets of seven ground motions selected and scaled using Group V methods.

					Individual Sets		All Subsets Combined	
Method Number	Method Tag	Method Name	Set Index	Num. of Rec.	Median MIDR	Ratio to POC	Median MIDR	Ratio to POC
500	27	$S_{di}(T_1, dy)$ Scaling	1	7	0.0287	1.51	0.0245	1.29
500	27	$S_{di}(T_1, dy)$ Scaling	2	7	0.0239	1.26		
500	27	$S_{di}(T_1, dy)$ Scaling	3	7	0.0283	1.49		
500	27	$S_{di}(T_1, dy)$ Scaling	4	7	0.0233	1.23		
501	6	Vector of Record Properties Identified by Proxy	1	7	0.0207	1.09	0.0183	0.96
501	6	Vector of Record Properties Identified by Proxy	2	7	0.0198	1.04		
501	6	Vector of Record Properties Identified by Proxy	3	7	0.0144	0.76		
501	6	Vector of Record Properties Identified by Proxy	4	7	0.0189	0.99		
502a	11	Inelastic Response Surface Scaling (1st mode)	1	7	0.0300	1.58	0.0227	1.19
502a	11	Inelastic Response Surface Scaling (1st mode)	2	7	0.0232	1.22		
502b	11	Inelastic Response Surface Scaling (1st-2nd modes)	3	7	0.0204	1.07		
502b	11	Inelastic Response Surface Scaling (1st-2nd modes)	4	7	0.0189	0.99		
503	35	IM1I&2E Selection/Scaling	1	7	0.0191	1.01	0.0225	1.18
503	35	IM1I&2E Selection/Scaling	2	7	0.0256	1.35		
503	35	IM1I&2E Selection/Scaling	3	7	0.0288	1.52		
503	35	IM1I&2E Selection/Scaling	4	7	0.0221	1.16		
				Median:	0.023	**1.19**	--	--
				Average:	0.023	1.20	--	--
				C.O.V.:	--	0.19	--	--
				Minimum:	0.014	0.76	--	--
				Maximum:	0.030	1.58	--	--

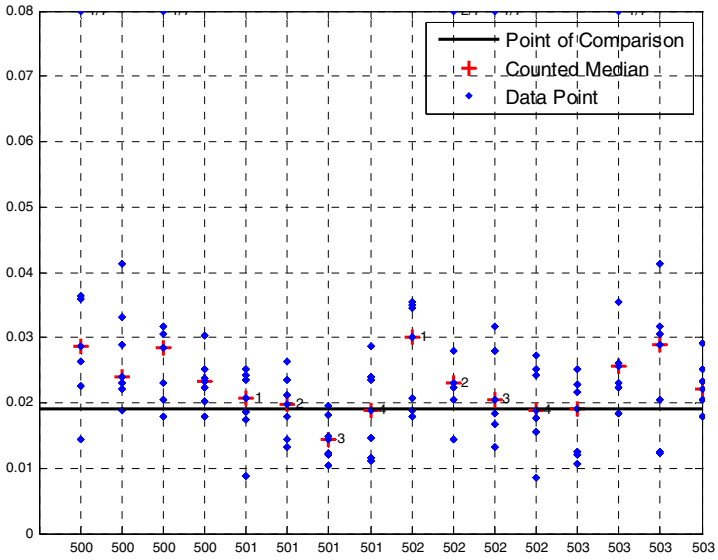

Fig. 8.12 Maximum interstory drift ratio responses for sets of seven ground motions selected and scaled using Group V methods.

Method 500 resulted in an average overprediction of MIDR response by 29%, but the scatter in these predictions is relatively small. As part of using this S_{di} method, one must determine the target S_{di} value that is consistent with the M7 scenario used in this study (which is based on an elastic acceleration spectral value). The author of this method (Tothong) suspects that the target S_{di} value used for selection may have been too large, which led to this consistent overprediction of MIDR response.

Method 503 tends to overpredict response similarly to the S_{di} method (method 500). This overestimation is an average of 18% for the four sets of seven records used. Similarly to method 500, this overestimation may come from the use of an inelastic target which was too high for the M7 scenario.

Method 501 results in much more consistent predictions that are only 4% lower than the POC, on average. Figure 8.13 shows that the average spectrum from this method matches closely to the CMS.

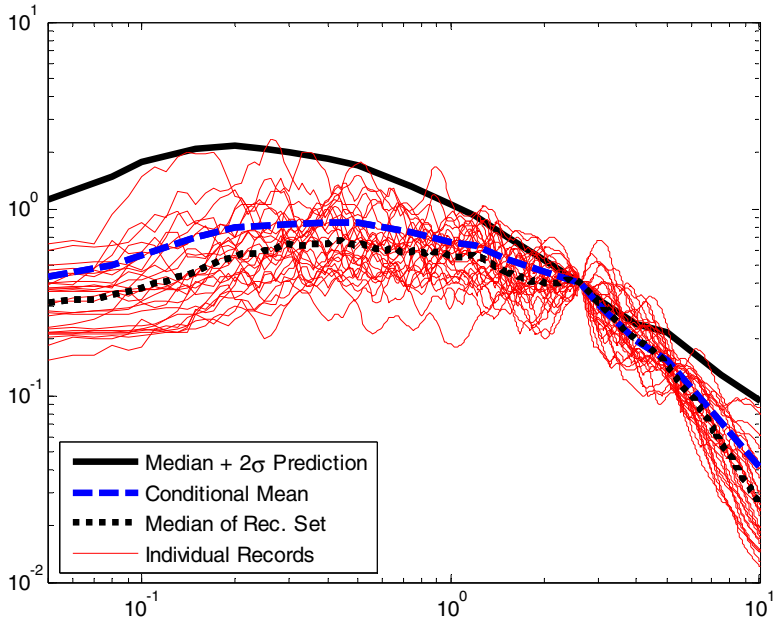

Fig. 8.13 Scaled acceleration spectra for combined set of 28 records selected based on method 501.

Method 502 has two variants. Ground motion sets 1–2 were selected without considering a second-mode term, and sets 3–4 were selected including this term. To illustrate this difference, Figure 8.14 shows the scaled response spectra for ground motion sets 2 and 4. When the second-mode (T_2 = 0.85s) is considered in selection, this method leads to an accurate prediction of MIDR, with a median overestimation of only 3%. In contrast, when the second-mode is not considered, the median overestimation is 40%.

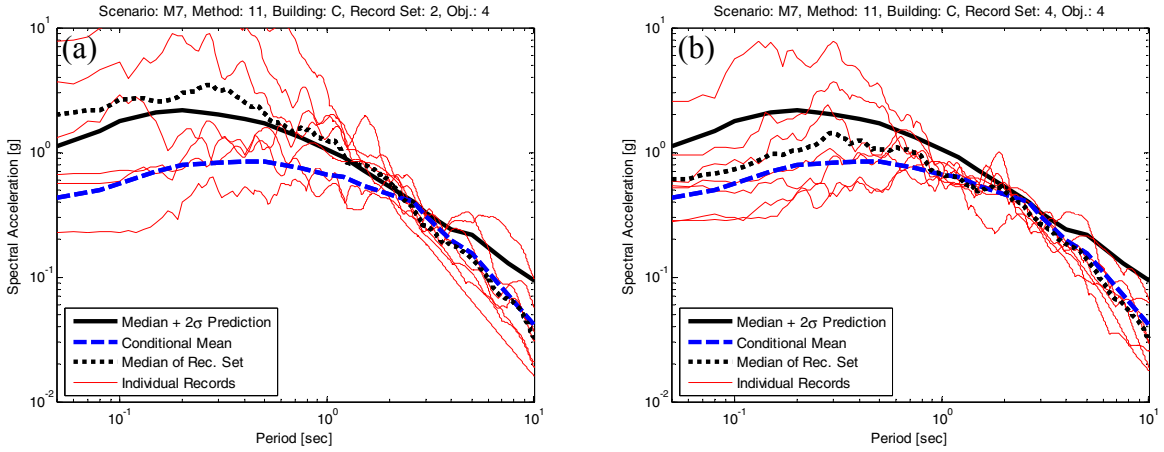

Fig. 8.14 Scaled acceleration spectra for two sets of seven records selected using two variants of method 502: (a) selected without consideration of the second-mode (set 2) and (b) selected to account for second-mode (set 4).

8.8 SUMMARY AND CONCLUSIONS

8.8.1 Summary of Results by Method Group

Table 8.6 summarizes the prediction accuracies by method group for this 20-story modern RC frame building. This table shows summary statistics for the estimation bias factor computed as the ratio of median MIDR response to the point-of-comparison (POC) prediction. This shows that the Group III (CMS matching) methods result in a prediction that is both highly accurate (with a median error of only 2%) and precise (with a coefficient of variation of only 0.09). In contrast, the methods that do not consider the CMS shape in any way (i.e., the Group I and Group II methods) lead to consistent overpredictions of response of 36% and 26%, respectively. This clearly shows that for predicting structural response under an extreme ground motion scenario (e.g., the M7 scenario), consideration of spectral shape is critical.

The Group IV methods use an *indicator,* or *proxy*, for spectral shape to select the records, which leads to higher scatter in the prediction (with a coefficient of variation of 0.33 instead of 0.09), and a slight bias in the prediction (with the median prediction being 6% over the POC).

Group V (inelastic) methods result in a slightly higher overprediction of response (a median overprediction of 19%), but the scatter is much smaller (coefficient of variation of 0.19). This chapter explains that the consistent overpredictions of the Group V methods may come from use of an inelastic target (e.g., S_{di}) that is too high the M7 scenario; if this is the case, further study may be able to remedy this bias problem.

Based on the results of this chapter (for predicting the median MIDR for Building C, subjected to the M7 scenario), the average prediction capability of the method groups can be ordered as follows. Note that these results are general to the method groups and the ordering does not always hold for individual methods within each grouping (as will be shown in the next section).

- Group III [CMS Matching]
- Group IV [proxy methods (e.g., ε)]
- Group V [inelastic-based methods]
- Group II [building code methods]
- Group I [Sa(T_1) methods]

Note that the results from the analyses of the other buildings (Chapters 5, 6, and 8) must be considered before these results can be generalized.

Table 8.6 Summary of response estimation bias factors by method group.

MIDR/POC	I: Sa(T_1)	II: UHS	III: CMS	IV: Proxy (i.e. ε)	V: Inelastic
Median:	1.36	1.26	**1.01**	1.06	1.19
Average:	1.55	1.36	**1.02**	1.15	1.20
C.O.V.:	0.36	0.23	**0.08**	0.32	0.19
Minimum:	1.07	0.91	0.91	0.79	0.76
Maximum:	2.74	2.07	1.17	1.88	1.58

8.8.2 Summary of Methods That Provided Accurate and Precise MIDR Response Predictions for 20-Story Modern RC Frame Building

This section summarizes results by individual method. In contrast, the summary statistics presented in the last section aggregate the results from all methods contained in each method group. The individual methods that work well are not all contained in Group III (which provided the best predictions on average). Table 8.7 presents the seven methods that produced the most accurate and precise predictions of the MIDR response for this modern 20-story RC frame building. *Seven* methods (rather than six or eight) were chosen for this table simply because this was a natural cut-off when trying to identify the methods that are both accurate and precise. To quantify accuracy, this table reports the median MIDR using the records in all ground motion sets submitted for each method (typically four sets of seven records). To roughly quantify precision, the table reports the minimum and maximum values of the median MIDR (computed for each set of seven records), as well as the range between these values. When fewer than four sets were submitted for a method, the above values are also reported, but "≥" and "≤" are added to indicate that the values may have been different if four ground motion sets were utilized.

Referring to Table 8.7, the methods are ranked accounting for both accuracy (with an average MIDR near 1.0 being desirable) and precision (with a range of MIDR near 0.0 being desirable). methods 300 and 303 resulted in the most accurate predictions (1–2% error) and the most precise predictions (with a range in prediction of only 13–20% for four sets of motions). These two methods are ranked as a tie because of the trade-off between accuracy and precision. Next in the ranking are methods 501 and 502b, which result in a median 3–4% overprediction of MIDR. It was not possible to identify which method should be ordered third or fourth because only two ground motion sets were provided for method 502b, and the standard four were provided for method 501; this made it impossible to consistently compare the precision of these two methods. method 302 is ordered in the fifth position, due to the low 7% prediction error. Methods 301 and 403 are also included in this table, since they resulted in accurate predictions with only 1–4% error. Even so, it is not possible to include them in the ordering with the other methods because only one ground motion set was submitted, so the precision of these methods is unknown. Note that the method 301 contributors only provided a single set of motions because the method is based on optimization, and a second set is suboptimal. method 403 contributors

provided only a single set because that method is expressly based on use of a single set of motions.

Table 8.7 Summary of prediction capabilities of selected GMSM methods.

				Ratio of MIDR to Point of Comparison			
Order	Method Name	Method Number	Record Sets	Median	Minimum of Four Sets	Maximum of Four Sets	Range of Four Sets
1 or 2	Design Ground Motion Library (DGML) (Objective 4)	303	4	1.00	0.95	1.15	0.20
1 or 2	Conditional Mean Spectrum Selection with Scaling	300	4	0.98	0.92	1.04	0.13
3 or 4	Vector of Record Properties Identified by Proxy	501	4	0.96	0.76	1.09	0.33
3 or 4	Inelastic Response Surface Scaling (1st-2nd modes)	502b	2	1.03	≤0.99	≥1.07	≥0.08
5	Semi-Automated Selection & Scaling (to match CMS)	302	2	1.07	≤0.91	≥1.17	≥0.26
unknown	Genetic Algorithm Selection (to match CMS)	301	1	1.01	--	--	--
unknown	ATC-63 Method Applied to MIDR - Near-Field Set	403	1	0.96	--	--	--

8.8.3 Closing Comments

This chapter presents many attempts to accurately predict the median MIDR response of a 20-story RC frame building (Building C), when subjected to an M_w = 7.0, R = 10 km, and ε = 2.0 ground motion scenario (the M7 scenario). These comparisons include 14 ground motion selection and modification (GMSM) methods (25 methods if variations are included), which come from five different method groupings.

This chapter concludes that for Building C subjected to the M7 scenario, consideration of proper spectral shape is critical when predicting MIDR under such an extreme ground motion. Methods that select and scale records such that they closely fit the CMS were more accurate and precise than methods that (a) did not utilize the CMS or (b) relied on some other type of selection and scaling that resulted in a looser fit to the CMS (e.g., Group IV methods). Of the specific methods considered, Table 8.7 lists the top seven methods for predicting response of this building. The prediction capabilities of these methods must also be verified for the other buildings utilized in this study (Chapters 6, 7, 9, and 10), in order to determine which methods should be recommended for use in GMSM for building structures, and for further study and verification. Such discussion is included later in Chapter 11.

9 Findings for Modern 12-Story Reinforced Concrete Shear Wall (Building D), Subjected to M 7.0 Scenario

Primary Author: F. Zareian

Associate Author: C. B. Haselton

9.1 INTRODUCTION AND OVERVIEW

This chapter evaluates the ability of 14 ground motion selection and modification (GMSM) methods (16 with method variations) in predicting the median value of maximum interstory drift ratio (MIDR) for a 12-story ductile reinforced concrete shear wall structure (Building D). Building D is the only shear wall structural system used in this study. It has the same number of stories as one of the frame buildings (Building B) and was selected in order to provide a check for a structural system other than frames.

GMSM methods are divided into five classes: $Sa(T_1)$ scaling methods, matching to the UHS methods, matching to CMS methods, ε-based (proxy) methods, and inelastic-based methods. For each class, the median of MIDR predictions for the M7 scenario (M_w = 7.0, R = 10 km, ε = 2.0) are presented for individual methods in that class. These predictions are compared to the point of comparison (POC), which we assume to be the best estimate for the median of MIDR for the M7 scenario. For Building D and the M7 scenario, the POC is 1.08% (Section 4.6). Comparing the predicted responses to the POC serves as the basis for evaluating the prediction capability of the class of methods. When appropriate, the results of individual methods within a class are also highlighted when their predictions differ substantially from other methods in their class.

Based on the results presented in this chapter, it is concluded that the methods that incorporate the proper shape of the spectrum associated with the design scenario (i.e., M7) provided a better estimate of median MIDR compared to other methods. These methods belong to the "Matching to the CMS" class of GMSM methods. It is illustrated that the methods belonging to the "ε-based (proxy)" methods provided the second most accurate response estimates for Building D.

9.1.1 Summary of Ductile 12-Story Shear Wall Building, Building D

Building D is a generic 12-story shear wall system with T_1 = 1.2 sec, and base shear coefficient V = 0.17W where W is the weight of the building. This design corresponds to a R_μ = 3 for the elastic design spectrum for soil type D in California (S_{DS} = 1.0g, S_{D1} = 0.6g). A uniform moment of inertia, mass, and strength is assumed over the height of the structure, and it is assumed the building can provide 5% critical damping in the first and third modes of vibration. The shear wall is modeled as a cantilever with 12 beam-column elements, each representing a story in the building, and each with a plastic hinge rotation capacity of 0.03. The model was created using Drain-2DX (Prakash and Powell 1993). Further information about the model can be found in Section 3.2 and in Zareian (2006).

9.1.2 Comparison to Other Chapters (Ground Motion Scenario, and Building)

The current chapter presents the results of simulations for a 12-story shear wall building (Building D) for the M7 scenario (M_w = 7.0, R = 10 km, ε = 2.0). This same ground motion scenario is considered in Chapters 6, 7, and 8, while Chapter 10 considers an additional M7.5 scenario.

Building D is a ductile reinforced concrete shear wall building, and it was selected so that an additional structural system was represented in the set of buildings used in this study. The 12-story height was chosen to allow direct comparisons to Building B (the 12-story RC frame building). Details about the design characteristics of this structure can be found in Section 3.2 and in Zareian (2006). For Building D and the M7 scenario, the point-of-comparison MIDR is 1.08% (Section 4.6).

9.1.3 Ground Motion Sets

Ground motion sets were selected according to the approach described in Section 3.4, which is the same method utilized for each building and ground motion scenario (Chapters 6-10).

Appendix C provides detailed documentation of each ground motion set, and the structural response predictions resulting from the set. This electronic Appendix includes Excel spreadsheet files with the ground motion filenames (from the PEER-NGA database; PEER 2006), the scale factors, and the resulting structural responses (including MIDR, individual drifts, floor accelerations, and many others). Also included are figure files showing the scaled acceleration spectra for each ground motion set.

Note that very few ground motions considered in this study caused collapse of this ductile RC wall building (only two motions).

9.2 METHOD CLASSIFICATIONS

The following sections present estimates of MIDR by method classification. The results are presented following the classes, which were established in Section 2.4. Chapter 2 explains the basis of each of these method classes.

- Group I: Sa(T_1) scaling (with bin selection)
- Group II: Building code methods (matching to the uniform hazard spectrum)
- Group III: Conditional mean spectrum (CMS) matching
- Group IV: methods using a proxy for the CMS (e.g., selection based on ε)
- Group V: Inelastic-based methods

9.3 RESPONSE RESULTS FOR GROUP I METHODS [SA(T_1) SCALING]

The basic process in the Sa(T_1) methods is to select a set of records from a ground motion bin, and scale this set to a target Sa(T_1) representing the ground motion scenario handoff interest. More detail about this class of GMSM methods can be found in Section 2.4.1.

Table 9.1 and Figure 9.1 illustrate the MIDR predictions of the Sa(T_1) class of GMSM methods (i.e., methods 100 and 101), and show a comparison to the POC prediction. Method 100 corresponds to a standard GMSM method that uses Sa(T_1) as a basis for scaling ground motion

records with a proper bin selection, and method 101 is the GMSM method recommended in the ATC-58 35% draft, which is similar to the latter but the ground motion record selection bin is limited to a group of 40 motions mandated by ATC-58 35% draft. Compared to the POC, the $Sa(T_1)$ class of GMSM methods have a median MIDR overestimation of 29%.

Table 9.1 Median MIDR estimated for Building D, using sets of seven ground motions selected and scaled using $Sa(T_1)$ methods.

					Individual Sets		All Subsets Combined	
Method Number	Method Tag	Method Name	GM Set Index	Number of Records	Median MIDR	Ratio to POC	Median MIDR	Ratio to POC
100	4	$Sa(T_1)$ Scaling with Bin Selection	1	7	0.0106	0.98	0.0108	1.00
100	4	$Sa(T_1)$ Scaling with Bin Selection	2	7	0.0124	1.15		
100	4	$Sa(T_1)$ Scaling with Bin Selection	3	7	0.0101	0.94		
100	4	$Sa(T_1)$ Scaling with Bin Selection	4	7	0.0155	1.44		
101	67	ATC-58 35% Draft Method	1	11	0.0168	1.56	0.0135	1.25
101	67	ATC-58 35% Draft Method	2	11	0.0126	1.17		
101	67	ATC-58 35% Draft Method	3	11	0.0153	1.42		
101	67	ATC-58 35% Draft Method	4	11	0.0153	1.42		
				Median:	0.0140	**1.29**	–	--
				Average:	0.0136	1.26	–	--
				C.O.V.:	--	0.18	–	--
				Minimum:	0.0101	0.94	–	--
				Maximum:	0.0168	1.56	–	--

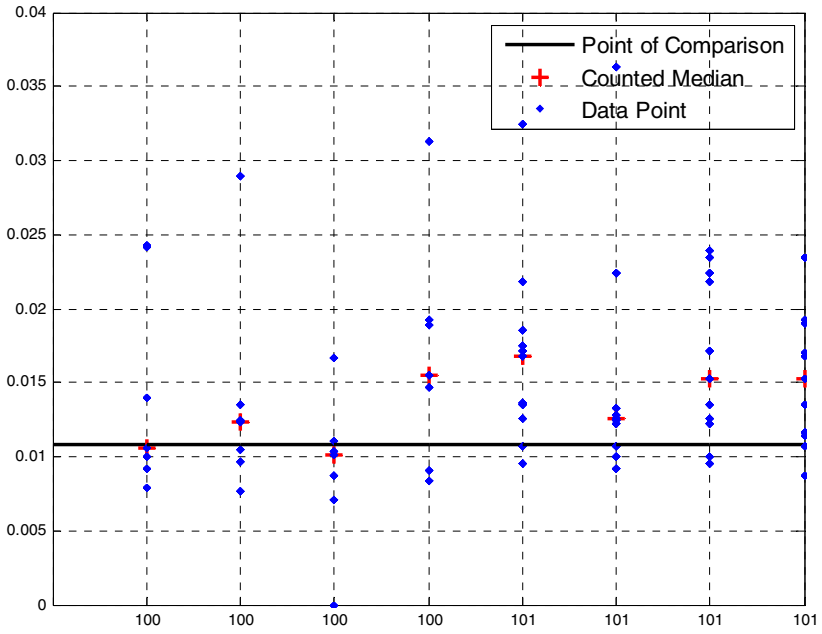

Fig. 9.1 MIDR estimated for Building D using sets of seven ground motions selected and scaled using Sa(T_1) methods.

As shown in Table 9.1, among methods in the Sa(T_1) GMSM class, method 101 overestimates the median of MIDR by 25%. This is due to the incompatibility of the spectral shapes of the ground motion records used in this GMSM method with the spectrum that represents ground motion intensity for the M7 scenario and Building D. On the other hand, GMSM class method 100 estimates POC very well, which is due to *accidental* compatibility of the spectral shapes of the ground motion records used. The previous chapters showed that this is not a general finding, and overall for all buildings considered in this study method 100 provides a median 46% overprediction of MIDR response.

Categorically, GMSM methods in this class do not appreciate the spectral shape in selection and scaling of ground motions for the target scenario, and typically lead to overprediction of response. This conclusion can be illustrated by observing the difference between the median spectra of ground motion records in each of the GMSM methods of this class and the expected spectrum, termed the conditional mean spectrum (CMS), for the scenario event. We consider the CMS to be the statistically appropriate spectral shape for a scenario ground motion. Figure 9.2 shows the scaled acceleration spectra for methods 100 and 101, along

with the CMS and uniform hazard spectrum (UHS) for this scenario and building. The solid black line shows the UHS for the M7 scenario, and the blue dashed line shows the CMS for the M7 scenario and period of 1.2 sec. The red lines in Figure 9.2 show 28 spectra included in the four sets of seven records for each GMSM method scaled to the target $Sa(T_1) = 0.92g$, and the dotted black line shows the median of the 28-record set. For GMSM method 100, Figure 9.2a, the median spectrum accidentally has a similar spectral acceleration for periods larger than the fundamental period of Building D. As Building D undergoes nonlinear behavior and period elongation, this similarity in spectral shape leads to similar estimates of MIDR for method 100 and the POC method (which reflects the proper CMS spectral shape).

Compared to the standard $Sa(T_1)$ scaling method, the ATC-58 35% draft method, method 101, has a median spectrum that is higher for periods larger than $T_1 = 1.2$ sec, which causes an overestimation of the median of MIDR (See Fig. 9.2b). The standard $Sa(T_1)$ scaling method (method 100) selects records from a bin that represents the $M_w = 7.0$ and R = 10 km scenario, while the ATC-58 35% draft method selects records from a near-field bin containing many pulse-type motions.

It needs to be emphasized that the ATC-58 35% draft method utilized in this research are subject to change. The ATC-58 project team has already indicated that spectral shape will be considered in future versions of the ATC-58 GMSM methodology, which can address the issue shown in these findings.

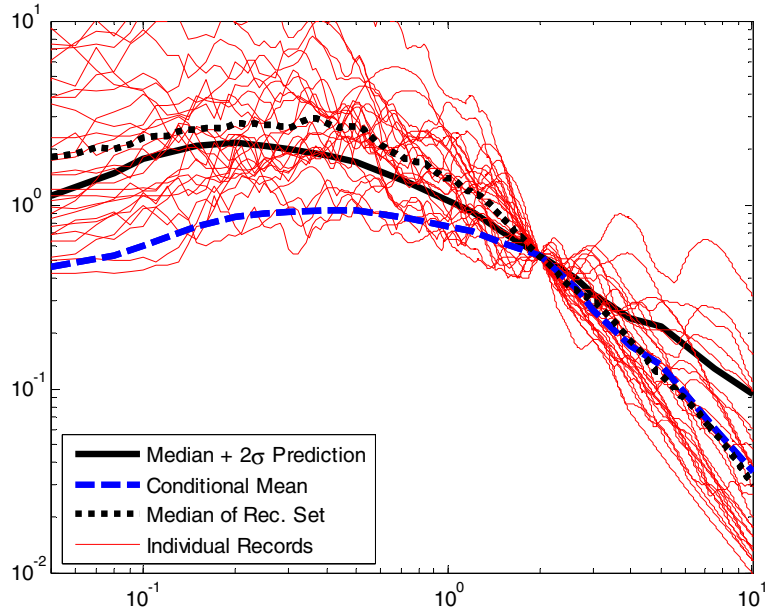

(a)

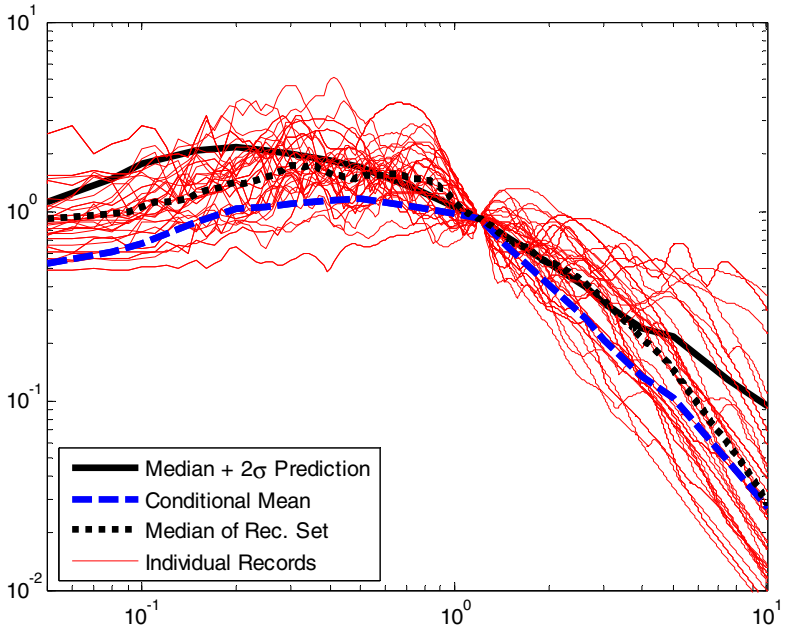

(b)

Fig. 9.2 Scaled acceleration spectra for combined set of 28 records (4 sets of 7 records each) selected using Sa(T_1) scaling methods for Building D: (a) 100 and (b) 101.

9.4 RESPONSE RESULTS FOR GROUP II METHODS (BUILDING CODE–BASED METHODS THAT MATCH UNIFORM HAZARD SPECTRUM)

The basic process for GMSM methods that use uniform hazard spectrum (UHS) for a target spectral shape is to select a set of records (based on some requirements, which are not consistent between various methods) and then scale the set so that the median spectrum of the set matches the target UHS. Such GMSM methods have been recommended by the Uniform Building Code (UBC 1997) and the ASCE 7-05 (ASCE 2005).

Table 9.2 and Figure 9.3 present the MIDR predictions for the single GMSM method (method 200) that matches the UHS. Compared with the POC value, this method results in a median overestimation of MIDR by 9%. Chapter 11 shows that this overestimation is lower than the average for all of the buildings in this study (which is 20% for this method); this occurs because the behavior of Building D is less nonlinear, on average, as compared to the other buildings (thus causing less period elongation, and causing spectral shape to be less important).

Figure 9.3 shows that two of the 28 ground motions from this method cause collapse of this structure. Of all GMSM methods considered in this chapter, this is the only method that results in a collapse prediction for this building.

Figure 9.4 shows the spectra for the four sets of seven records selected and scaled using method 200. The figure shows that the median spectrum for the selected and scaled records falls slightly above the CMS, which is assumed to be the best representative of spectral acceleration at all periods for Building D in the M7 scenario. As the building experiences period elongation, it is expected that by using the GMSM method that uses UHS, the MIDR will be overestimated.

The large overestimation (54%) and scatter in estimation of the median of MIDR using the second set of selected and scaled ground motion records using method 200 is due to large values of spectral acceleration at periods larger than T_1 = 1.2 sec. This can be seen in Figure 9.5 where the spectra for the four sets of seven records ground motions selected and scaled using method 200 are illustrated separately. As seen in Figure 9.5b, there is large scatter in the spectral values for periods larger than T_1 = 1.2 sec, and the ordinates of the median spectrum for the selected set falls above the CMS.

Table 9.2 Median of MIDR estimated for Building D, using sets of seven ground motions selected and scaled using building code–based methods (matching uniform hazard spectrum).

					Individual Sets		All Subsets Combined	
Method Number	Method Tag	Method Name	GM Set Index	Number of Records	Median MIDR	Ratio to POC	Median MIDR	Ratio to POC
200	9980/39	Building Code Selection and Scaling - Method A	1	7	0.0120	1.11	0.0119	1.10
200	9980/39	Building Code Selection and Scaling - Method A	2	7	0.0166	1.54		
200	9980/39	Building Code Selection and Scaling - Method A	3	7	0.0111	1.03		
200	9980/39	Building Code Selection and Scaling - Method A	4	7	0.0116	1.07		
				Median:	0.0118	**1.09**	--	--
				Average:	0.0128	1.19	--	--
				C.O.V.:	--	0.20	--	--
				Minimum:	0.0111	1.03	--	--
				Maximum:	0.0166	1.54	--	--

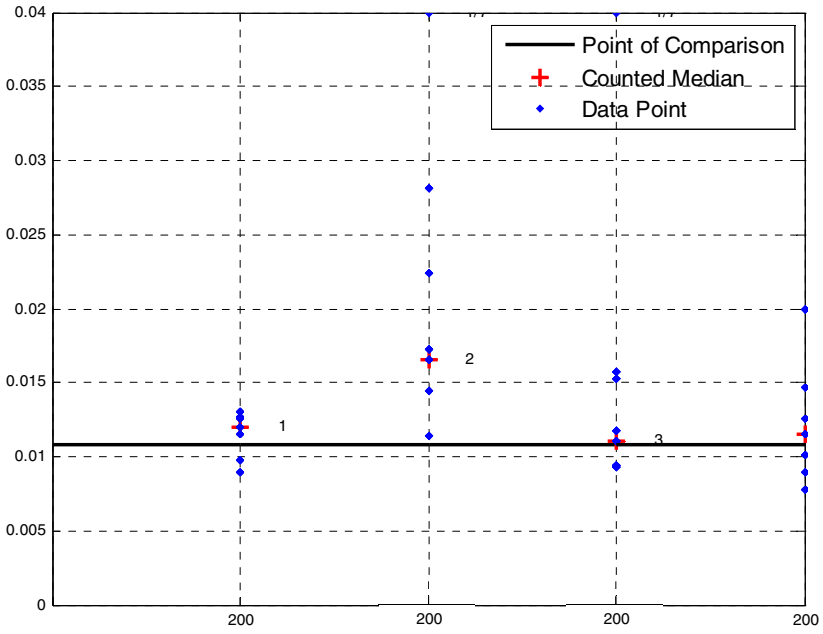

Fig. 9.3 MIDR estimated for Building D using sets of seven ground motions selected and scaled using building code–based methods (matching uniform hazard spectrum).

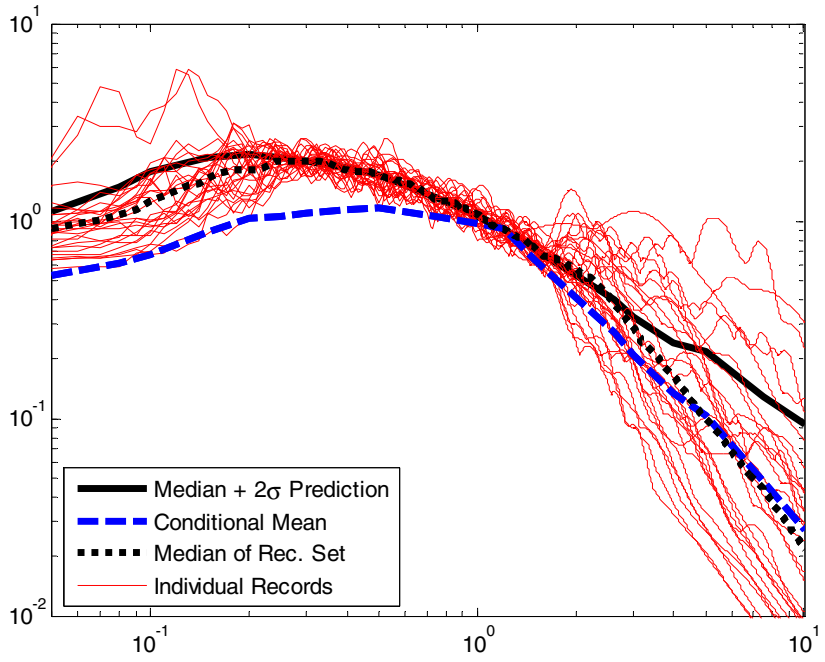

Fig. 9.4 Scaled acceleration spectra for combined set of 28 records (4 sets of 7 records each) selected using method 200 for Building D.

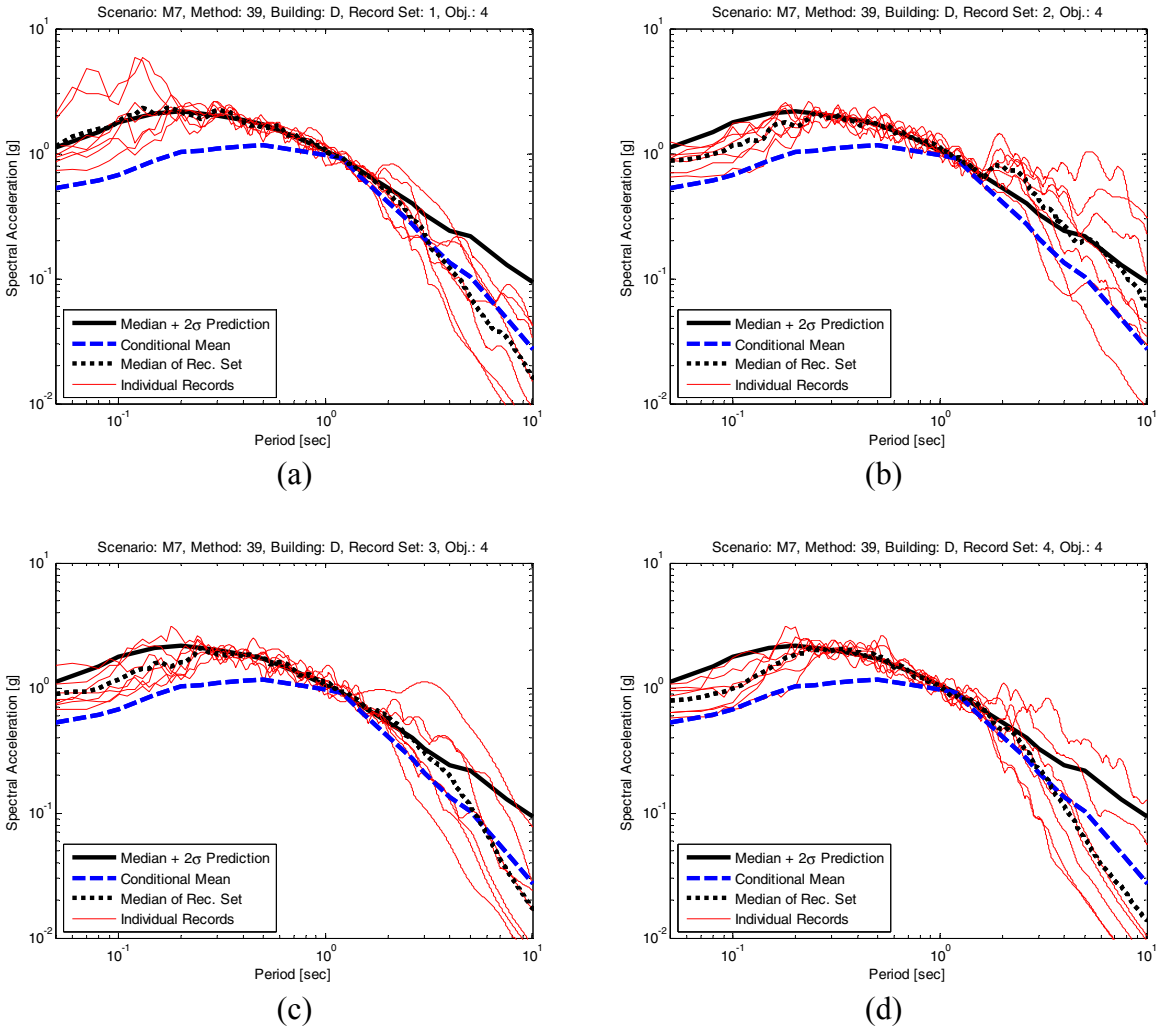

Fig. 9.5 Scaled acceleration spectra for individual sets of seven records selected using method 200 for Building D: (a) set 1, (b) set 2, (c) set 3 (d) set 4.

9.5 RESPONSE RESULTS FOR GROUP III METHODS [THAT MATCH CONDITIONAL MEAN SPECTRUM (CMS)]

Of all the methods considered in this study, GMSM methods that try to match the conditional mean spectrum (CMS) for the scenario earthquake (i.e., M7) provide the best estimate of the median MIDR response. A detailed discussion about this class of selection and scaling methods is provided in Section 2.4.3. In short, the conditional mean spectrum represents both the spectral

acceleration at the fundamental period of the structure, as well as the proper shape of the spectrum for the target ground motion scenario.

Table 9.3 and Figure 9.6 present the median of MIDR predictions from five different methods that match the CMS. These methods lead to a 5% median underestimation of MIDR, as compared to the POC. Among methods in the CMS selection and scaling group, the semi-automated algorithm for selection and scaling to match CMS, method 302, provides the most accurate and consistent prediction (i.e., an average of 1% overestimation of the median MIDR). Figure 9.7 shows the scaled acceleration spectra for the two set of seven ground motions selected to match the CMS using method 302. The close match between individual ground motion spectra and CMS is the reason for the close prediction of the median of MIDR using this method. Furthermore, the larger scatter in the prediction of the median of MIDR using the second set compared to the first set of method 302 (see Fig. 9.6) can be explained by the larger scatter around the CMS spectrum for the records in the first set.

Table 9.3 Median of MIDR estimated for Building D, using sets of seven ground motions selected and scaled to match conditional mean spectrum (CMS).

					Individual Sets		All Subsets Combined	
Method Number	Method Tag	Method Name	GM Set Index	Number of Records	Median MIDR	Ratio to POC	Median MIDR	Ratio to POC
300	10	Conditional Mean Spectrum Selection with Scaling	1	7	0.0108	1.00	0.0103	0.95
300	10	Conditional Mean Spectrum Selection with Scaling	2	7	0.0100	0.93		
300	10	Conditional Mean Spectrum Selection with Scaling	3	7	0.0101	0.94		
300	10	Conditional Mean Spectrum Selection with Scaling	4	7	0.0103	0.95		
301	15	Genetic Algorithm Selection (to match CMS)	1	7	0.0068	0.63	0.0068	0.63
302	24	Semi-Automated Selection & Scaling (to match CMS)	1	7	0.0110	1.02	0.0109	1.01
302	24	Semi-Automated Selection & Scaling (to match CMS)	2	7	0.0109	1.01		
304	45	Design Ground Motion Library (DGML) (Objective 3-4)	1	7	0.0097	0.90	0.0099	0.92
304	45	Design Ground Motion Library (DGML) (Objective 3-4)	2	7	0.0100	0.93		
304	45	Design Ground Motion Library (DGML) (Objective 3-4)	3	7	0.0099	0.92		
304	45	Design Ground Motion Library (DGML) (Objective 3-4)	4	7	0.0104	0.96		
				Median:	0.0103	**0.95**	--	--
				Average:	0.0100	0.92	--	--
				C.O.V.:	--	0.15	--	--
				Minimum:	0.0068	0.63	--	--
				Maximum:	0.0110	1.02	--	--

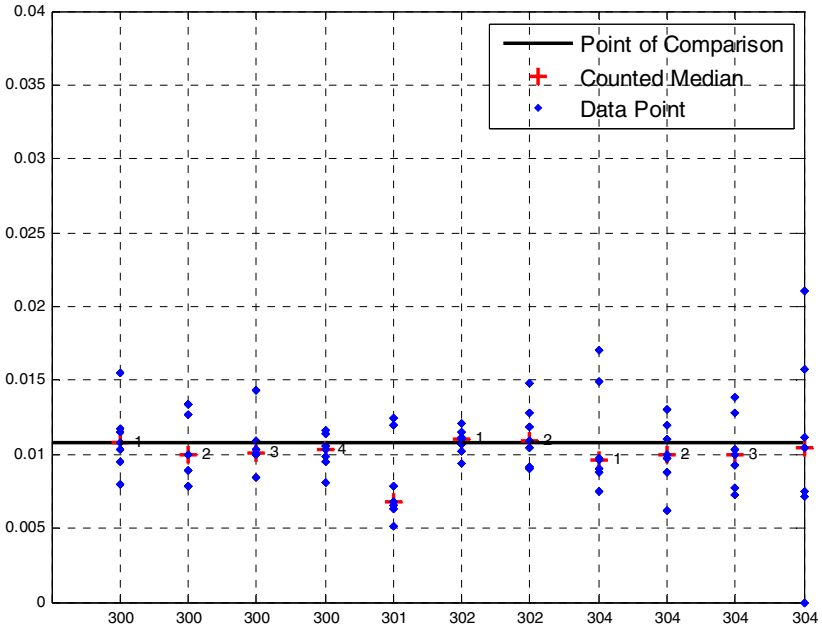

Fig. 9.6 MIDR estimated for Building D using sets of seven ground motions selected and scaled to match conditional mean spectrum (CMS).

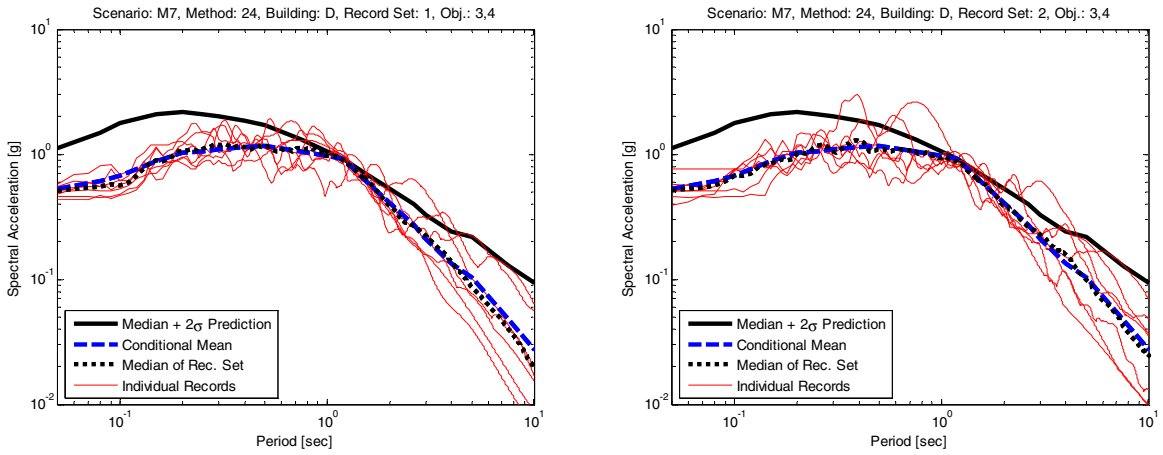

Fig. 9.7 Scaled acceleration spectra for sets of seven records selected using method 302 for Building D: (a) set 1, (b) set 2.

9.6 RESPONSE RESULTS FOR GROUP IV METHODS (METHODS THAT USE PROXY FOR CMS)

In the previous section, it was shown that using CMS for selection and scaling ground motions will result in good estimates for median MIDR. This efficiency in estimating median MIDR is due to the fact that by using the CMS, the set of selected and scaled ground motions will properly represent both the spectral amplitude and the spectral shape of a typical ground motion for the target scenario. In this section, methods are evaluated that use epsilon (ε) as a proxy for incorporating this target spectral shape. Table 9.4 and Figure 9.8 present the results for the three methods that use ε as a proxy for the CMS. The median overestimation of MIDR is 5% when the methods in this class are used.

This overestimation of 5% is not consistent between the methods in this class. Method 400 results in a 6% overestimation of the median MIDR, method 401 overestimates by 10%, and method 403 underestimates by 27%.

Figure 9.9 shows the acceleration spectra for the combined set of 28 records for method 400. This figure shows that using ε as a proxy for CMS leads to records that match the CMS well. Figure 9.10 shows the spectra for the individual sets of seven records selected and scaled using method 401. The figure shows that the median of spectral acceleration for seven motions in each set is larger than CMS in periods larger than T_1 = 1.2 sec; hence, the estimates of MIDR will be larger than POC.

Table 9.4 Median of MIDR estimated for Building D, using sets of seven ground motions selected and scaled to match conditional mean spectrum (CMS).

					Individual Sets		All Subsets Combined	
Method Number	Method Tag	Method Name	GM Set Index	Number of Records	Median MIDR	Ratio to POC	Median MIDR	Ratio to POC
400	20	Target Spectrum Based on Epsilon Correlations	1	7	0.0133	1.23	0.0114	1.06
400	20	Target Spectrum Based on Epsilon Correlations	2	7	0.0108	1.00		
400	20	Target Spectrum Based on Epsilon Correlations	3	7	0.0112	1.04		
400	20	Target Spectrum Based on Epsilon Correlations	4	7	0.0093	0.86		
401	31	ε Selection with $S_{de}(T_1)$ Scaling	1	7	0.0118	1.09	0.0119	1.10
401	31	ε Selection with $S_{de}(T_1)$ Scaling	2	7	0.0124	1.15		
401	31	ε Selection with $S_{de}(T_1)$ Scaling	3	7	0.0115	1.06		
401	31	ε Selection with $S_{de}(T_1)$ Scaling	4	7	0.0136	1.26		
402	43	ATC-63 Method Applied to MIDR - Far-Field Set	1	44	0.0079	0.73	0.0079	0.73
403	48	ATC-63 Method Applied to MIDR - Near-Field Set	1	56	0.0112	1.04	0.0112	1.04
				Median:	0.011	**1.05**	--	--
				Average:	0.011	1.05	--	--
				C.O.V.:	--	0.15	--	--
				Minimum:	0.008	0.73	--	--
				Maximum:	0.014	1.26	--	--

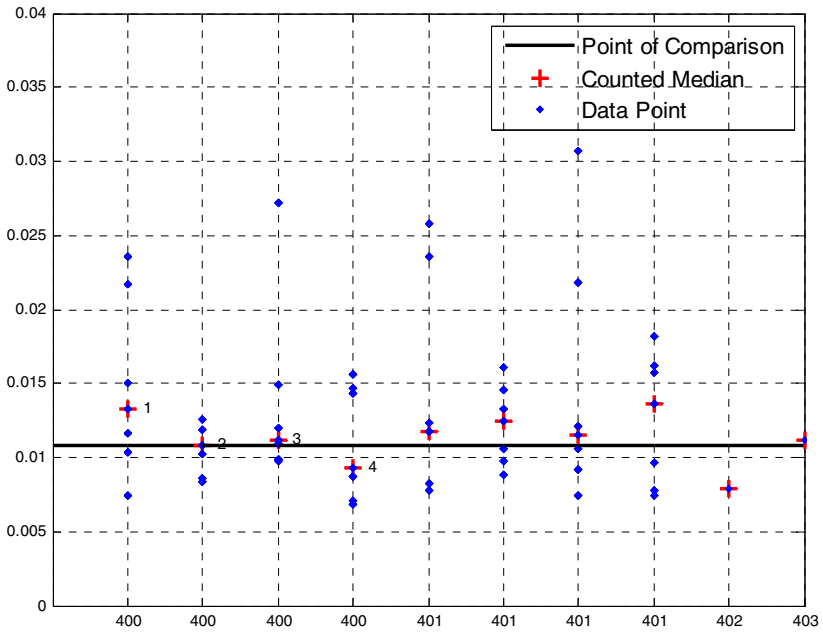

Fig. 9.8 Figure of MIDR estimated for Building D using sets of seven ground motions selected and scaled to match conditional mean spectrum (CMS).

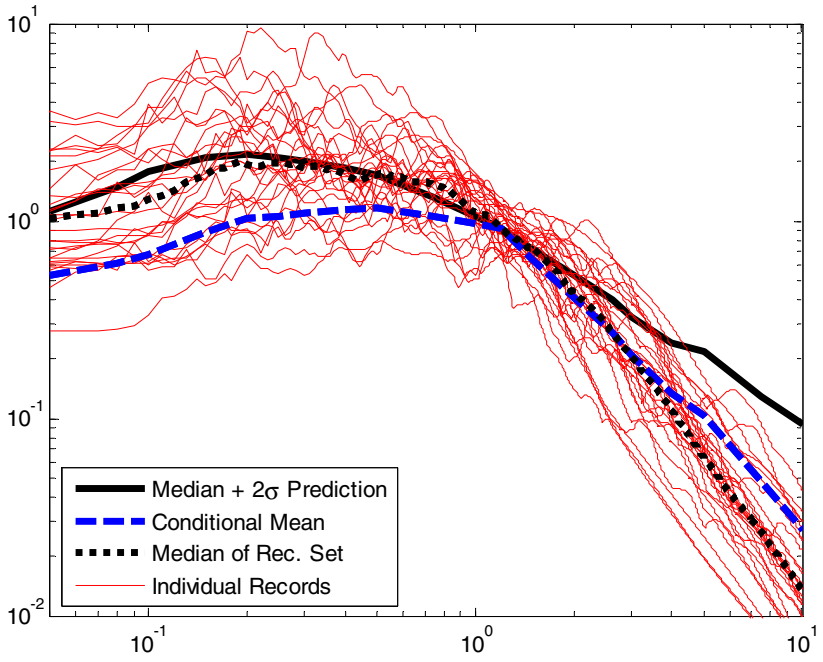

Fig. 9.9 Scaled acceleration spectra for combined set of 28 records selected using method 400 for Building D.

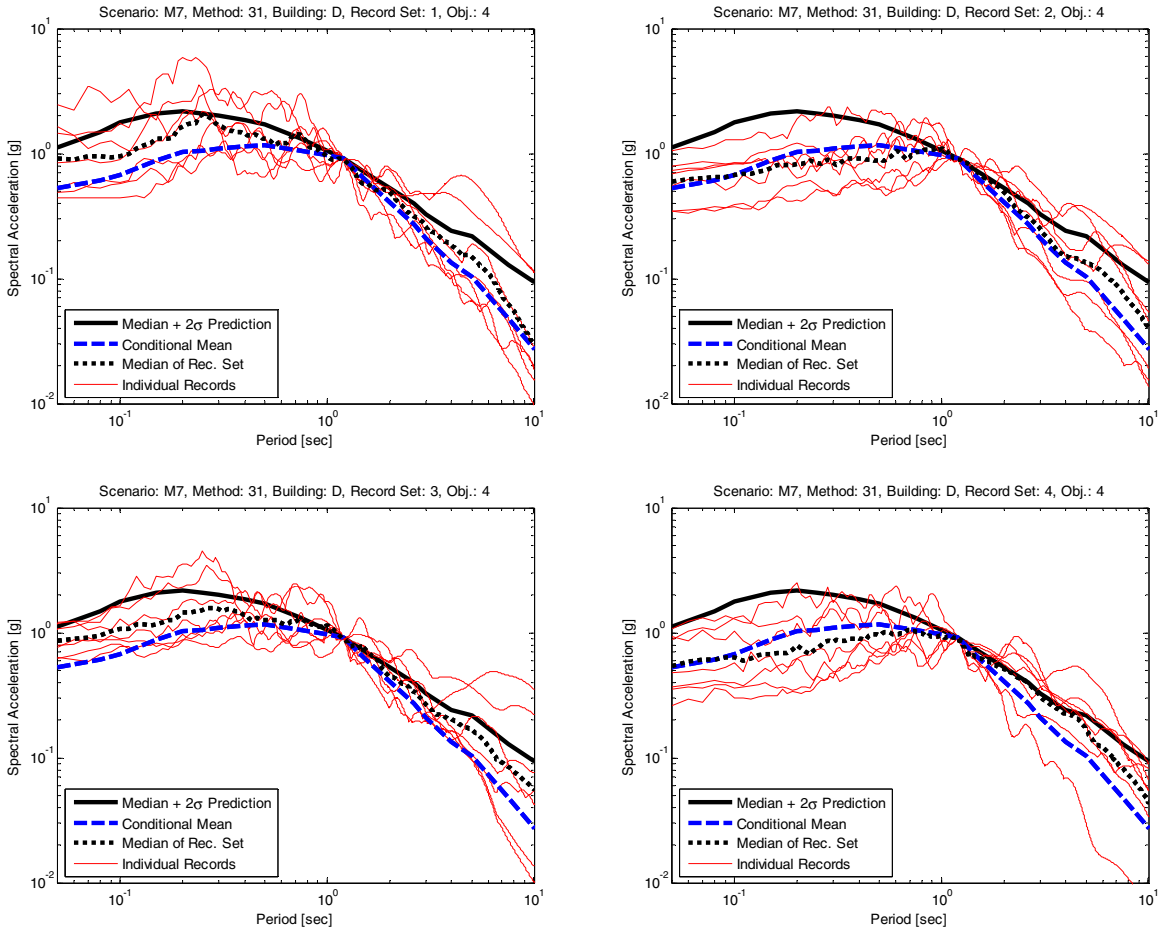

Fig. 9.10 Scaled acceleration spectra for each individual set of seven records selected using method 401 for Building D.

9.7 RESPONSE RESULTS FOR GROUP V METHODS (INELASTIC-BASED METHODS)

Table 9.5 and Figure 9.11 present the predictions of the median MIDR for the four GMSM methods that utilize some type of inelastic parameter (e.g., inelastic spectral displacement) and/or use results of inelastic structural analysis (e.g., nonlinear static pushover). In a median sense, these methods overpredict the POC by 4%. However, the differences between the estimates from each individual method are slightly larger.

Method 502a results in a median underprediction of response by only 2%, but the alternative version of the same method (which considers the second-mode spectral acceleration) results in a larger 16% underprediction.

Methods 500 and 503 overestimate the median of MIDR by 11% and 10%, respectively. As discussed in Section 3.3.1 and Chapter 5, this overestimation may come from the fact that the M7 scenario and the POC value are based on *elastic* spectral parameters, which are somewhat incompatible with these inelastic methods.

Method 501 underestimates the median of MIDR by 15%.

Table 9.5 Median of MIDR estimated for Building D, using sets of seven ground motions selected and scaled using inelastic-based methods.

					Individual Sets		All Subsets Combined	
Method Number	Method Tag	Method Name	GM Set Index	Number of Records	Median MIDR	Ratio to POC	Median MIDR	Ratio to POC
500	27	$S_{di}(T_1, dy)$ Scaling	1	7	0.0122	1.13	0.0120	1.11
500	27	$S_{di}(T_1, dy)$ Scaling	2	7	0.0117	1.08		
500	27	$S_{di}(T_1, dy)$ Scaling	3	7	0.0120	1.11		
500	27	$S_{di}(T_1, dy)$ Scaling	4	7	0.0133	1.23		
501	6	Vector of Record Properties Identified by Proxy	1	7	0.0101	0.94	0.0092	0.85
501	6	Vector of Record Properties Identified by Proxy	2	7	0.0094	0.87		
501	6	Vector of Record Properties Identified by Proxy	3	7	0.0083	0.77		
501	6	Vector of Record Properties Identified by Proxy	4	7	0.0099	0.92		
502a	11	Inelastic Response Surface Scaling (1st mode)	1	7	0.0109	1.01	0.0106	0.98
502a	11	Inelastic Response Surface Scaling (1st mode)	2	7	0.0103	0.95		
502b	11	Inelastic Response Surface Scaling (1st-2nd modes)	3	7	0.0091	0.84	0.0090	0.84
502b	11	Inelastic Response Surface Scaling (1st-2nd modes)	4	7	0.0078	0.72		
503	35	IM1I&2E Selection/Scaling	1	7	0.0120	1.11	0.0119	1.10
503	35	IM1I&2E Selection/Scaling	2	7	0.0116	1.07		
503	35	IM1I&2E Selection/Scaling	3	7	0.0130	1.20		
503	35	IM1I&2E Selection/Scaling	4	7	0.0120	1.11		
				Median:	0.011	**1.04**	--	--
				Average:	0.011	1.00	--	--
				C.O.V.:	--	0.15	--	--
				Minimum:	0.008	0.72	--	--
				Maximum:	0.013	1.23	--	--

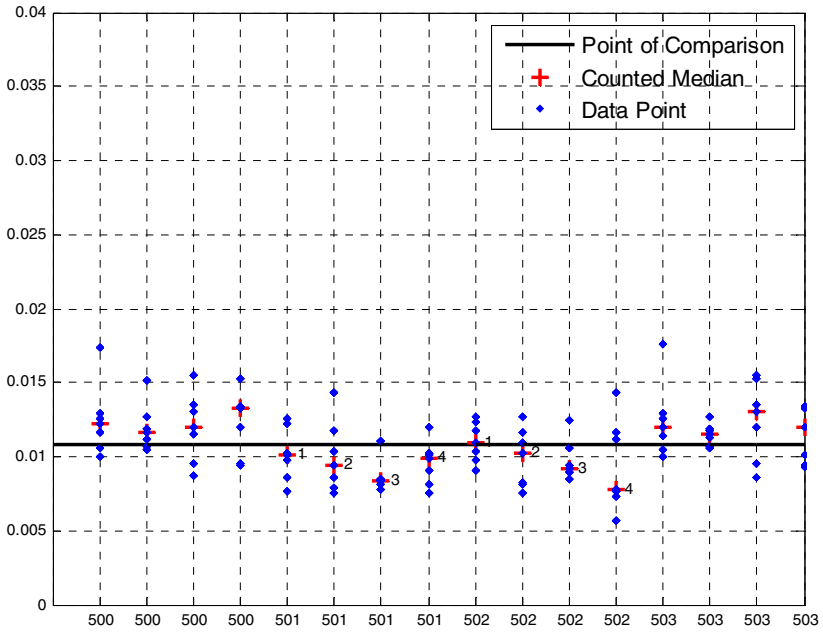

Fig. 9.11 MIDR estimated for Building D using sets of seven ground motions selected and scaled using inelastic-based methods.

9.8 SUMMARY AND CONCLUSIONS

9.8.1 Summary of Results by Method Group

Table 9.6 summarizes the ratio of the average of estimated values for the median of MIDR using individual classes of GMSM methods to the value of POC for Building D. The variation of estimates of the median of MIDR from using different methods belonging to each class is illustrated in the same table. Group III, IV, and V methods all result in predictions that are accurate and fairly precise, with median prediction errors of less than 5% and with coefficients of variation of 0.15. In contrast, the methods that do not consider the CMS shape in any way (Groups I and II) lead to overestimation of the median MIDR by 9%–29%. Note that the relatively accurate prediction of MIDR by the Group II methods is not a general observation, and occurs just because of the specific ground motions selection, which have relatively less damaging spectral shapes.

These results show that for predicting structural response under an extreme ground motion scenario (e.g., the M7 scenario), consideration of spectral shape is critical. Note that this statement is general to the overall method class and does not always hold for individual methods, as discussed in the next section. Additionally, the results from Buildings A–C (Chapters 6–8) must be considered before the results of this chapter can be generalized (e.g., the unusual results from Group II that are seen in this chapter).

Table 9.6 Summary of median of MIDR estimation bias factor by method class.

MIDR/POC	I: Sa(T_1)	II: UHS	III: CMS	IV: Proxy (i.e. ε)	V: Inelastic
Median:	1.29	1.09	**0.95**	**1.05**	**1.04**
Average:	1.26	1.19	0.92	1.05	1.00
C.O.V.:	0.18	0.20	**0.15**	**0.15**	**0.15**
Minimum:	0.94	1.03	0.63	0.73	0.72
Maximum:	1.56	1.54	1.02	1.26	1.23

9.8.2 Closing Comments

The significance of considering spectral shape in the selection and scaling of ground motion records for proper estimation of the median of MIDR was illustrated in this chapter for a generic shear wall that represents modern reinforced concrete shear wall structural systems (Building D) subjected to a M_w = 7.0, R = 10 km, and ε = 2.0 ground motion scenario (the M7 scenario). A total of 14 ground motion selection and modification (GMSM) methods (16 if variations are included) in five classes were evaluated.

For this building, this chapter has shown that for obtaining accurate and precise prediction of the median MIDR, an analyst can use some of the methods from Groups III, IV, and V, with Group III containing the most accurate and precise methods. The Group III (CMS matching) methods give consistently accurate and precise predictions. The Group IV methods (that use a proxy for spectral shape) show accurate estimates of the median of MIDR, but the scatter in response estimates was larger. Group V (inelastic) methods led to accurate predictions on average, but the predictions had wide variability and were not consistently accurate (i.e., not precise).

The prediction capabilities of these methods must also be verified for the other buildings utilized in this study (Chapters 6, 7, 8, and 10), in order to determine which methods should be recommended for use in GMSM for building structures, and for further study and verification. Such discussion is included later in Chapter 11.

10 Findings for Modern 20-Story Reinforced Concrete Moment-Frame Building (Building C) Subjected to M 7.5 Scenario

Primary Author: J. W. Baker

Associate Author: C. B. Haselton

10.1 INTRODUCTION AND OVERVIEW

In this chapter, we use 10 ground motion selection and modification (GMSM) methods to predict the maximum interstory drift ratio (MIDR) response of a modern (ductile) 20-story reinforced concrete (RC) frame building (termed Building C). This is the same building that was studied in Chapter 8, but here it is subjected to ground motions representing a Magnitude 7.5 event at a distance of 10 km, with an ε of 1.0. This scenario was described in Section 3.3 and is referred to hear as the "M7.5" scenario. The structure has been previously described in Chapter 8 and Section 3.2.1, so no further description is provided here.

The data from this chapter was collected and analyzed in order to study data from a ground motion scenario other than the M7 scenario that was the primary focus of this report. That scenario (and in particular the $\varepsilon = 2.0$ value) was of interest because the differences among the ground motion selection approaches are more substantial in that case, and investigating scenarios with substantial differences makes it easier to detect and explain any possible problems with particular approaches. The M7.5 scenario (with an $\varepsilon = 1.0$ value) is included to ensure that the results were consistent in other cases, and also because the $\varepsilon = 1.0$ case is consistent with some code-based analyses where design values from seismic hazard maps have a deterministic cap that approximately corresponds to an ε value of 1, as discussed previously in Section 3.3.

This chapter will follow the pattern of the previous four chapters, presenting MIDR predictions for the individual methods in each class of record selection approaches, as well as comparisons to the point of comparison (POC). For this building and scenario, the POC (i.e., the expected MIDR response) proposed in Chapter 4 is 1.6%. But as discussed in Chapter 5, that POC value changed if different regression models were used to predict structural response, and also changed significantly if the set of ground motions used to calibrate the regression model was changed. To reflect this apparent uncertainty, an alternate POC value of 1.48% from Chapter 5 is also considered here.

We will see that if the 1.6% POC value from Chapter 4 is correct for the point of comparison, then our findings regarding effective GMSM methods will be inconsistent with findings from previous chapters, and inconsistent with engineering intuition. When using the alternate POC value of 1.48%, our conclusions regarding the effectiveness of various ground motions selection methods is generally consistent with findings in previous chapters. But because the correct POC value is not known with certainty in this case, it is difficult to draw strong conclusions from the results in this chapter.

10.1.1 Summary of Modern 20-Story Reinforced Concrete Building (Building C)

The structural model utilized in this chapter is a 20-story RC perimeter frame building designed according to the ASCE 7-02 (ASCE 2002) and ACI 318-02 (ACI 2002) design requirements, and modeled utilizing the OpenSEES open source software package (OpenSEES 2006). Section 3.2, described the design and model in more detail, so please refer to that section if detailed information is desired. This model was created as part of the Applied Technology Council Project ATC-63 (FEMA 2009) and doctoral research by Haselton (Haselton and Deierlein 2007). In the course of those projects, the structural design was reviewed in detail by practicing structural engineers. The building fundamental period is 2.63 sec, and the second- and third-mode periods are 0.85 and 0.46 sec.

10.1.2 Comparison to Other Chapters (Ground Motion Scenario, and Building)

The current chapter presents the results of simulations for a 20-story building (Building C) for the M7.5 scenario (M_w = 7.0, R = 10 km, ε = 2.0). The previous chapters (6–9) were based on the M7 scenario, so the purpose of this chapter is to provide a comparison for a different ground motion scenario.

10.1.3 Ground Motion Sets

Ground motion sets were selected according to the approach described in Section 3.4, which is the same method utilized for each building and ground motion scenario (Chapters 6–10).

One difference from previous chapters is that fewer methods are included in the evaluation. Because the results were expected to confirm findings from previous chapters (especially given that the structure from Chapter 8 is used again here), only GMSM Program members submitted ground motion sets; the extra effort to solicit external submissions was deemed unnecessary to confirm the findings from previous chapters containing external submissions.

Appendix C provides detailed documentation of each ground motion set, and the structural response predictions resulting from the set. This electronic Appendix includes Excel spreadsheet files with the ground motion filenames (from the PEER-NGA database; PEER 2006), the scale factors, and the resulting structural responses (including MIDR, individual drifts, floor accelerations, and many others). Also included are figure files showing the scaled acceleration spectra for each ground motion set.

10.2 METHOD GROUPS

The following sections present the structural response results by method groups. The results are presented following the groups established in Section 2.4. Chapter 2 explains the basis of each of these method groups

- Group I: Sa(T_1) scaling (with bin selection)
- Group II: Building code methods (matching to the uniform hazard spectrum)
- Group III: Conditional mean spectrum (CMS) matching

- Group IV: methods using a proxy for the CMS (e.g., selection based on ε)
- Group V: Inelastic-based methods

10.3 RESPONSE RESULTS FOR GROUP I [SA(T_1) SCALING METHODS]

The Sa(T_1) methods involve selecting records from a ground motion bin, and then scaling the set of records to a target Sa(T_1) level. This is described in detail in Section 2.4.1.

Tables 10.1–10.2 and Figure 10.1 present the maximum interstory drift ratio response predictions for the two Sa(T1) methods. As mentioned in the introduction, these results will be compared to two potential POC values, given the uncertainty in the POC values developed in Chapters 4 and 5. Assuming a POC value of 1.6% (as in Table 10.1), these methods have a median MIDR prediction that is 22% larger than the POC. Assuming a POC value of 1.48% (as in Table 10.2), these methods' median predictions overpredict response by 31%. When this building was studied using the M7 scenario in Chapter 8, the Group I methods overpredicted the median MIDR by 36% relative to the POC, so the results seen here are consistent with that Chapter (noting that we might expect less conservatism in this case because of the smaller ε value associated with the M7.5 scenario considered here).

Table 10.1 Median MIDR responses for sets of seven ground motions scaled using Group I methods, assuming POC of 1.6%.

					Individual Sets		All Subsets Combined	
Method Number	Method Tag	Method Name	Set Index	Num. of Rec.	Median MIDR	Ratio to POC	Median MIDR	Ratio to POC
100	4	Sa(T_1) Scaling with Bin Selection	1	7	0.0178	1.11	0.0180	1.13
100	4	Sa(T_1) Scaling with Bin Selection	2	7	0.0163	1.02		
100	4	Sa(T_1) Scaling with Bin Selection	3	7	0.0211	1.32		
100	4	Sa(T_1) Scaling with Bin Selection	4	7	0.0220	1.38		
101	67	ATC-58 35% Draft Method	1	11	0.0240	1.50	0.0160	1.00
101	67	ATC-58 35% Draft Method	2	11	0.0143	0.89		
101	67	ATC-58 35% Draft Method	3	11	0.0212	1.33		
101	67	ATC-58 35% Draft Method	4	11	0.0151	0.94		
				Median:	0.019	1.22	0.017	1.06
				Average:	0.019	1.19	0.017	1.06
				C.O.V.:	--	0.19	--	0.08
				Minimum:	0.014	0.89	0.016	1.00
				Maximum:	0.024	1.50	0.018	1.13

Table 10.2 Median MIDR responses for sets of seven ground motions scaled using Group I methods, assuming POC of 1.48%.

					Individual Sets		All Subsets Combined	
Method Number	Method Tag	Method Name	Set Index	Num. of Rec.	Median MIDR	Ratio to POC	Median MIDR	Ratio to POC
100	4	Sa(T_1) Scaling with Bin Selection	1	7	0.0178	1.20	0.0180	1.22
100	4	Sa(T_1) Scaling with Bin Selection	2	7	0.0163	1.10		
100	4	Sa(T_1) Scaling with Bin Selection	3	7	0.0211	1.43		
100	4	Sa(T_1) Scaling with Bin Selection	4	7	0.0220	1.49		
101	67	ATC-58 35% Draft Method	1	11	0.0240	1.62	0.0160	1.08
101	67	ATC-58 35% Draft Method	2	11	0.0143	0.97		
101	67	ATC-58 35% Draft Method	3	11	0.0212	1.43		
101	67	ATC-58 35% Draft Method	4	11	0.0151	1.02		
				Median:	0.019	**1.31**	--	--
				Average:	0.019	1.28	--	--
				C.O.V.:	--	0.19	--	--
				Minimum:	0.014	0.97	--	--
				Maximum:	0.024	1.62	--	--

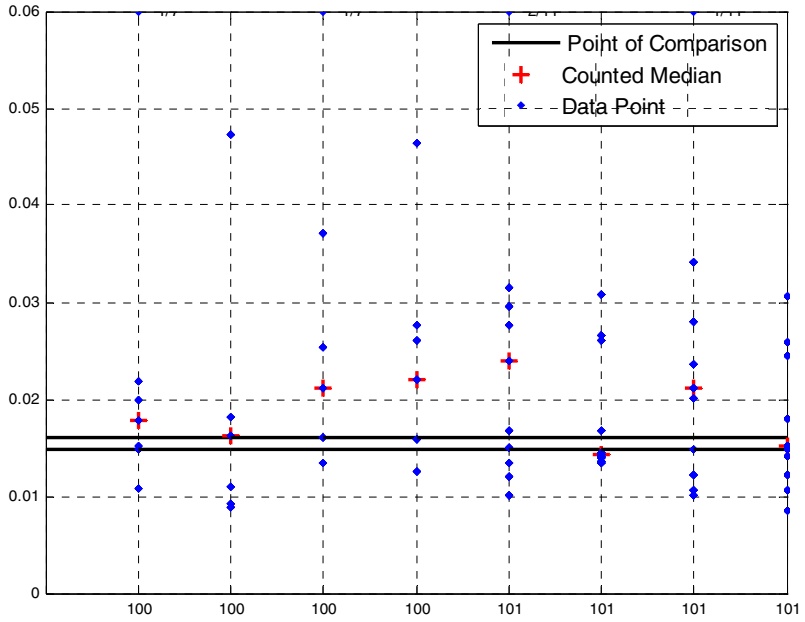

Fig. 10.1 Maximum interstory drift ratio responses for sets of seven ground motions scaled using Group I methods.

The tables and figure above suggest that the overestimation may not be consistent between the two Group 1 methods, with method 100 predicting approximately larger MIDR than method 101. Figure 10.2 shows the scaled acceleration spectra for the two methods; this figure shows that the average spectral shape differs somewhat between the two sets. Compared to the standard Sa(T_1) scaling method, the ATC-58 draft method has an average spectrum that is lower for $T < T_1$ (T_1 = 2.63 sec.) and slightly lower for $T > T_1$. This causes both a reduction in higher-mode response, as well as a reduction in nonlinear first-mode response, and explains why the ATC-58 draft method MIDR prediction is lower than that of the standard Sa(T_1) scaling method. These spectral shape differences come from fundamentally different ground motion bins being used for selection. The standard Sa(T_1) scaling method (method 100) was selected from a M_w = 7.5 and R = 10 km bin, while the ATC-58 draft method was selected from a near-field bin containing many pulse-type motions (some of which may have a "peak" in their spectra in the 2–3 sec range of importance when scaling these ground motions).

These observed trends are consistent with those seen in Chapter 8 for the same structure and selection methods. The slight reduction in biases here relative to Chapter 8 is likely due to the lower Sa(T1) target level, which means that the structure does not behave as nonlinearly, and thus is not as sensitive to the observed differences in spectral shape at longer periods, as well as the smaller associated ε value mentioned above. In summary, Sa(T_1) methods generally lead to overprediction of the MIDR response. The results show again that the prediction is sensitive to both the ground motion bin used for selection (i.e., the typical spectral shapes of the motions in the bin) and the period, T_1, used for ground motion scaling.

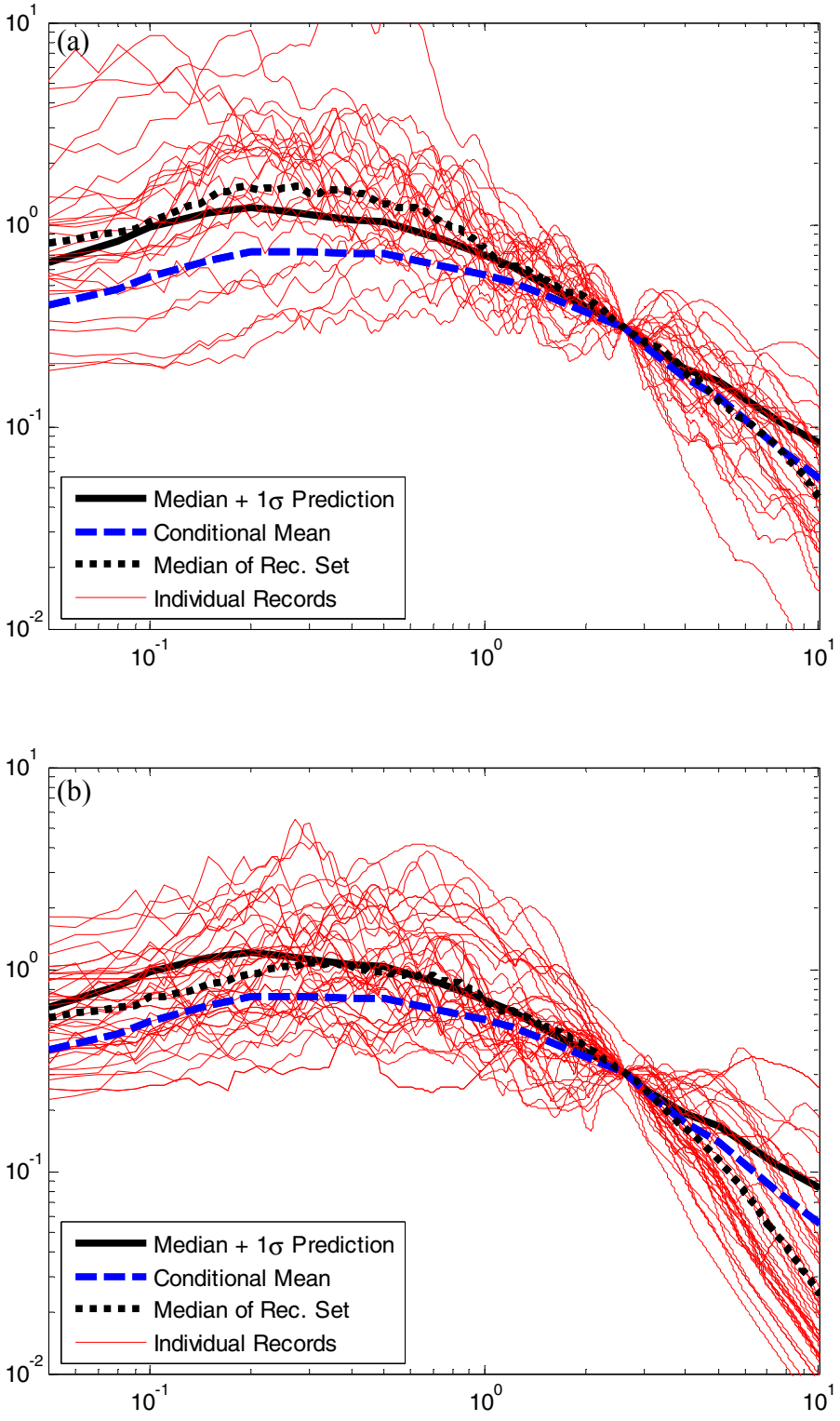

Fig. 10.2 Scaled acceleration spectra for 28 records (4 sets of 7 records each) for Sa(T_1) scaling methods: (a) 100 and (b) 101.

10.4 RESPONSE RESULTS FOR GROUP II METHODS (BUILDING CODE–BASED METHODS THAT MATCH UNIFORM HAZARD SPECTRUM)

The ground motions selected to represent this group are intended to represent the requirements of modern building codes (ASCE 2005). As in previous chapters, a principle feature of these ground motions is that they exceed the uniform hazard spectrum (UHS) at all periods from $0.2T_1$ to $1.5T_1$, as required by the building code provisions. Table 10.3 and Figure 10.3 illustrate MIDR results from ground motions selected using the building code-based method (only one of the building code methods presented earlier was analyzed here, as this chapter is intended to merely confirm the more general results seen earlier).

As compared to the POC value of 1.6% (Table 10.3), these methods overpredict MIDR response by a median of 8%. As compared to the POC value of 1.48% (Table 10.4), these methods overpredict MIDR response by 17%. In Chapter 8, these methods overpredicted response by 26%. Some reduction in overprediction is expected here, for the same reasons as discussed in the previous section. And compared to both POC values, these methods are still conservative, as expected.

Table 10.3 Median MIDR responses for sets of seven ground motions selected and scaled using Group II methods, assuming POC of 1.6%.

					Individual Sets		All Subsets Combined	
Method Number	Method Tag	Method Name	Set Index	Num. of Rec.	Median MIDR	Ratio to POC	Median MIDR	Ratio to POC
200	9980/39	Building Code Selection and Scaling - Method A	1	7	0.0170	1.06	0.0176	1.10
200	9980/39	Building Code Selection and Scaling - Method A	2	7	0.0176	1.10		
200	9980/39	Building Code Selection and Scaling - Method A	3	7	0.0254	1.59		
200	9980/39	Building Code Selection and Scaling - Method A	4	7	0.0146	0.91		
				Median:	0.017	1.08	0.018	1.10
				Average:	0.019	1.17	0.018	1.10
				C.O.V.:	--	0.25	--	--
				Minimum:	0.015	0.91	0.018	1.10
				Maximum:	0.025	1.59	0.018	1.10

Table 10.4 Median MIDR responses for sets of seven ground motions selected and scaled using Group II methods, assuming POC of 1.48%.

					Individual Sets		All Subsets Combined	
Method Number	Method Tag	Method Name	Set Index	Num. of Rec.	Median MIDR	Ratio to POC	Median MIDR	Ratio to POC
200	9980/39	Building Code Selection and Scaling - Method A	1	7	0.0170	1.15	0.0176	1.19
200	9980/39	Building Code Selection and Scaling - Method A	2	7	0.0176	1.19		
200	9980/39	Building Code Selection and Scaling - Method A	3	7	0.0254	1.72		
200	9980/39	Building Code Selection and Scaling - Method A	4	7	0.0146	0.99		
				Median:	0.017	**1.17**	--	--
				Average:	0.019	1.26	--	--
				C.O.V.:	--	0.25	--	--
				Minimum:	0.015	0.99	--	--
				Maximum:	0.025	1.72	--	--

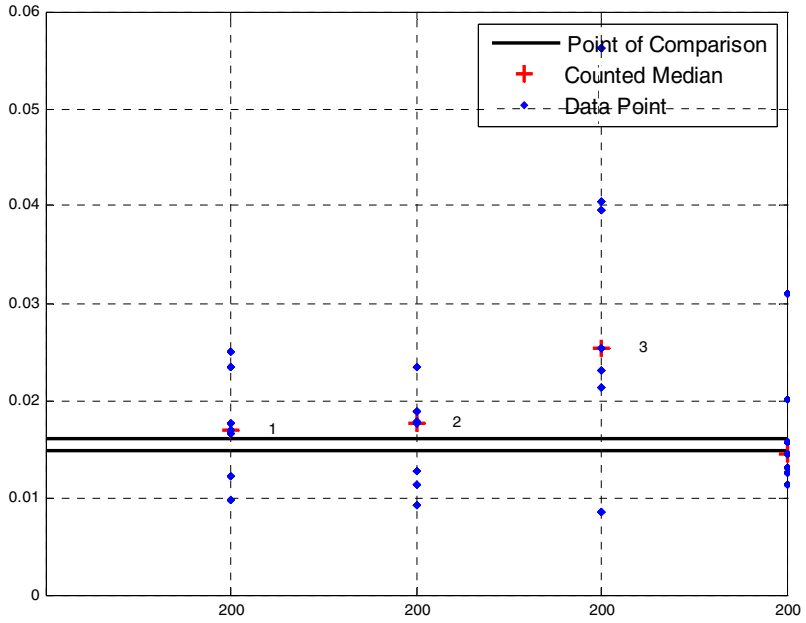

Fig. 10.3 Maximum interstory drift ratio responses for sets of seven ground motions selected and scaled using building code–based methods (matching uniform hazard spectrum).

10.5 RESPONSE RESULTS FOR GROUP III METHODS [METHODS THAT MATCH CONDITIONAL MEAN SPECTRUM (CMS)]

The methods discussed in this section match the conditional mean spectrum (CMS) using some type of numerical algorithm. Tables 10.5–10.6 and Figure 10.4 present the maximum interstory drift ratio response predictions from one method that matches the CMS. (Note again that only one of several methods from this group was considered here and was assumed to be representative of the general approach).

If the POC of 1.6% is used, the median prediction from this method underpredicts MIDR by 7%. If the POC of 1.48% is used, then this method is essentially unbiased (with an overprediction of 1%). This method was also essentially unbiased when the same building was studied under the M7 scenario (as well as for the other buildings studied in this report). If one assumes that this ground motion selection method is producing unbiased estimates here as well, this lends support to adopting the POC of 1.48% as the correct reference value. This will be supported by findings below as well.

Table 10.5 Median MIDR responses for sets of seven ground motions selected and scaled using Group III methods, assuming POC of 1.6%.

					Individual Sets		All Subsets Combined	
Method Number	Method Tag	Method Name	Set Index	Num. of Rec.	Median MIDR	Ratio to POC	Median MIDR	Ratio to POC
300	10	Conditional Mean Spectrum Selection with Scaling	1	7	0.0172	1.08	0.0143	0.89
300	10	Conditional Mean Spectrum Selection with Scaling	2	7	0.0131	0.82		
300	10	Conditional Mean Spectrum Selection with Scaling	3	7	0.0157	0.98		
300	10	Conditional Mean Spectrum Selection with Scaling	4	7	0.0142	0.89		
				Median:	0.015	0.93	0.014	0.89
				Average:	0.015	0.94	0.014	0.89
				C.O.V.:	--	0.12	--	--
				Minimum:	0.013	0.82	0.014	0.89
				Maximum:	0.017	1.08	0.014	0.89

Table 10.6 Median MIDR responses for sets of seven ground motions selected and scaled using Group III methods, assuming POC of 1.48%.

Method Number	Method Tag	Method Name	Set Index	Num. of Rec.	Individual Sets: Median MIDR	Individual Sets: Ratio to POC	All Subsets Combined: Median MIDR	All Subsets Combined: Ratio to POC
300	10	Conditional Mean Spectrum Selection with Scaling	1	7	0.0172	1.16	0.0143	0.97
300	10	Conditional Mean Spectrum Selection with Scaling	2	7	0.0131	0.89		
300	10	Conditional Mean Spectrum Selection with Scaling	3	7	0.0157	1.06		
300	10	Conditional Mean Spectrum Selection with Scaling	4	7	0.0142	0.96		
			Median:		0.015	**1.01**	--	--
			Average:		0.015	1.02	--	--
			C.O.V.:		--	0.12	--	--
			Minimum:		0.013	0.89	--	--
			Maximum:		0.017	1.16	--	--

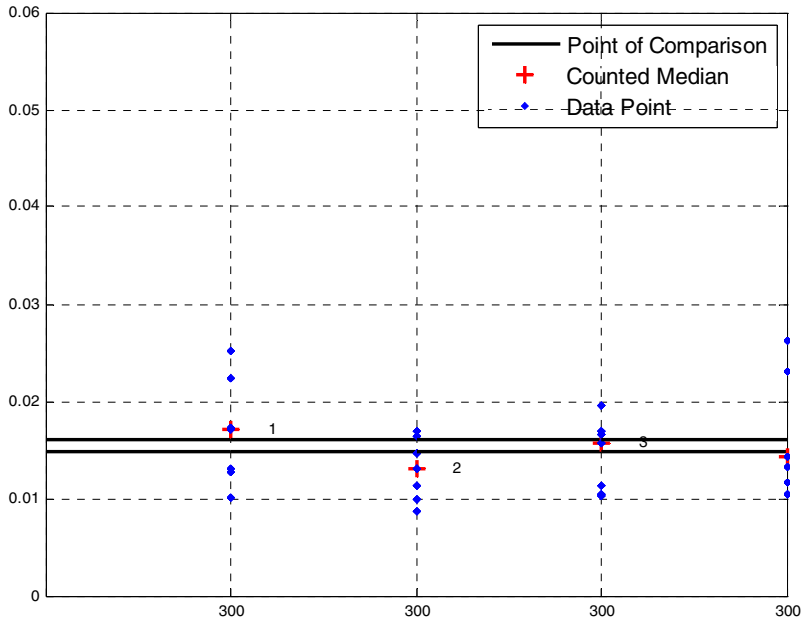

Fig. 10.4 Maximum interstory drift ratio responses for sets of seven ground motions selected and scaled using Group III methods.

10.6 RESPONSE RESULTS FOR GROUP IV METHODS (METHODS THAT USE EPSILON PROXY FOR CMS)

The methods of this class use a *proxy* for the spectral shape, rather than directly matching the shape of the CMS (typically the ε parameter discussed previously). Tables 10.7 and 10.8, and Figure 10.5 present the results for the three methods that use a proxy for the CMS.

Using a POC of 1.6% (in Table 10.7), this method is essentially unbiased with respect to the POC (having median difference of 1%). With respect to the POC of 1.48% (in Table 10.8), this method overpredicts the POC by 10%. Method 401 overpredicted the POC by 15% when this building was analyzed under the M7 scenario previously, and it over predicted the POC for buildings A, B, and D by 13%, 32%, and 10%, respectively. Given the relatively consistent overpredictions by this method in the other four analysis cases, the results in Table 10.8 suggest that the POC of 1.48% is again the most reasonable estimate of true median MIDR.

Table 10.7 Median MIDR responses for sets of seven ground motions selected and scaled using Group IV methods, assuming POC of 1.6%.

					Individual Sets		All Subsets Combined	
Method Number	Method Tag	Method Name	Set Index	Num. of Rec.	Median MIDR	Ratio to POC	Median MIDR	Ratio to POC
401	31	ε Selection with $S_{de}(T_1)$ Scaling	1	7	0.0253	1.58	0.0167	1.04
401	31	ε Selection with $S_{de}(T_1)$ Scaling	2	7	0.0165	1.03		
401	31	ε Selection with $S_{de}(T_1)$ Scaling	3	7	0.0169	1.06		
401	31	ε Selection with $S_{de}(T_1)$ Scaling	4	7	0.0131	0.82		
402	43	ATC-63 Method Applied to MIDR - Far-Field Set	1	44	0.0122	0.76	0.0122	0.76
403	48	ATC-63 Method Applied to MIDR - Near-Field Set	1	56	0.0160	1.00	0.0160	1.00
				Median:	0.016	**1.01**	0.016	1.00
				Average:	0.017	1.04	0.015	0.93
				C.O.V.:	--	0.28	--	0.16
				Minimum:	0.012	0.76	0.012	0.76
				Maximum:	0.025	1.58	0.017	1.04

Table 10.8 Median MIDR responses for sets of seven ground motions selected and scaled using Group IV methods, assuming POC of 1.48%.

Method Number	Method Tag	Method Name	Set Index	Num. of Rec.	Individual Sets: Median MIDR	Individual Sets: Ratio to POC	All Subsets Combined: Median MIDR	All Subsets Combined: Ratio to POC
401	31	ε Selection with $S_{de}(T_1)$ Scaling	1	7	0.0253	1.71	0.0167	1.13
401	31	ε Selection with $S_{de}(T_1)$ Scaling	2	7	0.0165	1.11		
401	31	ε Selection with $S_{de}(T_1)$ Scaling	3	7	0.0169	1.14		
401	31	ε Selection with $S_{de}(T_1)$ Scaling	4	7	0.0131	0.89		
402	43	ATC-63 Method Applied to MIDR - Far-Field Set	1	44	0.0122	0.82	0.0122	0.82
403	48	ATC-63 Method Applied to MIDR - Near-Field Set	1	56	0.0160	1.08	0.0160	1.08
				Median:	0.016	**1.10**	--	--
				Average:	0.017	1.13	--	--
				C.O.V.:	--	0.28	--	--
				Minimum:	0.012	0.82	--	--
				Maximum:	0.025	1.71	--	--

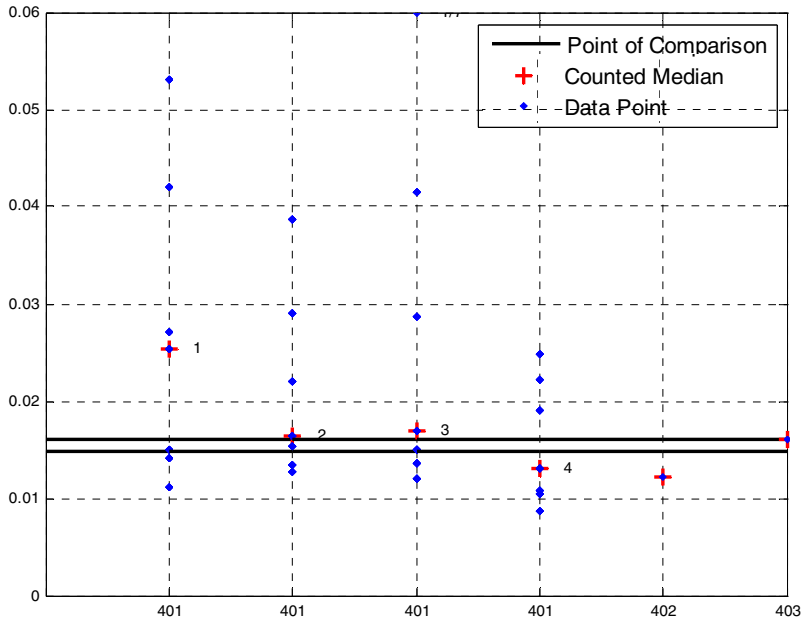

Fig. 10.5 Maximum interstory drift ratio responses for sets of seven ground motions selected and scaled using Group IV methods.

To better investigate the results from method 401, Figure 10.6 shows the combined set of 28 records for this method; this shows that epsilon selection leads to records that match the CMS well, on average. Figure 10.7 shows the spectra for the individual sets of seven records, and these spectra explain the observed MIDR responses for each ground motion set (as shown in Table

10.7). We see that the first set of seven records (in Fig. 10.7a) has a median spectrum that exceeds the CMS at periods both lower and higher than T_1; this set of seven records is thus not suprisingly associated with a median response prediction that is higher than the point of comparison (this statement is true whether the correct POC is 1.6% or 1.48%). Similarly, the records in Figure 10.7d have a median spectra lower than the CMS at most periods, and are associated with a median response prediction lower than the point of comparison. We thus see that elastic response spectra continue to provide a significant amount of insight into structural response.

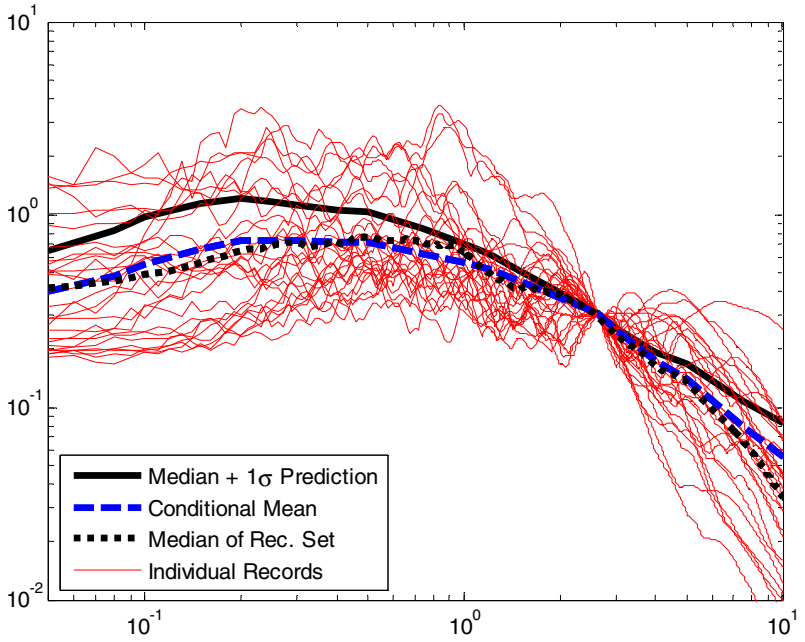

Fig. 10.6 Scaled acceleration spectra for combined set of 28 records selected based on ε (method 401).

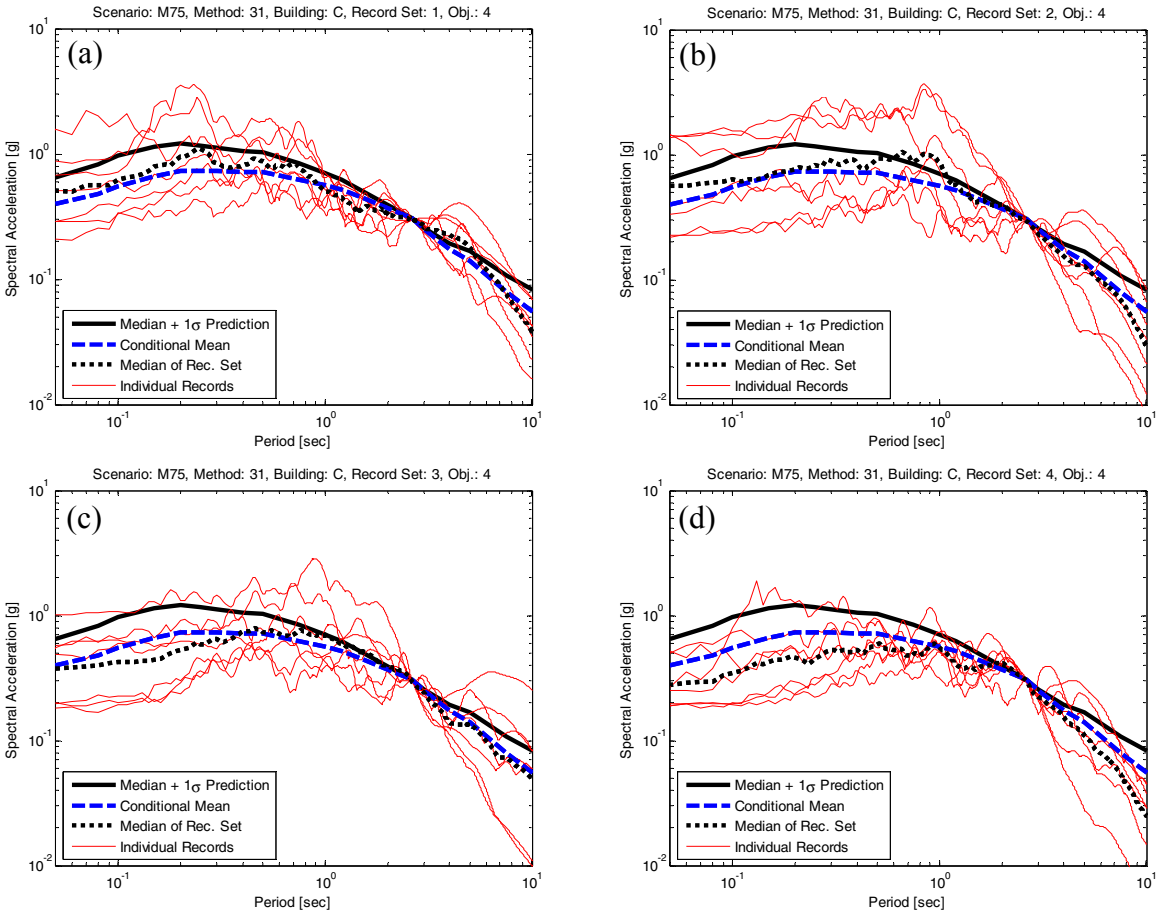

Fig. 10.7 Scaled acceleration spectra for each individual set of seven records selected based on ε (method 401).

10.7 RESPONSE RESULTS FOR GROUP V METHODS (INELASTIC-BASED METHODS)

The methods presented in this section utilize some type of inelastic parameter (e.g., inelastic spectral displacement) and/or results of inelastic structural analysis (e.g., nonlinear static pushover) to inform the record selection and scaling. Because several GMSM group members research selection methods in this Group, ground motions were obtained using several methods that fall within the Group V classification.

Tables 10.9–10.10 and Figure 10.8 present the results for the four inelastic-based methods. These methods produce a median MIDR that is 9% lower than the POC of 1.6%, but

essentially equal to the POC of 1.48%. As in the previous chapters, there is considerable scatter among the methods.

Table 10.9 Median MIDR responses for sets of seven ground motions selected and scaled using Group V methods, assuming POC of 1.6%.

					Individual Sets		All Subsets Combined	
Method Number	Method Tag	Method Name	Set Index	Num. of Rec.	Median MIDR	Ratio to POC	Median MIDR	Ratio to POC
500	27	$S_{di}(T_1, dy)$ Scaling	1	7	0.0202	1.26	0.0184	1.15
500	27	$S_{di}(T_1, dy)$ Scaling	2	7	0.0138	0.86		
500	27	$S_{di}(T_1, dy)$ Scaling	3	7	0.0193	1.21		
500	27	$S_{di}(T_1, dy)$ Scaling	4	7	0.0144	0.90		
501	6	Vector of Record Properties Identified by Proxy	1	7	0.0121	0.76	0.0128	0.80
501	6	Vector of Record Properties Identified by Proxy	2	7	0.0124	0.78		
501	6	Vector of Record Properties Identified by Proxy	3	7	0.0141	0.88		
501	6	Vector of Record Properties Identified by Proxy	4	7	0.0134	0.84		
502	11	Inelastic Response Surface Scaling	1	7	0.0159	0.99	0.0159	0.99
502	11	Inelastic Response Surface Scaling	2	7	0.0169	1.06		
502	11	Inelastic Response Surface Scaling	3	7	0.0159	0.99		
502	11	Inelastic Response Surface Scaling	4	7	0.0146	0.91		
503	35	IM1I&2E Selection/Scaling	1	7	0.0144	0.90	0.0141	0.88
503	35	IM1I&2E Selection/Scaling	2	7	0.0133	0.83		
503	35	IM1I&2E Selection/Scaling	3	7	0.0161	1.01		
503	35	IM1I&2E Selection/Scaling	4	7	0.0150	0.94		
			Median:		0.015	0.91	0.0150	0.94
			Average:		0.015	0.94	0.0153	0.96
			C.O.V.:		--	0.15	--	0.16
			Minimum:		0.012	0.76	0.013	0.80
			Maximum:		0.020	1.26	0.018	1.15

Table 10.10 Median MIDR responses for sets of seven ground motions selected and scaled using Group V methods, assuming POC of 1.48%.

					Individual Sets		All Subsets Combined	
Method Number	**Method Tag**	**Method Name**	**Set Index**	**Num. of Rec.**	**Median MIDR**	**Ratio to POC**	**Median MIDR**	**Ratio to POC**
500	27	$S_{di}(T_1, dy)$ Scaling	1	7	0.0202	1.36	0.0184	1.24
500	27	$S_{di}(T_1, dy)$ Scaling	2	7	0.0138	0.93		
500	27	$S_{di}(T_1, dy)$ Scaling	3	7	0.0193	1.30		
500	27	$S_{di}(T_1, dy)$ Scaling	4	7	0.0144	0.97		
501	6	Vector of Record Properties Identified by Proxy	1	7	0.0121	0.82	0.0128	0.86
501	6	Vector of Record Properties Identified by Proxy	2	7	0.0124	0.84		
501	6	Vector of Record Properties Identified by Proxy	3	7	0.0141	0.95		
501	6	Vector of Record Properties Identified by Proxy	4	7	0.0134	0.91		
502a	11	Inelastic Response Surface Scaling (1st mode)	1	7	0.0159	1.07	0.0159	1.07
502a	11	Inelastic Response Surface Scaling (1st mode)	2	7	0.0169	1.14		
502b	11	Inelastic Response Surface Scaling (1st-2nd modes)	3	7	0.0159	1.07		
502b	11	Inelastic Response Surface Scaling (1st-2nd modes)	4	7	0.0146	0.99		
503	35	IM1I&2E Selection/Scaling	1	7	0.0144	0.97	0.0141	0.95
503	35	IM1I&2E Selection/Scaling	2	7	0.0133	0.90		
503	35	IM1I&2E Selection/Scaling	3	7	0.0161	1.09		
503	35	IM1I&2E Selection/Scaling	4	7	0.0150	1.01		
			Median:		0.015	**0.98**	--	--
			Average:		0.015	1.02	--	--
			C.O.V.:		--	0.15	--	--
			Minimum:		0.012	0.82	--	--
			Maximum:		0.020	1.36	--	--

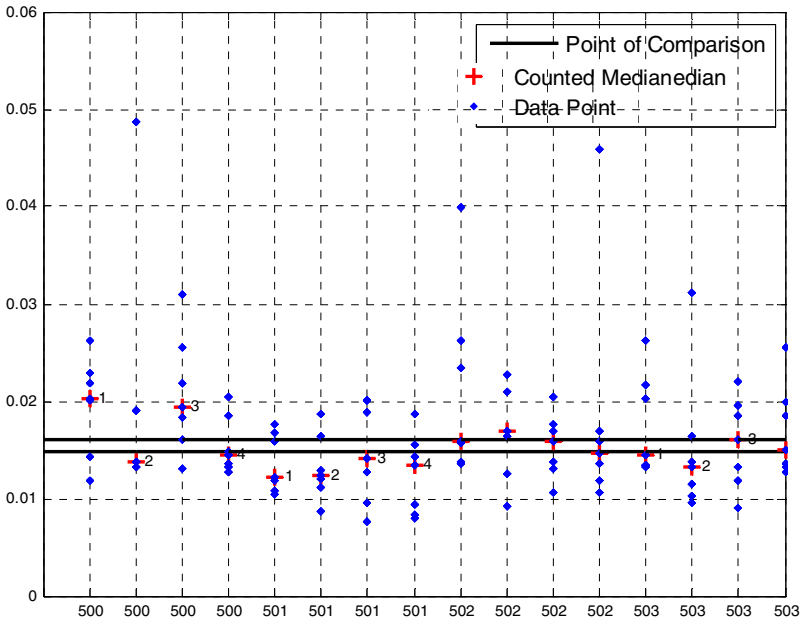

Fig. 10.8 Maximum interstory drift ratio responses for sets of seven ground motions selected and scaled using Group V methods.

The S_{di} method (method 500) resulted in an average overprediction of MIDR response by 15% or 24% (depending upon the reference POC value). As part of using the S_{di} method, one must determine the target S_{di} value that is consistent with the M7.5 scenario used in this study (which is based on an elastic acceleration spectral value). The author of this method suspects that the target S_{di} value used for selection may have been too large, being computed inaccurately for the M7.5 scenario which is defined based on solely elastic spectral values (Section 3.3.1), which led to this consistent overprediction of MIDR response (Polsak Tothong, personal communication 2008).

Conversely, the IM1I&2E method (method 503) tends to underpredict response by 12% or 5% (depending upon the reference POC value). Because methods 500 and 503 produced comparable responses for this structure in the M7 scenario, it is surprising to see this large difference here. Further, this method consistently overpredicted the POC in the previous four analysis cases, so the underprediction here is unexpected. It may be that apparent similarities

and differences in responses estimated by these two methods are simply due to variability caused by small record sets.

The vector of record properties identified by proxy method (method 501) results in consistent predictions that are 20% or 14% lower than the POC (depending upon the reference POC value). Figure 10.9 shows that the average spectrum from this method is lower than the CMS at all periods, which likely explains the underprediction of response. This method was observed to underpredict the POC by 6% when this building was studied with the M7 scenario, and underpredicted the POC for two out of three of the other buildings as well, so the result here is not unexpected.

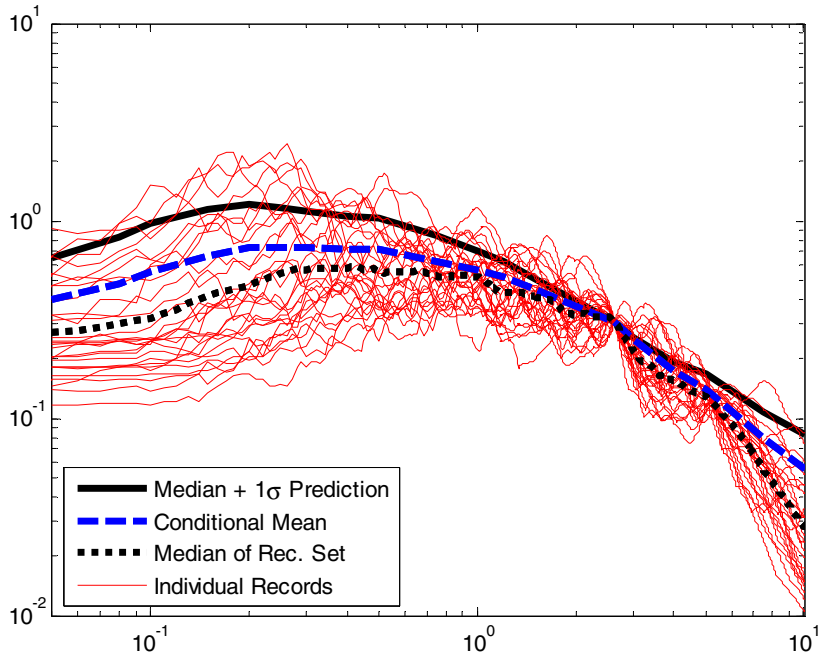

Fig. 10.9 Scaled acceleration spectra for the combined set of 28 records selected based on a vector of record properties identified by proxy (method 501).

The inelastic response surface scaling method (method 502) has two variants. Ground motion sets 1–2 were selected without considering a second-mode term, and sets 3–4 were selected including this term. To illustrate this difference, Figure 10.10 shows the scaled response spectra for ground motion sets 2 and 4. The predictions here (which are either unbiased or overpredict the POC by 7%, depending upon the reference POC) are consistent with predictions obtained from this method in the previous four chapters.

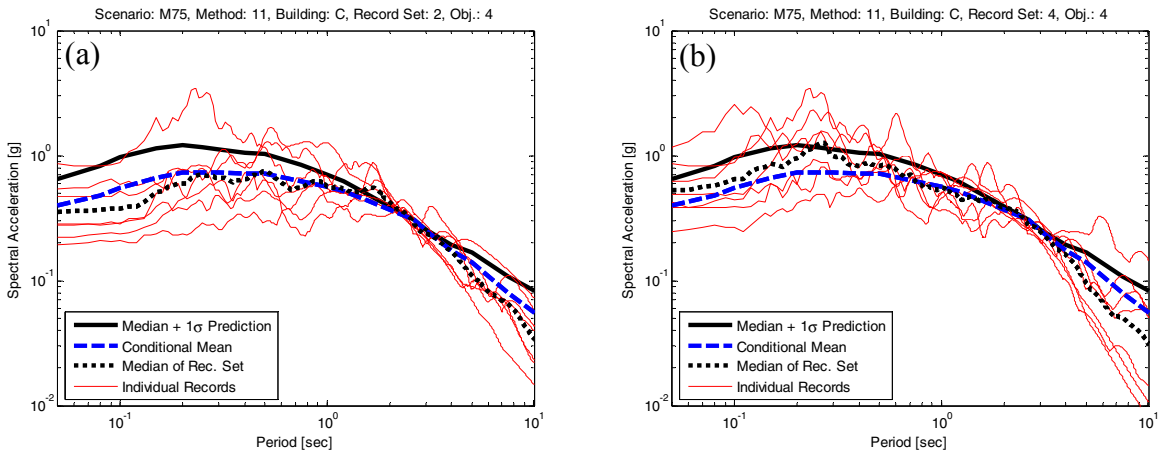

Fig. 10.10 Scaled acceleration spectra for two sets of seven records selected using two variants of inelastic response surface method (method 502): (a) was selected without consideration of second mode (set 2) and (b) selected to account for second mode (set 4).

10.8 SUMMARY AND CONCLUSIONS

10.8.1 Summary of Results by Method Group

Table 10.11 summarizes the prediction accuracies by method class for this 20-story modern RC frame building, assuming a POC of 1.6%. Similar results are shown in Table 10.12, assuming a POC of 1.48%. This table shows summary statistics for the estimation bias factor computed as the ratio of the median MIDR response to the point-of-comparison (POC) prediction.

If a POC of 1.6% is used, then the Group IV method was the best predictor of median response, while Groups III and V underpredict and Groups I and II overpredict. If a POC of 1.48% is assumed, then Groups III and V provide unbiased predictions of median response, with the other three groups overpredicting median response. In either case, Groups III and V provide the estimates of median MIDR that show the smallest variability among record sets (as measured by the coefficient of variation numbers presented in the tables).

For reference, comparable results for the same building under the M7 scenario (from Chapter 8, are reproduced here in Table 10.13. Comparison of the three tables shows that the results in Table 10.12 and Table 10.13 are strikingly similar (with the exception of Group V methods, and predictions from those methods were seen to have somewhat large variability). We do not expect to see any major changes in the performance of these selection methods under this

small change in the earthquake scenario except for perhaps a lessening of conservatism from methods I and II, as the associated ε value was reduced from 2 to 1 in the change from Chapter 8 to this chapter.

While this report generally assumes that the POC numbers from Chapter 4 are true response estimates to be (hopefully) reproduced by the ground motion selection methods, it is apparent from Chapter 5 and the results here that in this case the POC value is also uncertain. The results here, taken in conjunction with the conclusions of the previous four chapters, suggests that the POC value of 1.48% is likely to be a good estimate of the true median MIDR in this case.

Given that Chapter 5 and this chapter place some doubt on whether the POC prediction of 1.6% is correct, it does not seem reasonable to rank the ground motion selection methods based on their ability to reproduce the 1.6% prediction. Similarly, it does not seem reasonable to rank the methods based on the POC prediction of 1.48%, simply because the conclusions are consistent with conclusions from the previous four chapters. (And, in the interest of full disclosure, it should be noted that the additional analyses of Chapter 5 were undertaken partially in response to the apparent inconsistencies produced in this chapter by the POC of 1.6%). Therefore, the decision was made not to rank any of the selection methods based on these results, and instead to focus on the results from the previous four chapters, where the POC value is known with more certainty.

Table 10.11 Summary of response estimation bias factor by method class, assuming POC of 1.6%.

MIDR/POC	I: Sa(T_1)	II: UHS	III: CMS	IV: Proxy (i.e. ε)	V: Inelastic
Median:	1.22	1.08	0.93	**1.01**	0.91
Average:	1.19	1.17	0.94	**1.04**	0.94
C.O.V.:	0.19	0.25	**0.12**	0.28	**0.15**
Minimum:	0.89	0.91	0.82	0.76	0.76
Maximum:	1.50	1.59	1.08	1.58	1.26

Table 10.12 Summary of response estimation bias factor by method class, assuming POC of 1.48%.

MIDR/POC	I: Sa(T_1)	II: UHS	III: CMS	IV: Proxy (i.e. ε)	V: Inelastic
Median:	1.31	1.17	**1.01**	1.10	**0.98**
Average:	1.28	1.26	**1.02**	1.13	**1.02**
C.O.V.:	0.19	0.25	**0.12**	0.28	**0.15**
Minimum:	0.97	0.99	0.89	0.82	0.82
Maximum:	1.62	1.72	1.16	1.71	1.36

Table 10.13 Summary of response estimation bias factor for Building B under M7 scenario (from Chapter 7).

MIDR/POC	I: Sa(T_1)	II: UHS	III: CMS	IV: Proxy (i.e. ε)	V: Inelastic
Median:	1.36	1.26	**1.01**	1.06	1.19
Average:	1.55	1.36	**1.02**	1.15	1.20
C.O.V.:	0.36	0.23	**0.08**	0.32	0.19
Minimum:	1.07	0.91	0.91	0.79	0.76
Maximum:	2.74	2.07	1.17	1.88	1.58

10.8.2 Closing Comments

This chapter presents attempts to accurately predict the median MIDR response of a 20-story RC frame building (Building C), when subjected to a M_w = 7.5, R = 10 km, and ε = 1.0 ground motion scenario (the M7.5 scenario). These comparisons include 10 ground motion selection and modification methods. This chapter is primarily included in order to confirm that earlier findings are still valid for a ground motion scenario other than the M7 scenario that was the primary focus of this report. For this reason, a more limited number of GMSM methods were considered here.

Unfortunately, it was not possible to draw strong conclusions in this chapter, due to questions about the correct POC value to be used for evaluating the methods. The sensitivity of this POC to changes in the regression analysis was discussed in Chapter 5. And throughout this chapter, results were presented for two possible POC values. It was seen that if the POC value of 1.6% from Chapter 4 was used, the results in this chapter were somewhat inconsistent with the

results in the previous four chapters. If an alternate POC of 1.48% is used, then the findings here are very consistent with results from the previous four chapters (including Chapter 8, which studied this same building under a slightly different earthquake scenario). But, as also noted above, consistency of results is not reason enough to revise the POC value from Chapter 4 (and in fact, the alternate POC value was proposed after this chapter was completed and the inconsistencies observed). Due to these challenges, the decision was made to not draw any strong conclusions based on the results seen here. The final conclusions in the following chapter also not draw significantly from the results in this chapter. Further study into the observed instability of the POC prediction will be left for future research.

11 Summary of Results, Conclusions; Future Research

Primary Author: C. B. Haselton

Associate Authors: J. W. Baker, C. A. Goulet, N. Luco, T. Shantz, N. Shome

11.1 INTRODUCTION AND OVERVIEW

Chapters 6–10 presented the MIDR structural response predictions for each ground motion selection and modification method, for each of the four buildings and two ground motion scenarios considered in this study, including all the appropriate detail to explain observed trends.

The purpose of this chapter is to *concisely* summarize the results from Chapters 6 through 10, giving an overview of the findings from each of the five chapters, while avoiding detailed descriptions of results. For detailed descriptions of results, the reader is referred to the earlier chapters.

This chapter first presents the overall results for each of the five method groups, and then continues by presenting the results for each individual method. The chapter concludes by identifying individual methods that provided consistently accurate MIDR predictions, and then summarizing the overall findings and conclusions that came from this study.

This chapter closes by discussing the possible next steps in this GMSM research, as well as ideas for overall future research direction.

11.2 SUMMARY OF RESULTS BY METHOD GROUP, FOR ALL BUILDINGS

Tables 11.1 and 11.2 summarize the prediction accuracy and precision by method group for each test case considered in Chapters 6–9; these results include response predictions for four buildings under the M7 ground motion scenario. The results of Chapter 10 (Building C under the M7.5 scenario) are not included in this summative discussion because the point-of-comparison (POC) value is more variable for that case, as discussed in Chapters 5 and 10. Even so, the results for the M7.5 scenario are generally consistent with the results of the M7 scenario, so this exclusion does not affect the findings and conclusions of this chapter.

Tables 11.1 and 11.2 provide summary statistics for the prediction bias factor computed as the ratio of the median MIDR response to the point-of-comparison (POC) prediction; the bias factor will be referred to as "MIDR/POC". Table 11.1 presents the median MIDR/POC value for each building and scenario, as well as the overall median value for all four cases. These ratios give insight into the *accuracy* of the method relative to the POC predictions, and a median of 1.0 would mean perfect accuracy. Table 11.2 presents the coefficients of variation (c.o.v.) of the median MIDR/POC predictions, which describes the *precision* of the predictions. This c.o.v. value is not the record-to-record variability, but is rather the c.o.v. of individual *median* predictions, so a c.o.v. value of 0.0 would indicate perfect precision of the method, where each set of 7 records provides the exact same median MIDR/POC prediction.

Table 11.1 For each method class (and building/scenario), summary of median of MIDR/POC predictions from each set of seven records.

Method Class	Building A, M7	Building B, M7	Building C, M7	Building D, M7	Median
$Sa(T_1)$	1.48	1.55	1.36	1.29	**1.42**
UHS	1.40	1.33	1.26	1.09	**1.30**
CMS	1.04	1.01	1.01	0.95	**1.01**
Proxy (i.e. ε)	1.05	1.12	1.06	1.05	**1.06**
Inelastic	1.28	1.39	1.19	1.04	**1.24**

Table 11.2 For each method class (and building/scenario), summary of coefficient of variation (c.o.v.) of median MIDR/POC predictions from each set of seven records. This c.o.v. value is not the record-to-record variability.

Method Class	Building A, M7	Building B, M7	Building C, M7	Building D, M7	Median
$Sa(T_1)$	0.17	--	0.36	0.18	**0.18**
UHS	0.05	--	0.23	0.20	**0.20**
CMS	0.23	0.22	0.08	0.15	**0.19**
Proxy (i.e. ε)	0.24	0.29	0.32	0.15	**0.27**
Inelastic	0.21	0.31	0.19	0.15	**0.20**

Table 11.1 and Table 11.2 show that the Group III (CMS matching) methods result in a prediction that is both highly accurate (with a median error of only 1%) and reasonably precise (with a coefficient of variation of only 0.19). In contrast, the methods that do not consider the CMS shape in any way (i.e., the Group I and Group II methods) lead to consistent overpredictions of response of 42% and 30%, respectively. This clearly shows that for predicting structural response under an extreme ground motion scenario (with $\varepsilon = 2.0$), proper consideration of spectral shape can lead to an accurate prediction.

The reason that spectral shape is important is because as a building is damaged during the earthquake, the stiffness decreases and the effective building period elongates, making the spectral values at periods greater than the fundamental period of the building also affect the structural response (thus making the shape of the spectrum important). Additionally, spectral values at periods shorter than the building's fundamental period also affect structural response, as they are indicators of higher-mode excitation. These effects are not new findings, and have been shown in many previous studies (Baker and Cornell 2006, Goulet et al. 2007).

The Group IV methods use an *indicator,* or *proxy*, for spectral shape to select ground motion records. These methods also lead to an accurate prediction (with a median bias of only 6%), but the scatter is higher than the Group III methods (with a coefficient of variation of 0.27 compared to the value of 0.12 from Group III). This increased scatter results in slightly more variable predictions of median MIDR; this is undesirable if the goal is to predict only the median MIDR response. Note that the scope of this report includes prediction of only the median MIDR, and future work should look more carefully at prediction of the full response distribution.

Group V (inelastic) methods result in a greater overprediction of response (a median overprediction of 24%), but the scatter is smaller than for the Group IV methods (coefficient of variation of 0.20 compared to 0.27). Several previous sections of this report (Sections 3.3.1, 6.7, 7.7, 8.7, 9.7, and 10.7) suggested that these overpredictions may have resulted from some Group V methods using an inelastic target amplitude (e.g., Sdi) that was not consistent with the definition of the M7 scenario (which is defined based on *elastic* spectral values). Additionally, inelastic methods may not be consistent with the manner in which the point-of-comparison prediction was created, since it is also based on elastic spectral values (Section 5.2). It may be possible to remove some or all of this prediction bias through additional research to determine proper inelastic targets for ground motion scenarios like those used in this study (which are defined by *elastic* spectral acceleration parameters).

It is notable that the Group V methods work substantially better for Building D (M7), which comes from the fact that Building D is only mildly nonlinear for the M7 scenario, whereas Buildings A-C have much greater levels of nonlinear response.

As previously mentioned, Group I and II methods ($Sa(T_1)$ scaling, and matching to the UHS, respectively) both do not consider the unique spectral shape associated with rare $Sa(T_1)$ levels, and therefore consistently lead to overprediction of MIDR structural response (by 42% and 30%, respectively). When one desires an accurate prediction of structural response given $Sa(T_1)$, these methods should not be used. Similarly to the Group V methods, the predictions are more accurate for Building D, since Building D is only mildly nonlinear for the M7 scenario.

Based on these results, the prediction capability of the method groups can be ordered as follows, starting with the most accurate method Group. Note that these results are general to the method groups and the ordering does not always hold for individual methods within each grouping (as will be shown in the next section).

- Group III [CMS Matching]
- Group IV [proxy methods (e.g., ε)]
- Grooup V [inelastic-based methods]
- Group II [building code methods]
- Group I [$Sa(T_1)$ methods]

11.3 SUMMARY OF RESULTS FOR EACH INDIVIDUAL METHOD WITHIN EACH METHOD GROUP, FOR ALL BUILDINGS

Table 11.3 summarizes the prediction bias factors (ratios of median MIDR to the POC), for all Group I ($Sa(T_1)$ scaling) methods. This table includes data for each Group I method (only two methods in this case) and for each of the five building/scenario combinations that were used to evaluate the methods. This shows that both Group I methods result in MIDR predictions that are biased high, with the median predictions for each building/scenario ranging from +29% to +55% above the POC, with an overall median value of +42%. The median predictions for each individual method are consistent, being +46% high for each method.

A closer look at the median predictions for each building/scenario shows the effects of building nonlinearity. For the M7 scenario, the most nonlinear building is Building B and the least nonlinear is Building D; the results clearly show that the Group I methods become more biased as the building becomes more nonlinear. This occurs because when the building response becomes more nonlinear, the effective period of the structure increases, causing the spectral values at these longer periods to become more important to the response.

Table 11.3 Median MIDR/POC responses for sets of seven ground motions from Group I methods [$Sa(T_1)$ scaling methods], for all buildings and scenarios.

Ratio of Median MIDR to the Point of Comparison			Building A, M7		Building B, M7		Building C, M7		Building D, M7		Summary Stats. for All Bldgs./Scenarios			
Method Number	Method Tag	Method Name	Indiv. Sets of 7	All Rec.	Indiv. Sets of 7	All Rec.	Indiv. Sets of 7	All Rec.	Indiv. Sets of 7	All Rec.	Med. All Rec.	C.O.V. Set of 7	Min. Set of 7	Max. Set of 7
100	4	$Sa(T_1)$ Scaling with Bin Selection	1.23		1.19		1.52		0.98					
100	4	$Sa(T_1)$ Scaling with Bin Selection	1.20	1.26	2.63	1.66	2.74	1.68	1.15	1.00	**1.46**	--	**0.94**	***col.***
100	4	$Sa(T_1)$ Scaling with Bin Selection	1.41		*col.*		2.01		0.94					
100	4	$Sa(T_1)$ Scaling with Bin Selection	1.29		1.20		1.48		1.44					
101	67	ATC-58 35% Draft Method	1.92		1.25		1.07		1.56					
101	67	ATC-58 35% Draft Method	1.56	1.69	*col.*	1.67	1.20	1.18	1.17	1.25	**1.46**	--	**1.07**	***col.***
101	67	ATC-58 35% Draft Method	1.64		1.38		1.17		1.42					
101	67	ATC-58 35% Draft Method	1.61		1.72		1.24		1.42					
Median:			**1.48**	--	**1.55**	--	**1.36**	--	**1.29**	--	***Median all Buildings:***			
C.O.V.:			**0.17**	--	--	--	**0.36**	--	**0.18**	--	***1.42***			

Table 11.4 similarly summarizes the results for all Group II (building code) methods. This table includes data for each of the ten GMSM methods within Group II, and most of the results are for the M7 scenario for Buildings B and Building C. This shows that both Group II methods also result in MIDR predictions that are biased high, with the median predictions for

each building/scenario ranging from +9% to +40% above the POC, with an overall median value of +32%. The median predictions for each individual method have a slightly higher range over the ten methods, with the median predictions ranging from +20% to +61% above the POC.

When comparing the median predictions for each building/scenario, the effect of building nonlinearity again becomes clear (as with the Group I methods), showing that the Group II methods become more biased as the building response becomes more nonlinear. This occurs because Group II methods also fail to capture the proper spectral shape associated with rare $Sa(T_1)$ levels. The spectral shape dictates the spectral values at periods away from the undamaged fundamental period of the building, and the spectral values at extended periods become more important as the response becomes more nonlinear.

Table 11.4 Median MIDR/POC responses for sets of seven ground motions from Group II methods (building code–based methods that match uniform hazard spectrum), for all buildings and scenarios.

Ratio of Median MIDR to the Point of Comparison			Building A, M7		Building B, M7		Building C, M7		Building D, M7		Summary Stats. for All Bldgs./Scenarios			
Method Number	Method Tag	Method Name	Indiv. Sets of 7	All Rec.	Indiv. Sets of 7	All Rec.	Indiv. Sets of 7	All Rec.	Indiv. Sets of 7	All Rec.	Med. All Rec.	C.O.V. Set of 7	Min. Set of 7	Max. Set of 7
200	9980	Building Code Selection and Scaling - Method A	1.38		1.21		1.05		1.11					
200	9980	Building Code Selection and Scaling - Method A	1.53	1.40	0.96	1.20	1.18	1.19	1.54	1.10	**1.20**	**0.23**	**0.75**	**1.99**
200	9980	Building Code Selection and Scaling - Method A	1.41		1.45		1.99		1.03					
200	9980	Building Code Selection and Scaling - Method A	1.40		0.75		1.48		1.07					
201	9981	Building Code Selection and Scaling - Method B	--		1.21		1.18		--					
201	9981	Building Code Selection and Scaling - Method B	--	--	2.11	1.26	1.99	1.34	--	--	**1.30**	**0.31**	**0.91**	**2.11**
201	9981	Building Code Selection and Scaling - Method B	--		1.45		2.07		--					
201	9981	Building Code Selection and Scaling - Method B	--		0.91		1.26		--					
202	9982	Building Code Selection and Scaling - Method C	--		2.21		1.23		--					
202	9982	Building Code Selection and Scaling - Method C	--	--	*col.*	1.87	1.25	1.23	--	--	**1.55**	**--**	**0.91**	***col.***
202	9982	Building Code Selection and Scaling - Method C	--		1.36		1.46		--					
202	9982	Building Code Selection and Scaling - Method C	--		1.54		0.91		--					
203	9983	Building Code Selection and Scaling - Method D	--		1.22		1.08		--					
203	9983	Building Code Selection and Scaling - Method D	--	--	*col.*	1.24	1.27	1.16	--	--	**1.20**	**--**	**0.93**	***col.***
203	9983	Building Code Selection and Scaling - Method D	--		0.93		1.17		--					
203	9983	Building Code Selection and Scaling - Method D	--		1.30		1.13		--					
204	9984	Building Code Selection and Scaling - Method E	--		1.30		1.16		--					
204	9984	Building Code Selection and Scaling - Method E	--	--	1.36	1.55	1.26	1.19	--	--	**1.37**	**--**	**1.04**	***col.***
204	9984	Building Code Selection and Scaling - Method E	--		*col.*		1.04		--					
204	9984	Building Code Selection and Scaling - Method E	--		*col.*		1.47		--					
205	9985	Building Code Selection and Scaling - Method F	--		1.49		1.16		--					
205	9985	Building Code Selection and Scaling - Method F	--	--	1.87	1.45	1.66	1.39	--	--	**1.42**	**0.17**	**1.16**	**1.87**
205	9985	Building Code Selection and Scaling - Method F	--		1.42		1.48		--					
205	9985	Building Code Selection and Scaling - Method F	--		1.23		1.20		--					
206	9986	Building Code Selection and Scaling - Method G	--		1.64		1.29		--					
206	9986	Building Code Selection and Scaling - Method G	--	--	2.22	1.61	1.79	1.62	--	--	**1.61**	**0.20**	**1.27**	**2.22**
206	9986	Building Code Selection and Scaling - Method G	--		1.59		1.87		--					
206	9986	Building Code Selection and Scaling - Method G	--		1.27		1.38		--					
207	9975	Building Code Selection and Scaling - Method H	--		--		1.08		--					
207	9975	Building Code Selection and Scaling - Method H	--	--	--	--	1.57	1.37	--	--	**1.37**	**0.18**	**1.08**	**1.57**
207	9975	Building Code Selection and Scaling - Method H	--		--		1.53		--					
207	9975	Building Code Selection and Scaling - Method H	--		--		1.21		--					
208	9976	Building Code Selection and Scaling - Method I	--		--		1.49		--					
208	9976	Building Code Selection and Scaling - Method I	--	--	--	--	1.03	1.26	--	--	**1.26**	**0.36**	**0.92**	**1.97**
208	9976	Building Code Selection and Scaling - Method I	--		--		1.97		--					
208	9976	Building Code Selection and Scaling - Method I	--		--		0.92		--					
209	9989	Building Code Selection and Scaling - Method J	--	--	1.22	1.22	1.16	1.19	--	--	**1.20**	**--**	**1.16**	**1.23**
209	9989	Building Code Selection and Scaling - Method J	--		1.22		1.23		--					
Median:			**1.40**	**--**	**1.39**	**--**	**1.26**	**--**	**1.09**	**--**	***Median all Buildings:***			
C.O.V.:			**0.05**	**--**	**--**	**--**	**0.23**	**--**	**0.20**	**--**	***1.32***			

Table 11.5 summarizes the results for five methods within Group III (CMS matching). This shows that median predictions for each building/scenario are highly accurate, ranging from -5% below the POC to +4% above the POC, with an overall median value of only +1%. The median predictions for each individual method are similarly accurate, with one exception. method 301 results in very low predictions for two out of three cases, and a very high prediction for one case, with an overall median value of -18% below the POC. A possible explanation for this is explained in Chapter 7 (page 112); this is based on the fact that the expressed objective of method 301 differs slightly from the objective considered in this report (i.e., median interstory drift response). With the method 301 results excluded, the median predictions for the other individual methods are consistently accurate, with median predictions ranging only from -4% below the POC to +4% above the POC.

Table 11.5 Median MIDR/POC responses for sets of seven ground motions from Group III methods [methods that match conditional mean spectrum (CMS)], for all buildings and scenarios.

Ratio of Median MIDR to the Point of Comparison			Building A, M7		Building B, M7		Building C, M7		Building D, M7		Summary Stats. for All Bldgs./Scenarios			
Method Number	Method Tag	Method Name	Indiv. Sets of 7	All Rec.	Indiv. Sets of 7	All Rec.	Indiv. Sets of 7	All Rec.	Indiv. Sets of 7	All Rec.	Med. All Rec.	C.O.V. Set of 7	Min. Set of 7	Max. Set of 7
300	10	Conditional Mean Spectrum Selection with Scaling	1.02	1.01	1.04	0.92	0.92	0.98	1.00	0.95	**0.96**	**0.09**	**0.75**	**1.09**
300	10	Conditional Mean Spectrum Selection with Scaling	1.09		0.84		1.04		0.93					
300	10	Conditional Mean Spectrum Selection with Scaling	1.01		0.75		0.99		0.94					
300	10	Conditional Mean Spectrum Selection with Scaling	1.02		1.01		1.03		0.95					
301	15	Genetic Algorithm Selection (to match CMS)	1.67	1.67	0.51	0.51	1.01	1.01	0.63	0.63	**0.82**	**--**	**0.51**	**1.67**
302	24	Semi-Automated Selection & Scaling (to match CMS)	1.06	1.06	0.84	1.01	0.91	1.07	1.02	1.01	**1.04**	**0.12**	**0.84**	**1.19**
302	24	Semi-Automated Selection & Scaling (to match CMS)	--		1.19		1.17		1.01					
303	78	Design Ground Motion Library (DGML) (Objective 4)	--	--	1.23	1.05	0.95	1.00	--	--	**1.03**	**0.11**	**0.18**	**1.23**
303	78	Design Ground Motion Library (DGML) (Objective 4)	--		1.05		1.15		--					
303	78	Design Ground Motion Library (DGML) (Objective 4)	--		0.84		1.07		--					
303	78	Design Ground Motion Library (DGML) (Objective 4)	--		1.09		0.99		--					
304	45	Design Ground Motion Library (DGML) (Objective 3-4)	1.37	1.36	1.01	1.10	0.76	0.83	0.90	0.92	**1.01**	**0.39**	**0.76**	**2.39**
304	45	Design Ground Motion Library (DGML) (Objective 3-4)	1.09		0.94		1.51		0.93					
304	45	Design Ground Motion Library (DGML) (Objective 3-4)	0.97		2.13		1.11		0.92					
304	45	Design Ground Motion Library (DGML) (Objective 3-4)	1.53		2.39		0.81		0.96					
Median:			**1.04**	**--**	**1.01**	**--**	**1.01**	**--**	**0.95**	**--**	***Median all Buildings:***			
C.O.V.:			**0.23**	**--**	**0.22**	**--**	**0.08**	**--**	**0.15**	**--**	***1.01***			

*For consistency of comparisons, Objective 3 method is not included in the summary statistics.

Table 11.6 summarizes the results for four methods within Group IV (proxy for CMS). This shows that the median predictions are slightly higher than CMS methods, with predictions for each building/scenario ranging from +5% to +12% above the POC, with an overall median

value of +5%. The median predictions for each individual method have a bit more variability, ranging from -19% below to +14% above the POC. If slightly higher scatter is allowable, Group IV methods may have advantage over Group III methods, since they are often easier to use (e.g., only need to match an ε value instead of matching a full spectrum).

Methods 400 and 401 provide consistent overprediction of +10% to +14% above the POC. The two ATC-63 related methods give -19% below the POC for method 402 and +4% above the POC for method 403. This suggests that the ATC-63 near-field records are the more appropriate record set to use for these scenarios, which have a 10 km site to source distance[2].

It is interesting to note that the Group IV methods lead to slightly higher *variability* in both spectral values and the resulting response, and also slightly higher *median* response. While reviewing the results from this study (for Groups IV and V specifically), the observation was made multiple times that some methods which resulted in higher variability also resulted in higher median prediction. This suggests that the distribution of drift response might be non-symmetric (meaning that higher variability in response leads to a greater increase in larger responses, as compared with the amount of decrease in smaller responses). This observation has been documented in previous research studies as well (Carballo 2000, Bazzurro and Luco 2006). This study focused on predicting only median MIDR response, so the ground motion sets selected as part of this study did not allow a systematic investigation of this question. Possible future work, focusing on also predicting the variability in response, would help determine whether this observation is a real trend or just a coincidence.

[2] The observation that the near-field records result in higher interstory drift demands as compared with the far-field records is reasonable and consistent with comparisons done as part of the ATC-63 project (ATC 2008; Appendix A).

Table 11.6 Median MIDR/POC responses for sets of seven ground motions from Group IV methods [methods that use epsilon (ε) proxy for CMS], for all buildings and scenarios.

Ratio of Median MIDR to the Point of Comparison			Building A, M7		Building B, M7		Building C, M7		Building D, M7		Summary Stats. for All Bldgs./Scenarios			
Method Number	Method Tag	Method Name	Indiv. Sets of 7	All Rec.	Indiv. Sets of 7	All Rec.	Indiv. Sets of 7	All Rec.	Indiv. Sets of 7	All Rec.	Med. All Rec.	C.O.V. Set of 7	Min. Set of 7	Max. Set of 7
400	20	Target Spectrum Based on Epsilon Correlations	1.00	0.91	1.18	1.20	1.21	1.13	1.23	1.06	**1.10**	**0.16**	**0.76**	**1.28**
400	20	Target Spectrum Based on Epsilon Correlations	1.13		0.78		1.17		1.00					
400	20	Target Spectrum Based on Epsilon Correlations	0.76		1.28		1.15		1.04					
400	20	Target Spectrum Based on Epsilon Correlations	0.84		1.06		0.86		0.86					
401	31	ε Selection with $S_{de}(T_1)$ Scaling	1.64	1.13	0.74	1.32	1.88	1.15	1.09	1.10	**1.14**	**0.28**	**0.74**	**1.88**
401	31	ε Selection with $S_{de}(T_1)$ Scaling	1.18		1.57		1.69		1.15					
401	31	ε Selection with $S_{de}(T_1)$ Scaling	1.03		1.84		0.79		1.06					
401	31	ε Selection with $S_{de}(T_1)$ Scaling	1.07		1.33		0.94		1.26					
402	43	ATC-63 Method Applied to MIDR - Far-Field Set	--	--	0.92	0.92	0.81	0.81	0.73	0.73	**0.81**	**0.12**	**0.73**	**0.92**
403	48	ATC-63 Method Applied to MIDR - Near-Field Set	--	--	1.05	1.05	0.96	0.96	1.04	1.04	**1.04**	**0.05**	**0.96**	**1.05**
		Median:	**1.05**	**--**	**1.12**	**--**	**1.06**	**--**	**1.05**	**--**	***Median all Buildings:***			
		C.O.V.:	**0.24**	**--**	**0.29**	**--**	**0.32**	**--**	**0.15**	**--**	***1.05***			

Table 11.7 summarizes the results for five methods within Group V (inelastic-based methods). This shows that the median predictions are both higher and more variable as compared to both the CMS and proxy methods. The predictions for each building/scenario range from +4% to +39% above the POC, with an overall median value of +23%. The median predictions for each individual method are slightly more stable, with values ranging from -9% below to +33% above the POC.

Method 502b provides the most accurate prediction overall (with a median of +3% above the POC); however, the median predictions for each individual building/scenario have more variability as compared to CMS and proxy methods (ranging from -16% below to +55% above the POC), but this partially comes from the fact that the method 502b results are based on only 14 ground motions rather than the standard 28 motions.

It should be noted that there are still unresolved questions regarding the appropriateness of the inelastic targets used in methods 500 and 503, and the choice of these inelastic targets may have resulted in the overpredictions observed with these methods (discussed in Sections 3.3.1, 6.7, 7.7, 8.7, 9.7, and 10.7). This does not suggests that these methods should not be used, but simply means that they were designed for answering a question different than what was posed in this study (this study defines the scenario based on *elastic* spectral acceleration values). Note that further study of proper inelastic targets for use with such scenarios could resolve this issue

and remove the bias from these predictions. Even though these methods lead to predictions that are biased high (i.e., not *accurate*), it should be noticed that they still lead to reasonably *precise* predictions (with c.o.v. values of only 0.20).

Method 501 provides consistent underprediction of response, with a median value of 15% below the POC.

Table 11.7 Median MIDR/POC responses for sets of seven ground motions from Group V methods (inelastic-based), for all buildings and scenarios.

Ratio of Median MIDR to the Point of Comparison			Building A, M7		Building B, M7		Building C, M7		Building D, M7		Summary Stats. for All Bldgs./Scenarios			
Method Number	Method Tag	Method Name	Indiv. Sets of 7	All Rec.	Indiv. Sets of 7	All Rec.	Indiv. Sets of 7	All Rec.	Indiv. Sets of 7	All Rec.	Med. All Rec.	C.O.V. Set of 7	Min. Set of 7	Max. Set of 7
500	27	$S_{di}(T_1, dy)$ Scaling	1.28	1.38	1.69	1.50	1.51	1.29	1.13	1.11	**1.33**	**0.19**	**1.08**	**1.96**
500	27	$S_{di}(T_1, dy)$ Scaling	1.45		1.96		1.26		1.08					
500	27	$S_{di}(T_1, dy)$ Scaling	1.82		1.13		1.49		1.11					
500	27	$S_{di}(T_1, dy)$ Scaling	1.35		1.37		1.23		1.23					
501	6	Vector of Record Properties Identified by Proxy	1.06	1.06	0.83	0.80	1.09	0.96	0.94	0.85	**0.91**	**0.14**	**0.73**	**1.15**
501	6	Vector of Record Properties Identified by Proxy	1.02		0.73		1.04		0.87					
501	6	Vector of Record Properties Identified by Proxy	0.86		0.92		0.76		0.77					
501	6	Vector of Record Properties Identified by Proxy	1.15		0.74		0.99		0.92					
502a	11a	Inelastic Response Surface Scaling (1st mode)	1.17	1.17	2.11	1.90	1.58	1.35	1.01	0.98	**1.26**	**0.30**	**0.95**	**2.11**
502a	11a	Inelastic Response Surface Scaling (1st mode)	--		1.49		1.22		0.95					
502b	11b	Inelastic Response Surface Scaling (1st-2nd modes)	--	--	1.42	1.55	1.07	1.03	0.84	0.84	**1.03**	**0.36**	**0.72**	**1.83**
502b	11b	Inelastic Response Surface Scaling (1st-2nd modes)	--		1.83		0.99		0.72					
503	35	IM1I&2E Selection/Scaling	1.16	1.37	1.30	1.38	1.01	1.18	1.11	1.10	**1.28**	**0.17**	**1.01**	**1.72**
503	35	IM1I&2E Selection/Scaling	1.44		1.72		1.35		1.07					
503	35	IM1I&2E Selection/Scaling	1.71		1.14		1.52		1.20					
503	35	IM1I&2E Selection/Scaling	1.34		1.48		1.16		1.11					
		Median:	**1.28**	--	**1.39**	--	**1.19**	--	**1.04**	--	***Median all Buildings:***			
		C.O.V.:	**0.21**	--	**0.31**	--	**0.19**	--	**0.15**	--	***1.23***			

11.4 IDENTIFICATION OF INDIVIDUAL METHODS THAT PROVIDE ACCURATE AND PRECISE PREDICTIONS OF MIDR

The previous section presented detailed results for individual methods within each group. Using the results presented in Section 11.3, this section identifies the top methods that provide the best prediction capability.

Table 11.8 and Table 11.9 show summary statistics for the top eight methods that produced the most accurate and precise predictions of median MIDR. This is the short-list of methods an analyst might consider when predicting the median MIDR response (for structures and ground motion scenarios similar to those studied here). Table 11.8 shows the *accuracy* of

the methods by presenting the median MIDR/POC predictions for the combined records set (usually four sets of seven records, for a total of 28 records) for each building/scenario pair. Table 11.9 explains the *precision* of the methods by presenting the coefficients of variation (c.o.v.) of the median MIDR/POC predictions for each set of seven records; for a perfectly precise method which predicts the same MIDR value for each set of seven records, this c.o.v. value would be 0.0. Note that this value does not represent the record-to-record variability, but is rather the c.o.v. of several *median* predictions of MIDR.

The first three methods are from Group III (CMS matching), the following three methods are from Group IV (proxy for CMS), and the last two methods are from Group V (inelastic methods). This specific subset of methods was selected to be in this short list of methods because the median predictions are within 15% of the POC (and over half are within 5%), on average, over the four buildings considered.

From Table 11.8, the most accurate methods tend to be the Group III (CMS matching) methods, with all three methods providing median predictions within 4% of the POC. These methods also give consistently accurate predictions (have high *precision*), with c.o.v. values ranging on from 0.09 to 0.12. All three of the Group III methods provide accurate and precise predictions, but note that this conclusion is based on four buildings for methods 300 and 302, but only two buildings for method 303.

From Groups IV and V, the accuracy ranges from -9% below the POC to +14% above the POC. The two most accurate methods within this group are methods 403 and 502b. However, for method 403, the counterpart method 402 leads to underprediction of response, so this suggests that method 403 may not provide accurate predictions for all ground motion scenarios (e.g., if the source-to-site distance were longer, and the far-field ground motion set of method 402 were used, it may lead to slight underprediction of MIDR response). method 502b also has a drawback in that it is less *precise* as compared for the Group III methods (with a c.o.v. of 0.36).

In summary, the eight methods shown in Table 11.8 lead to accurate estimates of the median MIDR response (within 15%), but the first three methods (300, 302, and 303) provide the most accurate, and most consistently accurate, response predictions.

Table 11.8 Median MIDR/POC predictions for each building and scenario, presented for most accurate/precise individual GMSM methods. Data come from Tables 11.3–Table 11.7. Methods are not ranked within table, but are simply ordered by group and method number.

Method Information				Median(MIDR/POC) for Combined Record Set				
Method Group	Method Number	Method Name	Num. of G.M. Sets	Building A, M7	Building B, M7	Building C, M7	Building D, M7	Median
III	300	Conditional Mean Spectrum Selection with Scaling	4	1.01	0.92	0.98	0.95	**0.97**
III	302	Semi-Automated Selection & Scaling (to match CMS)	1-2	1.06	1.01	1.07	1.01	**1.04**
III	303	Design Ground Motion Library (DGML) (Objective 4)	4	--	1.05	1.00	--	**1.03**
IV	400	Target Spectrum Based on Epsilon Correlations	4	0.91	1.20	1.13	1.06	**1.10**
IV	401	ε Selection with Sde(T1) Scaling	4	1.13	1.32	1.15	1.10	**1.14**
IV	403	ATC-63 Method Applied to MIDR - Near-Field Set	1	--	1.05	0.96	1.04	**1.04**
V	501	Vector of Record Properties Identified by Proxy	4	1.06	0.80	0.96	0.85	**0.91**
V	502b	Inelastic Response Surface Scaling (1st-2nd modes)	2	--	1.55	1.03	0.84	**1.03**

Table 11.9 Coefficient of variation (c.o.v.) of median MIDR/POC predictions from each set of seven records, presented for most accurate/precise individual GMSM methods. Data come from Tables 11.3–11.7. Methods are not ranked within table, but are simply ordered by group and method number.

Method Information				c.o.v. of median MIDR/POC values for All Buildings and Scenarios
Method Group	Method Number	Method Name	Total Num. of G.M. Sets	
III	300	Conditional Mean Spectrum Selection with Scaling	20	**0.09**
III	302	Semi-Automated Selection & Scaling (to match CMS)	7	**0.12***
III	303	Design Ground Motion Library (DGML) (Objective 4)	8	**0.11***
IV	400	Target Spectrum Based on Epsilon Correlations	16	**0.16**
IV	401	ε Selection with Sde(T1) Scaling	20	**0.28**
IV	403	ATC-63 Method Applied to MIDR - Near-Field Set	4	**0.05***
V	501	Vector of Record Properties Identified by Proxy	20	**0.14**
V	502b	Inelastic Response Surface Scaling (1st-2nd modes)	8	**0.36***

* Note: Value is based on a relatively small number of data points.

11.5 OBSERVATIONS, CONCLUSIONS, AND SCOPING LIMITATIONS

11.5.1 Purpose and Scope

The purpose of this study is to provide the engineering community with a foundation, backed by supporting research, for choosing appropriate ground motion selection and modification (GMSM) methods for building structures. With this goal in mind, this study uses four reinforced concrete frame and wall structures and two ground motion scenarios as case studies; these are

used to evaluate the prediction capability of 14 ground motion selection and modification techniques (25 if variations are considered). The methods considered in this report cover the majority of common GMSM methods available to the engineering community.

The structures used in this study include reinforced concrete frames and walls from four to twenty stories. Strictly speaking, the results should be applied only to such systems. Even so, frame buildings of any material (steel, concrete, etc.) tend to behave in a similar manner, so these results should be applicable to many frame systems. The shear wall building used in this study fails in a flexural mode, rather than a shear mode; even so, the authors assume that these results would also be generally applicable to a wall failing in shear (as long as it is not an entirely brittle, strength controlled failure), but this should be considered carefully before applying these results to such a building. Regarding building height, the authors are comfortable with these results being applied over a slightly larger range of heights (than the four to twenty story models used in this study), since the fundamental behavior does not change immediately for buildings of other heights; a range of two to thirty stories seems like a reasonably acceptable range.

The ground motion scenarios used in this study were selected carefully to be consistent with the maximum considered earthquake (MCE) ground motions used in current building code provisions (ASCE 2005), for high seismic sites in California. Haselton (2008) used the full set of United State Geological Survey (USGS) deaggregation data (Harmsen et al. 2001) to show that the average ε value is 1.35 for a 2% in 50-year (or MCE) motion at high seismic California sites, with some sites reaching up to $\varepsilon = 2.0$. To cover this range of values, the M7.0 scenario is based on an expected $\varepsilon = 2.0$ motion, and the M7.5 scenario is based on an expected $\varepsilon = 1.0$ motion. Both scenarios are based on a source-to-site distance of 10 km. The findings of this report are limited to $\varepsilon = 1.0$ to 2.0 ground motion scenarios. For ground motion scenarios with lower ε values, we expect that the differences between methods will be less important.

When evaluating the seismic response of building structures, the interstory drift is typically the response of primary interest, though other parameters are also of interest for performance-based assessment methods (e.g., floor acceleration, element plastic rotations, base shear, etc.). This study is limited to prediction of peak interstory drift ratio (MIDR), so strictly speaking, the conclusions of this study should be applied only to prediction of this structural response. Realistically, element plastic rotation is closely related to interstory drift ratio (provided that the element is in the story that has the maximum drift, and the element is directly

contributing to that drift), so the conclusions of this report also gives guidance for estimation of element plastic rotations. Some other responses, such as peak floor accelerations for example, are not well related to peak interstory drift, so the findings of this report should not be applied to prediction of such responses (for example, floor accelerations are more closely related to peak ground acceleration that $Sa(T_1)$, and the methods are not consistent in how well they identify records with appropriate peak ground accelerations). Accurately predicting such responses will require additional study.

This work is limited to prediction of *median* response. Predicting the full distribution of response is a possible topic of future study for the Ground Motion Selection and Modification Program.

Additionally, collapsed cases were considered when computing the counted median MIDR values and computing the POC values (in Chapter 5), but collapse rates from the individual GMSM methods were not systematically investigated in this report. It was observed that various GMSM methods resulted in widely varying collapse rates, but understanding the precise cause of these differences will require future investigation.

11.5.2 Observations and Conclusions

This report showed that one way to obtain both an accurate and precise prediction of median interstory drift is to properly account for the expected spectral shape. This is necessary because the spectral shape is important to nonlinear drift response. Based on the findings of this report, and the methods considered in it, the most consistent way to obtain an accurate prediction is to match directly to the conditional mean spectrum (Group III methods 300, 302, and 303), ensuring a close match of the spectral shape at both periods longer than the fundamental period of the building (to capture nonlinear response), and periods shorter than the fundamental period of the building (to capture higher-mode effects). Spectral shape can also be accounted for by using some type of proxy (Group IV methods), such as ε, and this approach also consistently works well (methods 400, 401, and 403), yet has slightly higher scatter in the median predictions.

Inelastic methods (Group V methods) do not explicitly, but may implicitly, consider spectral shape. Even so, some inelastic methods still provide an accurate prediction (methods

501, 502b, and 503, with 502b providing the most accurate prediction). This is because they consider other factors important to nonlinear response (e.g., inelastic spectral displacement). However, the inelastic methods (502b and 503, specifically) had more variability in the median interstory drift predictions (a lower level of precision) for the buildings and scenarios considered in this study. Regarding some of the inelastic methods (specifically 500 and 503), it was suggested that an improper target may have been used for ground motion selection (e.g., improper inelastic spectral displacement target), leading to overprediction of response (see Sections 11.3 and 3.3.1). If the inelastic target can be improved, several of the inelastic methods may be able to provide both accurate and precise results. Future research is needed to develop improved inelastic targets for common ground motions scenarios like those used in this report (where the scenario definition is based on *elastic* spectral values).

The methods that did not consider proper spectral shape or a proper inelastic parameter (Group I and II methods, which are $Sa(T_1)$ scaling and matching to a UHS, respectively) led to consistent overpredictions of peak interstory drift response. When an accurate prediction of structural response is desired (i.e., not a conservative prediction) for the objective considered in this report (predicting median MIDR response for a positive ε motion), these methods should not be used.

Based on the above findings, the most general requirements to obtain an *accurate* and *precise* prediction of structural response are as follows:

1. Select ground motions based on record properties important to structural response (e.g., use the CMS for spectral shape, S_{di}, etc.). This will lead to a *precise* prediction of response.
2. Use the proper target for these record properties (e.g., use the CMS for spectral shape, use a proper S_{di} target, etc.). This will lead to an *accurate* prediction of response.

To illustrate the need for the above two requirements, we can consider the results from both the Group III (CMS matching) and Group IV (inelastic) methods. The Group III methods provided both *precise* and *accurate* predictions because they (a) selected and scaled motions based on spectral shape (providing a *precise* prediction), and (b) used the proper CMS target for that spectral shape (providing an *accurate* prediction). In contrast, two of the Group V methods (methods 500 and 503) (a) selected based on inelastic spectral displacement (which was correct,

and provided a *precise* prediction), and (b) used an improper inelastic target (which led to an *inaccurate* prediction).

It is important to note that the important record properties may differ depending on the structural response of interest. For the case of peak interstory drift ratio (considered in this report), we have shown that the spectral shape (of the elastic acceleration spectrum) and the inelastic spectral displacement are two important record properties. In contrast, for prediction of peak floor acceleration, past research has shown that the peak ground acceleration is an important record property that would need to be considered when selecting and scaling ground motions (Krawinkler et al. 2005).

11.6 FUTURE RESEARCH

The results of this report are an initial building block toward future studies that can grow increasingly more comprehensive, and can expand to cover more types of structural systems. This report provides guidance on GMSM for predicting *median* MIDR response of *building structures*. The vision of the GMSM Program is that future projects can continue this line of research by working on prediction of the *full distribution* of building MIDR response, and then prediction of building MIDR *hazard curves*. This progression of research (prediction of median response, full distribution of response, and then response hazard curves) is a template for possible future research.

Studies could then be expanded to consider other building responses (e.g., peak floor acceleration, collapse response, etc.), other types of structural systems, other types of ground motions, and other applications for which GMSM is an important consideration.

A summary of these possible research directions are as follows:

- GMSM for Building Structures:
  - Maximum interstory drift response (MIDR)
    - Prediction of the median MIDR response (completed in this report)
    - Prediction of the full distribution of MIDR response
    - Prediction of the full MIDR response hazard curve
  - Other structural responses such as peak floor acceleration (similar study to that of MIDR)

- Collapse fragility prediction
- Damage and closure fragility curves for essential facilities

- GMSM for Other Types of Structures and Systems (following the approach outlined above for the building study)
  - Bridge structures
  - Nuclear structures
  - Earth structures (levees and earthen dams)
  - Site response
- GMSM using Non-Recorded Ground Motions
  - Spectrum compatible motions
  - Synthetic motions

In addition to the possible overall research directions outline above, there are a few more immediate tasks that could be completed, in order to expand on this report regarding prediction of *median* MIDR response of *building structures*:

- Further investigation of short-list methods to verify their performance for a wider range of buildings (e.g., taller buildings) and scenarios (e.g., an ε neutral scenario)
- Expansion of the study on building code methods
- Further investigation of proper inelastic targets (e.g., S_{di}) for use with common ground motion scenarios such as those used in this report (which are defined in terms of *elastic* spectral demands)

REFERENCES

Agresti, A. (2002). Categorical data analysis, 2nd Ed., Wiley, New York.

Applied Technology Council (ATC) (2008). Recommended methodology for Quantification of Building System Performance and Response Parameters, ATC-63 (90% Draft), FEMA P695, Applied Technology Council, Redwood City, CA.

American Concrete Institute (2002). Building Code Requirements for Structural Concrete (ACI 318-02) and Commentary (ACI 318R-02), Farmington Hills, MI.

American Society of Civil Engineers. (2005). ASCE7-05: Minimum Design Loads for Buildings and Other Structures, Reston, VA.

American Society of Civil Engineers (2002). ASCE7-02: Minimum Design Loads for Buildings and Other Structures, Reston, VA.

Baker, J. W., and Jayaram, N. (2008). "Correlation of spectral acceleration values from NGA ground motion models." Earthquake Spectra, 24(1), 299-317

Baker, J. W., and Cornell, C. A. (2006). "Spectral shape, epsilon and record selection." Earthquake Engineering and Structural Dynamics, 35(9), 1077–1095.

Bazzurro, P. and Luco, N. (April 2006), "Do scaled and spectrum-matched near-source records produce biased nonlinear structural responses?", Proceedings of the Eighth U.S. National Conference on Earthquake Engineering, San Francisco, CA.

Benjamin, J. R., and Cornell, C. A. (1970). Probability, Statistics, and Decision for Civil Engineers, McGraw-Hill, New York.

Burnham, K., and Anderson, D. (2002). Model Selection and Multimodel Inference: A Practical Information-theoretic Approach, Springer.

Campbell, K.W. and Bozorgnia, Y. (2008). "NGA Ground Motion Model for the Geometric Mean Horizontal Component of PGA,. PGV, PGD and 5% Damped Linear Elastic Response Spectra for Periods Ranging from 0.01 to 10s." Earthquake Spectra, 24, 139-171.

Campbell, K.W. and Bozorgnia, Y. (2006). Campbell-Bozorgnia NGA Ground Motion Relations for the Geometric Mean Horizontal Component of Peak and Spectral Ground Motion Parameters, PEER Report 2007/02, Pacific Engineering Research Center, University of California, Berkeley, California.

Carballo, J. (2000). Probabilistic Seismic Demand Analysis: Spectrum Matching and Design, Ph.D. Dissertation, Department of Civil and Environmental Engineering, Stanford University.

Federal Emergency Management Agency (FEMA) (2009). Recommended methodology for Quantification of Building System Performance and Response Parameters, FEMA P695A, Prepared for the Federal Emergency Management Agency, Prepared by the Applied Technology Council, Redwood City, CA.

Fox, J. (2002). An R and S-Plus Companion to Applied Regression, Sage Publications.

Goulet, C., C.B. Haselton, J. Mitrani-Reiser, J. Beck, G.G. Deierlein, K.A. Porter, and J. Stewart, (2007). "Evaluation of the Seismic Performance of a Code-Conforming Reinforced-Concrete Frame Building - from seismic hazard to collapse Safety and Economic Losses," Earthquake Engineering and Structural Dynamics.

Harmsen, S.C., 2001, "Mean and Modal ε in the Deaggregation of Probabilistic Ground Motion", Bulletin of the Seismological Society of America, 91, 6, pp. 1537-1552, December 2001.

Haselton, C.B., J. Mitrani-Reiser, C. g1

Goulet, G.G. Deierlein, J. Beck, K.A. Porter, J. Stewart, and E. Taciroglu (2008). An Assessment to Benchmark the Seismic Performance of a Code-Conforming Reinforced-Concrete Moment-Frame Building, PEER Report 2007/12, Pacific Engineering Research Center, University of California, Berkeley, California.

Haselton, C.B., A.B. Liel, S. Taylor Lange, and G.G. Deierlein (2008). Beam-Column Element Model Calibrated for Predicting Flexural Response Leading to Global Collapse of RC Frame Buildings, PEER Report 2007/03, Pacific Engineering Research Center, University of California, Berkeley, California.

Haselton, C.B. and G.G. Deierlein (2007). Assessing Seismic Collapse Safety of Modern Reinforced Concrete Frame, PEER Report 2007/08, Pacific Engineering Research Center, University of California, Berkeley, California.

International Code Council. (2003). 2003 International Building Code, Falls Church, VA.

International Code Council. (2006). 2006 International Building Code, Falls Church, VA.

Jayaram, N., and Baker, J. W. (2008). "Statistical Tests of the Joint Distribution of Spectral Acceleration Values." Bulletin of the Seismological Society of America, 98(5), 2231-2243.

Ibarra, L.F., Medina, R.A., and Krawinkler, H. (2005). "Hysteretic models that incorporate strength and stiffness deterioration," Earthquake Engineering and Structural Dynamics, Vol. 34, pp. 1489-1511.

Kottke, Albert and Rathje, E. (2008). "A Semi-Automated Procedure for Selection and Scaling of Recorded Earthquake Motions for Dynamic Analysis." Earthquake Spectra, 24(4), 911-932.

Krawinkler, H. (2005). "Van Nuys Hotel Building Testbed Report: Exercising Seismic Performance Assessment," PEER Report 2005/11, PEER, UC Berkeley, 249 pp.

Kutner, M. H., Nachtsheim, C., and Neter, J. (2004). Applied linear regression models, 4th Ed., McGraw-Hill/Irwin, Boston; New York.

Luco, N. and C.A. Cornell (2007). "Structure-specific scalar intensity measures for near-source and ordinary earthquake ground motions," Earthquake Spectra, Vol. 23, No. 2, pp. 357-392.

McCullagh, P., and J. A. Nelder (1989). Generalized Linear Models, 2nd Edition. Chapman and Hall, New York, New York, USA. 511pp.

Matlab Inc. (2005). "Matlab 7.0 Release, Statistics toolbox."

Open System for Earthquake Engineering Simulation (OpenSEES) (2006). Pacific Earthquake Engineering Research Center, University of California, Berkeley, http://opensees.berkeley.edu/ (last accessed December 1, 2006).

PEER (2006). Pacific Earthquake Engineering Research Center: PEER NGA Database, University of California, Berkeley, http://peer.berkeley.edu/nga/ (last accessed October 22, 2006).

Prakash V, Powell G, Campbell S. (1993). DRAIN-2DX: Basic program description and user guide. Report No. UCB/SEMM-93/17, University California at Berkeley, Berkeley, CA.

Shome, N., and Cornell, C. A. (1999). "Probabilistic seismic demand analysis of nonlinear structures." RMS Program, Stanford, CA.

Shome, N., and Cornell, C. A. (2000). "Structural Seismic Demand Analysis: Consideration of "Collapse." 8th ASCE Specialty Conference on Probabilistic Mechanics and Structural Reliability, University of Notre Dame, South Bend, Indiana, 7.

UBC (1997), "Uniform Building Code," International Conference of Building Officials, Whittier, California.

Weisberg, S. (1985). Applied Linear Regression, John Wiley and Sons New York.

Zareian F. (2006). Simplified Performance-Based Earthquake Engineering. PhD Dissertation, Department of Civil and Environmental Engineering, Stanford University, Stanford, CA.

Appendix A: Summaries of Ground Motion Selection and Modification (GMSM) Methods

Author: N. Luco

A.1 SUMMARY OF GMSM METHODS

This appendix contains summaries of the GMSM methods that are investigated in this report. A list of the methods (Table 2.1), explanations of their objectives, and brief summaries of their selection and modification procedures by group are contained in Chapter 2. The intent of the summaries in this appendix is to help readers understand each of the individual GMSM methods to the extent that they could implement it on their own. The method summaries do not, for the most part, provide specific details about the ground motion sets selected and modified for this PEER GMSM Program study.

Each summary was written by the contributor of ground motion sets for the corresponding method, in some cases in collaboration with a (or another) member of the PEER GMSM Program. The author(s) are identified within each summary.

A.1.1 Method 100: $S_a(T_1)$ Scaling with Bin Selection

Name for Ground Motion Selection and Modification (GMSM) Method: "$S_a(T_1)$ Scaling"

Author(s) of Synopsis: Nilesh Shome, AIR Worldwide **Date**: 29 August 2007

Reference(s):

Shome N, Cornell CA, Bazzurro P, Carballo JE (1998). "Earthquakes, Records, and Nonlinear Responses", *Earthquake Spectra,* Vol. 14(3).

Objective: To obtain a set of ground-motion records for nonlinear structural dynamic analysis that will result in an accurate estimate of the cumulative distribution function (CDF) and the median of the engineering demand parameter (EDP) of interest for a given structure, earthquake magnitude (M), source-to-site distance (R), site classification (S) and style of faulting (F), or a given M, R, S, F and first-mode spectral acceleration ($S_a(T_1)$).

Brief Description of the Procedure:

1) Decide on an M-R-S-F bin that is consistent with the given scenario. An example of bin of records for magnitude M_w=7 at distance R=10km and for stiff soil sites ($V_{s,30} \approx 400$ m/s) is shown in Figure 1.
2) Select desired number of records randomly from the bin of records. The records should be selected from different earthquakes to capture the inter-event variability of response for a given $S_a(T_1)$.
3) Scale the records to the target $S_a(T_1)$. In the case of a given M, R, S, and F only, the target $S_a(T_1)$ is the median from a ground motion prediction equation (a.k.a., attenuation relation). The records as shown in Figure 1 are scaled to a target spectral acceleration and seven records are selected randomly for the bin of records.

The probability distribution of the EDP of interest is assumed to be lognormal. The parameters of the distribution are the following:

- The mean of the (natural) logarithms of the EDP values from nonlinear dynamic analysis of the given structure using the selected and scaled ground motions.
- In the case of a given M, R, S, F, and $S_a(T_1)$, the dispersion $\delta_{EDP}|M,R,SA_1$, which is the standard deviation of the logarithms of the EDP values.
- In the case of a given M, R, S and F only, the dispersion $\delta_{EDP}|M,R$, which is the square-root-of-the-sum-of-the-squares (SRSS) of the aforementioned $\delta_{EDP}|M,R,SA_1$ and the logarithmic standard deviation of $S_a(T_1)$ given by an attenuation function $\delta_{SA1}|M,R$. Here the slope of the EDP vs. $S_a(T_1)$ curve is assumed to be unity (i.e., $\beta = 1$ for $EDP = \alpha.(SA_1)^{\beta}$), which may be true for most structures. If β has any other values (e.g., $\beta > 1$ for tall structures that exhibit "softening" behavior because of P-Δ effects), $\delta_{EDP}|M,R$ can be estimated as follows:

$$\delta_{EDP}|M,R = \sqrt{[(\beta.\delta_{EDP}|M,R,SA_1)^2 + (\delta_{SA1}|M,R)^2]}.$$

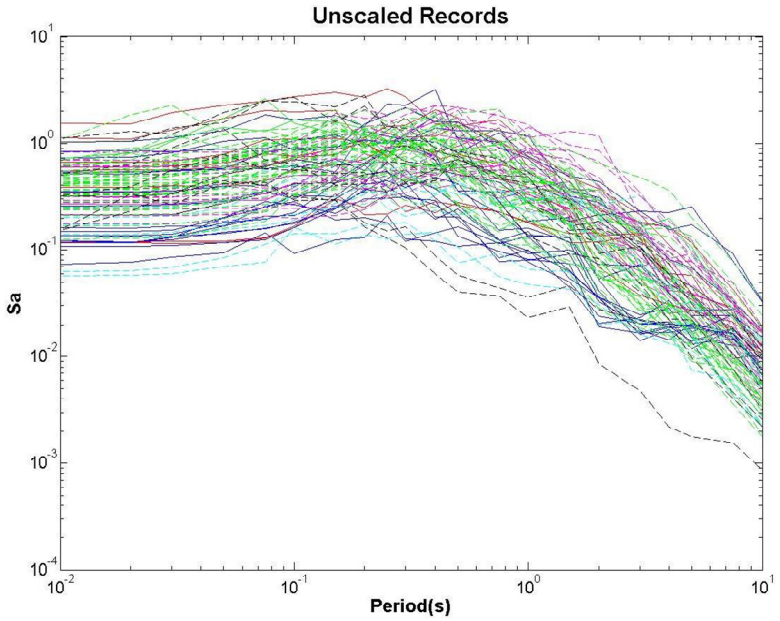

Figure 1: Spectrum of bin of records for earthquake events which have magnitude M_w= 7 and distance R = 10km at stiff soil sites ($V_s \approx 400$ m/s).

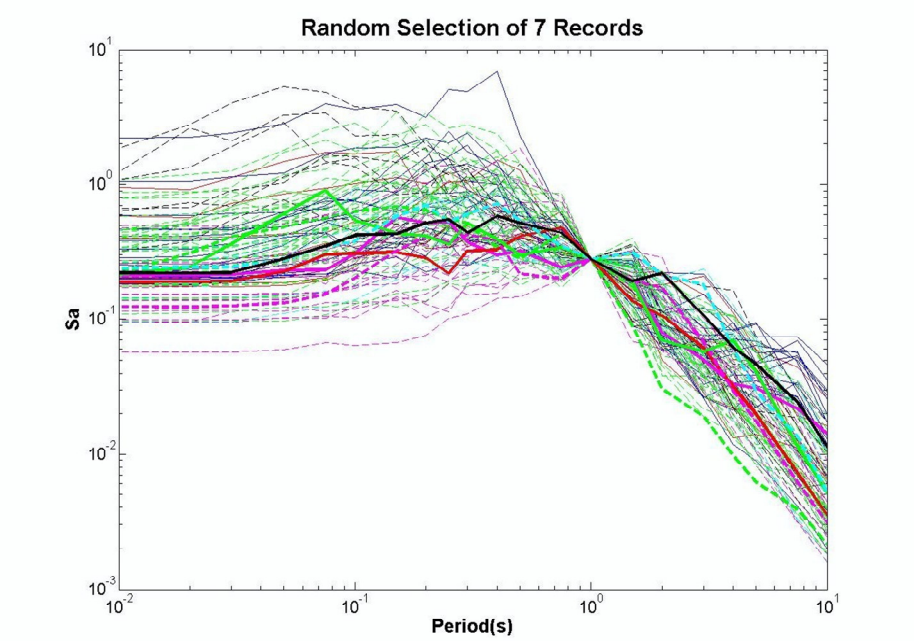

Figure 2: Records from the bin of records in Figure 1 are scaled to a target spectral acceleration 0.28g at period, T = 1 sec and 5% damping. Seven records are selected randomly from this bin for nonlinear time-history analysis of structures and are shown in thick lines.

A.1.2 Method 101: ATC-58 35% Draft Method

Name for Ground Motion Selection and Modification (GMSM) Method: "ATC-58 Intensity-Based Assessments Method"

Author(s) of Synopsis: Farzin Zareian **Date**: 21 October 2007

Reference(s):

ATC-58 35% Draft, "Guidelines for Seismic Performance Assessment of Buildings," *Applied Technology Council*, Redwood City, California.

Objective: To obtain a set of ground motion records for a two dimensional nonlinear response history analysis that will result in an accurate estimate of the joint cumulative distribution function (CDF) of the engineering demand parameters (EDP) of interest for a given structure, earthquake magnitude (M), source-to-site distance (R), and first-mode spectral acceleration (SA_1).

Brief Description/Example:

Selection Procedure:
1) Decide on an M-R bin that is consistent with the given M, R (e.g., one of the two bins listed in Tables B-3, and B-4.)
2) Randomly gather eleven ground motion records for the chosen M-R bin.

Modification Procedure:
1) Scale (in amplitude only) each of the eleven gathered ground motions by the ratio of SA_1 and the spectral acceleration value at the fundamental period of the structure for that ground motion, $Sa_i(T_1)$.

Additional Information: This GMSM method has been developed by the ATC-58 Project, "Guidelines for Seismic Performance Assessment of Buildings," whose mission is to provide practicing engineers with a methodology, procedures, and criteria to predict the probable performance of a building based on its structural, nonstructural and occupancy, and seismic hazard exposure characteristics. In this methodology, performance is defined in terms of economic loss, fatalities and injuries, and down-time loss of the building and its occupancy. However, the ground motion selection and scaling procedures suggested by ATC-58 are focused on developing the CDF of the EDPs that affect structural damage and consequently affect values of building loss parameters.

Table B-3 Bin 1–Near-Fault Ground Motions

Designation	Event	Station	M [1]	r [1]
NF1, NF2	Kobe 1995	SAC 2/50 for Los Angeles	6.9	3.4
NF3, NF4	Loma Prieta 1989		7.0	3.5
NF5, NF6	Northridge 1994		6.7	7.5
NF7, NF8	Northridge 1994		6.7	6.4
NF9, NF10	Tabas 1974		7.4	1.2
NF11, NF12	Elysian Park 1 (simulated)		7.1	17.5
NF13, NF14	Elysian Park 2 (simulated)		7.1	10.7
NF15, NF16	Elysian Park 3 (simulated)		7.1	11.2
NF17, NF18	Palos Verdes 1 (simulated)		7.1	1.5
NF19, NF20	Palos Verdes 2 (simulated)		7.1	1.5
NF21, NF22	Cape Mendocino 04/25/92	89156 Petrolia	7.1	9.5
NF23, NF24	Chi-Chi 09/20/99	TCU053	7.6	6.7
NF25, NF26	Chi-Chi 09/20/99	TCU056	7.6	11.1
NF27, NF28	Chi-Chi 09/20/99	TCU068	7.6	1.1
NF29, NF30	Chi-Chi 09/20/99	TCU101	7.6	11.1
NF31, NF32	Chi-Chi 09/20/99	TCUWGK	7.6	11.1
NF33, NF34	Duzce 11/12/99	Duzce	7.1	8.2
NF35, NF36	Erzinkan 03/13/92 17:19	95 Erzinkan	6.9	2.0
NF37, NF38	Imperial Valley 10/15/79	5057 El Centro Array #3	6.5	9.3
NF39, NF40	Imperial Valley 10/15/79	952 El Centro Array #5	6.5	1
NF41, NF42	Imperial Valley 10/15/79	942 El Centro Array #6	6.5	1
NF43, NF44	Kobe 01/16/95 20:46	Takarazu	6.9	1.2
NF45, NF46	Morgan Hill 04/24/84 04:24	57191 Halls Valley	6.2	3.4
NF47, NF48	Northridge 1/17/94 12:31	24279 Newhall	6.7	7.1
NF49, NF50	Northridge 1/17/94 12:31	0637 Sepulveda VA	6.7	8.9

1. M = moment magnitude; r = closest site-to-fault-rupture distance

Table B-4 Bin 2–Far-Field Ground Motions

Designation	Event	Station	M [1]	r [1]
FF1, FF2	Cape Mendocino 04/25/92	89509 Eureka—Myrtle & West	7.1	44.6
FF3, FF4	Cape Mendocino 04/25/92	89486 Fortuna—Fortuna Blvd	7.1	23.6
FF5, FF6	Coalinga 1983/05/02	36410 Parkfield—Cholame 3W	6.4	43.9
FF7, FF8	Coalinga 1983/05/02	36444 Parkfield—Fault Zone 10	6.4	30.4
FF9, FF10	Coalinga 1983/05/02	36408 Parkfield—Fault Zone 3	6.4	36.4
FF11, FF12	Coalinga 1983/05/02	36439 Parkfield—Gold Hill 3E	6.4	29.2
FF13, FF14	Imperial Valley 10/15/79	5052 Plaster City	6.5	31.7
FF15, FF16	Imperial Valley 10/15/79	724 Niland Fire Station	6.5	35.9
FF17, FF18	Imperial Valley 10/15/79	6605 Delta	6.5	43.6
FF19, FF20	Imperial Valley 10/15/79	5066 Coachella Canal #4	6.5	49.3
FF21, FF22	Landers 06/28/92	22074Yermo Fire Station	7.3	24.9
FF23, FF24	Landers 06/28/92	12025 Palm Springs Airport	7.3	37.5
FF25, FF26	Landers 06/28/92	12149 Desert Hot Springs	7.3	23.2
FF27, FF28	Loma Prieta 10/18/89	47524 Hollister—South & Pine	6.9	28.8
FF29, FF30	Loma Prieta 10/18/89	47179 Salinas—John &Work	6.9	32.6
FF31, FF32	Loma Prieta 10/18/89	1002 APEEL 2—Redwood City	6.9	47.9
FF33, FF34	Northridge 01/17/94	14368 Downey—Co Maint Bldg	6.7	47.6
FF35, FF36	Northridge 01/17/94	24271 Lake Hughes #1	6.7	36.3
FF37, FF38	Northridge 01/17/94	14403 LA—116th St School	6.7	41.9
FF39, FF40	San Fernando 02/09/71	125 Lake Hughes #1	6.6	25.8
FF41, FF42	San Fernando 02/09/71	262 Palmdale Fire Station	6.6	25.4
FF43, FF44	San Fernando 02/09/71	289 Whittier Narrows Dam	6.6	45.1
FF45, FF46	San Fernando 02/09/71 14:00	135 LA—Hollywood Stor Lot	6.6	21.2
FF47, FF48	Superstition Hills (A) 11/24/87	5210Wildlife Liquef. Array	6.3	24.7
FF49, FF50	Superstition Hills (B) 11/24/87	5210Wildlife Liquef. Array	6.7	24.4

1. M = moment magnitude; r = closest site-to-fault-rupture distance

A.1.3 Methods 200–209: Building Code Selection and Scaling — Methods A–J

Name for GMSM Method: Code-based record selection

Author of synopsis: Jack Baker, Stanford University **Date:** 10/19/2007

References:

American Society of Civil Engineers, 2005. *Minimum design loads for buildings and other structures*, American Society of Civil Engineers/Structural Engineering Institute, *SEI/ASCE 7-05*, Reston, VA, 388 pp.

International Council of Building Officials, 1997. *Uniform building code*, Whittier, CA.

Objective: To model the response of a structure to multiple input ground motions. The code allows the use of three input ground motions (in which case the maximum of the three response values is to be used for checking) or seven input ground motions (in which case the average value is to be used). The numbers three and seven are minimums for these two approaches, but more may be used if desired.

Brief description of the procedure

1. Compute the design response spectrum for the site of interest, using the code-specified spectrum or a site-specific response spectrum. The site-specific spectrum is generally interpreted as a uniform hazard spectrum. For the purposes of the GMSM evaluation, the design spectrum was taken to be a site-specific uniform hazard spectrum, having all spectral acceleration values equal to two standard deviations above the median spectrum associated with the design event.

2. Select representative ground motions for analysis. The UBC code states only that the motions should be "representative." ASCE 7-05 is more precise, specifying that the motions shall have "magnitudes, fault distances, and source mechanisms that are consistent with those that control the maximum considered earthquake." No guidance is given as to how close of a match these parameters should be with the controlling earthquake.

3. Scale the ground motions. The UBC code states only that the records should approximate the design spectrum. ASCE states that the average of the scaled ground motions' 5%-damped spectra should be greater than the design spectrum for periods ranging from $0.2T$ to $1.5T$, where T is the first-mode period of the structure.

Ambiguities and variations: Several questions are not explicitly answered by these criteria, as discussed below. Multiple selections were performed to evaluate the impact of these decisions on resulting structural responses.

- **Number of periods to compare against the target spectrum.** Here, 30 periods between $0.2T$ and $1.5T$ were checked to ensure that record response spectra did not fall below the target spectra.
- **Range of representative magnitudes and distances.** Here, a magnitude range of 6.5 to 7.6 and a distance range of 0 to 30 km was used to represent the magnitude=7, distance=10 km target. Only strike-slip events were considered. Separate analyses were performed using all of these criteria, some of these criteria, and using none of these restrictions. The case with no restrictions might still be considered consistent with the UBC criteria.
- **Limits on scaling.** While not specified by the building codes, some analysts prefer to limit the maximum amount by which a ground motion is scaled. Separate analyses were performed here, using a scale factor limit of 2, 4, or no limit.
- **Limits on the number of records from one earthquake.** While not specified by the building codes, some analysts prefer to use no more than one ground motion from a single earthquake. Analyses were performed here both with and without this restriction.

- **Filter frequencies.** Record processing limits the usable frequency range of ground motions. While no guidance is given in the codes, separate analyses were performed with and without the constraint that each selected ground motion's usable period range span from $0.2T$ to $1.5T$, where T is the first-mode period of the structure.
- **Definition of "average.**" The word average might be interpreted to refer to an arithmetic mean, a geometric mean, or a median of the response results. The geometric mean was used in the analyses performed here, as it is a stable estimate of the median, and is not as sensitive as the arithmetic mean to a single extreme response result.
- **Scaling of individual ground motions.** The ASCE code states only that the average of the spectra should be compared to the design spectrum. Records selected here were scaled so that their individual spectra closely match the design spectra, and then adjusted slightly upward if necessary to ensure that the average spectra also exceeded the design spectra.

A.1.4 Method 300: Conditional Mean Spectrum Selection with Scaling

Name for GMSM Method: Conditional Mean Spectrum with Scaling

Author of synopsis: Jack Baker, Stanford University **Date:** 1/9/2006

References:

Baker JW, Cornell CA (2006a). Spectral shape, epsilon and record selection. *Earthquake Engineering & Structural Dynamics*; 35(9):1077–95.

Baker JW, Cornell CA (2006b). Correlation of response spectral values for multi-component ground motions. *Bulletin of the Seismological Society of America*; 96(1):215-27.

Baker JW, Cornell CA (2005). A vector-valued ground motion intensity measure consisting of spectral acceleration and epsilon. *Earthquake Engineering & Structural Dynamics*; 34(10):1193-217.

Objective: To obtain the conditional mean values of spectral acceleration at all periods of interest, given the target spectral acceleration value at the first-mode period of the structure, $Sa(T_1)$, as well as causal magnitude and distance values. This "conditional mean spectrum" is then used as a target for record selection and scaling. Records selected and scaled to match this spectrum provide median responses equal to the median responses of ground motions naturally at the target $Sa(T_1)$ level of interest. The conditional standard deviation of the spectrum given $Sa(T_1)$ can also be calculated and presumably ensembles of records selected to match this standard deviation would provide an accurate representation of the complete distribution of response given $Sa(T_1)$, but this has not been tested in practice.

Brief description of the procedure

1. Compute the mean and standard deviation of logarithmic spectral acceleration at all periods for a target magnitude and distance. These are provided by standard ground motion prediction (attenuation) models. The predicted mean and standard deviation, given magnitude, distance, period, etc., are denoted $\overline{\ln Sa}(M,R,T)$ and $\sigma_{\ln Sa}(T)$, respectively.

2. Compute the target ε associated with $Sa(T_1)$, denoted $\varepsilon(T_1)$. This can be determined from direct back-calculation in the case where a deterministic magnitude and distance scenario was used, or from probabilistic seismic hazard analysis disaggregation.

3. Compute the conditional mean ε at other periods, given $\varepsilon(T_1)$. This can be shown to be a simple function of $\varepsilon(T_1)$ and the correlation coefficient between epsilons at the two periods of interest: $\overline{\varepsilon}(T_i) = \rho \cdot \varepsilon(T_1)$. Baker and Cornell (2006b) provide the following empirical model for this correlation coefficient

$$\rho = 1 - \cos\left(\frac{\pi}{2} - \left(0.359 + 0.163 I_{(T_{\min}<0.189)} \ln\frac{T_{\min}}{0.189}\right)\ln\frac{T_{\max}}{T_{\min}}\right)$$

   Where T_{min} and T_{max} are the smaller and larger values of T_1 and T_i.

4. Compute the spectral acceleration at all periods, using the information from steps 1-3. The conditional mean spectrum at T_2 can be computed using the following equation

$$\ln Sa(T_i)^* = \overline{\ln Sa}(M,R,T_i) + \sigma_{\ln Sa}(T_i)\cdot\overline{\varepsilon}(T_i)$$

5. Sum the squared differences between the (logarithms of the) conditional mean spectrum and a candidate ground motion at the periods of interest, after the candidate has been scaled to match the target $Sa(T_1)$. Select the ground motions with the minimum sum of squared differences. All available records are considered as candidates by the author, but it is possible to restrict the candidate records to only those falling within, e.g., a specified magnitude range. Unpublished results suggest that a reasonable period range is $0.2T_1$ to $2T_1$, and that 20 periods with uniform logarithmic spacing are sufficient to measure the spectral shape.

For extreme ground motion intensities associated with positive $\varepsilon(T_1)$ values, this spectrum will exhibit a peak at T_1 (see figures below). The peaked spectrum will fall below a uniform hazard target spectrum, which uses extreme spectral acceleration values at all periods simultaneously.

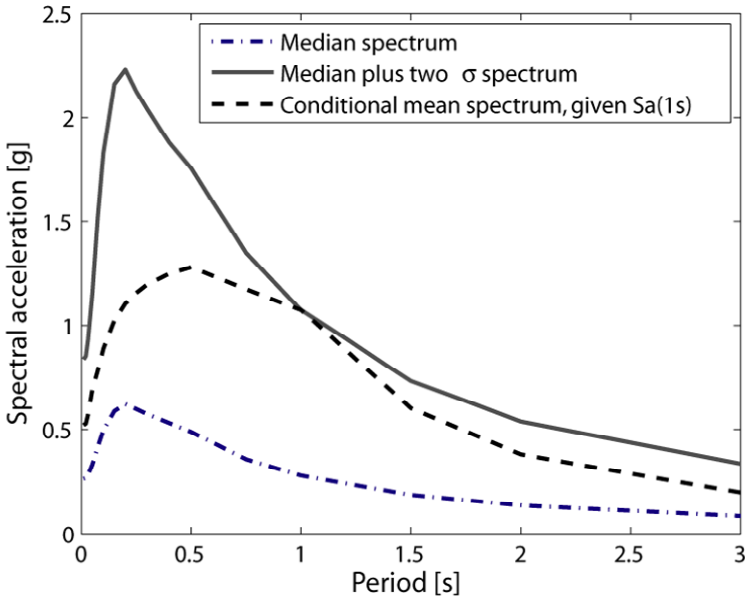

Figure 1: Comparison of the conditional mean spectrum associated with a magnitude 7, distance = 10km event and a target *Sa*(1s) that is two standard deviations larger than the median *Sa* for that magnitude and distance. The median spectrum and +2σ spectrum are also shown for comparison.

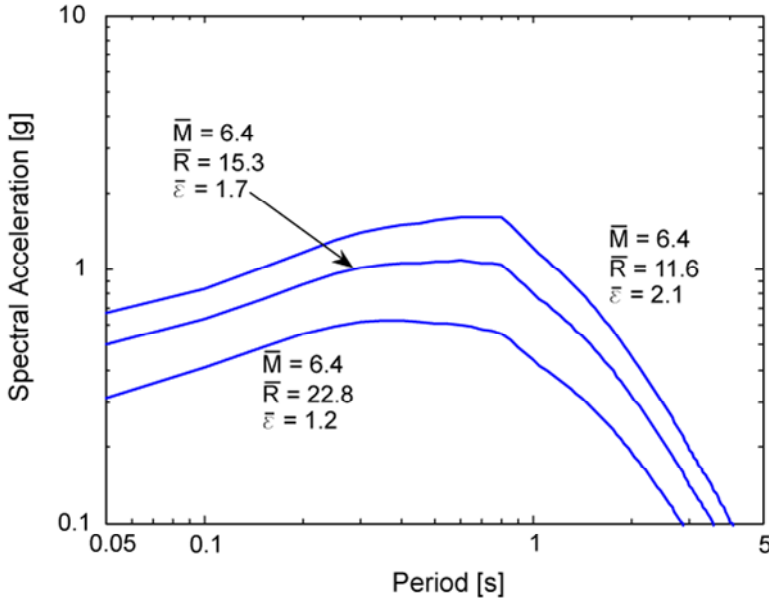

Figure 2: Conditional mean spectra for a site near Los Angeles, California, given occurrence of *Sa*(0.8s) values exceeded with 2%, 10% and 50% probabilities in 50 years, and the associated magnitude ($\bar{M}$), distance

A.1.5 Method 301: Genetic Algorithm Selection to Match CMS

Ground Motion Selection and Optimal Scaling Using Genetic Algorithms

Author(s) of Synopsis: Arzhang Alimoradi and Christine Goulet **Date**: 15 September 2008

References:

Alimoradi, A., S. Pezeshk, F. Naeim, and H. Frigui, (2005). "Fuzzy Pattern Classification of Strong Ground Motion Records," *Journal of Earthquake Engineering*, Vol. 9, No. 3, pp. 307-332, Imperial College Press, U.K.

Naeim, F., A. Alimoradi, and S. Pezeshk, (2004). "Selection and Scaling of Ground Motion Time Histories for Structural Design Using Genetic Algorithms," *Earthquake Spectra*, Vol. 20, No. 2, pp. 413-426, May 2004.

Objective: This method is designed to provide the best median estimate and/or the PDF of response (GMSM Objectives 3 and 4). This method has been coded as an in-house software developed by Alimoradi and Naeim at John A. Martin and Associates with support from the Mid-America Earthquake Center and The University of Memphis. The objective is to combine different ground motion records and scaling factors, using a genetic algorithm (GA) scheme, to match a given design response spectrum in an average sense, minimizing the mean square error. Contrary to most methods, the selection of record and scaling factor is done simultaneously, not sequentially. The concept of natural selection underlying the procedure is briefly summarized in the following section. Many options are available to the users through the Visual Basic (VB) interface. Options include: magnitude-distance and site definitions, the range of acceptable scaling factors, the database of records to choose from and other parameters related to the GA process (Figure 1).

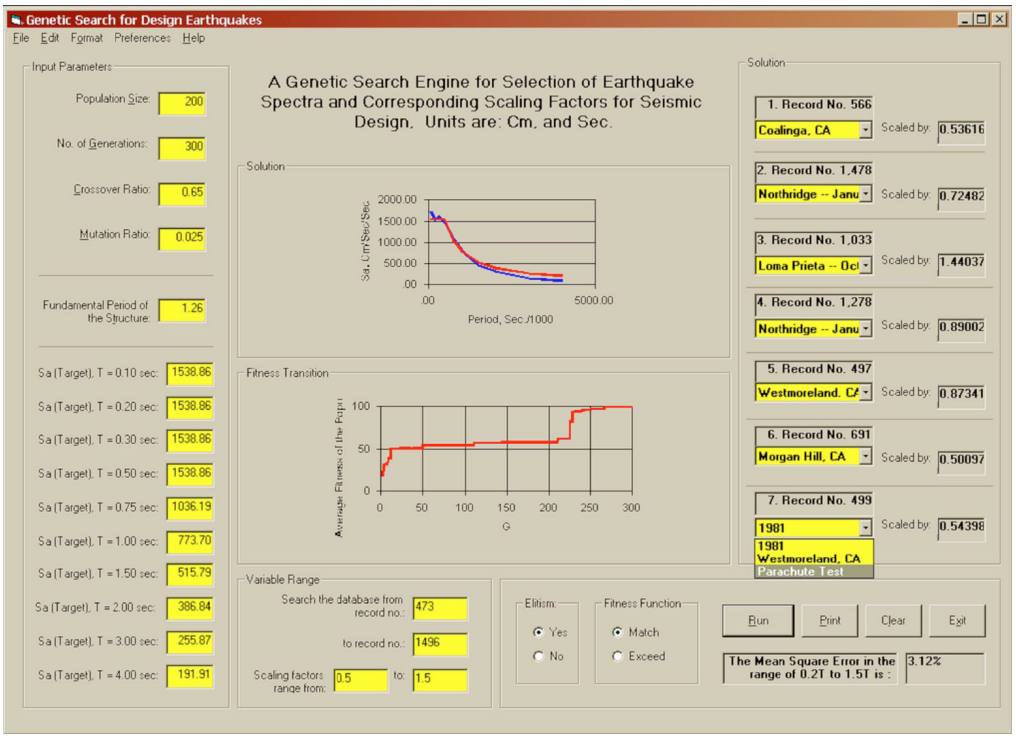

Figure 1. GUI showing some of the available options.

Brief Description:

Contrary to the prevailing scaling methods where a preset number of earthquake records (usually between a single component to seven pairs) are selected first and scaled to match the design spectrum next, the proposed method is capable of searching a set consisting of thousands of earthquake records and recommending a desired subset of records that match the target design spectrum. This task is achieved by using a genetic algorithm (GA), which treats the union of 7 records and corresponding scaling factors as a single ''individual.'' The first generation of individuals

may include a population of, for example, 200 records. A first individual is randomly selected and progressively modified through processes that mimic mating, natural selection, and mutation. New generations of individuals are produced and the process continues until an optimum individual (seven pairs and scaling factors) is obtained. A fitness function is used to quantify the goodness of fit of a specific individual and penalties can be attributed if the average spectrum falls below the target (to comply with the building-code requirements). The procedure is fast and reliable (much faster than considering all the possible solutions) and results in records that match the target spectrum with minimal modification (scaling factor could be limited by the user to fall close to 1.0) and the least mean square of deviation from the target spectrum. The selected records may individually or in combination pertain to various constraints that are set forward by design, geological settings, or geotechnical considerations.

The figure below shows the software algorithm or program flowchart. Please refer to the papers cited above for more information. The main steps of selection are as follow:

a. Randomly selecting a population of chromosomes (binary decoded record numbers in a database)
b. Evaluating the fitness of the chromosomes using a measure of distance from the selection criteria (e.g. the user specifies the objective: minimization of the second central moment of input spectra for dispersion and/or first central moment from median)
c. Selection of parent chromosomes based on 'survival of the fittest' and reproducing the offspring chromosomes through crossover and mutation
d. Evaluating the fitness of the next generation
e. Repeating for a number of generations until satisfactory adaptation of individuals is achieved

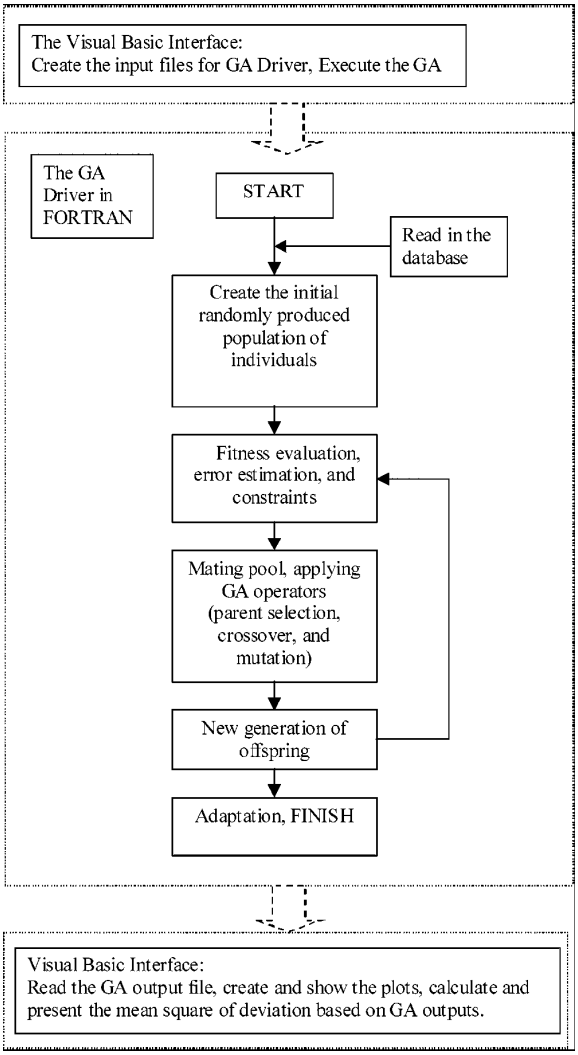

Figure 2. Program flowchart.

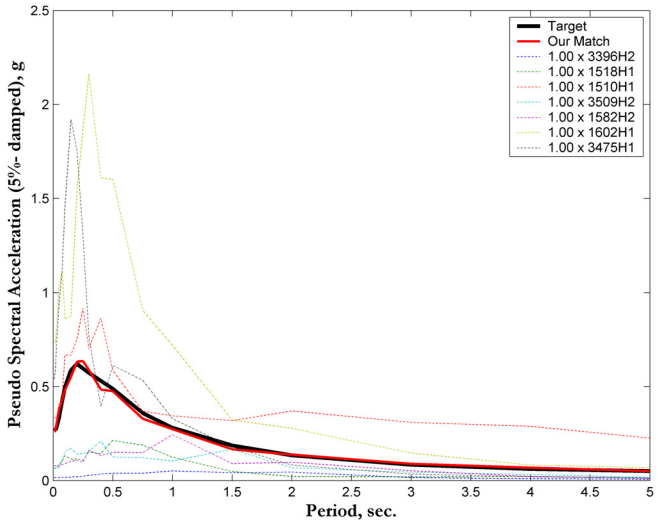

Figure 3: Selection without scaling that aims to minimize the average distance to target, without constraints on the dispersion.

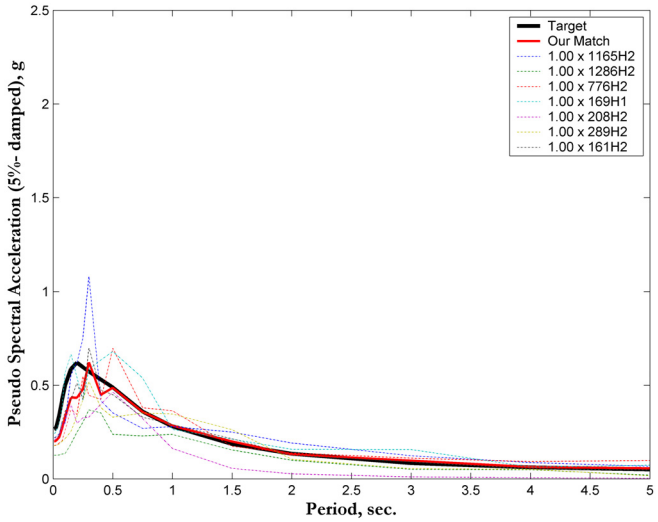

Figure 4: Selection without scaling that aims to minimize both the average distance to target and the dispersion.

A.1.6 Method 302: Semi-Automated Selection & Scaling to Match CMS

Semi-Automated Selection and Scaling

Author(s) of Synopsis: A. Kottke, E. Rathje, and J. Watson-Lamprey **Date**: 9 November 2006

Reference(s):

Kottke, Albert and E. Rathje (2008)

Objective: To obtain a set of ground motion seismograms for nonlinear dynamic structural analysis that will result in an accurate estimate of the cumulative distribution function (CDF) (for Methods #1 & 3) and the median (for Methods #2 & 4) of the engineering demand parameter (EDP) of interest for a given elastic response spectra.

Brief Description/Example:

A semi-automated approach for the selection and scaling of acceleration-time series was developed by Kottke and Rathje (2008). This method selects and scales a suite of acceleration-time series to fit a user-defined target response spectrum, while at the same time the procedure controls the variability within the ground motion suite. This procedure involves a two-step process to develop scale factors. First, an average scale factor is determined and applied to each motion to achieve an overall match to the target spectrum. Next, a second scale factor is derived for each motion that modifies the standard deviation within the suite.

The procedure starts by searching for a complementary set of motions, whose collective average spectral shape is similar to the target spectrum. An average scale factor (s_{avg}) is determined by minimizing the difference between the natural log of the target spectrum and the average natural log of the spectra of the individual time series, using:

$$\ln s_{avg} = \frac{1}{n_p} \sum_{j=1}^{n_p} \left[\ln\left(Sa_{target,Tj}\right) - \frac{1}{n_m} \sum_{i=1}^{n_m} \ln\left(Sa_{i,Tj}\right) \right] \qquad (3\text{-}4)$$

where n_p is the number of periods, n_m is the number of time series, $Sa_{target,Tj}$ is the target spectral acceleration at the j-th period, and $Sa_{i,Tj}$ is the spectral acceleration of the i-th time series at the j-th period. Each individual time series is then individually scaled by a second factor ($s2_i$) to achieve the desired variability within the suite. The total factor applied to each time series (SF_i) is:

$$\ln SF_i = \ln s_{avg} + \ln s2_i$$

There are two approaches to develop the second, motion-specific scale factor: the accordion method and the centroid method.

The accordion method calculates the second scale factor using a parameter, z, defined for each motion as the mean of the natural logs of response spectra for each motion subtracted from the mean natural log of the response spectra for the suite. These factors have a mean close to zero and, therefore, do not affect the amplitude of the average, scaled response spectrum when added to $\ln s_{avg}$. An influence factor, α, is applied to each of the scale factors and adjusted until the standard deviation of the suite matches the target standard deviation. The second scale factor derived from the accordion method is:

$$\ln s2_i = \alpha \cdot z_i = \alpha \cdot \frac{1}{n_p} \sum_{j=1}^{n_p} \left[\ln\left(Sa_{i,Tj}\right) - \frac{1}{n_m} \sum_{i=1}^{n_m} \ln\left(Sa_{i,Tj}\right) \right]$$

In the centroid method, the second scale factors are created by partitioning the unit normal distribution into equal probability sections with the number of sections equal to the number of motions in the suite. The second scale factors are derived from the locations of the centroid for each of the sections (ε_i). Motions are paired with an ε by ranking the motions by the average unscaled Sa over all periods, with the smallest motion being paired with the smallest ε. The standard deviation of the suite is adjusted to fit the target standard deviation by scaling these centroid locations (ε_i) by a scale factor (α) – effectively adjusting the standard deviation used in calculation of the ε values. The second scale factor derived from the centroid method is:

$$\ln s2_i = \alpha \cdot \varepsilon_i$$

A.1.7 Methods 303: Design Ground Motion Library (DGML) — Objectives 4

Application of DGML to Select Ground Motions for Nonlinear Structural Analysis

Author(s) of Synopsis: Gang Wang, Maury Power, Robert Youngs
AMEC Geomatrix Consultants

Date: 19 September 2008

Introduction to DGML

The Design Ground Motion Library (DGML) is a software package for searching for ground motion time histories suitable for use by engineering practitioners for the time history dynamic analysis of various facility types in California and other parts of the western United States. The DGML was developed in a project sponsored jointly by the California Geological Survey-Strong Motion Instrumentation Program (CGS-SMIP) and the Pacific Earthquake Engineering Research Center-Lifelines Program (PEER-LL). The project was carried out by a multidisciplinary project team of practitioners and researchers in structural engineering, geotechnical engineering, and seismology. The software package includes a database of ground motion records and a software tool for selecting, scaling, and evaluating time histories for applications. The DGML is currently on a DVD, and consideration is being given to converting the DGML to internet web-based usage. The ground motion database used in the DGML consists of the PEER-NGA data base created for the Next Generation of Attenuation (NGA) relationships project. The DGML is documented and supported by a Users Manual and a report.

The DGML has the broad capability to search for ground motion time history records on the basis of (1) the response spectral shape of the records in comparison to design or target response spectra and (2) other characteristics of the records. A key capability of the DGML software tool is searching for and ranking time history records on the basis of the degree of match of the response spectral shapes of the time histories with design or target spectra over a user-specified period range. To support this capability, the software tool can construct design or target spectra using different approaches. The user can also constrain searches for records by specifying search criteria, including, as desired: ranges of earthquake magnitude; type of faulting; ranges of distances from earthquake source to recording station; ranges of recording station site shear wave velocity in the upper 30 meters, Vs30; ranges of significant duration for records; presence of pulses in near-fault records; direction of horizontal component of records (fault-strike-normal (FN) direction, fault-strike-parallel (FP) direction, either FN or FP direction, or two-component pairs in FN and FP directions); and ranges of acceptable scaling factors for scaling records to the level of the target spectrum. The software tool includes a graphic interface for data input, processing, and plotting of target response spectra, spectra of individual or multiple time histories, and average spectra for selected time histories. In addition, acceleration, velocity, and displacement time histories can be plotted for the selected time histories.

Using the DGML, sets of time histories were developed for two different objectives. Method 303 selects sets of records to match the conditional mean spectrum (objective 4). In method 304, the DGML software package was modified to select a set of records that approximately match the distribution about the conditional mean spectrum (objective 3).

Method Objective: Match the Conditional Mean Spectrum

The median response of the engineering demand parameter can be estimated if the records are selected only to match the conditional mean spectrum using the unmodified DGML software package. The selection procedure of Method 303 is summarized as follows:

Selection Procedure:

1) The DGML package is used to identify records within a user-specified M-R bin that includes the given M, R and fault type (Figure 1). For example, in developing ground motion sets for building C, the data-bin contains records of M>=6.0, R=0-50 km, and all types of faults, resulting in a total of 1476 records (either FN or FP component) within the bin.

2) Scale (in amplitude only) the response spectrum of gathered records in the bin to the level of the given first-mode spectral acceleration $Sa(T_1)$, so each spectrum matches the target value at the given period. For building C, T_1 is known as 2.63 sec.

3) We calculated the mean squared error (MSE) of all records within M-R bin against the target conditional mean spectrum (see Equation 1) using DGML, and ranked them in ascending order of MSE over a specified period range of interest. We specified the period range to extend from the third mode period, T_3, to two and half times the first mode period, $2.5T_1$. In the building C example, the period range of interest is from 0.46-6.58 sec. We applied twice as much weight over the longer period range [T_1-$2.5T_1$] as the weight over the shorter period range [T_3 -T_1] to favor a better spectrum match over the long period range. The spectra of the best 28 records are compared in Figure 2 with the target spectrum. We grouped the 7 smallest MSE records into the first sub-group, and so on (see Figure 3). Each sub-group can be used to estimate median EDP.

Equation 1. The mean squared error (MSE) between the target spectrum and the response spectrum of a recorded time history is computed in terms of the difference in the natural logarithm of spectral acceleration. The periods are discretized as equally spaced in natural logarithm scale, with 100 points per period decade. The target and record response spectra are interpolated to provide spectral accelerations at each discrete period point. MSE is calculated as follows:

$$MSE = \frac{\sum_i w(t_i)\left[\ln\left\{SA^{target}(t_i)\right\} - \ln\left\{f \times SA^{recording}(t_i)\right\}\right]^2}{\sum_i w(t_i)}$$

where the summation is made for all discrete period points that are within the specified period range of interest. Parameter *f* is a linear scale factor applied to the entire response spectrum of the recording. By scaling the spectrum of records to the level of the target spectrum at the given first-mode spectral acceleration, the scaling factor is simply $f = SA^{target}(T_1)/SA^{recording}(T_1)$. Parameter w(ti) is a weight function that allows the user to assign relative weights to different parts of the period range of interest.

References:

"Design Ground Motion Library" (2008), Final Report Prepared for California Geological Survey – Strong Motion Instrumentation Program, and Pacific Earthquake Engineering Research Center – Lifelines Program. AMEC Geomatrix Consultants.

Youngs R.R., Power M.S., Wang G., Makdisi F., Chin C.C. (2007). "Design Ground Motion Library (DGML) – Tool for Selecting Time History Records for Specific Engineering Applications (Abstract)," *Proceedings of SMIP07 Seminar on Utilization of Strong-motion Data*, Sacramento, CA.

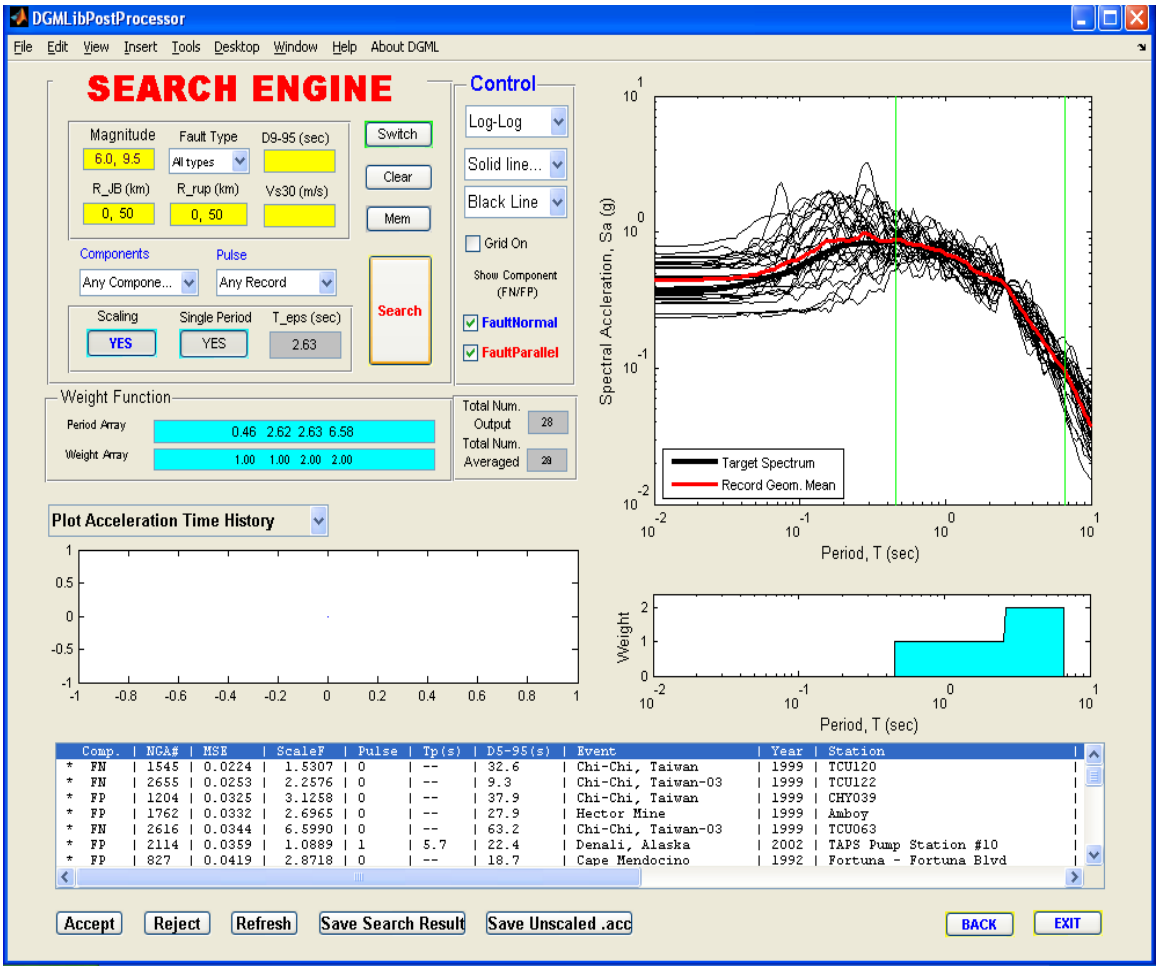

Figure 1. Search Engine Interface from DGML Software (Method 303, Building C)

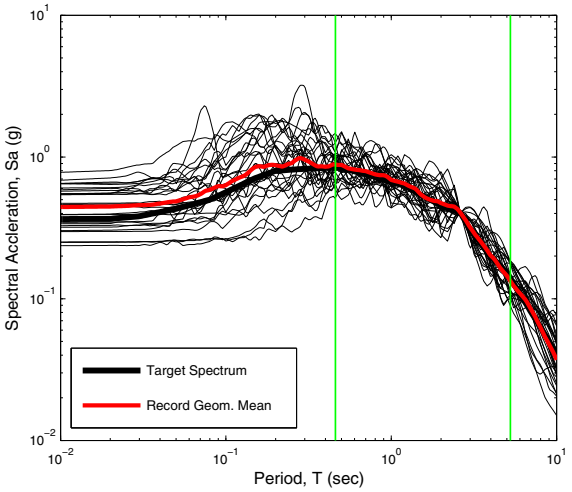

Figure 2 Mean of selected 28 Records vs Conditional Mean Target Spectrum (Method 303, Building C)

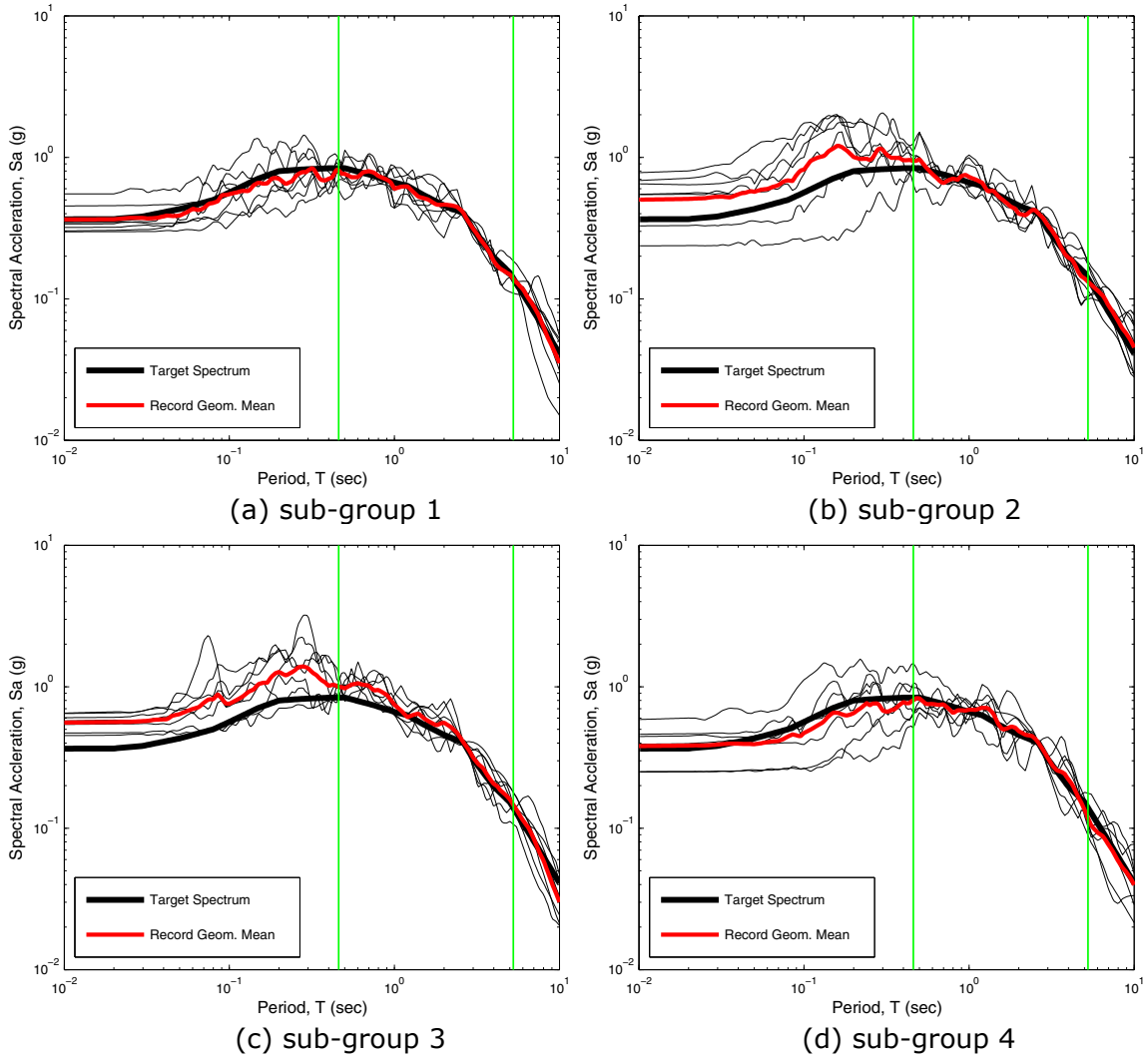

Figure 3. Dividing the Selected Records into 4 sub-groups of 7 records according to MSE Ranking (Method 303, Building C)

304: Design Ground Motion Library (DGML) — Objective 3

Application of DGML to Select Ground Motions for Nonlinear Structural Analysis

Author(s) of Synopsis: Gang Wang, Maury Power, Robert Youngs
AMEC Geomatrix Consultants
Date: 19 September 2008

Method Objective: **Match the Distribution about the Conditional Mean Spectrum**

A modified application of the DGML software package was used to obtain a set of ground motion acceleration time histories for nonlinear dynamic structural analysis that will result in an estimate of the cumulative distribution function (CDF) and the median of the engineering demand parameter (EDP) of interest for a given structure, earthquake magnitude (M), source-to-site distance (R), site classification (S), and a given first-mode spectral acceleration $Sa(T_1)$. For the method application, the DGML was modified to provide a set of records that would approximately match the distribution about the conditional mean target spectrum. This method provides a set of 28 records that matches the distribution about the conditional mean target spectrum for each building. The set of 28 records is used to estimate the cumulative distribution of the engineering demand parameter. The set of 28 records is further divided into 4 sets of 7 records sequentially, where each set can be used to estimate the median response of the engineering demand parameter. It is noted that Method 304 mainly aims at estimating the CDF of the EDP. It is recommended to use Method 303 if the main objective is to estimate the median of the EDP. In the following section, we illustrate the selection procedure using building C as an example.

Selection Procedure:

1) The DGML package is used to identify records within a user-specified M-R bin that includes the given M, R and fault type. For example, in developing ground motion sets for building C, the data bin contains records of M=6.0-7.5, R=0-30 km, and strike-slip faults, resulting in a total of 234 records (either FN or FP component) within the bin.

2) Scale (in amplitude only) the response spectrum of gathered records in the bin to the level of the given first-mode spectral acceleration $Sa(T_1)$, so each spectrum matches the target value at the given period. For bldg C, T_1 is known as 2.63 sec.

3) To capture the variability of record distribution, we calculate the theoretical conditional mean and conditional mean standard deviation (eg. see Equation 1) at a period T that is well away from T_1 (approximately 0.1 T_1). A given number of log-normally distributed points are randomly generated based on the theoretical distribution. For building C, we generated 28 points that are randomly distributed at T=0.26 sec according to the conditional mean and conditional mean standard deviation.

4) For each point of the distribution, select one scaled record within the data-bin that has Sa(T) closest to that point, which will result in a group of 28 records. Visually inspect the mean and distribution of the selected records against the theoretical

calculation to assess the reasonableness of the match. By repeating steps (3) and (4), one can select the realization that appears to best match the distribution over the full period range (see Figures 1 and 2).

5) We calculated the mean squared error (MSE) of the selected 28 records against the target conditional mean spectrum (see Equation 2) using DGML, and ranked them in ascending order of MSE over a specified period range of interest. We specified the period range to extend from the third mode period, T_3, to twice the first mode period, $2T_1$. In the building C example, the period range of interest is from 0.46-5.26 sec, and we applied equal weight over the period range. The 28 records can be further divided into 4 sub-groups of 7 records. We grouped the 7 smallest MSE records into the first sub-group, and so on (see Figure 3). Each sub-group can be used to estimate median EDP, and the combined group of 28 can be used to estimate CDF.

The records selected from the proposed method have the targeted Sa value at first mode period T_1, and they approximate the theoretical Sa distribution at other periods. So the selected records can be used in the analysis to estimate the median and cumulative distribution of the engineering demand parameter.

Equation 1. The theoretical conditional mean and conditional standard deviation of $\ln S_a(T_2)$ at period T_2, given $\ln S_a(T_2)$, can be calculated from the following equations (Baker and Cornell, 2005)

$$\mu_{\ln S_a(T_2)\,|\,\ln S_a(T_1)=x} = \mu_{\ln S_a(T_2)} + \rho_{\ln S_a(T_1),\ln S_a(T_2)} \cdot \sigma_{\ln S_a(T_2)} \cdot \varepsilon_{T_1}$$

$$\sigma_{\ln S_a(T_2)\,|\,\ln S_a(T_1)=x} = \sigma_{\ln S_a(T_2)} \sqrt{1 - \rho^2_{\ln S_a(T_1),\ln S_a(T_2)}}$$

where $\mu \ln S_a(T_2)$and $\sigma 1 \ln S_a(T_2)$ are the mean and standard deviation of the spectrum distribution that can be obtained from NGA models, and $\rho 1 \ln S_a(T_1)$,$1 \ln S_a(T_2)$ is the correlation coefficient that can be obtained from Baker and Jayaram (2008).

Equation 2. The mean squared error (MSE) between the target spectrum and the response spectrum of a recorded time history is computed in terms of the difference in the natural logarithm of spectral acceleration. The periods are discretized as equally spaced in natural logarithm scale, with 100 points per period decade. The target and record response spectra are interpolated to provide spectral accelerations at each discrete period point. MSE is calculated as follows:

$$MSE = \frac{\sum_i w(t_i)\left[\ln\left\{SA^{target}(t_i)\right\} - \ln\left\{f \times SA^{recording}(t_i)\right\}\right]^2}{\sum_i w(t_i)}$$

where the summation is made for all discrete period points that are within the specified period range of interest. Parameter *f* is a linear scale factor applied to the entire response spectrum of the recording. By scaling the spectrum of records to the level of the target spectrum at the given first-mode spectral acceleration, the scaling factor is simply $f = SA^{target}(T_1)/SA^{recording}(T_1)$. Parameter w(ti) is a

weight function that allows the user to assign relative weights to different parts of the period range of interest.

References:

"Design Ground Motion Library" (2008), Final Report Prepared for California Geological Survey – Strong Motion Instrumentation Program, and Pacific Earthquake Engineering Research Center – Lifelines Program. AMEC Geomatrix Consultants.

Youngs R.R., Power M.S., Wang G., Makdisi F., Chin C.C. (2007). "Design Ground Motion Library (DGML) – Tool for Selecting Time History Records for Specific Engineering Applications (Abstract)," *Proceedings of SMIP07 Seminar on Utilization of Strong-motion Data*, Sacramento, CA.

Baker J.W, Cornell C.A. (2005). "A Vector-Valued Ground Motion Intensity Measure Consisting of Spectral Acceleration and Epsilon", *Earthquake Engineering and Structural Dynamics*, 34: 1193-1217.

Baker J.W. and Jayaram N. (2008). "Correlation of spectral acceleration values from NGA ground motion models", *Earthquake Spectra*, 24 (1), 299-317.

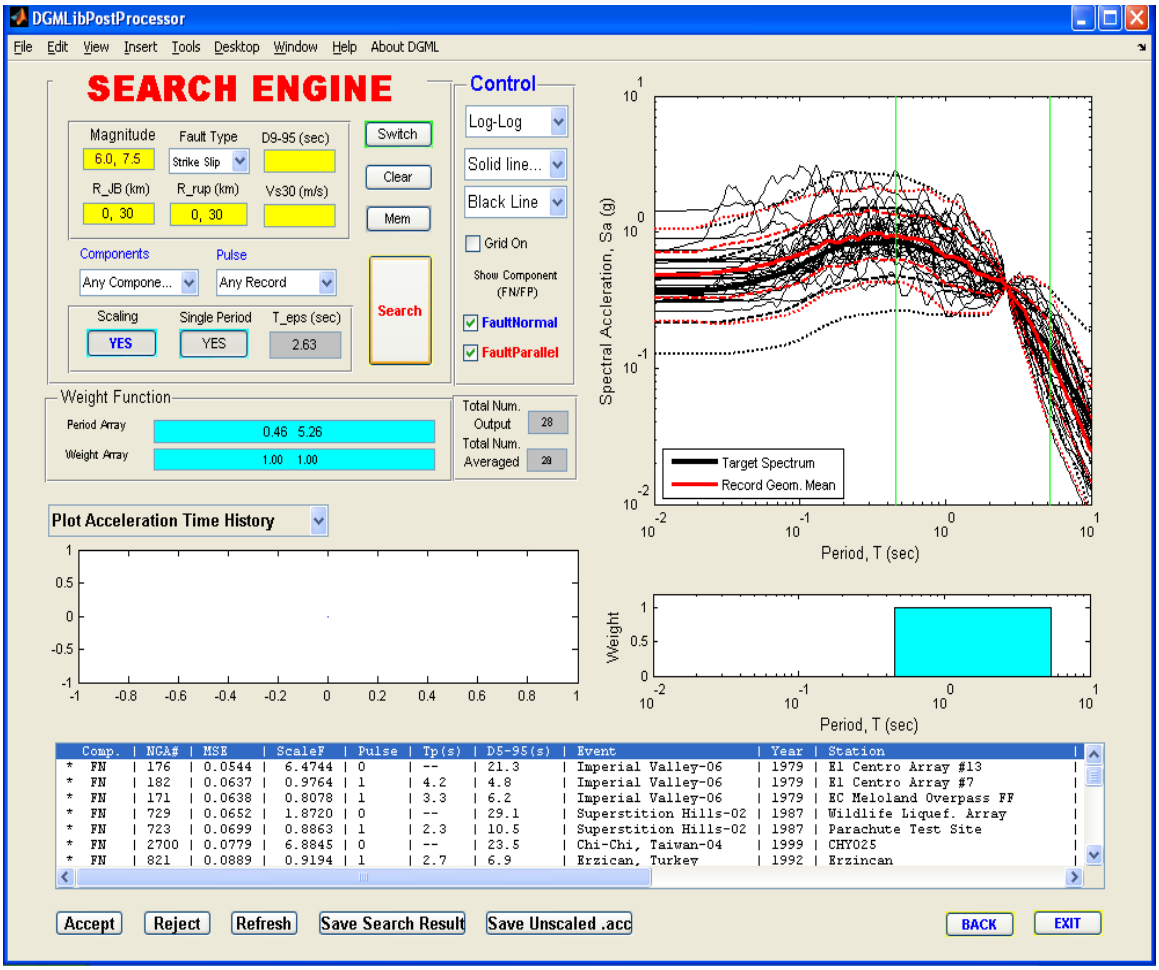

Figure 1. Search Engine Interface from DGML Software (Method 304, Building C)

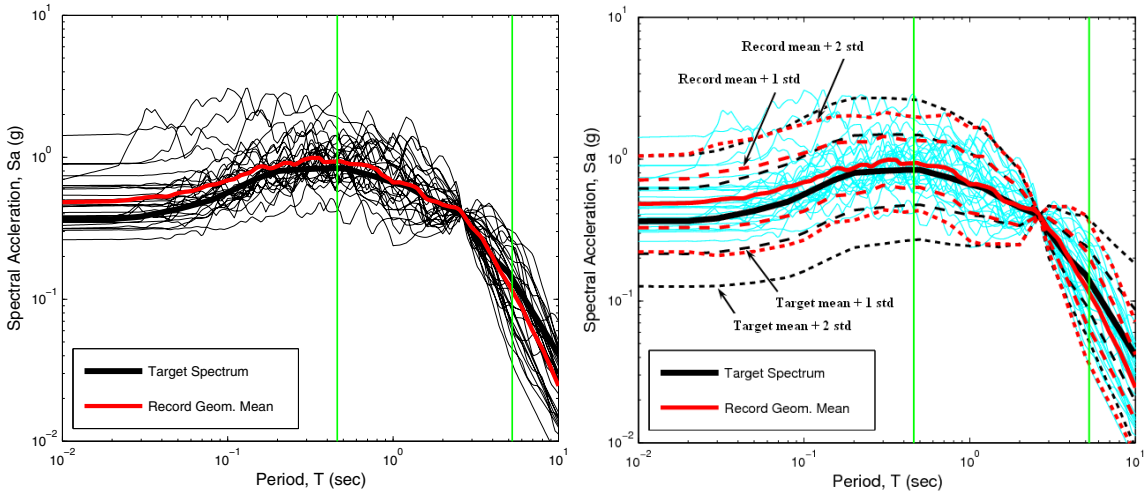

Figure 2. Comparison of the Distribution of Selected Records vs Conditional Mean Target Spectrum (Method 304, Building C)

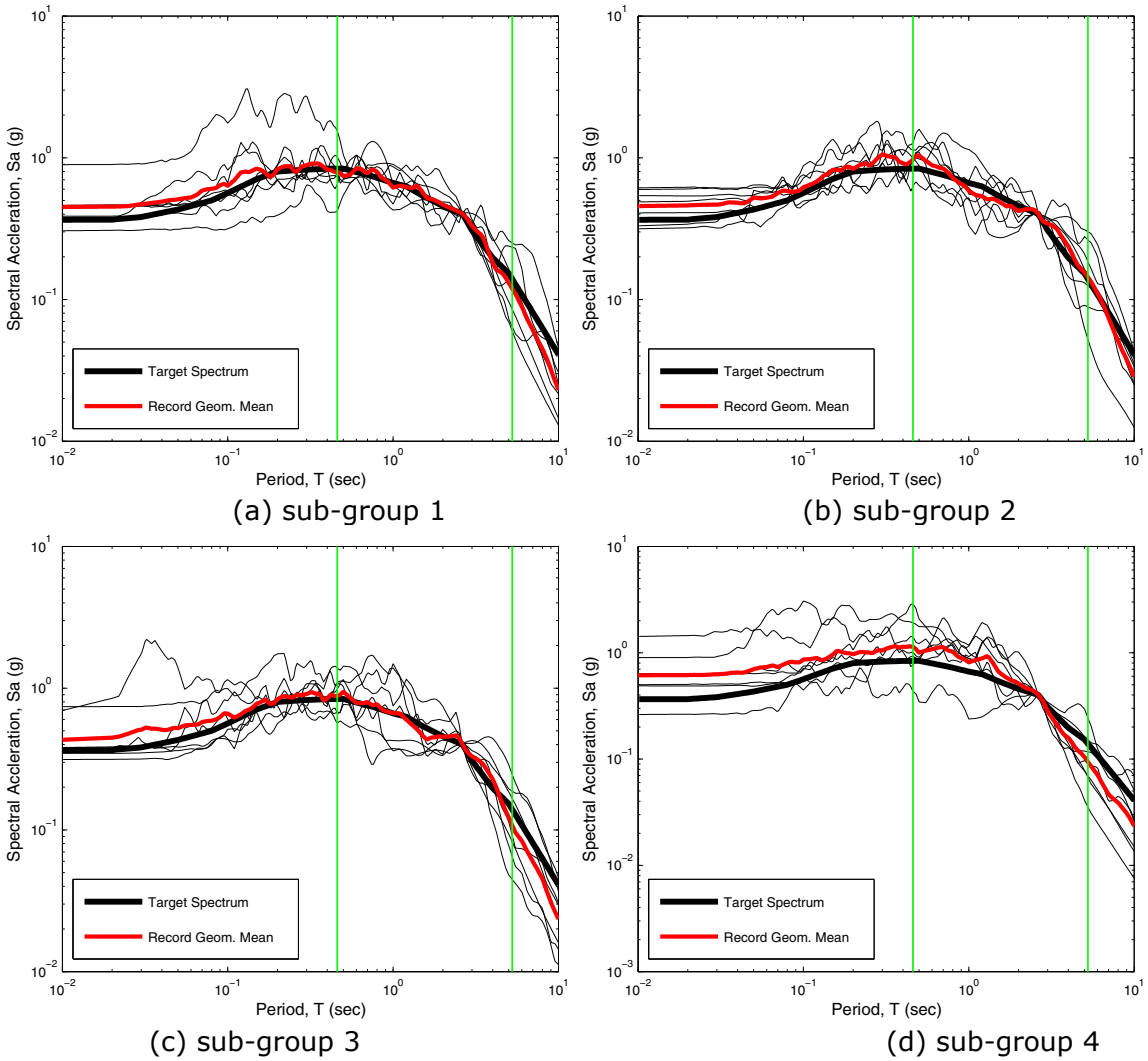

Figure 3. Dividing the Selected Records into 4 sub-groups of 7 records according to MSE Ranking (Method 304, Building C)

A.1.9 Method 400: Target Spectrum Based on Epsilon Correlations

Ground Motion Selection and Modification (GMSM) Method: Selection based on M, r and ε

Authors of Synopsis: Christine Goulet, UCLA
Jonathan Stewart, UCLA
Brian Skyers, Skyers and Associates.

Date: February 4th 2008

References:

Baker, J. W., and C. A. Cornell (2005). "A vector-valued ground motion intensity measure consisting of spectral acceleration and epsilon", Earthquake Eng. Struct. Dyn., 34(10), 1193–1217.

Goulet, C. (2008) "Improving the Characterization of Seismic Hazard for Performance-Based Earthquake Engineering Design" PhD Dissertation, Dept. of Environmental and Civil Eng., University of California, Los Angeles, California.

Goulet, C.A., Haselton, C.B., Mitrani-Reiser, Beck, J.L., Deierlein, G., Porter, K.A., Stewart, J.P. (2007) "Evaluation of the Seismic Performance of a Code-Conforming Reinforced-Concrete Frame Building - From Seismic Hazard to Collapse Safety and Economic Losses." *Earthquake Engineering and Structural Dynamics*, 36(13), 1973-1997.

Goulet, C.A., Haselton, C.B., Mitrani-Reiser, J., Deierlein, G., Stewart, J.P., Taciroglu, E. (2006) "Evaluation of the Seismic Performance of a Code-Conforming Reinforced-Concrete Frame Building - Part I: Ground Motion Selection and Structural Collapse Simulation." *8th National Conference on Earthquake Engineering (8NCEE)*. San Francisco, California: April 18-22, 2006.

General Objective

The objective of this method is to determine the probability density function (PDF) (or alternatively, the median) of MIDR from a limited number of ground motion records. The records are selected so that they are consistent with the disaggregation of hazard at the site of interest (or, in this case, match a deterministic scenario). The selection method utilizes metadata such as magnitude, rupture distance, site properties, etc. and ε as a proxy for spectral shape to improve the accuracy of structural response predictions.

Selection Method Description

Starting from a structure and a location (with site characteristics), define a target earthquake scenario (*M, r,* ε) based on the disaggregation results at the structure's first mode period (T_1). Alternatively, a deterministic scenario can also be defined. The disaggregation results generally provide information on the contribution of: magnitude, distance, ε, style of faulting (often as a list of contributing faults, from which the style of faulting is determined) and directivity.

The first step is to define the target magnitude-distance. It can be taken as the mode when a mode clearly dominates the hazard or two different magnitude-distance targets when the hazard is bi-modal. Then the other parameters associated with the magnitude-distance target(s) are defined: ε, style of faulting and directivity.

Procedure: The selection procedure is applied to an earthquake record database, such as the PEER NGA ground motion database (http://peer.berkeley.edu/nga/).

1. Constrain the usable periods (frequency bandwidth) to cover a range extending at least up to 1.5 T_1 (where T_1 = first mode period of the structure). Reject all the records that do not meet this criteria
2. Compute ε for the period of interest (T_1) for each record. Separate the ε values in bins, where $\Delta\varepsilon$ is the difference between the computed ε and the target defined by the scenario. The $\Delta\varepsilon$ bins are defined as:
   a. $(\Delta\varepsilon)_1 \leq 0.5$
   b. $0.5 < (\Delta\varepsilon)_2 \leq 1.0$
   c. $1.0 < (\Delta\varepsilon)_3$

1. Sort the data according to magnitude M bins and reject records with M significantly distinct from the target. The difference between the target and actual magnitude, ΔM, is binned, and the following bins are considered:
    a. $(\Delta \mathrm{M})_1 \leq 0.25$
    b. $0.25 < (\Delta \mathrm{M})_2 \leq 0.5$
2. Sort the data according to rupture distance (r) and reject records with r significantly distinct from the target. The following bins are considered, where Δr is the difference between the target and actual site-source distance:
    a. $(\Delta r)_1 \leq 10\text{km}$
    b. $10\text{ km} < (\Delta r)_2 \leq 20\text{km}$
    c. $20\text{ km} < (\Delta r)_3 \leq 30\text{km}$
3. Sort the data according to V_{s30} and reject records with V_{s30} significantly distinct from the target. The following bins are considered, where ΔV_{s30} is the difference between the target and actual V_{s30} parameter:
    a. $(\Delta V_{s30})_1 \leq 75$ m/s
    b. $75\text{ m/s} < (\Delta V_{s30})_2 \leq 150$ m/s
4. Sort the data according to the style of faulting using the following bins:
    a. Matches the style of faulting
    b. Does not match the style of faulting
5. Constrain the earthquake events so that not one event is over-represented in the selected motions (i.e. whenever possible, pick motions from different earthquake events).
6. Supplemental (often optional) parameters:
    a. Directivity (using directivity parameters Sommerville et al. 1997 or similar)
    b. Basin depth

Ideally, records that are simultaneously in the first bin for each parameter should be selected. Given the limited size of the strong motion database, this is often impossible. One has to apply judgment in relaxing some parameters and selecting records. With this method, the priority is given to matching ε closely, as long as the M, r and V_{s30} parameters are contained within one of the bins. From this subset, while making informed choices on the other parameters, the analyst must attempt to diversify the earthquake events so that a single event does not control the final selection. This is done to reduce bias that could come from one specific and potentially peculiar earthquake. If there are a sufficient number of records left in this subset, the user would ideally try to match the style of faulting, the directivity (in the case of relatively short distances) and other parameters. The priority given to each parameter may depend on the specifics of the scenario and is something that has to be evaluated on a case-by-case basis. In its present form, this method is not automated, and hence requires a lot of manipulations and judgment. Ultimately, the goal is to develop a set of database-enabled tools to facilitate the selection and to limit human intervention in the selection process.

A.1.10 Methods 401: ε Selection with $S_{de}(T_1)$ Scaling

Ground Motion Selection and Modification (GMSM) Method: "Advanced *IM* selection and scaling Method"

Author(s) of Synopsis: Polsak Tothong of AIR Worldwide Corporation
Nicolas Luco of USGS

Date: 18 October 2007

References:

Tothong, P. and Luco, N. (2007), "Probabilistic seismic demand analysis using advanced ground motion intensity measures," *Earthquake Engineering & Structural Dynamics*, **36**(13): 1837-1860.

Luco, N., and Cornell, C. A. (2007), "Structure-specific scalar intensity measures for near-source and ordinary earthquake ground motions," *Earthquake Spectra*, **23**(2): 357-392.

Tothong, P. and Cornell, C.A. (2006), "Probabilistic seismic demand analysis using advanced ground motion intensity measures, attenuation relationships, and near-fault effects," Pacific Earthquake Engineering Research Center, PEER Report 2006/11. University of California: Berkeley, CA. 2007; 205 pp.

Objective: To obtain a set of ground motion records for nonlinear dynamic analysis that will result in an accurate estimate of the cumulative distribution function (CDF) (for Method #3) and the median (for Method #4) of the engineering demand parameter (EDP) of interest for a given structure, earthquake magnitude (M_w), source-to-site distance (R), site classification, and a level of $S_{de}(T_1)$. *IM* used in this method refers to S_{de}, S_{di} and $IM_{1I\&2E}$.

Brief Description/Example:

<u>*Procedure for Method #3*</u>: To determine probability distribution function (PDF) of EDP (f_{EDP}) or the median (i.e., geometric mean) values

For given earthquake ground motion properties, e.g., M_w, R, soil type, faulting style, etc. and a level of $S_{de}(T_1)$

1. Determine the PDF of the *IM* (i.e., S_{de}, S_{di} or $IM_{1I\&2E}$) for the target earthquake scenario, i.e., the mean and standard deviation of ln*IM* (denoted $\mu_{\ln IM}$ and $\sigma_{\ln IM}$, respectively).
2. Divide the PDF of *IM* into a small number of bins, for example, seven.
   2.1. This step can be simplified by using Table 1 as guidance to assign the number of records into each bin. Then the range (or reference value) of ln*IM* in each bin is simply $\varepsilon_{\ln IM} \cdot \sigma_{\ln IM} + \mu_{\ln IM}$.
   2.2. Selection:
      2.2.1. For S_{de} (optional for S_{di} and $IM_{1I\&2E}$), select ground motions that have $\varepsilon_{\ln IM}$ close to the reference $\varepsilon_{\ln IM}$ of each bin with $\Delta\varepsilon$ of 0.5 or less.
   2.3. Scaling:
      2.3.1. Scale records to the ln*IM* values of each bin. For simplicity, just scale records to the reference *IM* value (i.e., exp(ln*IM*) determined in step 2.1) of each bin.
3. Simply perform nonlinear dynamic analyses of the records chosen above

<u>*Procedure for Method #4*</u>: To determine the median value of EDP using the first-order Taylor's series approximation

For given earthquake ground motion properties, e.g., M_w, R, soil type, faulting style, etc. and a level of $S_{de}(T_1)$

1. Determine the target median (i.e., geometric mean) value of the *IM* for the given earthquake scenario and level of $S_{de}(T_1)$.
2. Selection:
   2.1. For S_{de} (optional for S_{di} and $IM_{1I\&2E}$), select ground motions that have $\varepsilon_{\ln IM}$ close to that of the target median *IM* value.

1. Scale records to the median *IM* value.
2. Simply perform nonlinear dynamic analyses of the scaled records to determine the median value of EDP

Table 1. Example number of records in each bin

range $\varepsilon_{\ln IM}$	reference $\varepsilon_{\ln IM}$ value	probability	#records (9)	#records (28)	#records (40)	#records (192)
-0.5 - 0.5	0	0.384	3	10	16	74
0.5 - 1.5	1	0.242	2	7	10	46
1.5 - 2.5	2	0.060	1	2	2	12
2.5+	3	0.006	0	0	0	1

This methodology can also be used with a ground motion hazard curve encompassing multiple earthquake scenarios (i.e., not only for a specified M_w, R, $S_{de}(T_1)$ scenario). The users simply need to difference the ground motion hazard curve to obtain a probability density-like function. We can then bin the data in a fashion similar to that shown above.

It should be noted that when using S_{di} and $IM_{1I\&2E}$ this method is expected to work with near-source pulse-like ground motions as shown in Tothong and Luco (2007), Luco and Cornell (2007), and Tothong and Cornell (2006).

A.1.11 Methods 402: ATC-63 Method Applied to MIDR — Far-Field Set

Name for Ground Motion Selection and Scaling Method: "ATC-63 Method Applied to MIDR"

Date: 20 November 2008

Authors of Method: Curt B. Haselton, PhD, PE, California State University, Chico (synopsis author)
Charles Kircher, PhD, PE, SEBC, Kircher and Associates, Palo Alto, CA

Reference:

Haselton, C.B., J.W. Baker, A.B. Liel, and G.G. Deierlein (2008). "Accounting for Expected Spectral Shape (Epsilon) in Collapse Performance Assessment," *American Society of Civil Engineers Journal of Structural Engineering, Special Publication of Ground Motion Selection and Modification* (submitted).

Applied Technology Council (ATC) (2008). *Recommended Methodology for Quantification of Building System Performance and Response Parameters*, ATC-63 (90% Draft), Applied Technology Council, Redwood City, CA.

Objective:

The objective of the overall ATC-63 approach is to develop sets of strong ground motions (i.e. a Near-Field set and a Far-Field set) appropriate for collapse evaluation of structural systems using incremental dynamic analysis (IDA) methods. Records should be consistent (to the extent possible) with the ground motion requirements of Section 16.1.3.2 of ASCE7-05 (ASCE 2006). In this study, the general ATC-63 approach (which focuses on collapse) is adapted to be applicable for predicting median MIDR (Objective 4).

In ATC-63, it is desired that the record sets be generically applicable, independent of site, ground motion hazard-level, and structure type (e.g. building fundamental period). In addition, this set must contain strong motions (so the scaling is minimized), and include a large number of records so that predictions are statistically robust. Since the set must be independent of the building period and site, the set was selected without regard to spectral shape or ε. To account for the effects that ε has on the collapse fragility, Haselton (Haselton 2008 and 2006; ATC 2008, Appendix B) developed a post-processing correction procedure that can be used in combination with the ATC-63 ground motion sets. This post-processing correction procedure is utilized in the overall ATC-63 method, and is adapted here for use in predicting median MIDR response.

Brief Description:

Selection Criteria (consistent with ATC 2008):

1. Source Magnitude – M > 6.5
2. Source Type – Strike-slip and reverse (thrust) sources
3. Site Conditions – Soft-rock (Site Class C) and stiff soil (Site Class D)
4. Site-Source Distance – R > 10 km for the far-field set and R < 10 km for the near-field set (R is the average of Joyner-Boore and Campbell distances)
5. Number of Records per Event – Not more than two records per event (records with largest PGV when more than two are available)
6. Strong Ground Motion Records – Peak ground acceleration (PGA) > 0.2g and peak ground velocity (PGV) > 15 cm/sec
7. Strong Motion Instrument Capability – Lowest useable frequency < 0.25 Hz
8. Strong-Motion Instrument Location – Free-field or ground floor of a small building

Scaling Procedure (modified from ATC 2008):

This method uses basic amplitude scaling of each individual record to the target value of $Sa(T_1)$. Note that the overall ATC-63 method (ATC 2008) involves a more complex scaling method, which is not employed in this modified method.

Outline of Approach (modified from ATC 2008):

1. Use either the far-field set (44 records) or near-field set (56 records), based on selection criteria above.
2. Amplitude scale each ground motion to the target $Sa(T_1)$ value for the ground motion scenario of interest.
3. Perform nonlinear dynamic structural analyses using the scaled ground motions, and record the MIDR value (or any other EDP value of interest) for each ground motion record.
4. In order to correct the predictions for spectral shape, perform a linear regression analysis between the logarithm of MIDR (or any other EDP value of interest) and $\varepsilon(T_1)$, as shown in the following equation.
   $$LN[MIDR] = \beta_0 + \beta_1 * \varepsilon(T_1)$$
5. Now, solve the above equation by substituting the $\varepsilon(T_1)$ value from the ground motion scenario of interest. The resulting MIDR value is the median prediction for Objective 4.

References:

American Society of Civil Engineers. (2005). ASCE7-05: Minimum Design Loads for Buildings and Other Structures, Reston, VA.

Haselton, C.B. (2006). *Assessing Seismic Collapse Safety of Modern Reinforced Concrete Moment Frame Buildings*, Ph.D. Dissertation, Dept. of Civil and Environmental Engineering, Stanford University.

A.1.12 Methods 402: ATC-63 Method Applied to MIDR — Near-Field Set

The summary for this method is contained within the summary in section A.1.11 above.

A.1.13 Methods 500: $S_{di}(T_1,d_y)$ Scaling

Ground Motion Selection and Modification (GMSM) Method: "Advanced *IM* selection and scaling Method"

Author(s) of Synopsis: Polsak Tothong of AIR Worldwide Corporation
Nicolas Luco of USGS

Date: 18 October 2007

References:

Tothong, P. and Luco, N. (2007), "Probabilistic seismic demand analysis using advanced ground motion intensity measures," *Earthquake Engineering & Structural Dynamics*, **36**(13): 1837-1860.

Luco, N., and Cornell, C. A. (2007), "Structure-specific scalar intensity measures for near-source and ordinary earthquake ground motions," *Earthquake Spectra*, **23**(2): 357-392.

Tothong, P. and Cornell, C.A. (2006), "Probabilistic seismic demand analysis using advanced ground motion intensity measures, attenuation relationships, and near-fault effects," Pacific Earthquake Engineering Research Center, PEER Report 2006/11. University of California: Berkeley, CA. 2007; 205 pp.

Objective: To obtain a set of ground motion records for nonlinear dynamic analysis that will result in an accurate estimate of the cumulative distribution function (CDF) (for Method #3) and the median (for Method #4) of the engineering demand parameter (EDP) of interest for a given structure, earthquake magnitude (M_w), source-to-site distance (R), site classification, and a level of $S_{de}(T_1)$. *IM* used in this method refers to S_{de}, S_{di} and $IM_{1I\&2E}$.

Brief Description/Example:

<u>*Procedure for Method #3*</u>: To determine probability distribution function (PDF) of EDP (f_{EDP}) or the median (i.e., geometric mean) values

For given earthquake ground motion properties, e.g., M_w, R, soil type, faulting style, etc. and a level of $S_{de}(T_1)$

1. Determine the PDF of the *IM* (i.e., S_{de}, S_{di} or $IM_{1I\&2E}$) for the target earthquake scenario, i.e., the mean and standard deviation of ln*IM* (denoted $\mu_{\ln IM}$ and $\sigma_{\ln IM}$, respectively).
2. Divide the PDF of *IM* into a small number of bins, for example, seven.
   2.1. This step can be simplified by using Table 1 as guidance to assign the number of records into each bin. Then the range (or reference value) of ln*IM* in each bin is simply $\varepsilon_{\ln IM} \cdot \sigma_{\ln IM} + \mu_{\ln IM}$.
   2.2. Selection:
      2.2.1. For S_{di} and $IM_{1I\&2E}$, users can select randomly ground motion records from any M_w, R, etc. or
   2.3. Scaling:
      2.3.1. Scale records to the ln*IM* values of each bin. For simplicity, just scale records to the reference *IM* value (i.e., exp(ln*IM*) determined in step 2.1) of each bin.
3. Simply perform nonlinear dynamic analyses of the records chosen above

<u>*Procedure for Method #4*</u>: To determine the median value of EDP using the first-order Taylor's series approximation

For given earthquake ground motion properties, e.g., M_w, R, soil type, faulting style, etc. and a level of $S_{de}(T_1)$

1. Determine the target median (i.e., geometric mean) value of the *IM* for the given earthquake scenario and level of $S_{de}(T_1)$.
2. Selection:
   2.1. For S_{di} and $IM_{1I\&2E}$, users can randomly select ground motion records from any M_w, R, etc. or
3. Scale records to the median *IM* value.
4. Simply perform nonlinear dynamic analyses of the scaled records to determine the median value of EDP

Table 1. Example number of records in each bin

range $\varepsilon_{\ln IM}$	reference $\varepsilon_{\ln IM}$ value	probability	#records (9)	#records (28)	#records (40)	#records (192)
-0.5 - 0.5	0	0.384	3	10	16	74
0.5 - 1.5	1	0.242	2	7	10	46
1.5 - 2.5	2	0.060	1	2	2	12
2.5+	3	0.006	0	0	0	1

This methodology can also be used with a ground motion hazard curve encompassing multiple earthquake scenarios (i.e., not only for a specified M_w, R, $S_{de}(T_1)$ scenario). The users simply need to difference the ground motion hazard curve to obtain a probability density-like function. We can then bin the data in a fashion similar to that shown above.

It should be noted that when using S_{di} and $IM_{1I\&2E}$ this method is expected to work with near-source pulse-like ground motions as shown in Tothong and Luco (2007), Luco and Cornell (2007), and Tothong and Cornell (2006).

A.1.14 Methods 501: Vector of Record Properties Identified by Proxy

Name for Ground Motion Selection and Modification (GMSM) Method:
"Selection by Proxy Response"

Author(s) of Synopsis: Jennie Watson-Lamprey **Date**: 9 November 2006

Reference(s):

Watson-Lamprey, J.A. and N.A. Abrahamson (2006), "Selection of Ground Motion Time Series and Limits on Scaling", *Soil Dynamics and Earthquake Engineering*, 26(5) 477-482.

Watson-Lamprey, J.A. (2006). "Selection and Modification of Ground Motion Time Histories", *Thesis (Ph.D. in Engineering – Civil and Environmental Engineering) – University of California, Berkeley.*

Objective: To obtain a set of ground motion seismograms for nonlinear dynamic structural analysis that will result in an accurate estimate of the median of the engineering demand parameter (EDP) of interest for a given structure, earthquake magnitude (M), source-to-site distance (R), and elastic response spectrafirst-mode spectral acceleration [Sa(T1)].

Brief Description/Example:

Selection and Modification Procedure:
1) Compute the median and standard deviation of Dur_{UNI}, PGV and $Sa(2T_1)$ conditioned on M, R and $Sa(T_1)$.
2) Compute the median ratio of inelastic to elastic spectral displacement, Sd_I/Sd_E, for Dur_{UNI}, PGV, $Sa(T_1)$, $Sa(2T_1)$ and R.
3) Scale candidate records to $Sa(T_1)$.
4) Reject records whose Dur_{UNI}, PGV and $Sa(2T_1)$ are not within one-half standard deviation of the median.
5) Calculate the difference between the estimated Sd_I/Sd_E ratio for the design event to the -0.4 power and the expected Sd_I/Sd_E ratio for each time series to the -0.4 power.
6) Repeat Steps 2 and 5 for 1.5R, 1.2R and R/1.2
7) For records that appear on all four lists calculate the root mean square of the differences between the Sd_I/Sd_E ratio values.
8) Select the time series with the smallest differences.

A.1.15 Methods 502a: Inelastic Response Surface Scaling — 1st Mode

Name for GMSM Method: Inelastic Displacement Surface (IDS) Matching

Author of synopsis: Tom Shantz, Caltrans

References:

Shantz T (2006). Selection and Scaling of Earthquake Records for Nonlinear Dynamic Analysis of First Mode Dominate Bridge Structures, *Proceedings of the 8th National Conference on Earthquake Engineering, San Francisco,* Earthquake Engineering Research Institute. Oakland, California.

Baker JW, Cornell CA (2006a). Spectral shape, epsilon and record selection. *Earthquake Engineering & Structural Dynamics*, 35(9): 1077-95.

Objective: To select and individually scale a suite of earthquake records whose median structural response will provide an accurate estimate of the true median response of the structural system. The records are selected based on a magnitude – distance scenario and a prescribed $Sa(T_1)$.

Brief Description of Method

1. A conditional mean spectrum (CMS) is defined for the given M, r, ε scenario per Baker and Cornell (2006a).
2. An inelastic displacement surface (IDS) is defined by multiplying the elastic CMS displacement spectrum (step 1) by the function $C_R(R, T, \varepsilon)$. $C_R(R, T, \varepsilon)$ represents the ratio of inelastic to elastic displacement response of an elastic–perfectly plastic single-degree-of-freedom oscillator. The first argument, R, represents the strength ratio of the oscillator.

   A model for $C_R(R, T, \varepsilon)$ was regressed using over 1800 records from the NGA dataset. The resulting model is given in Figure 1. C_R dependence on R and ε for the case T=1s is shown in Figure 2. An example IDS is given in Figure 3.

3. A "target" region on the IDS is specified. Generally, the region is centered at the coordinate (R_0, T_1) where

$$R_0 = \frac{\Gamma_1 \cdot \phi_{1,1} \cdot S_{d-CMS}(T_1)}{D_y} \qquad (1)$$

   In (1) Γ_1 is the first mode modal amplification factor (from elastic modal analysis of the structure), $\phi_{1,1}$ is the component of the first mode eigenvector corresponding to the top of the structure, and D_y is the yield displacement resulting from a first mode pushover analysis of the structure.

The optimal size of the target region requires further study. Generally, it is thought that for structural systems that are strongly first-mode dominate and have pushover curves

that follow (approximately) elastic-perfectly plastic behavior, the target area can be fairly small. Complex structural systems, on the other hand, are likely to require larger target areas. An additional consideration is whether the structural model is likely to undergo significant change during design. If so, a larger target area should result in a suite of records that work well for a broader range of possible designs.

1. For each candidate record (typically selected from a broad magnitude bin) a scale factor is identified that results in an optimal fit to the target surface. The fit is measured in terms of an average absolute residual. Weighting schemes can be employed to give more weight to residuals near the center of the target region and less weight to residuals near the margins of the region. Records are ranked and selected by the closeness of their fit.
2. A refinement under investigation is consideration of how well the scaled record fits the CMS at T_2.

$C_R(R,T,\epsilon) = c1(R,T) + c2(R,T) * \epsilon$ where $0.5s \le T \le 5s$ and

$$c1(R,T) = s1(T)+s2(T) * R \qquad \text{for } R \le hp(T) \text{ AND } R \ge 1$$
$$= s1(T)+s2(T) * hp(T) + s3(T) * \text{Min}(R-hp(T), 8-hp(T)) \qquad \text{for } R>hp(T)$$

$$c2(R,T) = g1(T) + g2(T) * \text{Min}(\text{Max}(R,1),8) + g3(T) * \text{Min}(\text{Max}(R, 1), 8)^2$$

where
$$s1(T) = -.0019 + .0032\,T + .0024\,T^2 - .00048\,T^3 + .00011\,T^4$$
$$s2(T) = .0066 - .014\,T + .0052\,T^2 - .0016\,T^3 + .000092\,T^4$$
$$s3(T) = 0.249 - 0.285\,T + 0.149\,T^2 - 0.03416\,T^3 + 0.0027539\,T^4$$
$$hp(T) = -.17 + 2.93\,T - 1.63\,T^2 + .37\,T^3 - .029\,T^4$$

$$g1(T) = 0.2484 - 0.36269\,T + 0.2759\,T^2 - 0.09934\,T^3 + 0.01659\,T^4 - 0.0010387\,T^5$$
$$g2(T) = -0.2676 + 0.39212\,T - 0.29938\,T^2 + 0.10805\,T^3 - 0.01808\,T^4 + 0.0011332\,T^5$$
$$g3(T) = 0.0192 - 0.02943\,T + 0.0235\,T^2 - 0.00872\,T^3 + 0.001486\,T^4 - 0.00009446\,T^5$$

Figure 1: Model for $C_R(R, T, \epsilon)$

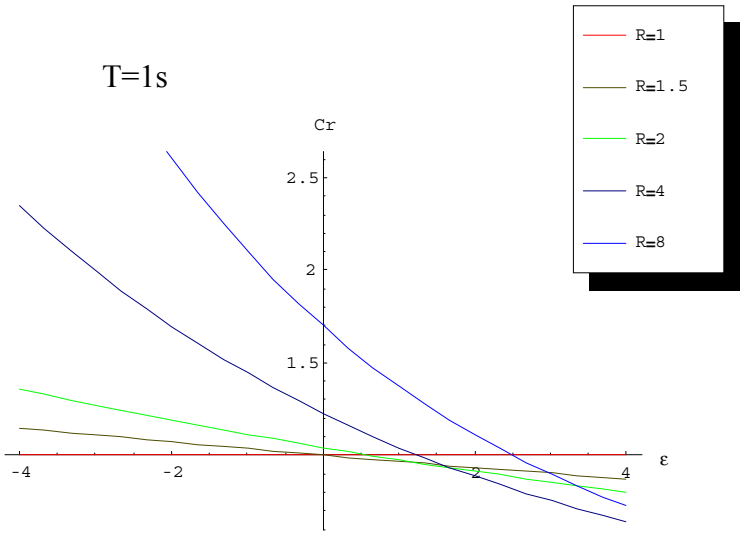

Figure 2: Inelastic displacement ratio $C_R(R, T, \varepsilon)$ for T=1 s

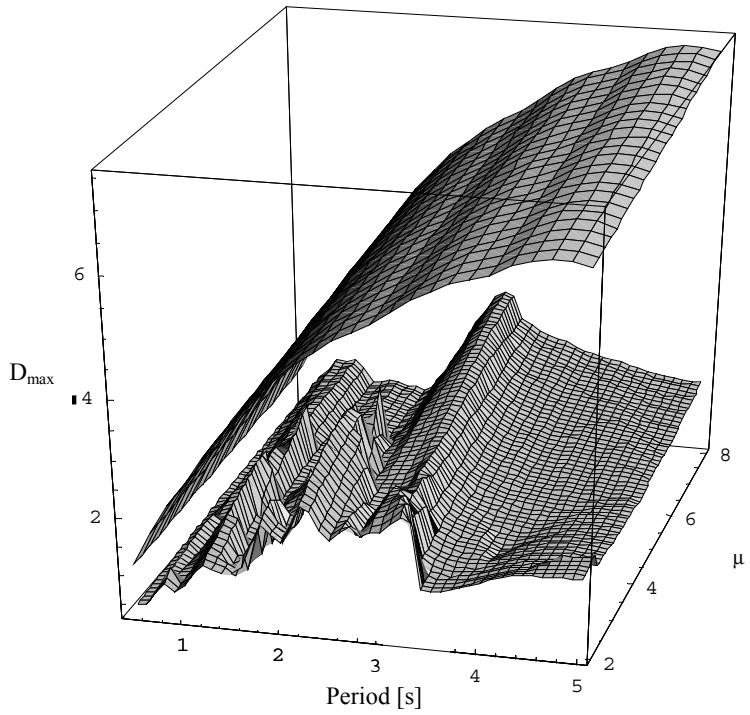

Figure 3. The inelastic displacement surface (IDS) for a magnitude 6.5, ε =0, strike-slip earthquake at 40 km distance (top) and the inelastic displacement response for the El Centro Array #9 record (C-ELC090) from the 1951 Imperial Valley earthquake (bottom).

A.1.16 Methods 502b: Inelastic Response Surface Scaling — 1st–2nd Modes

The summary for this method is contained within the summary in section A.1.15 above.

A.1.17 Methods 503: $IM_{1I\&2E}$ Scaling

The summary for this method is contained within the summary in section A.1.13 above.

Appendix B: Documentation of Public Solicitations for Community Collaboration in Submitting Ground Motion Sets

Author: C. B. Haselton

B.1 SUMMARY OF APPENDIX

This appendix documents the public announcements that were distributed, for the purpose of solicitating the collaboration and participation of the ground motion community in submitting ground motions for this research study.

B.2 SOLICITATION NUMBER ONE

To: Bob Youngs, Ellen Rathje, Yousef Bozorgnia, Jon Stewart, Nilesh Shome, Paolo Bazzurro, Polsak Tothong, Jack Baker, Farzad Naeim, Charlie Kircher, Jennie Watson-Lamprey, Nico Luco, CB Crouse, Tom Shantz

From: PEER Ground motion Selection & Modification (GMSM) Working Group

As part of the PEER Ground Motion Selection and Modification Working Group (GMSM), we are attempting an objective comparison of methods for ground motion time series selection and modification. At this time we are requesting suites of ground motions and scale factors that we will use to compute one or more of the maximum interstory drift ratio (MIDR) estimates listed below. They will be run through a nonlinear model of a 4-story reinforced concrete structure and compared with the response, as listed below. Information about the structure that we will analyze (T1, base shear, etc.) can be found in the attached PowerPoint slides.

The four estimates of maximum interstory drift ratio (MIDR) we are comparing are:

1. The cumulative distribution function of MIDR conditioned on a given earthquake event and site with a given 30m soil shear-wave velocity.
2. The median MIDR from the above distribution.
3. The cumulative distribution function of MIDR from (1) above additionally conditioned on a pseudo-spectral acceleration at the estimated fundamental period T1 (and a damping ratio of 5%).
4. The median MIDR from the above distribution.

Please let us know which measure the suite of time series you provide is attempting to estimate.

The event under consideration is a magnitude 7, at a distance of 10km from a strike-slip fault and a site with a 30m shear-wave velocity of 400 m/s. The corresponding median and one-sigma-level elastic response spectra are provided in the attached PowerPoint slides. Estimates 3 and 4 of the MIDR are to be conditioned on pseudo-spectral acceleration from the one-sigma-level spectrum at T1. The structural response values to which we will compare can be found in the attached PowerPoint slides.

This stage of the comparison is focused on analyses performed with few time series. Thus, we ask you to provide one or more suites of seven ground motions generated using your method, or a larger suite from which we will randomly select a suite of seven. Please select the time series from the PEER NGA database and provide us with the record number, component and scale factor for each selected time series. The PEER NGA database is available on the PEER web site: http://peer.berkeley.edu/nga/. The component is requested because the structural model we will analyze is 2D.

There will be a working group meeting on **October 27th** to present our method of comparison and discuss the preliminary results of these analyses. You are invited to attend this event and we would appreciate comments at that time. In order to have the analyses completed in time for this event we request that you provide us with your suite(s) no later than **October 16th**. A follow up meeting of GMSM will be held in a joint COSMOS-PEER session during COSMOS annual meeting on **November 17, 2006**.

This is not a blind prediction process, and we are interested in improving the existing GMSM methods and developing new procedures. Therefore, in order to provide an opportunity to possibly improve your method, we will send you the comparison between the results, based on your input motions, and one of the items listed above, as soon as possible.

An additional request for information about your method will be sent in the coming weeks. A request for information about your method will be sent in the coming weeks. Additionally, if you are interested in presenting a poster at the COSMOS-PEER technical session on your selection method, please contact Bob Bachman at REBachmanSE@aol.com or Yousef Bozorgnia at Yousef@Berkeley.edu.

If you have any questions, please let us know.

B.3 SOLICITATION NUMBER TWO, PART ONE

From: PEER Ground Motion Selection & Modification (GMSM) Working Group
Subject: Comparison of Ground Motion Selection and Modification Methods

Overview: As part of the PEER Ground Motion Selection and Modification Working Group (GMSM), we are attempting an objective comparison of methods for ground motion time series selection and modification. At this time we are requesting suites of ground motions and scale factors (if applicable) to predict the maximum interstory drift ratio (MIDR), for three different structural models.

Scenario: The event under consideration is a magnitude 7.0 earthquake occurring on a strike-slip fault, with the site being at a distance of 10km and having a 30m shear-wave velocity of 400 m/s. The corresponding median response spectrum and median+2σ acceleration demands are provided in the attached File #1.
The two estimates of MIDR we are attempting to predict are:

3. The cumulative distribution function of MIDR conditioned on event and site, and also conditioned on the observed $Sa(T_1)$ being median+2σ (where T_1 is the fundamental period of the structure).
4. The median MIDR from the above distribution.

File #1 also contains the conditional mean spectra, which are explained in that file.

Buildings: Three buildings are being considered, and we request that you submit sets of ground motions for each of these buildings. All buildings are reinforced-concrete structures, and File #2 gives more detail regarding each of these buildings.

Building B – Modern special moment frame (SMF) designed according to 2003 International Building Code and ASCE7-02, 12-story perimeter frame with 20' bay widths, with fundamental period (T_1) of 2.01s.

Building C – Modern SMF designed according to 2003 International Building Code and ASCE7-02, 20-story perimeter frame with 20' bay widths, with T_1 of 2.63s.

Building D – Modern (ductile) 12-story planar shear wall, with T_1 of 1.2s.

Record Sets: For each building, please provide four independent sets of 7 records each. Each set will be used to estimate median MIDR. In addition, these four sets will then be combined into a set of 28, in order to estimate both the median and standard deviation of MIDR (or just the median if that is the goal of your method). Therefore, the records of the four sets should not overlap, so that the combined set will have 28 distinct records. Please feel free to rank the sets (sets 1-4) if you feel one set is better than the other.

Record Formatting: When possible, please select the time series from the PEER NGA database (http://peer.berkeley.edu/nga/). To facilitate selection, the PEER NGA spectra are available by contacting Jennie Watson-Lamprey <jenniewl@ce.berkeley.edu>. A single component of ground motion (rather than a pair of horizontal components) is requested because the structural model is two-dimensional. If selection of PEER NGA records is not possible/convenient, please provide the acceleration time-history in a text file (single column vector of acceleration in g units). Please use the attached File #3 to submit each of your record sets.

Timeline:

5/2/07 – Please reply to indicate that you plan to collaborate and submit records sets (chaselton@csuchico.edu). This is not a hard deadline; we simply want to plan for how many sets will be submitted.

6/4/07 – Deadline for submitting records sets. Please submit sets to Curt Haselton (to both chaselton@csuchico.edu and cbhaselton@gmail.com, the later is for zipped files).

10/8/07 – Working group meeting to present preliminary results of analyses for the three structures and all selection/scaling methods (time and location TBD). You are invited to attend this event, as we would appreciate and value your comments and feedback. For those that submit sets of ground motion records, travel costs will be covered by the GMSM Working Group (please contact Curt Haselton for details).

11/9/07 – Joint COSMOS-PEER meeting where the findings of this study will be presented to obtain public feedback (time and location TBD).

Questions: Please contact Curt Haselton with any questions or comments, at chaselton@csuchico.edu or 530-898-5457.

B.4 SOLICITATION NUMBER TWO, PART TWO

From: PEER Ground Motion Selection & Modification (GMSM) Working Group

Overview: This document is meant to solicit sets of records for Building A (please see File #2 for details of this building). This document does not include all needed information, but only supplements the other more complete solicitation for Buildings B, C, and D (which was distributed by Curt Haselton by e-mail on 4-24-07). The only differences between this solicitation (for Building A) and the more complete solicitation (for Buildings B C, and D) are:

- This is for Building A.
- We are asking for records to estimate maximum interstory drift ratio (MIDR) for up to four cases instead of only two cases (#3 and #4; please see below).
- Four sets of seven records are not required. We instead ask you to provide one or more suites of seven ground motions. These suites will be used separately and will not be combined into one larger suite.

Scenario: The four estimates of MIDR we are comparing are as follows. You may submit sets of records for any number of cases. Please let us know which of the case(s) you are attempting to estimate (please indicate this in File #3).

1. The cumulative distribution function of MIDR conditioned on event and site.
2. The median MIDR from the above distribution.
3. The cumulative distribution function of MIDR conditioned on event and site, and also conditioned on the observed $Sa(T_1)$ being median+2σ (where T_1 is the fundamental period of the structure).
4. The median MIDR from the above distribution.

Spectra: File #1 includes the spectral values of interest for Building A.

Questions: Please contact Curt Haselton with any questions or comments, at chaselton@csuchico.edu or 530-898-5457.

B.5 SOLICITATION NUMBER TWO, PART THREE

To: Only GMSM Working Group members (others can submit if they would like, but we are not sending this as a public solicitation).
Date: April 26, 2007

Overview: At the April 4, 2007 meeting (and earlier meetings), we decided to use the 20-story modern RC building for a second scenario (M7.5 with +1σ).

The purpose of this study is primarily to use the results from these two scenarios (M7 and M7.5) to show the differences between the +2σ and a +1σ cases. Specifically, so we want to make the following comparisons: (a) M7 scenario (with median + 2σ) versus M7.5 scenario (with median + 1σ) (using both the sets of 7 and 28 records), and (b) 7 records versus

28 records (both for the M7.5 scenario), just to parallel the comparisons we will make for the M7 results. The vision is that our report/paper can use comparison (a) to address the concern that a +2σ scenario is too high, and our findings are therefore unrealistic.

Scenario: The event under consideration is a magnitude 7.5, at a distance of 10km from a strike-slip fault and a site with a 30m shear-wave velocity of 400 m/s. The corresponding median response spectrum and median+1σ acceleration demands are provided in the attached File #1. File #1 also contains the conditional mean spectrum. For this pilot study, we want to estimate.

3) The CDF of maximum interstory drift ratio (MIDR) conditioned on the event and site, and conditioned on $Sa(T_1=2.63s) = 0.308g$ (which is median + 1σ), or
4) The median MIDR of the above distribution.

Building: 20-story modern reinforce-concrete special moment frame (Building C). This is one of the same buildings used for the M7 scenario, and the information is included in the attached File #2.

Record Sets [same guidelines as M7 scenario]: For each building, please provide four independent sets of 7 records each. Each set will be used to estimate median MIDR. In addition, these four sets will then be combined into a set of 28, in order to estimate both the median and standard deviation of MIDR (or just the median if that is the goal of your method). Therefore, the records of the four sets should not overlap, so that the combined set will have 28 distinct records. Please feel free to rank the sets (sets 1-4) if you feel one set is better than the other.

Record Formatting [same guidelines as M7 scenario]: When possible, please select the time series from the PEER NGA database (http://peer.berkeley.edu/nga/). To facilitate selection, the PEER NGA spectra are available by contacting Jennie Watson-Lamprey <jenniewl@ce.berkeley.edu>. A single component of ground motion (rather than a pair of horizontal components) is requested because the structural model is two-dimensional. If selection of PEER NGA records is not possible/convenient, please provide the acceleration time-history in a text file (single column vector of acceleration in g units). Please use the attached File #3 to submit each of your record sets.

Timeline [same as M7 scenario]:

5/2/07 – Please reply to indicate that you plan to collaborate and submit records sets (chaselton@csuchico.edu). This is not a hard deadline; we simply want to plan for how many sets will be submitted.

6/4/07 – Deadline for submitting records sets. Please submit sets to Curt Haselton (to both chaselton@csuchico.edu and cbhaselton@gmail.com, the later is for zipped files).

10/8/07 – Working group meeting to present preliminary results of analyses for the three structures and all selection/scaling methods (time and location TBD). You are invited to attend this event, as we would appreciate and value your comments and feedback. For those that submit sets of ground motion records, travel costs will be covered by the GMSM Working Group (please contact Curt Haselton for details).

11/9/07 – Joint COSMOS-PEER meeting where the findings of this study will be presented to obtain public feedback (time and location TBD).

Questions: Please contact Curt Haselton with any questions or comments, at chaselton@csuchico.edu or 530-898-5457.

Appendix C: Documentation of Ground Motion Sets and Structural Response Results

Author: C. B. Haselton

SUMMARY OF APPENDIX

This is an electronic appendix, which is available at http://peer.berkeley.edu/publications/peer_reports.html. The content of this appendix is as follows:

- Full documentation of the ground motion sets used in this study, including:
  - filenames and scale factors (included electronically in both PDF and Excel file formats), and
  - figures of the scaled 5% damped acceleration response spectra (included electronically in both Matlab and .emf format).
- Full documentation of the structural response results for all ground motion sets (all buildings and ground motion scenarios) included in this study (included electronically in Excel file format). These response results include maximum interstory drift and a wide range of other structural response (e.g.. floor accelerations, plastic rotations, residual drifts, etc.).

The ground motions were, in almost all cases, selected from the PEER-NGA database (PEER 2008). In some cases, the rotated version of the database was used (which contains both fault-normal and fault-parallel horizontal components), and this is indicated by a "FN" or "FP" in the filename. For a single set of motions (method number 101), the ground motions were provided to the GMSM Working Group and were not selected from the PEER-NGA database; in this case, the filenames are consistent with the ATC-58 35% draft report numbering convention (ATC-58, 2007).

For each ground motion or each set, the following information is presented in this appendix: PEER-NGA records sequence number, horizontal component number, PEER-NGA record filename, and scale factor.

The ground motion data of this appendix are presented in the same order as the results in the body of this report. Ground motion sets for the Chapter 6 analyses (the M7 scenario for Building A) are presented first in section C.2. Section C.3 then presents the ground motion data used for the results of Chapter 7 (the M7 scenario for Building B). The appendix continues in the same order and finishes with section C.6, which presents the ground motion data used for the results of Chapter 10 (the M7.5 scenario for Building C).

Appendix D: Documentation of Ground Motions and Structural Responses Used to Create the POC Predictions

Author: J. Watson-Lamprey

SUMMARY OF APPENDIX

This is an electronic appendix, which is available at http://peer.berkeley.edu/publications/peer_reports.html. This appendix consists of the following tables:

- Table D-1: Documentation of the ground motion set utilized to create the POC predictions: M7 scenario
- Table D-2: Structural MIDR responses and spectral values used when creating the POC predictions: M7 scenario
- Table D-3: Documentation of the ground motion set utilized to create the POC predictions: M7 scenario
- Table D-4: Structural MIDR responses and spectral values used when creating the POC predictions: M7 scenario

PEER REPORTS

PEER reports are available individually or by yearly subscription. PEER reports can be ordered at http://peer.berkeley.edu/publications/peer_reports.html or by contacting the Pacific Earthquake Engineering Research Center, 1301 South 46th Street, Richmond, CA 94804-4698. Tel.: (510) 665-3448; Fax: (510) 665-3456; Email: peer_editor@berkeley.edu

PEER 2009/01 *Evaluation of Ground Motion Selection and Modification Methods: Predicting Median Interstory Drift Response of Buildings.* Curt B. Haselton, Ed. June 2009.

PEER 2008/10 *Technical Manual for Strata.* Albert R. Kottke and Ellen M. Rathje. February 2009.

PEER 2008/09 *NGA Model for Average Horizontal Component of Peak Ground Motion and Response Spectra.* Brian S.-J. Chiou and Robert R. Youngs. November 2008.

PEER 2008/08 *Toward Earthquake-Resistant Design of Concentrically Braced Steel Structures.* Patxi Uriz and Stephen A. Mahin. November 2008.

PEER 2008/07 *Using OpenSees for Performance-Based Evaluation of Bridges on Liquefiable Soils.* Stephen L. Kramer, Pedro Arduino, and HyungSuk Shin. November 2008.

PEER 2008/06 *Shaking Table Tests and Numerical Investigation of Self-Centering Reinforced Concrete Bridge Columns.* Hyung IL Jeong, Junichi Sakai, and Stephen A. Mahin. September 2008.

PEER 2008/05 *Performance-Based Earthquake Engineering Design Evaluation Procedure for Bridge Foundations Undergoing Liquefaction-Induced Lateral Ground Displacement.* Christian A. Ledezma and Jonathan D. Bray. August 2008.

PEER 2008/04 *Benchmarking of Nonlinear Geotechnical Ground Response Analysis Procedures.* Jonathan P. Stewart, Annie On-Lei Kwok, Yousseff M. A. Hashash, Neven Matasovic, Robert Pyke, Zhiliang Wang, and Zhaohui Yang. August 2008.

PEER 2008/03 *Guidelines for Nonlinear Analysis of Bridge Structures in California.* Ady Aviram, Kevin R. Mackie, and Božidar Stojadinović. August 2008.

PEER 2008/02 *Treatment of Uncertainties in Seismic-Risk Analysis of Transportation Systems.* Evangelos Stergiou and Anne S. Kiremidjian. July 2008.

PEER 2008/01 *Seismic Performance Objectives for Tall Buildings.* William T. Holmes, Charles Kircher, William Petak, and Nabih Youssef. August 2008.

PEER 2007/12 *An Assessment to Benchmark the Seismic Performance of a Code-Conforming Reinforced Concrete Moment-Frame Building.* Curt Haselton, Christine A. Goulet, Judith Mitrani-Reiser, James L. Beck, Gregory G. Deierlein, Keith A. Porter, Jonathan P. Stewart, and Ertugrul Taciroglu. August 2008.

PEER 2007/11 *Bar Buckling in Reinforced Concrete Bridge Columns.* Wayne A. Brown, Dawn E. Lehman, and John F. Stanton. February 2008.

PEER 2007/10 *Computational Modeling of Progressive Collapse in Reinforced Concrete Frame Structures.* Mohamed M. Talaat and Khalid M. Mosalam. May 2008.

PEER 2007/09 *Integrated Probabilistic Performance-Based Evaluation of Benchmark Reinforced Concrete Bridges.* Kevin R. Mackie, John-Michael Wong, and Božidar Stojadinović. January 2008.

PEER 2007/08 *Assessing Seismic Collapse Safety of Modern Reinforced Concrete Moment-Frame Buildings.* Curt B. Haselton and Gregory G. Deierlein. February 2008.

PEER 2007/07 *Performance Modeling Strategies for Modern Reinforced Concrete Bridge Columns.* Michael P. Berry and Marc O. Eberhard. April 2008.

PEER 2007/06 *Development of Improved Procedures for Seismic Design of Buried and Partially Buried Structures.* Linda Al Atik and Nicholas Sitar. June 2007.

PEER 2007/05 *Uncertainty and Correlation in Seismic Risk Assessment of Transportation Systems.* Renee G. Lee and Anne S. Kiremidjian. July 2007.

PEER 2007/04 *Numerical Models for Analysis and Performance-Based Design of Shallow Foundations Subjected to Seismic Loading.* Sivapalan Gajan, Tara C. Hutchinson, Bruce L. Kutter, Prishati Raychowdhury, José A. Ugalde, and Jonathan P. Stewart. May 2008.

PEER 2007/03 *Beam-Column Element Model Calibrated for Predicting Flexural Response Leading to Global Collapse of RC Frame Buildings.* Curt B. Haselton, Abbie B. Liel, Sarah Taylor Lange, and Gregory G. Deierlein. May 2008.

PEER 2007/02 *Campbell-Bozorgnia NGA Ground Motion Relations for the Geometric Mean Horizontal Component of Peak and Spectral Ground Motion Parameters.* Kenneth W. Campbell and Yousef Bozorgnia. May 2007.

PEER 2007/01 *Boore-Atkinson NGA Ground Motion Relations for the Geometric Mean Horizontal Component of Peak and Spectral Ground Motion Parameters.* David M. Boore and Gail M. Atkinson. May. May 2007.

PEER 2006/12 *Societal Implications of Performance-Based Earthquake Engineering.* Peter J. May. May 2007.

PEER 2006/11 *Probabilistic Seismic Demand Analysis Using Advanced Ground Motion Intensity Measures, Attenuation Relationships, and Near-Fault Effects.* Polsak Tothong and C. Allin Cornell. March 2007.

PEER 2006/10 *Application of the PEER PBEE Methodology to the I-880 Viaduct.* Sashi Kunnath. February 2007.

PEER 2006/09 *Quantifying Economic Losses from Travel Forgone Following a Large Metropolitan Earthquake.* James Moore, Sungbin Cho, Yue Yue Fan, and Stuart Werner. November 2006.

PEER 2006/08 *Vector-Valued Ground Motion Intensity Measures for Probabilistic Seismic Demand Analysis*. Jack W. Baker and C. Allin Cornell. October 2006.

PEER 2006/07 *Analytical Modeling of Reinforced Concrete Walls for Predicting Flexural and Coupled–Shear-Flexural Responses*. Kutay Orakcal, Leonardo M. Massone, and John W. Wallace. October 2006.

PEER 2006/06 *Nonlinear Analysis of a Soil-Drilled Pier System under Static and Dynamic Axial Loading.* Gang Wang and Nicholas Sitar. November 2006.

PEER 2006/05 *Advanced Seismic Assessment Guidelines.* Paolo Bazzurro, C. Allin Cornell, Charles Menun, Maziar Motahari, and Nicolas Luco. September 2006.

PEER 2006/04 *Probabilistic Seismic Evaluation of Reinforced Concrete Structural Components and Systems.* Tae Hyung Lee and Khalid M. Mosalam. August 2006.

PEER 2006/03 *Performance of Lifelines Subjected to Lateral Spreading*. Scott A. Ashford and Teerawut Juirnarongrit. July 2006.

PEER 2006/02 *Pacific Earthquake Engineering Research Center Highway Demonstration Project.* Anne Kiremidjian, James Moore, Yue Yue Fan, Nesrin Basoz, Ozgur Yazali, and Meredith Williams. April 2006.

PEER 2006/01 *Bracing Berkeley. A Guide to Seismic Safety on the UC Berkeley Campus.* Mary C. Comerio, Stephen Tobriner, and Ariane Fehrenkamp. January 2006.

PEER 2005/16 *Seismic Response and Reliability of Electrical Substation Equipment and Systems.* Junho Song, Armen Der Kiureghian, and Jerome L. Sackman. April 2006.

PEER 2005/15 *CPT-Based Probabilistic Assessment of Seismic Soil Liquefaction Initiation.* R. E. S. Moss, R. B. Seed, R. E. Kayen, J. P. Stewart, and A. Der Kiureghian. April 2006.

PEER 2005/14 *Workshop on Modeling of Nonlinear Cyclic Load-Deformation Behavior of Shallow Foundations.* Bruce L. Kutter, Geoffrey Martin, Tara Hutchinson, Chad Harden, Sivapalan Gajan, and Justin Phalen. March 2006.

PEER 2005/13 *Stochastic Characterization and Decision Bases under Time-Dependent Aftershock Risk in Performance-Based Earthquake Engineering*. Gee Liek Yeo and C. Allin Cornell. July 2005.

PEER 2005/12 *PEER Testbed Study on a Laboratory Building: Exercising Seismic Performance Assessment*. Mary C. Comerio, editor. November 2005.

PEER 2005/11 *Van Nuys Hotel Building Testbed Report: Exercising Seismic Performance Assessment.* Helmut Krawinkler, editor. October 2005.

PEER 2005/10 *First NEES/E-Defense Workshop on Collapse Simulation of Reinforced Concrete Building Structures.* September 2005.

PEER 2005/09 *Test Applications of Advanced Seismic Assessment Guidelines.* Joe Maffei, Karl Telleen, Danya Mohr, William Holmes, and Yuki Nakayama. August 2006.

PEER 2005/08 *Damage Accumulation in Lightly Confined Reinforced Concrete Bridge Columns.* R. Tyler Ranf, Jared M. Nelson, Zach Price, Marc O. Eberhard, and John F. Stanton. April 2006.

PEER 2005/07 *Experimental and Analytical Studies on the Seismic Response of Freestanding and Anchored Laboratory Equipment.* Dimitrios Konstantinidis and Nicos Makris. January 2005.

PEER 2005/06 *Global Collapse of Frame Structures under Seismic Excitations*. Luis F. Ibarra and Helmut Krawinkler. September 2005.

PEER 2005//05 *Performance Characterization of Bench- and Shelf-Mounted Equipment*. Samit Ray Chaudhuri and Tara C. Hutchinson. May 2006.

PEER 2005/04 *Numerical Modeling of the Nonlinear Cyclic Response of Shallow Foundations.* Chad Harden, Tara Hutchinson, Geoffrey R. Martin, and Bruce L. Kutter. August 2005.

PEER 2005/03 *A Taxonomy of Building Components for Performance-Based Earthquake Engineering.* Keith A. Porter. September 2005.

PEER 2005/02 *Fragility Basis for California Highway Overpass Bridge Seismic Decision Making*. Kevin R. Mackie and Božidar Stojadinović. June 2005.

PEER 2005/01 *Empirical Characterization of Site Conditions on Strong Ground Motion.* Jonathan P. Stewart, Yoojoong Choi, and Robert W. Graves. June 2005.

PEER 2004/09 *Electrical Substation Equipment Interaction: Experimental Rigid Conductor Studies.* Christopher Stearns and André Filiatrault. February 2005.

PEER 2004/08 *Seismic Qualification and Fragility Testing of Line Break 550-kV Disconnect Switches.* Shakhzod M. Takhirov, Gregory L. Fenves, and Eric Fujisaki. January 2005.

PEER 2004/07 *Ground Motions for Earthquake Simulator Qualification of Electrical Substation Equipment.* Shakhzod M. Takhirov, Gregory L. Fenves, Eric Fujisaki, and Don Clyde. January 2005.

PEER 2004/06 *Performance-Based Regulation and Regulatory Regimes.* Peter J. May and Chris Koski. September 2004.

PEER 2004/05 *Performance-Based Seismic Design Concepts and Implementation: Proceedings of an International Workshop.* Peter Fajfar and Helmut Krawinkler, editors. September 2004.

PEER 2004/04 *Seismic Performance of an Instrumented Tilt-up Wall Building*. James C. Anderson and Vitelmo V. Bertero. July 2004.

PEER 2004/03 *Evaluation and Application of Concrete Tilt-up Assessment Methodologies.* Timothy Graf and James O. Malley. October 2004.

PEER 2004/02 *Analytical Investigations of New Methods for Reducing Residual Displacements of Reinforced Concrete Bridge Columns.* Junichi Sakai and Stephen A. Mahin. August 2004.

PEER 2004/01 *Seismic Performance of Masonry Buildings and Design Implications.* Kerri Anne Taeko Tokoro, James C. Anderson, and Vitelmo V. Bertero. February 2004.

PEER 2003/18 *Performance Models for Flexural Damage in Reinforced Concrete Columns.* Michael Berry and Marc Eberhard. August 2003.

PEER 2003/17 *Predicting Earthquake Damage in Older Reinforced Concrete Beam-Column Joints.* Catherine Pagni and Laura Lowes. October 2004.

PEER 2003/16 *Seismic Demands for Performance-Based Design of Bridges.* Kevin Mackie and Božidar Stojadinović. August 2003.

PEER 2003/15 *Seismic Demands for Nondeteriorating Frame Structures and Their Dependence on Ground Motions.* Ricardo Antonio Medina and Helmut Krawinkler. May 2004.

PEER 2003/14 *Finite Element Reliability and Sensitivity Methods for Performance-Based Earthquake Engineering.* Terje Haukaas and Armen Der Kiureghian. April 2004.

PEER 2003/13 *Effects of Connection Hysteretic Degradation on the Seismic Behavior of Steel Moment-Resisting Frames.* Janise E. Rodgers and Stephen A. Mahin. March 2004.

PEER 2003/12 *Implementation Manual for the Seismic Protection of Laboratory Contents: Format and Case Studies.* William T. Holmes and Mary C. Comerio. October 2003.

PEER 2003/11 *Fifth U.S.-Japan Workshop on Performance-Based Earthquake Engineering Methodology for Reinforced Concrete Building Structures.* February 2004.

PEER 2003/10 *A Beam-Column Joint Model for Simulating the Earthquake Response of Reinforced Concrete Frames.* Laura N. Lowes, Nilanjan Mitra, and Arash Altoontash. February 2004.

PEER 2003/09 *Sequencing Repairs after an Earthquake: An Economic Approach.* Marco Casari and Simon J. Wilkie. April 2004.

PEER 2003/08 *A Technical Framework for Probability-Based Demand and Capacity Factor Design (DCFD) Seismic Formats*. Fatemeh Jalayer and C. Allin Cornell. November 2003.

PEER 2003/07 *Uncertainty Specification and Propagation for Loss Estimation Using FOSM Methods.* Jack W. Baker and C. Allin Cornell. September 2003.

PEER 2003/06 *Performance of Circular Reinforced Concrete Bridge Columns under Bidirectional Earthquake Loading*. Mahmoud M. Hachem, Stephen A. Mahin, and Jack P. Moehle. February 2003.

PEER 2003/05 *Response Assessment for Building-Specific Loss Estimation.* Eduardo Miranda and Shahram Taghavi. September 2003.

PEER 2003/04 *Experimental Assessment of Columns with Short Lap Splices Subjected to Cyclic Loads*. Murat Melek, John W. Wallace, and Joel Conte. April 2003.

PEER 2003/03 *Probabilistic Response Assessment for Building-Specific Loss Estimation.* Eduardo Miranda and Hesameddin Aslani. September 2003.

PEER 2003/02 *Software Framework for Collaborative Development of Nonlinear Dynamic Analysis Program*. Jun Peng and Kincho H. Law. September 2003.

PEER 2003/01 *Shake Table Tests and Analytical Studies on the Gravity Load Collapse of Reinforced Concrete Frames.* Kenneth John Elwood and Jack P. Moehle. November 2003.

PEER 2002/24 *Performance of Beam to Column Bridge Joints Subjected to a Large Velocity Pulse.* Natalie Gibson, André Filiatrault, and Scott A. Ashford. April 2002.

PEER 2002/23 *Effects of Large Velocity Pulses on Reinforced Concrete Bridge Columns.* Greg L. Orozco and Scott A. Ashford. April 2002.

PEER 2002/22 *Characterization of Large Velocity Pulses for Laboratory Testing.* Kenneth E. Cox and Scott A. Ashford. April 2002.

PEER 2002/21 *Fourth U.S.-Japan Workshop on Performance-Based Earthquake Engineering Methodology for Reinforced Concrete Building Structures*. December 2002.

PEER 2002/20 *Barriers to Adoption and Implementation of PBEE Innovations.* Peter J. May. August 2002.

PEER 2002/19 *Economic-Engineered Integrated Models for Earthquakes: Socioeconomic Impacts.* Peter Gordon, James E. Moore II, and Harry W. Richardson. July 2002.

PEER 2002/18 *Assessment of Reinforced Concrete Building Exterior Joints with Substandard Details.* Chris P. Pantelides, Jon Hansen, Justin Nadauld, and Lawrence D. Reaveley. May 2002.

PEER 2002/17 *Structural Characterization and Seismic Response Analysis of a Highway Overcrossing Equipped with Elastomeric Bearings and Fluid Dampers: A Case Study*. Nicos Makris and Jian Zhang. November 2002.

PEER 2002/16 *Estimation of Uncertainty in Geotechnical Properties for Performance-Based Earthquake Engineering.* Allen L. Jones, Steven L. Kramer, and Pedro Arduino. December 2002.

PEER 2002/15 *Seismic Behavior of Bridge Columns Subjected to Various Loading Patterns.* Asadollah Esmaeily-Gh. and Yan Xiao. December 2002.

PEER 2002/14 *Inelastic Seismic Response of Extended Pile Shaft Supported Bridge Structures.* T.C. Hutchinson, R.W. Boulanger, Y.H. Chai, and I.M. Idriss. December 2002.

PEER 2002/13 *Probabilistic Models and Fragility Estimates for Bridge Components and Systems.* Paolo Gardoni, Armen Der Kiureghian, and Khalid M. Mosalam. June 2002.

PEER 2002/12 *Effects of Fault Dip and Slip Rake on Near-Source Ground Motions: Why Chi-Chi Was a Relatively Mild M7.6 Earthquake*. Brad T. Aagaard, John F. Hall, and Thomas H. Heaton. December 2002.

PEER 2002/11 *Analytical and Experimental Study of Fiber-Reinforced Strip Isolators*. James M. Kelly and Shakhzod M. Takhirov. September 2002.

PEER 2002/10 *Centrifuge Modeling of Settlement and Lateral Spreading with Comparisons to Numerical Analyses***.** Sivapalan Gajan and Bruce L. Kutter. January 2003.

PEER 2002/09 *Documentation and Analysis of Field Case Histories of Seismic Compression during the 1994 Northridge, California, Earthquake.* Jonathan P. Stewart, Patrick M. Smith, Daniel H. Whang, and Jonathan D. Bray. October 2002.

PEER 2002/08 *Component Testing, Stability Analysis and Characterization of Buckling-Restrained Unbonded Braces™*. Cameron Black, Nicos Makris, and Ian Aiken. September 2002.

PEER 2002/07 *Seismic Performance of Pile-Wharf Connections.* Charles W. Roeder, Robert Graff, Jennifer Soderstrom, and Jun Han Yoo. December 2001.

PEER 2002/06 *The Use of Benefit-Cost Analysis for Evaluation of Performance-Based Earthquake Engineering Decisions*. Richard O. Zerbe and Anthony Falit-Baiamonte. September 2001.

PEER 2002/05 *Guidelines, Specifications, and Seismic Performance Characterization of Nonstructural Building Components and Equipment*. André Filiatrault, Constantin Christopoulos, and Christopher Stearns. September 2001.

PEER 2002/04 *Consortium of Organizations for Strong-Motion Observation Systems and the Pacific Earthquake Engineering Research Center Lifelines Program: Invited Workshop on Archiving and Web Dissemination of Geotechnical Data, 4–5 October 2001*. September 2002.

PEER 2002/03 *Investigation of Sensitivity of Building Loss Estimates to Major Uncertain Variables for the Van Nuys Testbed.* Keith A. Porter, James L. Beck, and Rustem V. Shaikhutdinov. August 2002.

PEER 2002/02 *The Third U.S.-Japan Workshop on Performance-Based Earthquake Engineering Methodology for Reinforced Concrete Building Structures*. July 2002.

PEER 2002/01 *Nonstructural Loss Estimation: The UC Berkeley Case Study.* Mary C. Comerio and John C. Stallmeyer. December 2001.

PEER 2001/16 *Statistics of SDF-System Estimate of Roof Displacement for Pushover Analysis of Buildings.* Anil K. Chopra, Rakesh K. Goel, and Chatpan Chintanapakdee. December 2001.

PEER 2001/15 *Damage to Bridges during the 2001 Nisqually Earthquake.* R. Tyler Ranf, Marc O. Eberhard, and Michael P. Berry. November 2001.

PEER 2001/14 *Rocking Response of Equipment Anchored to a Base Foundation.* Nicos Makris and Cameron J. Black. September 2001.

PEER 2001/13 *Modeling Soil Liquefaction Hazards for Performance-Based Earthquake Engineering.* Steven L. Kramer and Ahmed-W. Elgamal. February 2001.

PEER 2001/12 *Development of Geotechnical Capabilities in OpenSees.* Boris Jeremi . September 2001.

PEER 2001/11 *Analytical and Experimental Study of Fiber-Reinforced Elastomeric Isolators*. James M. Kelly and Shakhzod M. Takhirov. September 2001.

PEER 2001/10 *Amplification Factors for Spectral Acceleration in Active Regions.* Jonathan P. Stewart, Andrew H. Liu, Yoojoong Choi, and Mehmet B. Baturay. December 2001.

PEER 2001/09 *Ground Motion Evaluation Procedures for Performance-Based Design.* Jonathan P. Stewart, Shyh-Jeng Chiou, Jonathan D. Bray, Robert W. Graves, Paul G. Somerville, and Norman A. Abrahamson. September 2001.

PEER 2001/08 *Experimental and Computational Evaluation of Reinforced Concrete Bridge Beam-Column Connections for Seismic Performance*. Clay J. Naito, Jack P. Moehle, and Khalid M. Mosalam. November 2001.

PEER 2001/07 *The Rocking Spectrum and the Shortcomings of Design Guidelines*. Nicos Makris and Dimitrios Konstantinidis. August 2001.

PEER 2001/06 *Development of an Electrical Substation Equipment Performance Database for Evaluation of Equipment Fragilities*. Thalia Agnanos. April 1999.

PEER 2001/05 *Stiffness Analysis of Fiber-Reinforced Elastomeric Isolators.* Hsiang-Chuan Tsai and James M. Kelly. May 2001.

PEER 2001/04 *Organizational and Societal Considerations for Performance-Based Earthquake Engineering.* Peter J. May. April 2001.

PEER 2001/03 *A Modal Pushover Analysis Procedure to Estimate Seismic Demands for Buildings: Theory and Preliminary Evaluation.* Anil K. Chopra and Rakesh K. Goel. January 2001.

PEER 2001/02 *Seismic Response Analysis of Highway Overcrossings Including Soil-Structure Interaction.* Jian Zhang and Nicos Makris. March 2001.

PEER 2001/01 *Experimental Study of Large Seismic Steel Beam-to-Column Connections.* Egor P. Popov and Shakhzod M. Takhirov. November 2000.

PEER 2000/10 *The Second U.S.-Japan Workshop on Performance-Based Earthquake Engineering Methodology for Reinforced Concrete Building Structures.* March 2000.

PEER 2000/09 *Structural Engineering Reconnaissance of the August 17, 1999 Earthquake: Kocaeli (Izmit), Turkey*. Halil Sezen, Kenneth J. Elwood, Andrew S. Whittaker, Khalid Mosalam, John J. Wallace, and John F. Stanton. December 2000.

PEER 2000/08 *Behavior of Reinforced Concrete Bridge Columns Having Varying Aspect Ratios and Varying Lengths of Confinement.* Anthony J. Calderone, Dawn E. Lehman, and Jack P. Moehle. January 2001.

PEER 2000/07 *Cover-Plate and Flange-Plate Reinforced Steel Moment-Resisting Connections.* Taejin Kim, Andrew S. Whittaker, Amir S. Gilani, Vitelmo V. Bertero, and Shakhzod M. Takhirov. September 2000.

PEER 2000/06 *Seismic Evaluation and Analysis of 230-kV Disconnect Switches.* Amir S. J. Gilani, Andrew S. Whittaker, Gregory L. Fenves, Chun-Hao Chen, Henry Ho, and Eric Fujisaki. July 2000.

PEER 2000/05 *Performance-Based Evaluation of Exterior Reinforced Concrete Building Joints for Seismic Excitation.* Chandra Clyde, Chris P. Pantelides, and Lawrence D. Reaveley. July 2000.

PEER 2000/04 *An Evaluation of Seismic Energy Demand: An Attenuation Approach.* Chung-Che Chou and Chia-Ming Uang. July 1999.

PEER 2000/03 *Framing Earthquake Retrofitting Decisions: The Case of Hillside Homes in Los Angeles.* Detlof von Winterfeldt, Nels Roselund, and Alicia Kitsuse. March 2000.

PEER 2000/02 *U.S.-Japan Workshop on the Effects of Near-Field Earthquake Shaking.* Andrew Whittaker, ed. July 2000.

PEER 2000/01 *Further Studies on Seismic Interaction in Interconnected Electrical Substation Equipment.* Armen Der Kiureghian, Kee-Jeung Hong, and Jerome L. Sackman. November 1999.

PEER 1999/14 *Seismic Evaluation and Retrofit of 230-kV Porcelain Transformer Bushings*. Amir S. Gilani, Andrew S. Whittaker, Gregory L. Fenves, and Eric Fujisaki. December 1999.

PEER 1999/13 *Building Vulnerability Studies: Modeling and Evaluation of Tilt-up and Steel Reinforced Concrete Buildings.* John W. Wallace, Jonathan P. Stewart, and Andrew S. Whittaker, editors. December 1999.

PEER 1999/12 *Rehabilitation of Nonductile RC Frame Building Using Encasement Plates and Energy-Dissipating Devices.* Mehrdad Sasani, Vitelmo V. Bertero, James C. Anderson. December 1999.

PEER 1999/11 *Performance Evaluation Database for Concrete Bridge Components and Systems under Simulated Seismic Loads*. Yael D. Hose and Frieder Seible. November 1999.

PEER 1999/10 *U.S.-Japan Workshop on Performance-Based Earthquake Engineering Methodology for Reinforced Concrete Building Structures.* December 1999.

PEER 1999/09 *Performance Improvement of Long Period Building Structures Subjected to Severe Pulse-Type Ground Motions*. James C. Anderson, Vitelmo V. Bertero, and Raul Bertero. October 1999.

PEER 1999/08 *Envelopes for Seismic Response Vectors.* Charles Menun and Armen Der Kiureghian. July 1999.

PEER 1999/07 *Documentation of Strengths and Weaknesses of Current Computer Analysis Methods for Seismic Performance of Reinforced Concrete Members.* William F. Cofer. November 1999.

PEER 1999/06 *Rocking Response and Overturning of Anchored Equipment under Seismic Excitations.* Nicos Makris and Jian Zhang. November 1999.

PEER 1999/05 *Seismic Evaluation of 550 kV Porcelain Transformer Bushings.* Amir S. Gilani, Andrew S. Whittaker, Gregory L. Fenves, and Eric Fujisaki. October 1999.

PEER 1999/04 *Adoption and Enforcement of Earthquake Risk-Reduction Measures.* Peter J. May, Raymond J. Burby, T. Jens Feeley, and Robert Wood.

PEER 1999/03 *Task 3 Characterization of Site Response General Site Categories*. Adrian Rodriguez-Marek, Jonathan D. Bray, and Norman Abrahamson. February 1999.

PEER 1999/02 *Capacity-Demand-Diagram Methods for Estimating Seismic Deformation of Inelastic Structures: SDF Systems*. Anil K. Chopra and Rakesh Goel. April 1999.

PEER 1999/01 *Interaction in Interconnected Electrical Substation Equipment Subjected to Earthquake Ground Motions.* Armen Der Kiureghian, Jerome L. Sackman, and Kee-Jeung Hong. February 1999.

PEER 1998/08 *Behavior and Failure Analysis of a Multiple-Frame Highway Bridge in the 1994 Northridge Earthquake.* Gregory L. Fenves and Michael Ellery. December 1998.

PEER 1998/07 *Empirical Evaluation of Inertial Soil-Structure Interaction Effects.* Jonathan P. Stewart, Raymond B. Seed, and Gregory L. Fenves. November 1998.

PEER 1998/06 *Effect of Damping Mechanisms on the Response of Seismic Isolated Structures.* Nicos Makris and Shih-Po Chang. November 1998.

PEER 1998/05 *Rocking Response and Overturning of Equipment under Horizontal Pulse-Type Motions.* Nicos Makris and Yiannis Roussos. October 1998.

PEER 1998/04 *Pacific Earthquake Engineering Research Invitational Workshop Proceedings, May 14–15, 1998: Defining the Links between Planning, Policy Analysis, Economics and Earthquake Engineering.* Mary Comerio and Peter Gordon. September 1998.

PEER 1998/03 *Repair/Upgrade Procedures for Welded Beam to Column Connections.* James C. Anderson and Xiaojing Duan. May 1998.

PEER 1998/02 *Seismic Evaluation of 196 kV Porcelain Transformer Bushings.* Amir S. Gilani, Juan W. Chavez, Gregory L. Fenves, and Andrew S. Whittaker. May 1998.

PEER 1998/01 *Seismic Performance of Well-Confined Concrete Bridge Columns.* Dawn E. Lehman and Jack P. Moehle. December 2000.

ONLINE REPORTS

The following PEER reports are available by Internet only at http://peer.berkeley.edu/publications/peer_reports.html

PEER 2008/104 *Experimental and Analytical Study of the Seismic Performance of Retaining Structures.* Linda Al Atik and Nicholas Sitar. January 2009.

PEER 2008/103 *Experimental and Computational Evaluation of Current and Innovative In-Span Hinge Details in Reinforced Concrete Box-Girder Bridges. Part 1: Experimental Findings and Pre-Test Analysis.* Matias A. Hube and Khalid M. Mosalam. January 2009.

PEER 2008/102 *Modeling of Unreinforced Masonry Infill Walls Considering In-Plane and Out-of-Plane Interaction.* Stephen Kadysiewski and Khalid M. Mosalam. January 2009.

PEER 2008/101 *Seismic Performance Objectives for Tall Buildings.* William T. Holmes, Charles Kircher, William Petak, and Nabih Youssef. August 2008.

PEER 2007/101 *Generalized Hybrid Simulation Framework for Structural Systems Subjected to Seismic Loading.* Tarek Elkhoraibi and Khalid M. Mosalam. July 2007.

PEER 2007/100 *Seismic Evaluation of Reinforced Concrete Buildings Including Effects of Masonry Infill Walls.* Alidad Hashemi and Khalid M. Mosalam. July 2007.